

**Removal of Chromium from Water using Manganese Oxide Based Adsorbents:  
Adsorption of Cr(III) and Cr(VI)**

BY

LISHA WU

B.S., Chemical Engineering, Wuhan Institute of Technology, China, 2011  
M.S., Beijing University of Chemical Engineering, China, 2014

Thesis submitted as partial fulfillment of the requirements  
for the degree of Doctor of Philosophy in Civil Engineering  
in the Graduate College of the  
University of Illinois at Chicago, 2020

Chicago, Illinois

Defense Committee:

Dr. Amid Khodadoust, Chair and Advisor

Dr. Krishna Reddy

Dr. Michael McNallan

Dr. Eduard Karpov

Dr. Suresh Aggarwal, Mechanical & Industrial Engineering

**This thesis is dedicated to  
my parents, Changqing Wu and Xiaohong Lyu,  
for their endless love and support.**

## ACKNOWLEDGEMENTS

First, I would like to express my sincerest gratitude toward my advisor Professor Amid Khodadoust for his enormous patience and professional guidance during the course of my PhD study and research. This thesis would be impossible without his constant support and help and his professionalism will be my cornerstone for whatever profession I will take on in the future.

Second, my deepest appreciation goes to my thesis committee members Dr. Krishna Reddy, Dr. Michael McNallan, Dr. Eduard Karpov, and Dr. Suresh Aggarwal. Their professional opinions and guidance benefit my research and thesis profoundly. I also would like to give thanks to my dear friends and lab mates at UIC, Snover, Karoline, Abhilasha, Masha, Morvarid, Nick, Mohsen, and Jose for their constant company and precious friendship.

At last, I also would like to thank my family and friends in China. Even they are not with me physically, but their encouragement and support have been with me for every step of the way. I also would like to express my greatest appreciation toward my husband, Zhen Luo, for his endless support, encouragement and challenge.

## TABLE OF CONTENTS

<u>CHAPTER</u>	<u>PAGE</u>
<b>I. INTRODUCTION.....</b>	<b>1</b>
1.1 Introduction.....	1
1.2 Environmental chemistry of chromium .....	1
1.2.1 Cr(III).....	3
1.2.2 Cr(VI) .....	3
1.2.3 Oxidation-reduction of chromium .....	5
1.2.3.1 Oxidation of Cr(III) .....	5
1.2.3.2 Reduction of Cr(VI).....	6
1.2.4 Adsorption-desorption of chromium .....	7
1.3 Sources of chromium.....	7
1.3.1 Natural sources .....	7
1.3.2 Anthropogenic sources .....	9
1.4 Toxicology of chromium .....	10
1.4.1 Human nutrient .....	10
1.4.2 Toxicology.....	11
1.5 Treatment technologies of chromium.....	11
1.5.1 Reduction.....	12
1.5.2 Ion exchange.....	12
1.5.3 Membrane filtration.....	13
1.5.4 Adsorption .....	14
1.5.4.1 Activated carbon.....	14
1.5.4.2 Biosorbents .....	15
1.5.4.4 Minerals .....	17
1.2 Research objectives .....	19
1.2.1 Adsorption capacity and adsorption mechanism .....	19
1.2.2 Adsorbent characterization .....	20
1.2.3 Geochemical modeling .....	20
1.2.4 Adsorption system/adsorber sustainability analysis .....	20
1.3 Reference .....	22
<b>II. DEVELOPMENT OF MANGANESE-COATED SAND.....</b>	<b>36</b>
2.1 Introduction.....	36

## TABLE OF CONTENTS (continued)

<u>CHAPTER</u>	<u>PAGE</u>
2.2 Materials and methods .....	38
2.2.1 Chemicals .....	38
2.2.2 Coating method.....	38
2.3 Results and discussion .....	39
2.4 Reference .....	39
<b>III. ADSORPTION OF CHROMIUM ONTO MANGANESE-COATED SAND: BATCH STUDY.....</b>	<b>49</b>
3.1 Introduction.....	49
3.2 Materials and method .....	51
3.2.1 Chemicals .....	51
3.2.2 Batch adsorption experiments.....	51
3.2.3 Zeta potential measurement.....	52
3.2.4 Adsorption kinetics.....	52
3.2.5 Coexisting ions study.....	52
3.2.6 Sorbent recycling and regeneration experiments.....	53
3.2.7 Analytical methods .....	53
3.3 Results and discussion .....	55
3.3.1 Effect of MCS dosage.....	55
3.3.2 Isotherm studies .....	56
3.3.3 Effect of pH .....	67
3.3.4 Effect of surface charge .....	69
3.3.5 Effect of contacting time and adsorption kinetic study .....	71
3.3.6 Effect of coexisting ions .....	79
3.3.7 Sorbent reuse and regeneration.....	83
3.4 Conclusion .....	85
3.5 Reference .....	86
<b>IV. SURFACE CHARACTERIZATION OF MANGANESE-COATED SAND.....</b>	<b>95</b>
4.1 Introduction.....	95
4.2 Materials and methods .....	96
4.2.1 Materials .....	96
4.2.2 Sorbent characterization .....	96
4.3 Results and discussion .....	97
4.3.1 X-ray Diffraction .....	97
4.3.2 SEM-EDX.....	102

## TABLE OF CONTENTS (continued)

<u>CHAPTER</u>	<u>PAGE</u>
4.3.3 X-ray Photoelectron Spectroscopy .....	107
4.4 Conclusion .....	112
4.5 Reference .....	113
<b>V. ADSORPTION OF CR(III) AND CR(VI) FROM WATER USING CRYSTALLINE MANGANESE (II, III) OXIDES.....</b>	<b>118</b>
5.1 Introduction.....	118
5.2 Materials and methods.....	121
5.2.1 Chemicals and reagents .....	121
5.2.2 Sorbent characterization .....	121
5.2.3 Batch adsorption experiments.....	123
5.2.4 pH experiments .....	123
5.2.5 Zeta potential measurements .....	124
5.3 Results and discussion .....	125
5.3.1 Adsorption isotherm experiments.....	125
5.3.2 Effect of pH on adsorption .....	132
5.3.3 Effect of surface charge on adsorption .....	137
5.3.4 Surface characterization.....	140
5.5 Conclusion .....	147
5.5 Reference .....	148
<b>VI. SURFACE COMPLEXATION MODELING OF CHROMATE ADSORPTION ON MANGANESE OXIDES.....</b>	<b>155</b>
6.1 Introduction.....	155
6.2 Materials and methods.....	157
6.2.1 Description of SCM model.....	157
6.2.2 Adsorption studies .....	157
6.3 Results and discussion .....	158
6.3.1 Surface complexation modeling .....	159
6.3.2 Reduction modeling.....	163
6.4 Conclusion .....	166
6.5 Reference .....	167
<b>VII. SUSTAINABILITY ASSESSMENT OF DIFFERENT CR(VI) REMOVAL TECHNOLOGIES: ADSORPTION, ION-EXCHANGE, AND REDUCTION-COAGULATION-FILTRATION .....</b>	<b>172</b>
7.1 Introduction.....	172
7.2 Method.....	175

## TABLE OF CONTENTS (continued)

<u>CHAPTER</u>	<u>PAGE</u>
7.2.1 Goal and scope.....	175
7.2.2 Functional unit selection.....	176
7.2.3 Technical design.....	176
7.3 Results and discussion.....	180
7.3.1 LCA inventory.....	180
7.3.2 Environmental sustainability.....	181
7.3.3 Economic sustainability.....	185
7.3.4 Social sustainability.....	186
7.4 Conclusion.....	188
7.5 Reference.....	189
<b>VIII. CONCLUSIONS.....</b>	<b>193</b>
8. Conclusions.....	193
<b>CITED LITERATURE.....</b>	<b>196</b>
<b>APPENDIX.....</b>	<b>226</b>
<b>VITA.....</b>	<b>239</b>

## LIST OF TABLES

<u>TABLE</u>	<u>PAGE</u>
<b>I. INTRODUCTION</b>	
Table 1. 1 Physicochemical properties of chromium .....	1
Table 1. 2 Chromium concentration in earth crust and rocks.....	8
Table 1. 3 Common chromium alloys .....	9
Table 1. 4 Different sources and chromium concentration in water and soil .....	10
Table 1. 5 Adsorption capacity for different activated carbons.....	15
Table 1. 6 Adsorption capacity of hexavalent chromium by different biosorbents.....	16
Table 1. 7 Adsorption capacity of trivalent chromium by different biosorbents.....	17
Table 1. 8 Adsorption capacity of hexavalent chromium by different minerals .....	18
Table 1. 9 Adsorption capacity of trivalent chromium by different minerals .....	18
<b>II. DEVELOPMENT OF MANGANESE-COATED SAND</b>	
Table 2. 1 Adsorption efficiency and manganese content of different manganese sources .....	39
<b>III. ADSORPTION OF CHROMIUM ONTO MANGANESE-COATED SAND: BATCH STUDY</b>	
Table 3. 1 Adsorption parameters for chromium adsorption onto MCS .....	64
Table 3. 2 Adsorption capacity of different metal oxides based adsorbents for Cr(VI).....	66
Table 3. 3 Adsorption capacity of different metal oxides based adsorbents for Cr(III).....	66
Table 3. 4 Adsorption kinetic parameters of chromium on MCS sorbent.....	75

## LIST OF TABLES (continued)

<u>TABLE</u>	<u>PAGE</u>
<b>V. ADSORPTION OF CR(III) AND CR(VI) FROM WATER USING CRYSTALLINE MANGANESE (II, III) OXIDES</b>	
Table 5. 1 Adsorption parameters for adsorption of Cr(III) and Cr(VI) onto the MnO sorbent .....	130
Table 5. 2 Adsorption parameters for adsorption of Cr(III) and Cr(VI) onto the Mn <sub>2</sub> O <sub>3</sub> sorbent.....	130
<b>VI. SURFACE COMPLEXATION MODELING OF CHROMATE ADSORPTION ON MANGANESE OXIDES</b>	
Table 6. 1 The Input Values for TLM model .....	161
Table 6. 2 Stability Constants for TLM model.....	161
<b>VII. SUSTAINABILITY ASSESSMENT OF DIFFERENT CR(VI) REMOVAL TECHONOLOGIES: ADSORPTION, ION-EXCHANGE, AND REDUCTION-COAGULATION-FILTRATION</b>	
Table 7. 1 Design parameters in SBA and Adsorber system.....	179
Table 7. 2 Design parameters in RCF system.....	179
Table 7. 3 LCA inventory of adsorber, ion-exchange and RCF .....	180
Table 7. 4 Overall costs for adsorber, ion-exchange and RCF systems .....	186
Table 7. 5 Social sustainability matrix for adsorber, ion-exchange and RCF systems .....	187

## LIST OF FIGURES

<u>FIGURE</u>	<u>PAGE</u>
<b>I. INTRODUCTION</b>	
Figure 1. 1 The Frost diagram for chromium (Cr) species .....	2
Figure 1. 2 Eh-pH diagram for chromium .....	4
<b>II. DEVELOPMENT OF MANGANESE-COATED SAND</b>	
Figure 2. 1 Comparison of MCS coated with pH adjusted solution and no pH adjusted solution on Cr(VI) removal .....	40
Figure 2. 2 Comparison of MCS coated at different coating temperature on Cr(VI) removal.....	42
Figure 2. 3 Mn concentration in solution after batch adsorption tests with MCS coated at different temperatures.....	42
<b>III. ADSORPTION OF CHROMIUM ONTO MANGANESE-COATED SAND: BATCH STUDY</b>	
Figure 3. 1 The effect of MCS dosage on chromium removal .....	56
Figure 3. 2 Adsorption equilibrium isotherm data for Cr(III) and Cr(VI).....	59
Figure 3. 3 Langmuir isotherm for (a) Cr(III) and (b) Cr(VI) adsorption onto MCS sorbent.....	60
Figure 3. 4 Freundlich isotherm for (a) Cr(III) and (b) Cr(VI) adsorption onto MCS sorbent .....	61
Figure 3. 5 Temkin isotherm for (a) Cr(III) and (b) Cr(VI) adsorption onto MCS sorbent .....	62
Figure 3. 6 D-R isotherm for (a) Cr(III) and (b) Cr(VI) adsorption onto MCS sorbent.....	63
Figure 3. 7 Adsorption of chromium onto MCS as function of pH: (a) Cr(III) and (b) Cr(VI) .....	68
Figure 3. 8 Zeta potential of the MCS sorbent in the presence of Cr(III) and Cr(VI).....	70
Figure 3. 9 Effect of contact time on adsorption of (a) Cr(III) and (b) Cr(VI) onto MCS sorbent .....	72
Figure 3. 10 Pseudo-first order kinetic plots for the sorption of (a) Cr(III) and (b) Cr(VI) .....	76
Figure 3. 11 Pseudo-second order kinetic plots for the sorption of (a) Cr(III) and (b) Cr(VI) .....	77
Figure 3. 12 Intraparticle diffusion kinetic plots for the sorption of (a) Cr(III) and (b) Cr(VI).....	78

## LIST OF FIGURES (continued)

<u>FIGURE</u>	<u>PAGE</u>
Figure 3. 13 Effect of $\text{Ca}^{2+}$ ions on the adsorption of chromium onto MCS.....	81
Figure 3. 14 Effect of $\text{HCO}_3^-$ ions on the adsorption of chromium onto MCS .....	81
Figure 3. 15 Effect of $\text{SO}_4^{2-}$ ions on the adsorption of chromium onto MCS .....	82
Figure 3. 16 Effect of $\text{PO}_4^{3-}$ ions on the adsorption of chromium onto MCS .....	82
Figure 3. 17 Reuse of MCS sorbent in five adsorption cycles .....	83
Figure 3. 18 Effect of different NaOH concentrations on regeneration of MCS sorbent.....	84
 <b>IV. SURFACE CHARACTERIZATION OF MANGANESE-COATED SAND</b>	
Figure 4. 1 XRD pattern of MCS (Temperature = $120^\circ\text{C}$ ).....	98
Figure 4. 2 XRD pattern of MCS (Temperature = $150^\circ\text{C}$ ).....	98
Figure 4. 3 XRD pattern of MCS (Temperature = $180^\circ\text{C}$ ).....	99
Figure 4. 4 XRD pattern of MCS (Temperature = $220^\circ\text{C}$ ).....	99
Figure 4. 5 XRD pattern of MCS (Temperature = $330^\circ\text{C}$ ).....	100
Figure 4. 6 XRD pattern of MCS (Temperature = $440^\circ\text{C}$ ).....	100
Figure 4. 7 XRD pattern of MCS (Temperature = $550^\circ\text{C}$ ).....	101
Figure 4. 8 SEM image of virgin silica sand .....	103
Figure 4. 9 SEM image of MCS overloaded with Cr(III).....	103
Figure 4. 10 EDX mapping analysis of different elements for MCS overloaded with Cr(III).....	104
Figure 4. 11 EDX spectrum of MCS overloaded with Cr(III).....	104
Figure 4. 12 SEM image of MCS overloaded with Cr(VI) .....	106
Figure 4. 13 EDX mapping analysis of different elements for MCS overloaded with Cr(VI).....	106
Figure 4. 14 EDX spectrum of MCS overloaded with Cr(VI) .....	107
Figure 4. 15 XPS spectra of the MCS sorbent coated at different temperatures .....	108

## LIST OF FIGURES (continued)

<u>FIGURE</u>	<u>PAGE</u>
Figure 4. 16 XPS all element spectra of the MCS surface after adsorption of (a) Cr(III) and (b) Cr(VI) .....	110
Figure 4. 17 XPS Cr spectra of the MCS sorbent surface after adsorption of (a) Cr(III) and (b) Cr(VI) .....	111
<b>V. ADSORPTION OF CR(III) AND CR(VI) FROM WATER USING CRYSTALLINE MANGANESE (II, III) OXIDES</b>	
Figure 5. 1 X-ray diffraction pattern of the MnO sorbent .....	122
Figure 5. 2 X-ray diffraction pattern of the Mn <sub>2</sub> O <sub>3</sub> sorbent .....	122
Figure 5. 3 Adsorption isotherm data for chromium: (a) Cr(III) and (b) Cr(VI) onto the MnO sorbent .....	128
Figure 5. 4 Adsorption isotherm data for chromium: (a) Cr(III) and (b) Cr(VI) onto the Mn <sub>2</sub> O <sub>3</sub> sorbent .....	129
Figure 5. 5 Eh-pH diagram for manganese.....	134
Figure 5. 6 Adsorption of chromium onto the MnO sorbent as function of pH: (a) Cr(III) and (b) Cr(VI) .....	135
Figure 5. 7 Adsorption of chromium onto the Mn <sub>2</sub> O <sub>3</sub> sorbent as function of pH: (a) Cr(III) and (b) Cr(VI) .....	136
Figure 5. 8 Zeta potential of the MnO sorbent in the presence of Cr(III) and Cr(VI).....	138
Figure 5. 9 Zeta potential of the Mn <sub>2</sub> O <sub>3</sub> sorbent in the presence of Cr(III) and Cr(VI).....	139
Figure 5. 10 XPS all element spectra of the MnO surface after adsorption of (a) Cr(III) and (b) Cr(VI) .....	143
Figure 5. 11 XPS all element spectra of the Mn <sub>2</sub> O <sub>3</sub> surface after adsorption of (a) Cr(III) and (b) Cr(VI) .....	144
Figure 5. 12 XPS Cr spectra of the MnO sorbent surface after adsorption of (a) Cr(III) and (b) Cr(VI) .....	145

## LIST OF FIGURES (continued)

<u>FIGURE</u>	<u>PAGE</u>
Figure 5. 13 XPS Cr spectra of the Mn <sub>2</sub> O <sub>3</sub> sorbent surface after adsorption of (a) Cr(III) and (b) Cr(VI) .....	146
 <b>VI. SURFACE COMPLEXATION MODELING OF CHROMATE ADSORPTION ON MANGANESE OXIDES</b>	
Figure 6. 1 Different surface planes in SCM models (a) constant capacitance model; (b) diffuse layer model; (c) triple layer model. ....	158
Figure 6. 2 Cr photoemission spectra of Mn <sub>2</sub> O <sub>3</sub> .....	160
Figure 6. 3 (a) Eh-pH diagram of manganese species; (b) Eh-pH diagram of chromium species. ....	162
Figure 6. 4 The experimental and model data of adsorption of at $8 \times 10^{-6}$ M Cr(VI) on Mn <sub>2</sub> O <sub>3</sub> .....	163
Figure 6. 5 Cr photoemission spectra of MnO .....	164
Figure 6. 6 The experimental and model data of adsorption of at $8 \times 10^{-6}$ M Cr(VI) on MnO.....	165
 <b>VII. SUSTAINABILITY ASSESSMENT OF DIFFERENT CR(VI) REMOVAL TECHONOLOGIES: ADSORPTION, ION-EXCHANGE, AND REDUCTION- COAGULATION-FILTRATION</b>	
Figure 7. 1 Chromium(VI) distribution in U.S. tap water .....	173
Figure 7. 2 Block diagram of boundaries of the system under study .....	175
Figure 7. 3 Diagram for an SBA treatment system .....	177
Figure 7. 4 (a)Diagram for an adsorber system; (b)diagram for an RCF system .....	178
Figure 7. 5 Characterization and normalization of environmental impacts using TRACI 2.1 method: adsorption, ion-exchange and RCF system .....	183
Figure 7. 6 Characterization of environmental impacts for adsorption, ion-exchange and RCF systems of different input materials and processes .....	184

## SUMMARY

The removal of chromium from water down to environmentally acceptable levels is required because of the toxicity of this contaminant species. The removal of chromium from water should be achieved in an effective manner using relatively simple and inexpensive technology. Various technologies such as ion exchange, membrane filtration, adsorption and reduction-filtration-precipitation have been employed for removal of chromium from water. Adsorption is considered as a relatively simple and effective technology with low operational cost.

Metal oxides such as manganese oxides have commonly been used as potential adsorbents for the removal of heavy metals. However, the application of pure manganese oxides as viable adsorbents or filter media in a flow-through (adsorber) column system is limited due to the low hydraulic conductivity and extant colloidal form of the pure manganese oxides. Manganese-coated sand (MCS) has exhibited a considerably appreciable adsorption capacity toward several heavy metal species which are present in water as cations or as oxyanions. In this study, we focused on synthesizing and evaluating a novel MCS sorbent with a high hydraulic conductivity as a potential sorbent for removal of two chromium species [Cr(III) and Cr(VI)] from water. In order to investigate the adsorption mechanism and interactions between the two chromium species with the MCS sorbent, we employed several surface characterization techniques to analyze the crystallinity and surface oxides on the surface of the MCS sorbent, surface charge, surface elemental composition and oxidation states of manganese and chromium before and after adsorption. A surface complexation model was developed for the adsorption process based on the experimental adsorption data and surface characterization results. A sustainability assessment was performed to compare the sustainability of the MCS adsorber system with two other technologies used for the removal of chromium from water.

## SUMMARY(continued)

Adsorption of chromium species onto pure manganese oxides was investigated to better understand how the chromium species would interact with the more reduced forms of manganese oxides. The adsorption of Cr(III) and Cr(VI) was evaluated using manganese (II) oxide (MnO) and manganese (III) oxide (Mn<sub>2</sub>O<sub>3</sub>). A similar pattern of zeta potential measurements was observed for adsorption of Cr(III) and Cr(VI) onto the MnO sorbent without a major PZC shift, suggesting the possible reduction of Cr(VI) to Cr(III), which was later confirmed by the X-ray Photoelectron Spectroscopy (XPS) spectra analysis that Cr(VI) was completely reduced to Cr(III) on the surface of the MnO sorbent concomitant with the oxidation of Mn(II) to Mn(III). The appearance of both Cr(III) and Cr(VI) species on the surface of the Mn<sub>2</sub>O<sub>3</sub> sorbent after the adsorption of Cr(III) and Cr(VI) onto the surface of the Mn<sub>2</sub>O<sub>3</sub> sorbent may be attributed to the intermediate oxidation state of manganese (III), enabling manganese (III) oxide to serve as either a reductant or an oxidant for the transformation of chromium species.

The MCS sorbent was developed through the formulation of a coating of manganese (II,III) oxides on the surface of silica sand at a coating temperature of 220C° using manganese sulfate as manganese source without adjusting the pH of the coating solution. The Langmuir and Freundlich adsorption equations displayed favorable adsorption of Cr(III) and Cr(VI) onto the surface of the MCS sorbent, suggesting the adsorption of chromium is a monolayer adsorption on the heterogenous MCS surface. The MCS sorbent exhibited favorable adsorption toward both chromium species over a wide pH range of 3-10. According to the adsorption parameters obtained from four adsorption equations (Langmuir, Freundlich, Temkin, Dubinin–Radushkevich), the MCS sorbent displayed a stronger binding for Cr(VI) than for Cr(III). The significant shift in the point of zero charge (PZC) observed for adsorption of Cr(III) and Cr(VI) onto the surface of the MCS sorbent indicated that specific adsorption would be the main adsorption mechanism. The coexistence of anions (HCO<sub>3</sub><sup>-</sup>, SO<sub>4</sub><sup>2-</sup> and PO<sub>4</sub><sup>3-</sup>) showed no negative impact on the adsorption of Cr(III) onto the surface of the MCS sorbent, while the effect of the anions on the

## SUMMARY(continued)

adsorption of Cr(VI) followed the order:  $\text{PO}_4^{3-} > \text{HCO}_3^- > \text{SO}_4^{2-}$ . The MCS sorbent can be re-used in multiple adsorption cycles, and can be successfully regenerated using 0.01 N NaOH solution without a major loss of adsorption capacity. The X-ray Diffraction (XRD) patterns along with XPS spectra results confirmed that the surface oxides coated onto the MCS were a mixture of manganese (II) oxide and manganese (III) oxide. The Scanning Electron Microscopy coupled with Energy Dispersive X-ray (SEM-EDX) analysis indicated that the MCS sorbent employed in this study has a surface heterogeneity with a non-uniform coating of manganese oxides. Partial reduction or oxidation of Cr(III) and Cr(VI) on the surface of the MCS sorbent can be attributed to manganese (II, III) oxides present on the surface of the MCS sorbent which may act as either a reductant or an oxidant.

The sustainability of the MCS adsorber system was quantified and compared with other commonly used heavy metal removal technologies such as ion-exchange and reduction-filtration-precipitation from environmental, social and economic perspectives. Overall, the MCS adsorber system was determined to be the preferred technology for removal of chromium from water with intermediate environmental impact, lowest economic burden and best social equity.

# CHPATER I

## I. INTRODUCTION

### 1.1 Introduction

Chromium(Cr) is the 21<sup>st</sup> most abundance naturally occurring element in earth's crust with average concentration ranging from 80 mg/kg to 200 mg/kg [1]. It is the 24<sup>th</sup> element on the periodic table between vanadium and manganese and has an atomic mass of 51.996 g/mol. It is a lustrous and brittle metal that shows silver-gray color. Chromium will immediately form a thin oxide layer when it is directly exposed to oxygen. Chromium exists in several oxidation states, ranging from chromium (-II) to chromium (+VI), while it is mostly present in two valence states of trivalent chromium [Cr (III)] and hexavalent chromium [Cr (VI)] in environment [2], [3]. Basic chemical and physical properties are listed in Table 1.1. Cr(III) is not toxic to plants and is an essential nutrient for animals and humans, while Cr(VI) is a potential carcinogen and can pose health threat on human beings [4], [5].

Table 1. 1 Physicochemical properties of chromium

Density (at 20°C)	Melting Point	Boiling point	Vander Waals radius	Ionic radius	Standard potential
7.19g/cm <sup>3</sup>	1907°C	2672°C	0.127nm	0.061nm(+3); 0.044nm(+6)	0.71V(Cr/Cr <sup>3+</sup> )

### 1.2 Environmental chemistry of chromium

Degrees of mobility, toxicity, and bioavailability of chromium species depend on the specific oxidation states [2]. The Cr(III) oxidation state lying lowest in the Frost diagram indicates that Cr(III) is the most stable oxidation state and obtains the lowest standard reaction Gibbs energy (Figure 1.1) in acidic solution [6].

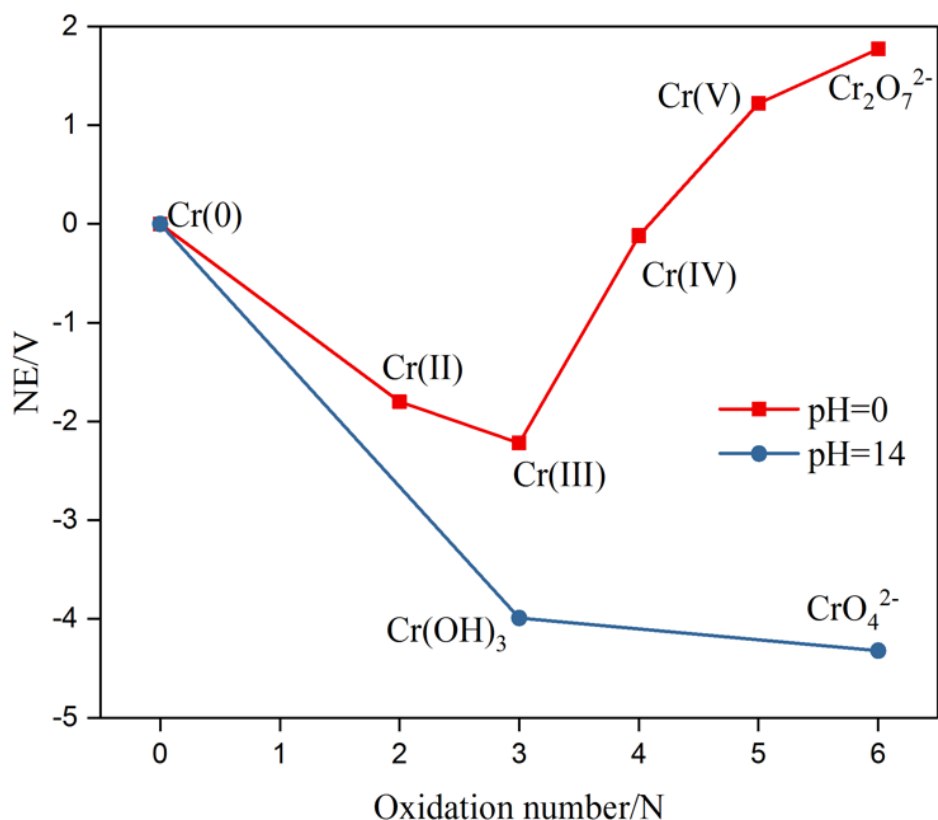


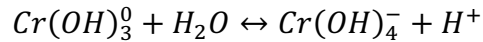
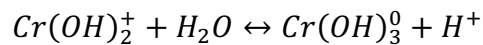
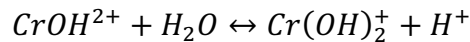
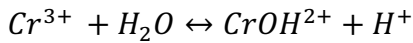
Figure 1. 1 The Frost diagram for chromium (Cr) species

Oxidation states -2, -1, 0, and +1 majorly appears in synthetic organic-chromium compounds such as the chromium carbonyls, chromium bipyridine and organometallic complexes [7]. Cr (0), which occurs in metallic or native chromium, is rarely found in nature. Cr(III) generally occurs either as insoluble chromium oxide(Cr<sub>2</sub>O<sub>3</sub>) and chromium hydroxide [Cr(OH)<sub>3</sub>] or as soluble chromium hydroxide cations. Cr(VI) primarily occurs as soluble chromate(CrO<sub>4</sub><sup>2-</sup>) and dichromate(Cr<sub>2</sub>O<sub>7</sub><sup>2-</sup>) anions. The chemical form of chromium species and equilibria between them in aerated solution are depended on pH and redox potential [8], [9].

### 1.2.1 Cr(III)

Cr(III) generally forms insoluble chromic oxide( $\text{Cr}_2\text{O}_3$ ) from approximately pH 5.0 to 13.5 with approximately Eh from +0.8 to -0.75V (volts). When pH is slightly less than 5.0, it dissolves to soluble chromium hydroxide ( $\text{CrOH}^{2+}$ ). At a pH of greater than 13 with Eh from 0.05 to -0.8V, soluble anion  $\text{CrO}_2^-$  appears (Figure 1.2) [10].

The main Cr(III) species formed in aqueous system are  $\text{Cr}^{3+}$ ,  $\text{Cr}(\text{OH})^{2+}$ ,  $\text{Cr}(\text{OH})_3^0$  and  $\text{Cr}(\text{OH})_4^-$  [11], [12]. The predominant reactions are:

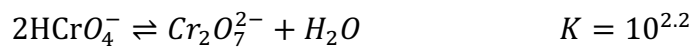


Polymeric species such as  $\text{Cr}_2(\text{OH})_2^{4+}$ ,  $\text{Cr}_3(\text{OH})_4^{5+}$  and  $\text{Cr}_4(\text{OH})_6^{6+}$  can occur due to solution polymerization of Cr(III) hydrolysis species [13], [14]. Low solubility of  $\text{Cr}(\text{OH})_3$  limits aqueous Cr(III) concentration at pH values greater than 5.0. Cr(III) typically behaves as “hard” Lewis acid and readily couple with a variety of ligands: ammonium, cyanide, fluoride and sulfate and natural and synthetic organic ligands containing oxygen, nitrogen or sulphur donor atoms [15]. Strong retention of Cr(III) on soil surface greatly limits its bioavailability and mobility in soils and water.

### 1.2.2 Cr(VI)

In aqueous environment, under oxidized conditions, Cr(VI) is the most thermodynamically stable oxidation state. Cr(VI) species primarily occurs soluble chromate ( $\text{CrO}_4^{2-}$ ) from approximately pH 6.0 to 14.0 with approximately Eh from -0.1V to +0.9V (Figure 1.2) [16]. In the pH between 1 and 6,  $\text{HCrO}_4^-$  is the predominant species until Cr(VI) concentration  $> 10^{-2.1}$  M then dichromate ion ( $\text{Cr}_2\text{O}_7^{2-}$ )

is formed, which is rarely found in natural waters [17].



Cr(VI) exhibits a much greater bioavailability and mobility in natural environment than Cr(III) because of solubility difference. In natural systems, the presence and distribution of different Cr(III) and Cr(VI) species depend on various processes including oxidation/reduction and adsorption/desorption reactions.

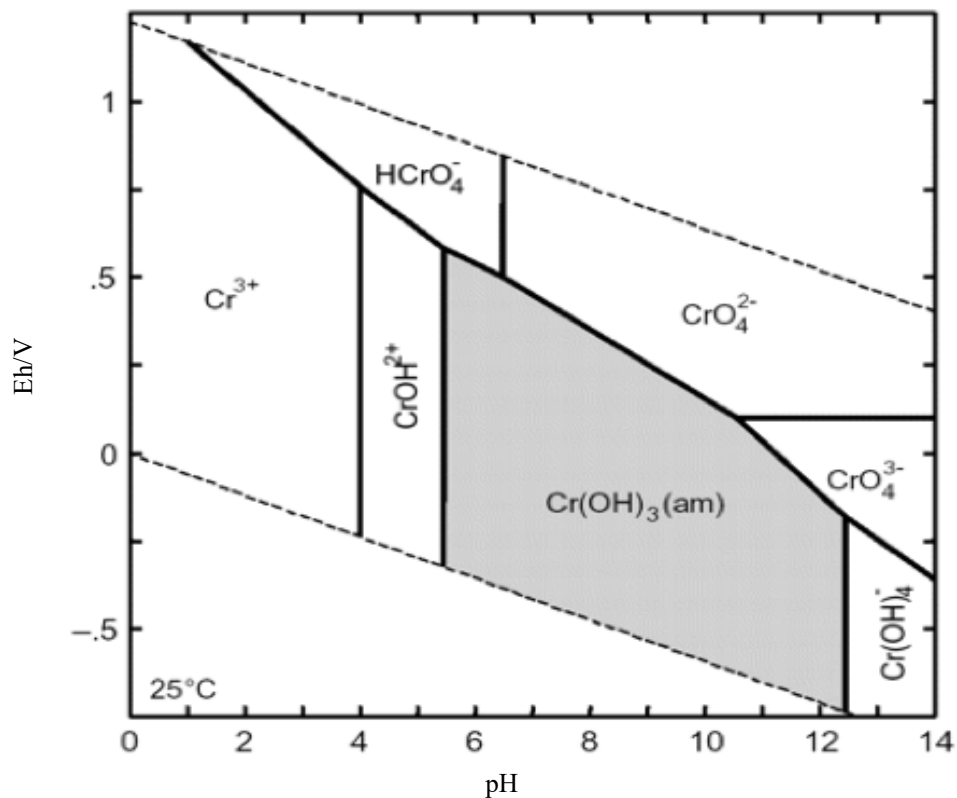


Figure 1. 2 Eh-pH diagram for chromium

### 1.2.3 Oxidation-reduction of chromium

Eh-pH diagram for chromium can provide a generalized distribution of aqueous species and their redox stabilities based on chemical equilibrium. Chromium may undergo changes if the redox conditions are altered in the environment. The redox reactions of Cr(III) and Cr(VI) require another redox couple functioning as electron donor or acceptor. In natural aquatic systems, there are several predominant redox couples including  $\text{H}_2\text{O}/\text{O}_2(\text{aq})$ ,  $\text{Mn(II)}/\text{Mn(IV)}$ ,  $\text{Fe(II)}/\text{Fe(III)}$  and  $\text{CH}_4/\text{CO}_2$  [18].

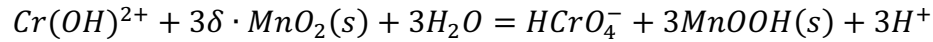
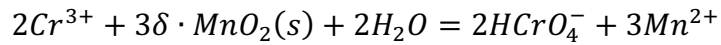
#### 1.2.3.1 Oxidation of Cr(III)

Chromium(VI) is a strong oxidizing agent and the Cr(VI)/Cr(III) couple obtains a relatively high redox potential. There are merely a handful of oxidants existed in natural environments that are capable of oxidizing Cr(III) to Cr(VI) [19]. Dissolved oxygen was found to oxidize Cr(III) into Cr(VI) at a relatively slow rate at room temperature [20]. Therefore, it enables Cr(III) to be involved in faster reactions (sorption or precipitation). Manganese oxides have proven to be responsible for most Cr(III) oxidation in natural systems [21], [22]. Manganese oxides appear in the subsurface as grain coatings, deposits in fractures, or as finely disseminated grains. Bacterial metabolic activities sometimes are in relation with this presence [23]. The reaction rate is likely related to amount, surface area and crystalline structure of manganese oxides. The kinetic of Cr(III) oxidation is initially rapid and then slow down drastically. Direct microscopic and spectroscopic evidence revealed that a new phase of  $\text{Cr(OH)}_3 \cdot n\text{H}_2\text{O}$  precipitate was formed on the Mn surface and then inhibited oxidation [24].

The oxidation reaction between manganese oxides and Cr(III) occurs as three sequential steps:

- (1) Cr(III) is first sorbed onto the activate sites of the  $\text{MnO}_2$  surface,
- (2) Cr(III) is oxidized to Cr(VI) by surface Mn(IV),
- (3) Cr(VI) and Mn(II) are produced by the redox reaction taken place on the surface.

The redox reaction occurred on the MnO<sub>2</sub> surface can be expressed as [19]:



#### 1.2.3.2 Reduction of Cr(VI)

Cr(VI) can be readily reduced to Cr(III) forms in presence of numerous reducing agents commonly found in the environment. Dissolved Fe(II), minerals with Fe(II), sulfides and organic matter appear to be the predominant reductants for chromium species [9], [25], [26]. Dissolved sulfides can be generated from industrial wastes and decomposition of organic matter. Weathering of minerals with Fe(II) and industrial wastes produce dissolved ferrous ion. Eary and Rai [27] discovered that Cr(VI) is reduced by dissolved ferrous ions in seconds and by Fe(II)-containing oxides and silicate minerals in hours to days. The reduction of Cr(VI) by Fe(II) can be expressed as follow:

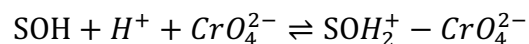


This reaction can be complete in less than 5 min in laboratory studies. In acidic waters, this reduction yields Cr(III) and Fe(III) or Cr(III)/Fe(III) co-precipitates in form of (Cr, Fe)(OH)<sub>3</sub> in groundwater of pH more than 4 [28]. Cr(OH)<sub>3</sub> is probably the end product under neutral to alkaline conditions because of the relatively low solubility of Fe(OH)<sub>3</sub>. There are a diverse and widely distributed group of bacteria capable of reducing iron oxides while oxidizing organic compounds. This metabolic pathway can produce Fe(II) and catalyze the reduction of Cr(VI). The capacity for soils to reduce and immobilize Cr(VI) could improve dramatically by iron respiration [9].

Organic matter high in soils such as amino-acids, humic and fulvic acids can also reduce Cr(VI) to Cr(III) [29]. The reduction was only appreciable in soils of pH less than 3. Intermediate Cr(VI) species are formed and gradually decay into Cr(III).

#### 1.2.4 Adsorption-desorption of chromium

Cr(III) can be readily and specifically adsorbed by Fe and Mn oxides, clay minerals and sand as a cationic metal [22]. The experimental data showed that the adsorption of Cr(III) onto clay minerals and Fe oxides is rapid, with about 90% Cr(III) being adsorbed in 24 hours [30]. The adsorption of Cr(III) increases with pH as the mineral surfaces becomes more negatively charged and decreases with other competing inorganic cations or dissolved organic ligands present [31]. Cr(VI) is generally adsorbed by minerals that obtain positively charged surfaces due to its anionic nature. Mn, Al and Fe oxides and hydroxides that have exposed inorganic hydroxyl groups on their surfaces often are present at significant level in environment [32]. Adsorption of Cr(VI) can be described as a surface complexation reaction between chromate ions and hydroxyl sites on mineral surface [33]:



Cr(VI) adsorption is controlled by the solution pH, surface sites concentration, reaction equilibrium constant and competing anion present.

#### 1.3 Sources of chromium

Chromium(Cr) can be found in various environmental media including surface and ground water, soil and sediments, air and all biota [21]. Chromium enters into the environment via either naturally occurring or anthropogenic pathways.

##### 1.3.1 Natural sources

Chromium (Cr) has been reported as the 21<sup>st</sup> most abundance element in Earth crust. Cr levels average from 5 mg/kg in coal to 20 mg/kg in limestone and to 300 mg/kg in basaltic rock and 2300 mg/kg in ultramafic rock (Table 1.2) [34]. Cr occurs naturally in two minerals: chromite and crocoite. Crocoite is unusual in appearance but rarely found. The chief commercial source of Cr is chromite (FeCr<sub>2</sub>O<sub>4</sub>). The chromite ore found as bands, layers, pods and lenses are mostly in magnesium-rich ultramafic rocks [20]. Cr can be replaced by Mg, Al, Fe and Ca because of their crystallochemical similarity, reducing the Cr

concentration in chromite mineral to about 40%. Chromite is physically refractory and chemically inert. Cr is locked up in immobile Cr(III) state. When the basic anhydrides, such as MgO, FeO, and CaO come in contact with water, they can release their hydroxides to create an alkaline environment [35]. The diuretic alkaline environment at the chromite-water interface in an oxidized chromite-bearing ultramafic rocks indicates the possibility of Cr(III)/Cr(VI) transformation and therefore poses hazards of Cr(VI) contamination to the adjacent water bodies [36]. Mining activities can increase the rate and intensity of the process of mobilization of Cr species. Godgul et al. [37] conducted a combined field and laboratory study on chromite-bearing oxidized serpentinite rocks of Sukinda in Orissa, India. The results of chemical analysis of stream water and hydrolysate incrustation on detrital grains taken from stream beds indicate the possible mobilization of chromium from the chromite ores. Elevation of chromium concentration in groundwater has been detected in Leon Guanajuato Valley, Central-Mexico. Studies showed that ultramafic units and their alteration products obtain highest possibility to liberate chromium into water bodies [38]. Recent and past tectonic and hydrothermal activities have enhanced the process of chromium leaching into water.

Table 1. 2 Chromium concentration in earth crust and rocks

Material	Cr concentration (mg/kg)
Bulk continental crust	126
Upper continental crust	35
Ultramafic rock	2300
Ocean ridge basalt	300
Limestone	5
Coal	20

### 1.3.2 Anthropogenic sources

Chromium is an important industrial metal in a variety of diverse products and process and has been majorly consumed by chemical (15%), metallurgical (67%) and refractory (18%) industries. Metallurgical industry uses Cr as an alloy element to produce a series of alloys including Fe, Ni and Co (Table 1.3) [39]. The primary source of chromium contamination originated in industrial processes such as electroplating, leather tanning operations, pigment manufacturing and textile manufacturing (Table 1.4) [34], [40]–[43]. Cr and other metals are released into soils and ground water by leachate generated from solid waste landfills and mining wastes, seepage from lagoon wastewater treatment system, and leakage from industrial process such as metal plating and wood preserving, whereas emission to the atmosphere is a result of fossil fuel combustion, steel production and stainless steel welding [44].

Table 1. 3 Common chromium alloys

Alloy	Cr Concentration (%)
Low Cr steel	0.5-5
Low Cr iron	0.2-4
Medium Cr steel	3-12
Stainless steel	12-18
Stainless irons	12-15
Cr-Ni-Fe alloys	14-30
Cr-Co alloys	20-35

Table 1. 4 Different sources and chromium concentration in water and soil

Country	Species	Media	Source	Concentration
				(soil mg/kg)
				(water mg/L)
USA (New Jersey)	Cr(total)	Water	Mining	30
USA (New Jersey)	Cr(total)	Soil	Mining	53,000
UK (Glasgow)	Cr(total)	Water	Mining	169
Brazil (Iraja river)	Cr(total)	Sediment	Electroplating	60,000
USA (Oregon)	Cr(total)	Soil	Electroplating	60,000
USA (Oregon)	Cr(VI)	Water	Electroplating	19,000
Poland	Cr(total)	Water	Tannery	1.18
Poland	Cr(total)	Soil	Tannery	5.79

## 1.4 Toxicology of chromium

### 1.4.1 Human nutrient

The role of chromium to maintain normal glucose tolerance in animals was reported almost five decades ago. Improved glucose tolerance by chromium supplementation in human was then reported. The Food and Nutrition Board of the U.S. categorized trivalent chromium as an essential nutrient and the estimated safe and adequate dietary intake for Cr is 50-200 µg/day [45]. The results of several human studies suggested that 1) chromium deficiency can cause insulin resistance. 2) chromium supplementation can alleviate the symptom of insulin resistance triggered by chromium deficiency. 3) chromium deficiency can be a major cause of insulin resistance [46]. Several risk factors of cardiovascular disease, in addition to insulin resistance, can be improved by Cr supplementation. Chromium is an essential microelement for carbohydrate, lipid, and protein metabolism [47]. There still are some uncertainties of specific mechanism.

## 1.4.2 Toxicology

Trivalent chromium is considered as an essential element for humans in moderate intake whereas hexavalent chromium is considered harmful even in small dosage. Hexavalent chromium is classified as a known human carcinogen via inhalation [48]. Cr(VI) generated from anthropogenic and natural sources has relatively high environmental mobility and bioavailability in water bodies compared to Cr(III). Structural similarity of chromate ion, the predominant form of Cr(VI), to sulfate ion allows its easy entry through general sulfate channels [49]. Cellular metabolism of Cr(VI) can cause both oxidative and nonoxidative forms of DNA damage. Occupational exposures to Cr(VI) via inhalation has been extensively studied and consistently been found to increase the cancer risks in respiratory system whereas epidemiological evidence about the carcinogenicity of Cr(VI) via ingestion in humans is limited [50], [51]. Zhang and Li [52] reported that the drinking water heavily contaminated with Cr(VI) that released by chromate ore mining activities in Liaoning Province of China increased mortality from stomach cancers among the rural residents there. Exposure of Cr(VI) in drinking water induced tumors in the alimentary tract in the mouse small intestine. Bioavailability studies suggest that 10-20% of ingested low-dose Cr(VI) escapes human gastric inactivation [48]. The similar structural of chromate ion and sulfate ion allows the chromate ion entry through cell membrane sulfate channel. The biological reduction of Cr(VI) *in vivo* by ascorbate, small thiols and cysteine can produce highly mutagenic chromium species. Cancer-promoting Cr-DNA damage is induced in cells of human digestive system. The primary type of DNA damage is Cr-DNA adducts, which cause mutations and chromosomal breaks [49]. Multispecies and multisite carcinogenicity of Cr(VI) strongly suggest Cr(VI) exposure via oral route by drinking water ingestion is classified as likely to be carcinogenic to humans.

## 1.5 Treatment technologies of chromium

The properties of Cr are highly dependent on the oxidation state of Cr. Cr(VI) species, mainly in forms of oxyanions, are soluble in water and therefore considerably more mobile and accessible than Cr(III) species, mainly in forms of cations, which may easily precipitate by raising the pH. It is

considered as more challenging to remove Cr(VI) species from water. Trivalent chromium is considered as an essential element for humans in moderate intake whereas hexavalent chromium is considered harmful even in small dosage. There are several treatment technologies can be applied to remove Cr(VI) from water discussed as follows.

#### 1.5.1 Reduction

Laboratory and pilot-studies with different electron donors as S, Fe(II) or Fe(0) have demonstrated that there is a high potential of successful removal [53]–[55]. Powell et al. [56] studied the reduction of Cr(VI) by elemental iron and the kinetics and mechanism of Cr(VI) reduction. Experimental data confirmed that Cr(VI) was reduced to Cr(III) by Fe<sup>0</sup> and co-precipitated with iron as Cr<sub>x</sub>Fe<sub>(1-x)</sub>(OH)<sub>3</sub>. The use of zero-valent iron nanoparticles with a diameter of 10-30nm supported on a polymer resin as reductant for hexavalent chromium was reported by Ponder et al. [57]. The supported zero-valent iron can reduced Cr(VI) 7-12 times faster than the same amount of iron powder and reduce Cr(VI) 5 times more than iron filings over the same period of 60 days. Cr(VI) was reduced into Cr(III) while zero-valent iron was oxidized into goethite. Hydrogen sulfide was also proven to be an effective reductant for Cr(VI) [58]. The reduction of Cr(VI) into Cr(III) by chromium reducing bacteria, yeast, and fungi was also extensively studied [59]–[62]. Kang et al. [61] investigated the biosorption of both chromium species onto the cell surface of *Pseudomonas aeruginosa*. Cr(III) ions mainly adsorbed by formation of complexation with the functional groups such as carboxyl and amino groups appeared on the cell surface, while Cr(VI) acted as an electron acceptor and was reduced into Cr(III) on the cell wall.

#### 1.5.2 Ion exchange

The application of ion exchange for heavy metal removal from water or industrial wastewater is well established for its high selectivity and chemical and mechanical stability [63]–[65]. Trivalent chromium species, as cation ions, can be removed through acidic cation exchanger, while hexavalent chromium species, as oxyanions, can be removed through basic anion exchanger. Co-existence of both chromium species in industrial wastewater generally involves two stages for removal of chromium using ion-

exchanger. Cr(III) is first oxidized into Cr(VI) and the wastewater was introduced to a strong base anion exchange column [63]. Sapari et al. [64] employed Amberlite IR-120 as a cation exchanger for Cr(III) removal and Dowex 2-X4 as an anion exchanger for Cr(VI) removal and the results showed that the total removal for both chromium species were achieved. Aliquat 336, a common liquid-liquid extractant, was impregnated onto a strong base ion exchange resin (Amberlite XAD-4) to increase the stability of the ion exchange system. The removal of Cr(VI) was performed on the modified anion exchange resin in a column setting. Aliquat 336 modified Amberlite XAD-4 can be used for five consecutive adsorption cycles without significant removal loss. The existence of chloride ions showed low impact on Cr(VI) removal, while the presence of sulfate ions decreased the removal of Cr(VI) by 14% for this novel solvent modified resin.

### 1.5.3 Membrane filtration

Membrane filtration is another widely used and studied technique for chromium removal due to its simple operation and high flexibility [66]–[70]. A multi-layer ceramic membrane was developed for the removal of trivalent chromium and the results showed a 99% removal of Cr(III) was achieved at the contact time of 1 hour with the initial concentration of 1mg/L [68]. Hexavalent chromium, existing as an oxyanion in aqueous environment, may be removed by anion-exchange membrane. Dzyazko et al. [71] synthesized and investigated a microporous composite ceramic membrane using hydrated zirconium dioxide as effective ion-exchange component for hexavalent chromium removal. The ceramic membrane developed in this study was proven to be permeable to chromate ions at acidic pH and successfully remove Cr(VI) from water. Bohdziewicz [72] studied the removal of Cr(VI) from abyssal water by ultrafiltration process using two different membranes both produced from a non-matted polyacrylonitrile fiber (PAN). The ultrafiltration process can be enhanced by addition of complexing agent (hexadecylpyridine chloride) into the solution. The results showed that the maximum chromium removal efficiency reached at 97.8% when the ratio of chromate to complexing agent is 1:5 and pH of the solution is 6. A combination of ultrafiltration with other removal technologies such as adsorption

and complexation can be effective alternative for improving chromium removal efficiency from water or wastewater.

#### 1.5.4 Adsorption

Adsorption is regarded as a relatively effective and promising technology with low operational and maintenance cost due to the high capacity toward heavy metals and the regenerability of the most adsorbents. Various natural or synthetic materials such as activated carbon, biosorbents and minerals have been considered and evaluated as a potentially cost-effective adsorbent for chromium removal [32], [73]–[76].

##### 1.5.4.1 Activated carbon

Activated carbon is the most studied potential adsorbent for chromium removal from water or wastewater and can be produced from a variety of raw materials. Activated carbon is considered to be an desirable adsorbent material for chromium removal because its properties such as high porosity and surface area can contribute to more active adsorption sites, which is beneficial for adsorption process [77]. The presence of a wide spectrum of functional groups such as carbonyl and hydroxyl groups on the surface of activated carbon can also facilitate the adsorption process. Powder-activated carbon (PAC), granular-activated carbon (GAC), activated carbon fibrous (ACF), and activated carbon clothe (ACC) are the four main types of activated carbon employed in application of water or wastewater treatment [73]. Different raw materials selection and chemical activation process can result in vastly different surface chemical or physical characteristics of activated carbon such as shape, porosity, particle size, surface area and surface functional groups that can be either beneficial or detrimental for chromium removal from water or wastewater [78]–[81]. However, activated carbon is not commonly considered at Cr-contaminated sites, owing to practical considerations. Studies showed that chromium adsorption onto activated carbon is controlled by solution pH and the maximum adsorption capacity generally achieved at extremely acidic level (pH 1-3), which renders chemical pretreatment necessary. There are also activated carbon prepared from other sources such as coconut shell, hazelnut shell and dust coal

[82]–[84].

Table 1. 5 Adsorption capacity for different activated carbons

Activated carbon	Cr uptake (mg/g)	Surface area	pH	Reference
PAC	390.00	1264	2.0	[77]
PAC	145.00	-	2.5-3.0	[85]
GAC	53.19	832	2.0	[86]
ACF	40	-	-	[87]

#### 1.5.4.2 Biosorbents

Biosorbent has been considered to an ideal alternative adsorbent for removal of chromium from water due to its naturally availability, low operational cost and environmental benignity. Various biosorbents such as agricultural waste, chitosan based composite, plants and bacteria biomass have been applied to remove heavy metals [88]–[91].

Agricultural and industrial wastes such as saw dust, straw, grape fruit peelings and waste fertilizer slurry were studied as possible inexpensive biosorbents for chromium decontamination. Saha et al. [92] reported chromium removal from contaminated water using devil tree saw dust. The maximum uptake of chromium (333.33mg/g) achieved at extreme acid environment of pH 2.0 and the adsorption can be better described by pseudo-first-order kinetics. Sorghum straw, oats straw and agave bagasse were also explored for chromium removal [93]. Agave bagasse exhibited the highest adsorption capacity towards chromium among these three agro-waste biosorbents. The functional groups of carboxyl and hydroxyl groups commonly existed in agro-waste materials were the major chromium-binding sites and the possible mechanisms of chromium adsorption onto agriculture waste were ion exchange and complexation [92]–[95]. Chitosan, a product of deacetylation of chitin, has been intensively investigated and identified as a superior adsorbent for heavy metal removal [96]. In order to facilitate the

commercialization of the chitosan based sorbent, the attempts have been made to modify and improve the chitosan sorbent by developing chitosan composite biosorbents. Kumar et al. [97] investigated chromium removal from industrial wastewater by cellulose-montmorillonite composite material and their results showed that this biopolymer composite was effective for chromium adsorption. The maximum adsorption capacity was found to be 22.2mg/g at pH 5.0 and the adsorption process followed the second order kinetics. Boddu et al. [89] developed and characterized an alumina supported chitosan sorbent for treatment of chromium in wastewater. The maximum adsorption capacity was obtained by fitting the adsorption equilibrium data to Langmuir isotherm model as 153.85 mg/g. The chromium adsorption by chitosan coated with poly 3-methyl thiophene for chromium removal was studied as a function of contact time, initial chromium concentration, adsorbent dosage, pH and temperature[98]. The optimum adsorption pH was determined to be pH 2.0 and the higher temperature enhanced the chromium adsorption process. Chitosan coated with poly 3-methyl thiophene can be successfully regenerated using 0.01 M NaOH without significant loss of sorption capacity. Table 1.6 and 1.7 summarized adsorption capacity of chromium by a series of biosorbents.

Table 1. 6 Adsorption capacity of hexavalent chromium by different biosorbents

Adsorbent	pH	Initial concentration (mg/L)	Adsorbent dosage (g/L)	Adsorption isotherm model used	Adsorption capacity (mg/g)	Ref.
Cellulose-clay composite	5	20	20	Langmuir	22.2	[97]
Devil tree saw dust	2	400	20	Langmuir	333.33	[92]
Seaweed	2	650	4	Langmuir	38	[94]
Alumina supported chitosan	4	1200	10	Langmuir	153.8	[89]
Grapefruit peelings	5.5	35	24	Langmuir	39.0628	[91]
Chitosan coated with poly 3-methyl thiophene polymer	2	200	1	Langmuir	99.02	[98]

Table 1. 7 Adsorption capacity of trivalent chromium by different biosorbents

Adsorbent	pH	Initial concentration (mg/L)	Adsorbent dosage (g/L)	Adsorption isotherm model used	Adsorption capacity (mg/g)	Ref.
Sorghum straw	4	100	1	Langmuir	6.96	[93]
Oats straw	4	100	1	Langmuir	12.97	[93]
Agava bagasse	4	100	1	Langmuir	11.44	[93]
Seaweed	4	650	4	Langmuir	40	[94]

#### 1.5.4.3 Minerals

Natural or modified minerals have gained excessive attention for removal of heavy metals in aqueous environment because of its ubiquitous appearance in the environment and economic feasibility [99]. Natural minerals such as diatomite, dolomite, bentonite and vermiculite have been proven to be effective adsorbents for chromium species [100]–[103].

Natural clay minerals including bentonite, vermiculite and montmorillonite are vastly employed as an effective adsorbent for the treatment of heavy metals in water body [103], [104]. Khan et al. [102] evaluated bentonite as a possible sorbent for the removal of chromium (III), chromium (VI) and silver (I) from industrial waste water. The adsorption mean energy (E) obtained from Dubinin-Radushkevich (D-R) isotherm equation was indicative of the mechanism of Cr(VI) adsorption onto bentonite was through ion-exchange process, while the adsorption of Cr(III) and Ag(I) did not fit the D-R equation. The optimum pH for adsorption processes were selected as 6.5 for Ag(I), 3.5 for Cr(III) and 2.0 for Cr(VI). They also discovered that the adsorption of Cr(III) and Ag(I) were favored at lower temperature, whereas the adsorption of Cr(VI) was favored at higher temperature. El-Bayaa et al. [103] assessed the effect of ion strength on the adsorption of copper and chromium onto vermiculite. The studied vermiculite exhibited higher adsorption capacity towards Cr(III) than Cu(II) and this preferential adsorption can be attributed to that Cr(III) obtains a larger charge and smaller ion radius resulting in greater accessibility to the active adsorption sites. Dolomite is another potential low-cost sorbent for

chromium removal from wastewater stream [101]. Batch adsorption tests have been carried out at different contact time and temperature to study the kinetics and thermodynamics of chromium adsorption onto dolomite. The experimental data showed that this adsorption process can be better explained by pseudo first-order kinetic model and the sorption of chromium is exothermic in nature. The application of negative-charged mineral for Cr(VI) removal is limited due to the possible electrostatic repulsion between the negative-charged surface and anionic chromate. Modifying mineral with cationic surfactant provides an alternative approach to circumvent this limitation. Montmorillonite modified by cetylpyridinium bromide was investigated for removal of hexavalent chromium from water as a function of pH and contact time [105]. The results showed that modified montmorillonite was effective over a wide pH range and the adsorption equilibrium data can be best described by Langmuir isotherm. Adsorption capacity for chromium using different minerals were summarized in Table 1.8 and 1.9.

Table 1. 8 Adsorption capacity of hexavalent chromium by different minerals

Adsorbent	pH	Initial concentration (mg/L)	Adsorbent dosage (g/L)	Surface area (m <sup>2</sup> /g)	Adsorption capacity (mg/g)	Ref.
Modified kaolinite	4	20	10	7.02	27.8	[106]
Modified montmorillonite	4.5	150	10	10	18.05	[105]
Maghemite nanoparticles	4	0.5	1.5	73.8	10.01	[107]
Dolomite	2	50	1	4.63	40	[101]

Table 1. 9 Adsorption capacity of trivalent chromium by different minerals

Adsorbent	pH	Initial concentration (mg/L)	Adsorbent dosage (g/L)	Surface area (m <sup>2</sup> /g)	Adsorption capacity (mg/g)	Ref.
Vermiculite	4	200	1.25	8.257	46.948	[103]
Bentonite	3.5	15.6	50	34	20.8	[102]
Clay mineral	2.6	520	2.5	16	24.96	[108]
Bentonite clay	2.5	200	10	46.61	49.75	[104]

## 1.2 Research objectives

Metal oxides such as iron oxides and manganese oxides have been commonly used as effective adsorbents of heavy metals. The heavy metal species can be adsorbed through electrostatic forces or formation of surface complexes or reduction followed by precipitation on the metal oxides [109]–[114]. Nevertheless, the application of pure manganese oxides as viable adsorbents or filter media in a column setting is limited due to that manganese oxides have relatively low hydraulic conductivity and generally exist in colloidal form or nonmaterial form resulting in difficult separation from water body after use [115]. Therefore, manganese oxides have been coated onto various supporting medias such as zeolite, bentonite, alumina and silica sand to improve the mechanical stability [16], [22]–[24]. Manganese-coated sand (MCS) has been used for removal of a variety of heavy metals either in the formats of cations such as lead ( $\text{Pb}^{2+}$ ), copper ( $\text{Cu}^{2+}$ ), zinc ( $\text{Zn}^{2+}$ ) or in the formats of oxyanions such as arsenic ( $\text{H}_2\text{AsO}_3^-$ ) and uranium [ $\text{UO}_2(\text{CO}_3)_2^{2-}$ ] and has the potential to be an effective adsorbent for the removal of chromium from water [115], [119]–[122]. Modifying the procedure of synthesizing the manganese oxide coated sand to get a re-usable and re-generable sorbent is another focus of this project. In this research project, we plan to synthesize the MCS sorbent as an efficient, applicable and inexpensive sorbent for removal of chromium from water and then investigate the interactions between chromium species with manganese oxide at solid/solution interfaces.

### 1.2.1 Adsorption capacity and adsorption mechanism

The adsorption of chromium from water onto the MCS sorbent will be evaluated as function of sorbent dosage, time, solution ionic strength and co-existing ions, and solution pH. The (batch) adsorption capacity will be determined by performing adsorption equilibrium isotherm experiments. The adsorption mechanism will be investigated by performing adsorption kinetics experiments, surface charge analysis, evaluation of adsorption equations, determination of surface oxides, the effect of pH, and possible other

factors. The potential for the re-use of the MCS sorbent will be determined after the regeneration of the spent MCS sorbent.

### 1.2.2 Adsorbent characterization

The MCS will be characterized in terms of its material matrix, manganese content, surface area, crystallinity and oxide constituents, surface elemental composition, surface oxide (groups) and surface charge. The surface area will be determined using BET surface area analyzer. The crystallinity (and oxide constituents) and particle size/clusters will be determined using X-ray Diffraction (XRD). The surface elemental composition will be determined using Scanning Electron Microscope (SEM) coupled with Electron Dispersive Spectroscopy (EDS). The surface manganese oxides will be investigated using X-ray Photoelectron Spectroscopy (XPS). The surface charge will be determined by the measurement of the zeta-potential.

### 1.2.3 Geochemical modeling

The adsorption of chromium species onto the MCS sorbent will be evaluated with respect to the interaction of chromium species with the solution/sorbent interface. The predominance and stability of the major chromium species in the solution will be determined by geochemical modeling using the “Geochemist Work Bench” and “Visual MINTEQ”.

### 1.2.4 Adsorption system/adsorber sustainability analysis

The MCS adsorption treatment technology for the removal of Cr(VI) will be assessed by a life cycle analysis (LCA) using SimaPro with comparison to two other Cr(VI) removal technologies. The treatment system is divided into two main processes: upstream processes (adsorber construction) and operation processes (operation and maintenance). Materials and energy inputs, such as electricity and chemicals, are calculated based on technical design parameters and functional unit. In this way, an inventory of materials and energy of construction and operation phases are developed for the MCS adsorber system.

The environmental impact assessment will be evaluated using TRACI method. TRACI, the tool for the Reduction and Assessment of Chemical and Other Environmental Impacts, is a database developed for North America. The capital costs including equipment, construction, professional services and discharge fees and annual operational & maintenance costs including chemicals, labor, energy, and analytical cost will be estimated. Moreover, social impacts of three technologies will be evaluated using comprehensive indicators over the different life stages.

### 1.3 Reference

- [1] J. Barnhart, "Occurrences, uses, and properties of chromium," *Regul. Toxicol. Pharmacol.*, vol. 26, no. 1, pp. S3–S7, Aug. 1997, doi: 10.1006/rtph.1997.1132.
- [2] J. Kotaś and Z. Stasicka, "Chromium occurrence in the environment and methods of its speciation," *Environ. Pollut.*, vol. 107, no. 3, pp. 263–283, Mar. 2000, doi: 10.1016/S0269-7491(99)00168-2.
- [3] R. E. Cranston and J. W. Murray, "The determination of chromium species in natural waters," *Anal. Chim. Acta*, vol. 99, no. 2, pp. 275–282, Aug. 1978, doi: 10.1016/S0003-2670(01)83568-6.
- [4] S. A. Katz and H. Salem, "The toxicology of chromium with respect to its chemical speciation: A review," *J. Appl. Toxicol.*, vol. 13, no. 3, pp. 217–224, May 1993, doi: 10.1002/jat.2550130314.
- [5] I. Moffat, N. Martinova, C. Seidel, and C. M. Thompson, "Hexavalent chromium in drinking water," *J. - AWWA*, vol. 110, no. 5, pp. E22–E35, Apr. 2018, doi: 10.1002/awwa.1044.
- [6] S. E. Fendorf, "Surface reactions of chromium in soils and waters," *Geoderma*, vol. 67, no. 1–2, pp. 55–71, Jun. 1995, doi: 10.1016/0016-7061(94)00062-F.
- [7] F. M. G. Tack and M. G. Verloo, "Chemical speciation and fractionation in soil and sediment heavy metal analysis: A review," *Int. J. Environ. Anal. Chem.*, vol. 59, no. 2–4, pp. 225–238, Apr. 1995, doi: 10.1080/03067319508041330.
- [8] D. C. Schroeder and G. F. Lee, "Potential transformations of chromium in natural waters," *Water. Air. Soil Pollut.*, vol. 4, no. 3, pp. 355–365, Sep. 1975, doi: 10.1007/BF00280721.
- [9] S. E. Fendorf and G. Li, "Kinetics of chromate reduction by ferrous iron," *Environ. Sci. Technol.*, vol. 30, no. 5, pp. 1614–1617, Jan. 1996, doi: 10.1021/es950618m.
- [10] P. M. Jardine, S. E. Fendorf, M. A. Mayes, I. L. Larsen, S. C. Brooks, and W. B. Bailey, "Fate and transport of hexavalent chromium in undisturbed heterogeneous soil," *Environ. Sci. Technol.*, vol. 33, no. 17, pp. 2939–2944, Sep. 1999, doi: 10.1021/es981211v.
- [11] F. Y. Salem, T. F. Parkerton, R. V. Lewis, J. H. Huang, and K. L. Dickson, "Kinetics of chromium transformations in the environment," *Sci. Total Environ.*, vol. 86, no. 1, pp. 25–41, Oct. 1989, doi: 10.1016/0048-9697(89)90190-3.

- [12] W. Cui *et al.*, “Cr(III) adsorption by cluster formation on boehmite nanoplates in highly alkaline solution,” *Environ. Sci. Technol.*, vol. 53, no. 18, pp. 11043–11055, Sep. 2019, doi: 10.1021/acs.est.9b02693.
- [13] C. Oze, D. K. Bird, and S. Fendorf, “Genesis of hexavalent chromium from natural sources in soil and groundwater,” *Proc. Natl. Acad. Sci.*, vol. 104, no. 16, pp. 6544–6549, Apr. 2007, doi: 10.1073/pnas.0701085104.
- [14] S. Egodawatte, A. Datt, E. A. Burns, and S. C. Larsen, “Chemical insight into the adsorption of chromium(III) on iron oxide/mesoporous silica nanocomposites,” *Langmuir*, vol. 31, no. 27, pp. 7553–7562, Jul. 2015, doi: 10.1021/acs.langmuir.5b01483.
- [15] M. Tuzen and M. Soylak, “Multiwalled carbon nanotubes for speciation of chromium in environmental samples,” *J. Hazard. Mater.*, vol. 147, no. 1, pp. 219–225, Aug. 2007, doi: 10.1016/j.jhazmat.2006.12.069.
- [16] Y. Li *et al.*, “Hexavalent chromium removal from aqueous solution by adsorption on aluminum magnesium mixed hydroxide,” *Water Res.*, vol. 43, no. 12, pp. 3067–3075, Jul. 2009, doi: 10.1016/j.watres.2009.04.008.
- [17] F. C. Richard and A. C. M. Bourg, “Aqueous geochemistry of chromium: A review,” *Water Res.*, vol. 25, no. 7, pp. 807–816, Jul. 1991, doi: 10.1016/0043-1354(91)90160-R.
- [18] A. C. M. Bourg and J. P. G. Loch, “Mobilization of heavy metals as affected by pH and redox conditions,” in *Biogeochemistry of Pollutants in Soils and Sediments: Risk Assessment of Delayed and Non-Linear Responses*, W. Salomons and W. M. Stigliani, Eds. Berlin, Heidelberg: Springer, 1995, pp. 87–102.
- [19] M. L. Peterson, G. E. Brown, G. A. Parks, and C. L. Stein, “Differential redox and sorption of Cr (III/VI) on natural silicate and oxide minerals: EXAFS and XANES results,” *Geochim. Cosmochim. Acta*, vol. 61, no. 16, pp. 3399–3412, Aug. 1997, doi: 10.1016/S0016-7037(97)00165-8.

- [20] G. Choppala, N. Bolan, and J. H. Park, "Chromium contamination and its risk management in complex environmental settings," in *Advances in Agronomy*, vol. 120, Elsevier, 2013, pp. 129–172.
- [21] J. Gorny, G. Billon, C. Noiriél, D. Dumoulin, L. Lesven, and B. Madé, "Chromium behavior in aquatic environments: a review," *Environ. Rev.*, vol. 24, no. 4, pp. 503–516, Dec. 2016, doi: 10.1139/er-2016-0012.
- [22] J. Wu, J. Zhang, and C. Xiao, "Focus on factors affecting pH, flow of Cr and transformation between Cr(VI) and Cr(III) in the soil with different electrolytes," *Electrochimica Acta*, vol. 211, pp. 652–662, Sep. 2016, doi: 10.1016/j.electacta.2016.06.048.
- [23] J. E. Johnson, S. M. Webb, C. Ma, and W. W. Fischer, "Manganese mineralogy and diagenesis in the sedimentary rock record," *Geochim. Cosmochim. Acta*, vol. 173, pp. 210–231, Jan. 2016, doi: 10.1016/j.gca.2015.10.027.
- [24] X. H. Feng, L. M. Zhai, W. F. Tan, W. Zhao, F. Liu, and J. Z. He, "The controlling effect of pH on oxidation of Cr(III) by manganese oxide minerals," *J. Colloid Interface Sci.*, vol. 298, no. 1, pp. 258–266, Jun. 2006, doi: 10.1016/j.jcis.2005.12.012.
- [25] I. J. Buerge and S. J. Hug, "Kinetics and pH Dependence of Chromium(VI) Reduction by Iron(II)," *Environ. Sci. Technol.*, vol. 31, no. 5, pp. 1426–1432, May 1997, doi: 10.1021/es960672i.
- [26] L. Di Palma, M. T. Gueye, and E. Petrucci, "Hexavalent chromium reduction in contaminated soil: A comparison between ferrous sulphate and nanoscale zero-valent iron," *J. Hazard. Mater.*, vol. 281, pp. 70–76, Jan. 2015, doi: 10.1016/j.jhazmat.2014.07.058.
- [27] L. E. Eary and Dhanpat. Rai, "Chromate removal from aqueous wastes by reduction with ferrous ion," *Environ. Sci. Technol.*, vol. 22, no. 8, pp. 972–977, Aug. 1988, doi: 10.1021/es00173a018.
- [28] J. D. Hem, "Reactions of metal ions at surfaces of hydrous iron oxide," *Geochim. Cosmochim. Acta*, vol. 41, no. 4, pp. 527–538, Apr. 1977, doi: 10.1016/0016-7037(77)90290-3.

- [29] H.-B. Kim, J.-G. Kim, S.-H. Kim, E. E. Kwon, and K. Baek, "Consecutive reduction of Cr(VI) by Fe(II) formed through photo-reaction of iron-dissolved organic matter originated from biochar," *Environ. Pollut.*, vol. 253, pp. 231–238, Oct. 2019, doi: 10.1016/j.envpol.2019.07.026.
- [30] K. H. Shah *et al.*, "Native and magnetic oxide nanoparticles (Fe<sub>3</sub>O<sub>4</sub>) impregnated bentonite clays as economic adsorbents for Cr(III) removal," *J. Solut. Chem.*, vol. 48, no. 11, pp. 1640–1656, Dec. 2019, doi: 10.1007/s10953-019-00912-z.
- [31] R. A. Griffin, A. K. Au, and R. R. Frost, "Effect of pH on adsorption of chromium from landfill-leachate by clay minerals," *J. Environ. Sci. Health Part Environ. Sci. Eng.*, vol. 12, no. 8, pp. 431–449, Jan. 1977, doi: 10.1080/10934527709374769.
- [32] M. Hua, S. Zhang, B. Pan, W. Zhang, L. Lv, and Q. Zhang, "Heavy metal removal from water/wastewater by nanosized metal oxides: A review," *J. Hazard. Mater.*, vol. 211–212, pp. 317–331, Apr. 2012, doi: 10.1016/j.jhazmat.2011.10.016.
- [33] K. Mesuere and W. Fish, "Chromate and oxalate adsorption on goethite. 2. Surface complexation modeling of competitive adsorption," *Environ. Sci. Technol.*, vol. 26, no. 12, pp. 2365–2370, Dec. 1992, doi: 10.1021/es00036a005.
- [34] A. B. Mukherjee, "Chromium in the environment of Finland," *Sci. Total Environ.*, vol. 217, no. 1, pp. 9–19, Jun. 1998, doi: 10.1016/S0048-9697(98)00163-6.
- [35] B. M. Sass and D. Rai, "Solubility of amorphous chromium(III)-iron(III) hydroxide solid solutions," *Inorg. Chem.*, vol. 26, no. 14, pp. 2228–2232, Jul. 1987, doi: 10.1021/ic00261a013.
- [36] R. Mattuck and N. P. Nikolaidis, "Chromium mobility in freshwater wetlands," *J. Contam. Hydrol.*, vol. 23, no. 3, pp. 213–232, Jul. 1996, doi: 10.1016/0169-7722(95)00097-6.
- [37] G. Godgul and K. C. Sahu, "Chromium contamination from chromite mine," *Environ. Geol.*, vol. 25, no. 4, pp. 251–257, Jun. 1995, doi: 10.1007/BF00766754.
- [38] J. Robles-Camacho and M. A. Armienta, "Natural chromium contamination of groundwater at León Valley, México," *J. Geochem. Explor.*, vol. 68, no. 3, pp. 167–181, Apr. 2000, doi: 10.1016/S0375-6742(99)00083-7.

- [39] R. Saha, R. Nandi, and B. Saha, "Sources and toxicity of hexavalent chromium," *J. Coord. Chem.*, vol. 64, no. 10, pp. 1782–1806, May 2011, doi: 10.1080/00958972.2011.583646.
- [40] Burke T, Fagliano J, Goldoft M, Hazen R E, Iglewicz R, and McKee T, "Chromite ore processing residue in Hudson County, New Jersey.," *Environ. Health Perspect.*, vol. 92, pp. 131–137, May 1991, doi: 10.1289/ehp.9192131.
- [41] C. P. Jordão, J. L. Pereira, and G. N. Jham, "Chromium contamination in sediment, vegetation and fish caused by tanneries in the State of Minas Gerais, Brazil," *Sci. Total Environ.*, vol. 207, no. 1, pp. 1–11, Nov. 1997, doi: 10.1016/S0048-9697(97)00232-5.
- [42] S. G. Sturges, P. McBeth, and R. C. Pratt, "Performance of soil flushing and groundwater extraction at the United Chrome Superfund site," *J. Hazard. Mater.*, vol. 29, no. 1, pp. 59–78, Dec. 1991, doi: 10.1016/0304-3894(91)87074-C.
- [43] Z. Stępniewska and K. Bucior, "Chromium contamination of soils, waters, and plants in the vicinity of a tannery waste lagoon," *Environ. Geochem. Health*, vol. 23, no. 3, pp. 241–245, Sep. 2001, doi: 10.1023/A:1012247230682.
- [44] A. Zahoor and A. Rehman, "Isolation of Cr(VI) reducing bacteria from industrial effluents and their potential use in bioremediation of chromium containing wastewater," *J. Environ. Sci.*, vol. 21, no. 6, pp. 814–820, Jan. 2009, doi: 10.1016/S1001-0742(08)62346-3.
- [45] W. Mertz, "Chromium in human nutrition: A review," *J. Nutr.*, vol. 123, no. 4, pp. 626–633, Apr. 1993, doi: 10.1093/jn/123.4.626.
- [46] R. A. Anderson, "Chromium as an essential nutrient for humans," *Regul. Toxicol. Pharmacol.*, vol. 26, no. 1, pp. S35–S41, Aug. 1997, doi: 10.1006/rtph.1997.1136.
- [47] A. Zhitkovich, "Importance of chromium–DNA adducts in mutagenicity and toxicity of chromium(VI)," *Chem. Res. Toxicol.*, vol. 18, no. 1, pp. 3–11, Jan. 2005, doi: 10.1021/tx049774+.
- [48] C.-H. Tseng, C. Lei, and Y.-C. Chen, "Evaluating the health costs of oral hexavalent chromium exposure from water pollution: A case study in Taiwan," *J. Clean. Prod.*, vol. 172, pp. 819–826, Jan. 2018, doi: 10.1016/j.jclepro.2017.10.177.

- [49] G. Quievryn, E. Peterson, J. Messer, and A. Zhitkovich, "Genotoxicity and mutagenicity of chromium(VI)/ascorbate-generated DNA adducts in human and bacterial cells," *Biochemistry*, vol. 42, no. 4, pp. 1062–1070, Feb. 2003, doi: 10.1021/bi0271547.
- [50] G. Quievryn, J. Messer, and A. Zhitkovich, "Carcinogenic chromium(VI) induces cross-linking of vitamin C to DNA in vitro and in human lung A549 cells," *Biochemistry*, vol. 41, no. 9, pp. 3156–3167, Mar. 2002, doi: 10.1021/bi011942z.
- [51] P. A. Lay and A. Levina, "Activation of molecular oxygen during the reactions of chromium(VI/V/IV) with biological reductants: Implications for chromium-induced genotoxicities<sup>1</sup>," *J. Am. Chem. Soc.*, vol. 120, no. 27, pp. 6704–6714, Jun. 1998, doi: 10.1021/ja974240z.
- [52] J. D. Zhang and X. L. Li, "Chromium pollution of soil and water in Jinzhou," *Zhonghua Yu Fang Yi Xue Za Zhi*, vol. 21, no. 5, pp. 262–264, Sep. 1987.
- [53] C. E. Barrera-Díaz, V. Lugo-Lugo, and B. Bilyeu, "A review of chemical, electrochemical and biological methods for aqueous Cr(VI) reduction," *J. Hazard. Mater.*, vol. 223–224, pp. 1–12, Jul. 2012, doi: 10.1016/j.jhazmat.2012.04.054.
- [54] M. J. Alowitz and M. M. Scherer, "Kinetics of nitrate, nitrite, and Cr(VI) reduction by iron metal," *Environ. Sci. Technol.*, vol. 36, no. 3, pp. 299–306, Feb. 2002, doi: 10.1021/es011000h.
- [55] J. B. Fein, D. A. Fowle, J. Cahill, K. Kemner, M. Boyanov, and B. Bunker, "Nonmetabolic reduction of Cr(VI) by bacterial surfaces under nutrient-absent conditions," *Geomicrobiol. J.*, vol. 19, no. 3, pp. 369–382, May 2002, doi: 10.1080/01490450290098423.
- [56] R. M. Powell, R. W. Puls, S. K. Hightower, and D. A. Sabatini, "Coupled iron corrosion and chromate reduction: Mechanisms for subsurface remediation," *Environ. Sci. Technol.*, vol. 29, no. 8, pp. 1913–1922, Aug. 1995, doi: 10.1021/es00008a008.
- [57] S. M. Ponder, J. G. Darab, and T. E. Mallouk, "Remediation of Cr(VI) and Pb(II) aqueous solutions using supported, nanoscale zero-valent iron," *Environ. Sci. Technol.*, vol. 34, no. 12, pp. 2564–2569, Jun. 2000, doi: 10.1021/es9911420.

- [58] X. Cheng *et al.*, “Electrochemical behaviour of chromium in acid solutions with H<sub>2</sub>S,” *Corros. Sci.*, vol. 41, no. 4, pp. 773–788, Apr. 1999, doi: 10.1016/S0010-938X(98)00150-4.
- [59] H. Shen and Y. T. Wang, “Characterization of enzymatic reduction of hexavalent chromium by *Escherichia coli* ATCC 33456,” *Appl. Environ. Microbiol.*, vol. 59, no. 11, pp. 3771–3777, Nov. 1993.
- [60] C. Cervantes *et al.*, “Interactions of chromium with microorganisms and plants,” *FEMS Microbiol. Rev.*, vol. 25, no. 3, pp. 335–347, May 2001, doi: 10.1111/j.1574-6976.2001.tb00581.x.
- [61] S.-Y. Kang, J.-U. Lee, and K.-W. Kim, “Biosorption of Cr(III) and Cr(VI) onto the cell surface of *Pseudomonas aeruginosa*,” *Biochem. Eng. J.*, vol. 36, no. 1, pp. 54–58, Aug. 2007, doi: 10.1016/j.bej.2006.06.005.
- [62] M. X. Loukidou, A. I. Zouboulis, T. D. Karapantsios, and K. A. Matis, “Equilibrium and kinetic modeling of chromium(VI) biosorption by *Aeromonas caviae*,” *Colloids Surf. Physicochem. Eng. Asp.*, vol. 242, no. 1–3, pp. 93–104, Aug. 2004, doi: 10.1016/j.colsurfa.2004.03.030.
- [63] N. Sapari, A. Idris, and N. H. Ab. Hamid, “Total removal of heavy metal from mixed plating rinse wastewater,” *Desalination*, vol. 106, no. 1, pp. 419–422, Aug. 1996, doi: 10.1016/S0011-9164(96)00139-7.
- [64] S. H. Lin and C. D. Kiang, “Chromic acid recovery from waste acid solution by an ion exchange process: equilibrium and column ion exchange modeling,” *Chem. Eng. J.*, vol. 92, no. 1, pp. 193–199, Apr. 2003, doi: 10.1016/S1385-8947(02)00140-7.
- [65] N. Kabay *et al.*, “Packed column study of the sorption of hexavalent chromium by novel solvent impregnated resins containing aliquat 336: Effect of chloride and sulfate ions,” *React. Funct. Polym.*, vol. 64, no. 2, pp. 75–82, Aug. 2005, doi: 10.1016/j.reactfunctpolym.2005.05.002.
- [66] J. Sánchez and B. L. Rivas, “Cationic hydrophilic polymers coupled to ultrafiltration membranes to remove chromium (VI) from aqueous solution,” *Desalination*, vol. 279, no. 1, pp. 338–343, Sep. 2011, doi: 10.1016/j.desal.2011.06.029.

- [67] S. Nosrati, N. S. Jayakumar, and M. A. Hashim, "Extraction performance of chromium (VI) with emulsion liquid membrane by Cyanex 923 as carrier using response surface methodology," *Desalination*, vol. 266, no. 1, pp. 286–290, Jan. 2011, doi: 10.1016/j.desal.2010.08.023.
- [68] M. Soylak, U. Divrikli, S. Saracoglu, and L. Elci, "Membrane filtration – atomic absorption spectrometry combination for copper, cobalt, cadmium, lead and chromium in environmental samples," *Environ. Monit. Assess.*, vol. 127, no. 1, pp. 169–176, Apr. 2007, doi: 10.1007/s10661-006-9271-0.
- [69] G.-R. Xu, J.-N. Wang, and C.-J. Li, "Preparation of hierarchically nanofibrous membrane and its high adaptability in hexavalent chromium removal from water," *Chem. Eng. J.*, vol. 198–199, pp. 310–317, Aug. 2012, doi: 10.1016/j.cej.2012.05.104.
- [70] R. Yang *et al.*, "Thiol-modified cellulose nanofibrous composite membranes for chromium (VI) and lead (II) adsorption," *Polymer*, vol. 55, no. 5, pp. 1167–1176, Mar. 2014, doi: 10.1016/j.polymer.2014.01.043.
- [71] Yu. S. Dzyazko, A. Mahmoud, F. Lapique, and V. N. Belyakov, "Cr(VI) transport through ceramic ion-exchange membranes for treatment of industrial wastewaters," *J. Appl. Electrochem.*, vol. 37, no. 2, pp. 209–217, Feb. 2007, doi: 10.1007/s10800-006-9243-7.
- [72] J. Bohdziewicz, "Removal of chromium ions (VI) from underground water in the hybrid complexation-ultrafiltration process," *Desalination*, vol. 129, no. 3, pp. 227–235, Aug. 2000, doi: 10.1016/S0011-9164(00)00063-1.
- [73] D. Mohan and C. U. Pittman Jr., "Activated carbons and low cost adsorbents for remediation of tri- and hexavalent chromium from water," *J. Hazard. Mater.*, vol. 137, no. 2, pp. 762–811, Sep. 2006, doi: 10.1016/j.jhazmat.2006.06.060.
- [74] S. Kuppusamy, P. Thavamani, M. Megharaj, K. Venkateswarlu, Y. B. Lee, and R. Naidu, "Potential of *Melaleuca diosmifolia* leaf as a low-cost adsorbent for hexavalent chromium removal from contaminated water bodies," *Process Saf. Environ. Prot.*, vol. 100, pp. 173–182, Mar. 2016, doi: 10.1016/j.psep.2016.01.009.

- [75] M. Owlad, M. K. Aroua, W. A. W. Daud, and S. Baroutian, "Removal of hexavalent chromium-contaminated water and wastewater: A review," *Water. Air. Soil Pollut.*, vol. 200, no. 1–4, pp. 59–77, Jun. 2009, doi: 10.1007/s11270-008-9893-7.
- [76] D. Pradhan, L. B. Sukla, M. Sawyer, and P. K. S. M. Rahman, "Recent bioreduction of hexavalent chromium in wastewater treatment: A review," *J. Ind. Eng. Chem.*, vol. 55, pp. 1–20, Nov. 2017, doi: 10.1016/j.jiec.2017.06.040.
- [77] M. Pérez-Candela, JoséM. Martín-Martínez, and R. Torregrosa-Maciá, "Chromium(VI) removal with activated carbons," *Water Res.*, vol. 29, no. 9, pp. 2174–2180, Sep. 1995, doi: 10.1016/0043-1354(95)00035-J.
- [78] A. S. Thajeel, "Modeling and optimization of adsorption of heavy metal ions onto local activated carbon," *Aquat. Sci. Technol.*, vol. 1, no. 2, pp. 108–134, Jun. 2013, doi: 10.5296/ast.v1i2.3890.
- [79] G. M. Ayoub, A. Damaj, H. El-Rassy, M. Al-Hindi, and R. M. Zayyat, "Equilibrium and kinetic studies on adsorption of chromium(VI) onto pine-needle-generated activated carbon," *SN Appl. Sci.*, vol. 1, no. 12, p. 1562, Dec. 2019, doi: 10.1007/s42452-019-1617-7.
- [80] J. Fang, Z. Gu, D. Gang, C. Liu, E. S. Ilton, and B. Deng, "Cr(VI) removal from aqueous solution by activated carbon coated with quaternized poly(4-vinylpyridine)," *Environ. Sci. Technol.*, vol. 41, no. 13, pp. 4748–4753, Jul. 2007, doi: 10.1021/es061969b.
- [81] S. Pap *et al.*, "Evaluation of the adsorption potential of eco-friendly activated carbon prepared from cherry kernels for the removal of  $Pb^{2+}$ ,  $Cd^{2+}$  and  $Ni^{2+}$  from aqueous wastes," *J. Environ. Manage.*, vol. 184, pp. 297–306, Dec. 2016, doi: 10.1016/j.jenvman.2016.09.089.
- [82] J. Acharya, J. N. Sahu, B. K. Sahoo, C. R. Mohanty, and B. C. Meikap, "Removal of chromium(VI) from wastewater by activated carbon developed from Tamarind wood activated with zinc chloride," *Chem. Eng. J.*, vol. 150, no. 1, pp. 25–39, Jul. 2009, doi: 10.1016/j.cej.2008.11.035.
- [83] N. F. Fahim, B. N. Barsoum, A. E. Eid, and M. S. Khalil, "Removal of chromium(III) from tannery wastewater using activated carbon from sugar industrial waste," *J. Hazard. Mater.*, vol. 136, no. 2, pp. 303–309, Aug. 2006, doi: 10.1016/j.jhazmat.2005.12.014.

- [84] M. Owlad, M. K. Aroua, and W. M. A. Wan Daud, "Hexavalent chromium adsorption on impregnated palm shell activated carbon with polyethyleneimine," *Bioresour. Technol.*, vol. 101, no. 14, pp. 5098–5103, Jul. 2010, doi: 10.1016/j.biortech.2010.01.135.
- [85] M. K. Rai *et al.*, "Removal of hexavalent chromium Cr (VI) using activated carbon prepared from mango kernel activated with H<sub>3</sub>PO<sub>4</sub>," *Resour.-Effic. Technol.*, vol. 2, pp. S63–S70, Dec. 2016, doi: 10.1016/j.reffit.2016.11.011.
- [86] N. K. Hamadi, X. D. Chen, M. M. Farid, and M. G. Q. Lu, "Adsorption kinetics for the removal of chromium(VI) from aqueous solution by adsorbents derived from used tyres and sawdust," *Chem. Eng. J.*, vol. 84, no. 2, pp. 95–105, Oct. 2001, doi: 10.1016/S1385-8947(01)00194-2.
- [87] S.-J. Park and W.-Y. Jung, "Adsorption behaviors of chromium(III) and (VI) on electroless Cu-plated activated carbon fibers," *J. Colloid Interface Sci.*, vol. 243, no. 2, pp. 316–320, Nov. 2001, doi: 10.1006/jcis.2001.7910.
- [88] S. Ricordel, S. Taha, I. Cisse, and G. Dorange, "Heavy metals removal by adsorption onto peanut husks carbon: characterization, kinetic study and modeling," *Sep. Purif. Technol.*, vol. 24, no. 3, pp. 389–401, Sep. 2001, doi: 10.1016/S1383-5866(01)00139-3.
- [89] V. M. Boddu, K. Abburi, J. L. Talbott, and E. D. Smith, "Removal of hexavalent chromium from wastewater using a new composite chitosan biosorbent," *Environ. Sci. Technol.*, vol. 37, no. 19, pp. 4449–4456, Oct. 2003, doi: 10.1021/es021013a.
- [90] Y.-Y. Deng, X.-F. Xiao, D. Wang, B. Han, Y. Gao, and J.-L. Xue, "Adsorption of Cr(VI) from aqueous solution by ethylenediaminetetraacetic acid-chitosan-modified metal-organic framework.," *J. Nanosci. Nanotechnol.*, vol. 20, no. 3, pp. 1660–1669, Mar. 2020, doi: 10.1166/jnn.2020.17157.
- [91] E. Rosales, J. Meijide, T. Tavares, M. Pazos, and M. A. Sanromán, "Grapefruit peelings as a promising biosorbent for the removal of leather dyes and hexavalent chromium," *Process Saf. Environ. Prot.*, vol. 101, pp. 61–71, May 2016, doi: 10.1016/j.psep.2016.03.006.

- [92] R. Saha *et al.*, “Application of Chattim tree (devil tree, *Alstonia scholaris*) saw dust as a biosorbent for removal of hexavalent chromium from contaminated water,” *Can. J. Chem. Eng.*, vol. 91, no. 5, pp. 814–821, 2013, doi: 10.1002/cjce.21703.
- [93] G.-R. R. Bernardo, R.-M. J. Rene, and A.-D. la T. Ma. Catalina, “Chromium (III) uptake by agro-waste biosorbents: Chemical characterization, sorption–desorption studies, and mechanism,” *J. Hazard. Mater.*, vol. 170, no. 2, pp. 845–854, Oct. 2009, doi: 10.1016/j.jhazmat.2009.05.046.
- [94] D. Kratochvil, P. Pimentel, and B. Volesky, “Removal of trivalent and hexavalent chromium by seaweed biosorbent,” *Environ. Sci. Technol.*, vol. 32, no. 18, pp. 2693–2698, Sep. 1998, doi: 10.1021/es971073u.
- [95] N. K. Akunwa, M. N. Muhammad, and J. C. Akunna, “Treatment of metal-contaminated wastewater: A comparison of low-cost biosorbents,” *J. Environ. Manage.*, vol. 146, pp. 517–523, Dec. 2014, doi: 10.1016/j.jenvman.2014.08.014.
- [96] V. A. Spinelli, M. C. M. Laranjeira, and V. T. Fávere, “Preparation and characterization of quaternary chitosan salt: adsorption equilibrium of chromium(VI) ion,” *React. Funct. Polym.*, vol. 61, no. 3, pp. 347–352, Nov. 2004, doi: 10.1016/j.reactfunctpolym.2004.06.010.
- [97] A. S. K. Kumar, S. Kalidhasan, V. Rajesh, and N. Rajesh, “Application of cellulose-clay composite biosorbent toward the effective adsorption and removal of chromium from industrial wastewater,” *Ind. Eng. Chem. Res.*, vol. 51, no. 1, pp. 58–69, Jan. 2012, doi: 10.1021/ie201349h.
- [98] S. Hena, “Removal of chromium hexavalent ion from aqueous solutions using biopolymer chitosan coated with poly 3-methyl thiophene polymer,” *J. Hazard. Mater.*, vol. 181, no. 1, pp. 474–479, Sep. 2010, doi: 10.1016/j.jhazmat.2010.05.037.
- [99] V. Dimos, K. J. Haralambous, and S. Malamis, “A review on the recent studies for chromium species adsorption on raw and modified natural minerals,” *Crit. Rev. Environ. Sci. Technol.*, vol. 42, no. 19, pp. 1977–2016, Oct. 2012, doi: 10.1080/10643389.2011.574102.

- [100] M. Gürü, D. Venedik, and A. Murathan, "Removal of trivalent chromium from water using low-cost natural diatomite," *J. Hazard. Mater.*, vol. 160, no. 2, pp. 318–323, Dec. 2008, doi: 10.1016/j.jhazmat.2008.03.002.
- [101] A. B. Albadarin, C. Mangwandi, A. H. Al-Muhtaseb, G. M. Walker, S. J. Allen, and M. N. M. Ahmad, "Kinetic and thermodynamics of chromium ions adsorption onto low-cost dolomite adsorbent," *Chem. Eng. J.*, vol. 179, pp. 193–202, Jan. 2012, doi: 10.1016/j.cej.2011.10.080.
- [102] S. A. Khan, Riaz-ur-Rehman, and M. A. Khan, "Adsorption of chromium (III), chromium (VI) and silver (I) on bentonite," *Waste Manag.*, vol. 15, no. 4, pp. 271–282, Jan. 1995, doi: 10.1016/0956-053X(95)00025-U.
- [103] A. A. El-Bayaa, N. A. Badawy, and E. A. AlKhalik, "Effect of ionic strength on the adsorption of copper and chromium ions by vermiculite pure clay mineral," *J. Hazard. Mater.*, vol. 170, no. 2, pp. 1204–1209, Oct. 2009, doi: 10.1016/j.jhazmat.2009.05.100.
- [104] S. S. Tahir and R. Naseem, "Removal of Cr(III) from tannery wastewater by adsorption onto bentonite clay," *Sep. Purif. Technol.*, vol. 53, no. 3, pp. 312–321, Mar. 2007, doi: 10.1016/j.seppur.2006.08.008.
- [105] M. C. Brum, J. L. Capitaneo, and J. F. Oliveira, "Removal of hexavalent chromium from water by adsorption onto surfactant modified montmorillonite," *Miner. Eng.*, vol. 23, no. 3, pp. 270–272, Feb. 2010, doi: 10.1016/j.mineng.2009.10.008.
- [106] X. Jin, M. Jiang, J. Du, and Z. Chen, "Removal of Cr(VI) from aqueous solution by surfactant-modified kaolinite," *J. Ind. Eng. Chem.*, vol. 20, no. 5, pp. 3025–3032, Sep. 2014, doi: 10.1016/j.jiec.2013.11.038.
- [107] J. Hu, G. Chen, and I. M. C. Lo, "Removal and recovery of Cr(VI) from wastewater by maghemite nanoparticles," *Water Res.*, vol. 39, no. 18, pp. 4528–4536, Nov. 2005, doi: 10.1016/j.watres.2005.05.051.

- [108] M. G. da Fonseca, M. M. de Oliveira, and L. N. H. Arakaki, "Removal of cadmium, zinc, manganese and chromium cations from aqueous solution by a clay mineral," *J. Hazard. Mater.*, vol. 137, no. 1, pp. 288–292, Sep. 2006, doi: 10.1016/j.jhazmat.2006.02.001.
- [109] K. Babaeivelni and A. P. Khodadoust, "Removal of arsenic from water using manganese (III) oxide: Adsorption of As(III) and As(V)," *J. Environ. Sci. Health Part A*, vol. 51, no. 4, pp. 277–288, Mar. 2016, doi: 10.1080/10934529.2015.1109382.
- [110] Bajpai Sanjeev and Chaudhuri Malay, "Removal of arsenic from ground water by manganese dioxide-coated sand," *J. Environ. Eng.*, vol. 125, no. 8, pp. 782–784, Aug. 1999, doi: 10.1061/(ASCE)0733-9372(1999)125:8(782).
- [111] F. A. Al-Sagheer and M. I. Zaki, "Synthesis and surface characterization of todorokite-type microporous manganese oxides: implications for shape-selective oxidation catalysts," *Microporous Mesoporous Mater.*, vol. 67, no. 1, pp. 43–52, Jan. 2004, doi: 10.1016/j.micromeso.2003.10.005.
- [112] R. G. Burns, "The uptake of cobalt into ferromanganese nodules, soils, and synthetic manganese (IV) oxides," *Geochim. Cosmochim. Acta*, vol. 40, no. 1, pp. 95–102, Jan. 1976, doi: 10.1016/0016-7037(76)90197-6.
- [113] R. Rao. Gadde and H. A. Laitinen, "Heavy metal adsorption by hydrous iron and manganese oxides," *Anal. Chem.*, vol. 46, no. 13, pp. 2022–2026, Nov. 1974, doi: 10.1021/ac60349a004.
- [114] W. Xu, H. Lan, H. Wang, H. Liu, and J. Qu, "Comparing the adsorption behaviors of Cd, Cu and Pb from water onto Fe-Mn binary oxide, MnO<sub>2</sub> and FeOOH," *Front. Environ. Sci. Eng.*, vol. 9, no. 3, pp. 385–393, Jun. 2015, doi: 10.1007/s11783-014-0648-y.
- [115] S. D. Rachmawati, C. Tizaoui, and N. Hilal, "Manganese coated sand for copper (II) removal from water in batch mode," *Water*, vol. 5, no. 4, pp. 1487–1501, Dec. 2013, doi: 10.3390/w5041487.

- [116] S. M. Maliyekkal, L. Philip, and T. Pradeep, "As(III) removal from drinking water using manganese oxide-coated-alumina: Performance evaluation and mechanistic details of surface binding," *Chem. Eng. J.*, vol. 153, no. 1, pp. 101–107, Nov. 2009, doi: 10.1016/j.cej.2009.06.026.
- [117] S. M. Maliyekkal, A. K. Sharma, and L. Philip, "Manganese-oxide-coated alumina: A promising sorbent for defluoridation of water," *Water Res.*, vol. 40, no. 19, pp. 3497–3506, Nov. 2006, doi: 10.1016/j.watres.2006.08.007.
- [118] E. Eren, B. Afsin, and Y. Onal, "Removal of lead ions by acid activated and manganese oxide-coated bentonite," *J. Hazard. Mater.*, vol. 161, no. 2, pp. 677–685, Jan. 2009, doi: 10.1016/j.jhazmat.2008.04.020.
- [119] N. Boujelben, J. Bouzid, Z. Elouear, and M. Feki, "Retention of nickel from aqueous solutions using iron oxide and manganese oxide coated sand: kinetic and thermodynamic studies," *Environ. Technol.*, vol. 31, no. 14, pp. 1623–1634, Dec. 2010, doi: 10.1080/09593330.2010.482148.
- [120] S. A. Chaudhry, T. A. Khan, and I. Ali, "Adsorptive removal of Pb(II) and Zn(II) from water onto manganese oxide-coated sand: Isotherm, thermodynamic and kinetic studies," *Egypt. J. Basic Appl. Sci.*, vol. 3, no. 3, pp. 287–300, Sep. 2016, doi: 10.1016/j.ejbas.2016.06.002.
- [121] R. Han, W. Zou, Y. Wang, and L. Zhu, "Removal of uranium(VI) from aqueous solutions by manganese oxide coated zeolite: discussion of adsorption isotherms and pH effect," *J. Environ. Radioact.*, vol. 93, no. 3, pp. 127–143, Jan. 2007, doi: 10.1016/j.jenvrad.2006.12.003.
- [122] Y.-Y. Chang, K.-H. Song, M.-R. Yu, and J.-K. Yang, "Removal of arsenic from aqueous solution by iron-coated sand and manganese-coated sand having different mineral types," *Water Sci. Technol.*, vol. 65, no. 4, pp. 683–688, Feb. 2012, doi: 10.2166/wst.2012.910.

## CHAPTER II

### II. DEVELOPMENT OF MANGANESE-COATED SAND

#### 2.1 Introduction

Chromium (Cr) is a metal that exists in several oxidation states, ranging from chromium (-II) to chromium (+VI), whereas it is mostly present in two valence states of trivalent chromium and hexavalent chromium in natural water [1], [2]. Hexavalent chromium compounds are well known as laboratory reagents and manufacturing intermediates. Major sources of hexavalent chromium in drinking water are discharged from steel industry, pulp mills, or metal plating operations [3]. There is strong evidence to consider hexavalent chromium as carcinogen that can pose serious hazards towards human beings, therefore the removal of hexavalent chromium from source of drinking water is an important health concern [4], [5]. The removal of chromium from natural waters down to environmentally acceptable levels is required because of the genotoxic, mutagenic and carcinogenic effects of chromium species. The U.S. EPA Safe Drinking Water Act regulated that the maximum allowed total chromium in drinking water is 0.1 mg/L.

Therefore, the application of a technology that is easy to operate and maintain for the removal of chromium from water to ensure regulatory compliance is necessary. Various technologies for the removal of chromium from water including ion exchange, reduction/filtration/precipitation and membrane processes have been used [6], [7]. Hexavalent chromium may be removed from water using adsorption. Adsorption is regarded as a relatively effective and promising technology with low operational and maintenance cost due to the high capacity toward heavy metals and the regenerability of the most adsorbents. A wide range of adsorbents have been considered for adsorption of chromium including activated carbon, natural fibers, agricultural and industrial wastes, clays, zerovalent iron, metal oxides and hybrid adsorbents [8]–[14].

Metal oxides such as iron oxides and manganese oxides have been commonly used as effective adsorbents of heavy metals. The heavy metal species can be adsorbed through electrostatic forces or formation of surface complexes or reduction followed by precipitation on the metal oxides [15]–[20].

Nevertheless, the application of pure manganese oxides as viable adsorbents or filter media in a column setting is limited due to that manganese oxides have relatively low hydraulic conductivity and generally exist in colloidal form or nonmaterial form resulting in difficult separation from water body after use [21]. Therefore, manganese oxides have been coated onto various supporting medias such as zeolite, bentonite, alumina and silica sand to improve the mechanical stability [16], [22]–[24]. Manganese-coated sand (MCS) has been used for removal of a variety of heavy metals either in the formats of cations such as lead ( $\text{Pb}^{2+}$ ), copper ( $\text{Cu}^{2+}$ ), zinc ( $\text{Zn}^{2+}$ ) or in the formats of oxyanions such as arsenic ( $\text{H}_2\text{AsO}_3^-$ ) and uranium [ $\text{UO}_2(\text{CO}_3)_2^{2-}$ ] and has the potential to be an effective adsorbent for the removal of chromium from water [21], [25]–[28]. In this study, we plan to modify the procedure of synthesizing the manganese-coated sand (MCS) including changing the source of manganese and coating temperature and adjusting pH value to get an efficient, applicable and inexpensive sorbent for removal of chromium from water.

## 2.2 Materials and methods

### 2.2.1 Chemicals

The white quartz sand ( $\text{SiO}_2$ ) with 50-70 mesh particle size was obtained from Sigma-Aldrich (St. Louis, MO, USA). De-ionized (DI) water was produced inside the laboratory with a resistance of greater than  $18 \text{ M}\Omega$ . All other chemicals employed in this study were analytical grade. Manganese sulfate monohydrate ( $\text{MnSO}_4 \cdot \text{H}_2\text{O}$ , 99+% purity, extra pure) and manganese chloride tetrahydrate ( $\text{MnCl}_2 \cdot 4\text{H}_2\text{O}$ , 99+% purity, for analysis) were purchased from Acros Organics (Fair Lawn, NJ, USA) and used as manganese source for coating solution. Sodium hydroxide (NaOH, 99.5% purity, ACS grade), sodium carbonate ( $\text{Na}_2\text{CO}_3$ , 100% purity, ACS grade), hydrochloric acid (HCl, ACS plus grade) and nitric acid ( $\text{HNO}_3$ , trace metal grade) were obtained from Fisher Scientific (Fair Lawn, NJ, USA).

### 2.2.2 Coating method

40g silica sand was first soaked in 0.1M hydrochloride acid (HCl) solution for 3 hours and then rinsed with deionized(DI) water to remove possible surface impurities. After dried in an oven at  $110^\circ\text{C}$ , the acid-washed sand was stirred in 50mL of 1mol/L  $\text{Na}_2\text{CO}_3$  solution where 50mL of 1mol/L of manganese source solution was added with or without additional pH adjustment using 6N sodium hydroxide (NaOH). The sand and the coating solution were mixed for 24 hours to facilitate the coating procedure and the solution residual was poured out. The coated sand were air dried for 12 hours and again dried in an oven at  $110^\circ\text{C}$  for 4 hours before it was introduced into a furnace at different temperatures for 24 hours to finish the coating process. Manganese coated sand (MCS) was cooled down and stored in an airtight polyethylene container for future experimental use.

### 2.3 Results and discussion

In order to optimize the preparation conditions for manganese-coated sand (MCS), we synthesized MCS with different sources of manganese, pH values of the coating solution and coating temperatures to select the final optimum MCS that will be used for all future studies.

Manganese chloride ( $\text{MnCl}_2$ ) and manganese sulfate ( $\text{MnSO}_4$ ) are two widely used manganese sources for manganese oxides coated sorbents [28]–[31]. The sand was coated with 1M of  $\text{MnCl}_2$  solution and 1M of  $\text{MnSO}_4$  solution and the removal of hexavalent chromium [Cr(VI)] and manganese content coated onto the sand were evaluated to decide which manganese source is more suitable for the purpose of chromium removal. Results of chromium removal and manganese content shown in Table 2.1 are indicative of the superior manganese source for this study of chromium removal is  $\text{MnSO}_4$ . MCS coated with  $\text{MnSO}_4$  obtained twice more chromium uptake and more manganese deposited on the sand than MCS coated with  $\text{MnCl}_2$ . Therefore,  $\text{MnSO}_4$  was selected in this study as manganese sources in coating solution.

Table 2. 1 Adsorption efficiency and manganese content of different manganese sources

Manganese Source	Removal(%)	Manganese Content (mg/g)
	1mg/L Cr(VI) + DI solution	
$\text{MnCl}_2$	48.16	0.78
$\text{MnSO}_4$	89.04	1.76

The pH value of the coating solution can be another important factor that affects the Cr(VI) uptake on the final synthesized MCS [26], [32]–[34]. The pH of the coating solution (mixture of 50mL 1M of  $\text{Mn}_2\text{SO}_4$  solution and 50mL 1M of  $\text{Na}_2\text{CO}_3$  solution) without any pH adjustment is determined to be 10. The coating process was also carried out with adjusting pH of the same solution mixture into 7, 9 and 11 to determine the optimum pH for coating the silica sand. From the results shown in Figure 2.1, it can be seen that when the pH of the coating solution was adjusted to 9, the removal of Cr(VI) reached the

highest level at 92%, compared to a merely 1.8% at pH 7 and 25% at pH 11. However, MCS coated with no pH adjustment coating solution also exhibited a relatively high 89% Cr(VI) removal. Therefore, MCS developed for future studies was coated with the coating solution mixture without pH adjustment because this coating procedure can not only eliminate the use of strong acid such as hydrochloric acid to adjust pH value of the coating solution without compromising the Cr(VI) uptake but also make the MCS adsorbent more affordable and environmental benign.

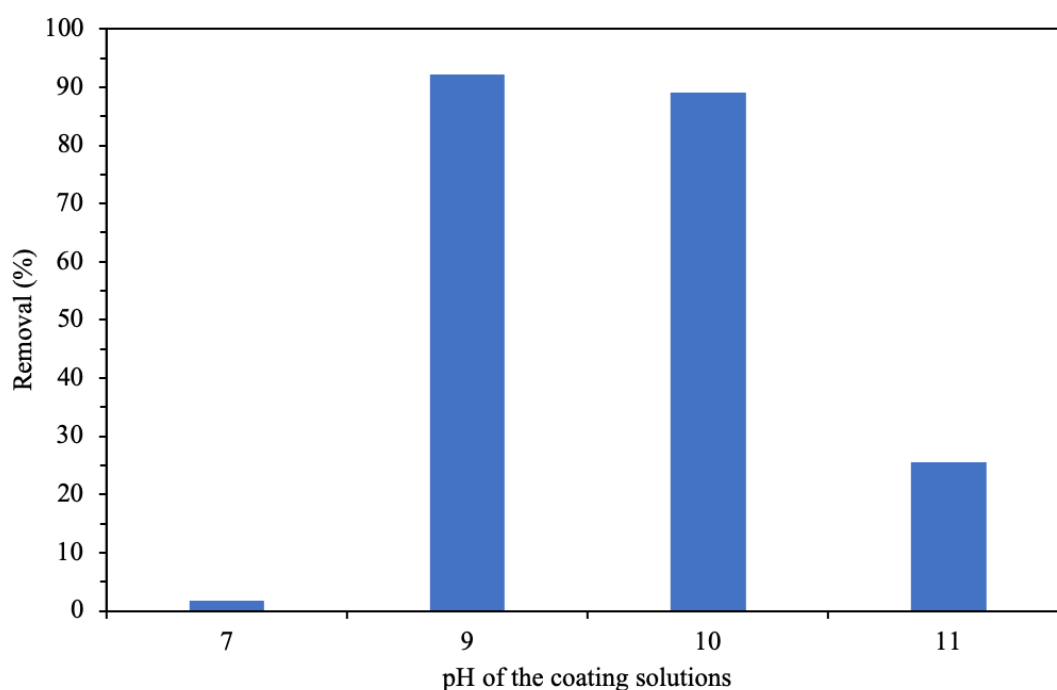


Figure 2. 1 Comparison of MCS coated with pH adjusted solution and no pH adjusted solution on Cr(VI) removal

The coating temperature has been known to control the mineralogy of metal oxides deposited onto the surface of the metal oxides coated silica sand. Lo et al. [35] found that no crystalline iron oxide formed at 60°C, goethite and hematite formed at 150°C, only hematite formed at 300°C and 500°C while all other coating conditions such concentration and pH value remained the same. Chang et al. [36] discovered that MCS prepared at 150°C obtained a mixture of pyrolusite and ramsdellite on the surface, which changed to high crystalline pyrolusite when the coating temperature went up over 300°C. We selected a series of different coating temperatures while other coating parameters such as manganese source and pH value of the coating solution were adjusted to the same level. The batch adsorption test were carried out with the final MCS coated under different coating temperatures. As shown in Figure 2.2, the removal of Cr(VI) decreases when the coating temperature increases. At the temperature range of 120°C to 220°C, the highest removal of 96% was reached at the lowest coating temperature of 120°C and a minor loss of the Cr(VI) removal (9%) can be observed when the coating temperature was raised to 220°C. The Cr(VI) removal suddenly experienced a drastic drop from 87% to a merely 8% when the coating temperature was further increased to 330°C and eventually exhibited no adsorption towards Cr(VI) when the coating temperature reached the highest temperature at 550°C. This observation suggests that the coating temperature is another crucial factor that controls both the structure and type of manganese oxides finally formed on the silica sand surface, which can affect the hexavalent chromium adsorption process profoundly. In contrast to the MCS coated at higher temperature, the manganese oxides formed at lower coating temperature were likely in a more reduced form such as Mn(II) and Mn(III). Therefore, the reduced form of manganese can be a potential way to reduce the hexavalent chromium into less toxic trivalent chromium. The higher coating temperature can result in higher attachment strength between silica sand and manganese oxides and less manganese leachate into solution after adsorption (Figure 2.3). In order to remove hexavalent chromium without introducing excessive manganese into the water system, 220°C is selected as the optimum coating temperature for this research. Further microscopic investigations are necessary to confirm the mineralogy of the manganese oxides coated onto MCS surface.

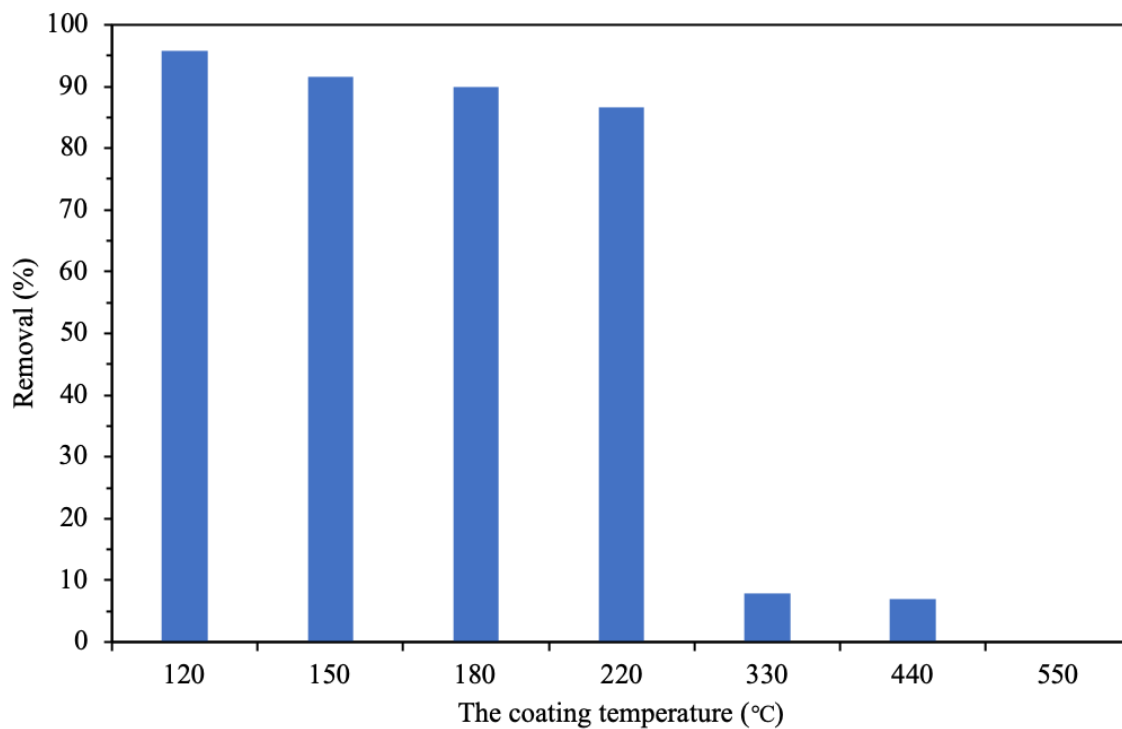


Figure 2. 2 Comparison of MCS coated at different coating temperature on Cr(VI) removal

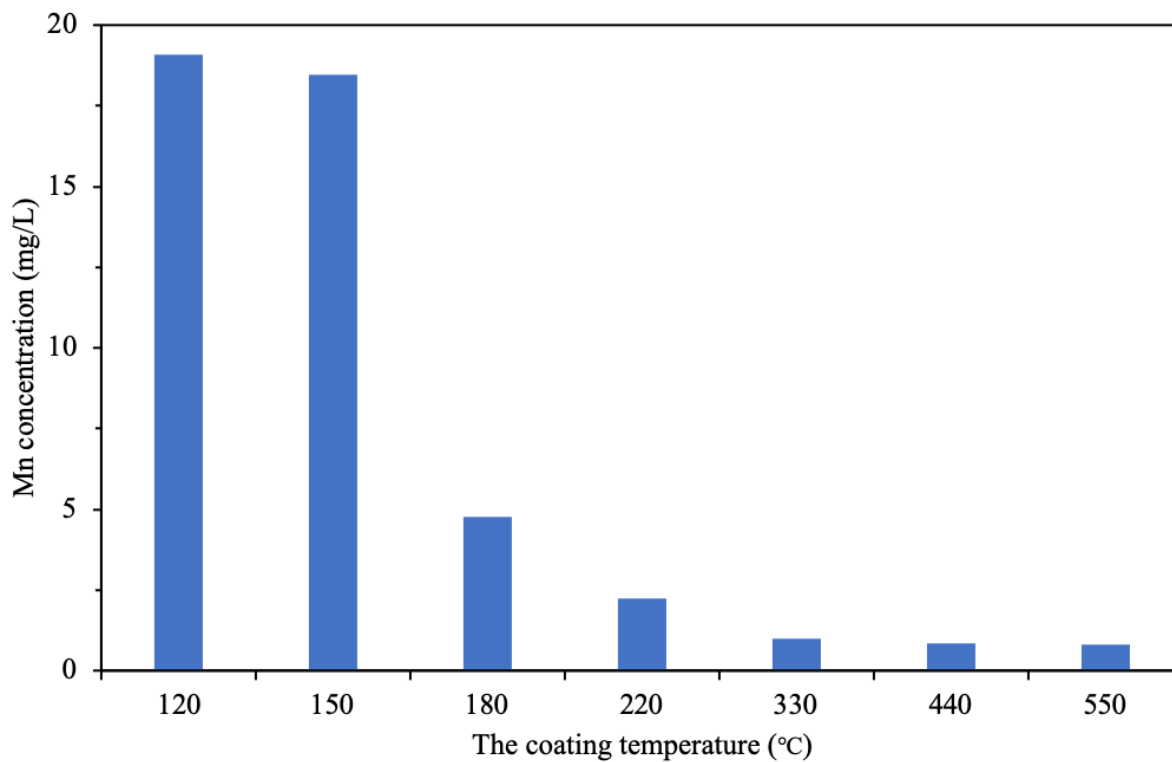


Figure 2. 3 Mn concentration in solution after batch adsorption tests with MCS coated at different temperatures

## 2.4 Conclusion

In order to develop a process to coat manganese oxides onto silica sand and utilize the adsorption capacity for hexavalent chromium of the coated sand, we investigated three coating parameters including the source of manganese, the coating pH and the coating temperature.

The source of manganese played an important role in final adsorption capacity of manganese oxides coated sand (MCS) toward hexavalent chromium [Cr(VI)] and the optimum manganese source for the coating onto silica sand is  $\text{MnSO}_4$ . The coating temperature exhibited a significant effect on the mineralogy of the manganese oxides coated onto silica sand. Comparing the MCS coated at different temperature, it can be observed that the removal of chromium decreases drastically when temperature was raised above  $220^\circ\text{C}$ . The weak attachment strength between the manganese oxides and silica sand formed at low temperature range from  $120^\circ\text{C}$  to  $180^\circ\text{C}$  resulted in the excessive release of manganese ion into the solution. Therefore,  $220^\circ\text{C}$  is determined to be the optimum coating temperature because MCS coated at  $220^\circ\text{C}$  obtained relatively high removal efficiency of Cr(VI) without releasing high level of manganese ion into water system. Despite that the highest Cr(VI) uptake was achieved at 92% when the pH of the coating solution was adjusted to 9, MCS coated without pH adjustment was considered to more suitable for this study due to the fact that we successfully eliminated the use of a strong acid with a negligible loss of the removal efficiency of Cr(VI).

## 2.5 Reference

- [1] J. Kotaś and Z. Stasicka, “Chromium occurrence in the environment and methods of its speciation,” *Environ. Pollut.*, vol. 107, no. 3, pp. 263–283, Mar. 2000, doi: 10.1016/S0269-7491(99)00168-2.
- [2] F. C. Richard and A. C. M. Bourg, “Aqueous geochemistry of chromium: A review,” *Water Res.*, vol. 25, no. 7, pp. 807–816, Jul. 1991, doi: 10.1016/0043-1354(91)90160-R.
- [3] J. Barnhart, “Occurrences, uses, and properties of chromium,” *Regul. Toxicol. Pharmacol.*, vol. 26, no. 1, pp. S3–S7, Aug. 1997, doi: 10.1006/rtph.1997.1132.
- [4] S. A. Katz and H. Salem, “The toxicology of chromium with respect to its chemical speciation: A review,” *J. Appl. Toxicol.*, vol. 13, no. 3, pp. 217–224, May 1993, doi: 10.1002/jat.2550130314.
- [5] A. Zhitkovich, “Chromium in drinking water: sources, metabolism, and cancer risks,” *Chem. Res. Toxicol.*, vol. 24, no. 10, pp. 1617–1629, Oct. 2011, doi: 10.1021/tx200251t.
- [6] K. Loska and D. Wiechuła, “Application of principal component analysis for the estimation of source of heavy metal contamination in surface sediments from the Rybnik Reservoir,” *Chemosphere*, vol. 51, no. 8, pp. 723–733, Jun. 2003, doi: 10.1016/S0045-6535(03)00187-5.
- [7] R. A. Wuana and F. E. Okieimen, “Heavy metals in contaminated soils: A review of sources, chemistry, risks and best available strategies for remediation,” *ISRN Ecol.*, vol. 2011, pp. 1–20, Apr. 2011, doi: 10.5402/2011/402647.
- [8] V. Dimos, K. J. Haralambous, and S. Malamis, “A review on the recent studies for chromium species adsorption on raw and modified natural minerals,” *Crit. Rev. Environ. Sci. Technol.*, vol. 42, no. 19, pp. 1977–2016, Oct. 2012, doi: 10.1080/10643389.2011.574102.
- [9] D. Mohan and C. U. Pittman Jr., “Activated carbons and low cost adsorbents for remediation of tri- and hexavalent chromium from water,” *J. Hazard. Mater.*, vol. 137, no. 2, pp. 762–811, Sep. 2006, doi: 10.1016/j.jhazmat.2006.06.060.
- [10] S. Yadav, V. Srivastava, S. Banerjee, C.-H. Weng, and Y. C. Sharma, “Adsorption characteristics of modified sand for the removal of hexavalent chromium ions from aqueous solutions: Kinetic,

- thermodynamic and equilibrium studies,” *CATENA*, vol. 100, pp. 120–127, Jan. 2013, doi: 10.1016/j.catena.2012.08.002.
- [11] M. X. Loukidou, A. I. Zouboulis, T. D. Karapantsios, and K. A. Matis, “Equilibrium and kinetic modeling of chromium(VI) biosorption by *Aeromonas caviae*,” *Colloids Surf. Physicochem. Eng. Asp.*, vol. 242, no. 1–3, pp. 93–104, Aug. 2004, doi: 10.1016/j.colsurfa.2004.03.030.
- [12] S. Chen, J. Zhang, H. Zhang, and X. Wang, “Removal of hexavalent chromium from contaminated water by Chinese herb-extraction residues,” *Water. Air. Soil Pollut.*, vol. 228, no. 4, p. 145, Apr. 2017, doi: 10.1007/s11270-017-3329-1.
- [13] S. Kuppusamy, P. Thavamani, M. Megharaj, K. Venkateswarlu, Y. B. Lee, and R. Naidu, “Potential of *Melaleuca diosmifolia* leaf as a low-cost adsorbent for hexavalent chromium removal from contaminated water bodies,” *Process Saf. Environ. Prot.*, vol. 100, pp. 173–182, Mar. 2016, doi: 10.1016/j.psep.2016.01.009.
- [14] M. Owlad, M. K. Aroua, W. A. W. Daud, and S. Baroutian, “Removal of hexavalent chromium-contaminated water and wastewater: A Review,” *Water. Air. Soil Pollut.*, vol. 200, no. 1–4, pp. 59–77, Jun. 2009, doi: 10.1007/s11270-008-9893-7.
- [15] K. Babaeiveli and A. P. Khodadoust, “Removal of arsenic from water using manganese (III) oxide: Adsorption of As(III) and As(V),” *J. Environ. Sci. Health Part A*, vol. 51, no. 4, pp. 277–288, Mar. 2016, doi: 10.1080/10934529.2015.1109382.
- [16] B. Sanjeev and C. Malay, “Removal of arsenic from ground water by manganese dioxide-coated Sand,” *J. Environ. Eng.*, vol. 125, no. 8, pp. 782–784, Aug. 1999, doi: 10.1061/(ASCE)0733-9372(1999)125:8(782).
- [17] F. A. Al-Sagheer and M. I. Zaki, “Synthesis and surface characterization of todorokite-type microporous manganese oxides: implications for shape-selective oxidation catalysts,” *Microporous Mesoporous Mater.*, vol. 67, no. 1, pp. 43–52, Jan. 2004, doi: 10.1016/j.micromeso.2003.10.005.

- [18] R. G. Burns, "The uptake of cobalt into ferromanganese nodules, soils, and synthetic manganese (IV) oxides," *Geochim. Cosmochim. Acta*, vol. 40, no. 1, pp. 95–102, Jan. 1976, doi: 10.1016/0016-7037(76)90197-6.
- [19] R. Rao. Gadde and H. A. Laitinen, "Heavy metal adsorption by hydrous iron and manganese oxides," *Anal. Chem.*, vol. 46, no. 13, pp. 2022–2026, Nov. 1974, doi: 10.1021/ac60349a004.
- [20] W. Xu, H. Lan, H. Wang, H. Liu, and J. Qu, "Comparing the adsorption behaviors of Cd, Cu and Pb from water onto Fe-Mn binary oxide, MnO<sub>2</sub> and FeOOH," *Front. Environ. Sci. Eng.*, vol. 9, no. 3, pp. 385–393, Jun. 2015, doi: 10.1007/s11783-014-0648-y.
- [21] S. D. Rachmawati, C. Tizaoui, and N. Hilal, "Manganese coated sand for copper (II) removal from water in batch mode," *Water*, vol. 5, no. 4, pp. 1487–1501, Dec. 2013, doi: 10.3390/w5041487.
- [22] S. M. Maliyekkal, L. Philip, and T. Pradeep, "As(III) removal from drinking water using manganese oxide-coated-alumina: Performance evaluation and mechanistic details of surface binding," *Chem. Eng. J.*, vol. 153, no. 1, pp. 101–107, Nov. 2009, doi: 10.1016/j.cej.2009.06.026.
- [23] S. M. Maliyekkal, A. K. Sharma, and L. Philip, "Manganese-oxide-coated alumina: A promising sorbent for defluoridation of water," *Water Res.*, vol. 40, no. 19, pp. 3497–3506, Nov. 2006, doi: 10.1016/j.watres.2006.08.007.
- [24] E. Eren, B. Afsin, and Y. Onal, "Removal of lead ions by acid activated and manganese oxide-coated bentonite," *J. Hazard. Mater.*, vol. 161, no. 2, pp. 677–685, Jan. 2009, doi: 10.1016/j.jhazmat.2008.04.020.
- [25] N. Boujelben, J. Bouzid, Z. Elouear, and M. Feki, "Retention of nickel from aqueous solutions using iron oxide and manganese oxide coated sand: kinetic and thermodynamic studies," *Environ. Technol.*, vol. 31, no. 14, pp. 1623–1634, Dec. 2010, doi: 10.1080/09593330.2010.482148.
- [26] S. A. Chaudhry, T. A. Khan, and I. Ali, "Adsorptive removal of Pb(II) and Zn(II) from water onto manganese oxide-coated sand: Isotherm, thermodynamic and kinetic studies," *Egypt. J. Basic Appl. Sci.*, vol. 3, no. 3, pp. 287–300, Sep. 2016, doi: 10.1016/j.ejbas.2016.06.002.

- [27] R. Han, W. Zou, Y. Wang, and L. Zhu, "Removal of uranium(VI) from aqueous solutions by manganese oxide coated zeolite: discussion of adsorption isotherms and pH effect," *J. Environ. Radioact.*, vol. 93, no. 3, pp. 127–143, Jan. 2007, doi: 10.1016/j.jenvrad.2006.12.003.
- [28] Y.-Y. Chang, K.-H. Song, M.-R. Yu, and J.-K. Yang, "Removal of arsenic from aqueous solution by iron-coated sand and manganese-coated sand having different mineral types," *Water Sci. Technol.*, vol. 65, no. 4, pp. 683–688, Feb. 2012, doi: 10.2166/wst.2012.910.
- [29] A. Georgiadis and T. Rennert, "A simple method to produce birnessite-coated quartz sand," *J. Plant Nutr. Soil Sci.*, vol. 180, no. 4, pp. 491–495, 2017, doi: 10.1002/jpln.201700024.
- [30] R. S. Stahl and B. R. James, "Zinc sorption by manganese-oxide-coated sand as a function of pH," *Soil Sci. Soc. Am. J.*, vol. 55, no. 5, pp. 1291–1294, Oct. 1991, doi: 10.2136/sssaj1991.03615995005500050016x.
- [31] Q. Su, B. Pan, S. Wan, W. Zhang, and L. Lv, "Use of hydrous manganese dioxide as a potential sorbent for selective removal of lead, cadmium, and zinc ions from water," *J. Colloid Interface Sci.*, vol. 349, no. 2, pp. 607–612, Sep. 2010, doi: 10.1016/j.jcis.2010.05.052.
- [32] D. Tiwari, C. Laldanwngliana, C.-H. Choi, and S. M. Lee, "Manganese-modified natural sand in the remediation of aquatic environment contaminated with heavy metal toxic ions," *Chem. Eng. J.*, vol. 171, no. 3, pp. 958–966, Jul. 2011, doi: 10.1016/j.cej.2011.04.046.
- [33] K. Laatikainen, J. Pakarinen, M. Laatikainen, R. Koivula, R. Harjula, and E. Paatero, "Preparation of silica-supported nanoporous manganese oxides," *Sep. Purif. Technol.*, vol. 75, no. 3, pp. 377–384, Nov. 2010, doi: 10.1016/j.seppur.2010.09.007.
- [34] N. Boujelben, F. Bouhamed, Z. Elouear, J. Bouzid, and M. Feki, "Removal of phosphorus ions from aqueous solutions using manganese-oxide-coated sand and brick," *Desalination Water Treat.*, vol. 52, no. 10–12, pp. 2282–2292, Mar. 2014, doi: 10.1080/19443994.2013.822324.
- [35] S.-L. Lo, H.-T. Jeng, and C.-H. Lai, "Characteristics and adsorption properties of iron-coated sand," *Water Sci. Technol.*, vol. 35, no. 7, pp. 63–70, Apr. 1997, doi: 10.2166/wst.1997.0261.

- [36] Y.-Y. Chang, K.-H. Song, and J.-K. Yang, "Removal of As(III) in a column reactor packed with iron-coated sand and manganese-coated sand," *J. Hazard. Mater.*, vol. 150, no. 3, pp. 565–572, Feb. 2008, doi: 10.1016/j.jhazmat.2007.05.005.

## CHAPTER III

### III. ADSORPTION OF CHROMIUM ONTO MANGANESE-COATED SAND: BATCH STUDY

#### 3.1 Introduction

Chromium (Cr) is a metal that exists in several oxidation states, ranging from chromium (-II) to chromium (+VI), whereas it is mostly present in two valence states of trivalent chromium and hexavalent chromium in natural water [1], [2]. The properties of chromium are highly dependent on the oxidation state of chromium. Hexavalent chromium is considerably more mobile and toxic than trivalent chromium, and is more difficult to remove from water due to the fact that Cr(VI) appears mainly as the soluble oxy-anionic species of chromate ( $\text{CrO}_4^{2-}$ ) from pH 6.5 to 14, whereas the cationic Cr(III) may precipitate as insoluble  $\text{Cr}(\text{OH})_3$  in the same pH range [3], [4]. Several studies have shown that Cr(VI) appears to be 10-100 times more toxic than Cr(III) via oral ingestion mainly because Cr(VI) exhibits higher oxidizing strength and membrane transport [5]–[7]. While Cr(VI) has been categorized as known human carcinogen via inhalation by the International Agency for Research on Cancer(IARC), Cr(VI) ingestion via oral route has not been confirmed as carcinogenic for humans due to the lack of epidemiological studies. But genotoxic, mutagenic and carcinogenic effects in multispecies produced by consumption of Cr(VI) in drinking water were firmly established in multiple studies and there is adequate evidence to classify Cr(VI) consumption through drinking water as likely to be carcinogenic to humans [8]–[11]. Therefore, the application of a technology that is easy to operate and maintain for the removal of chromium from water to ensure regulatory compliance is necessary. Various technologies for the removal of chromium from water including ion exchange, reduction/filtration/precipitation and membrane processes have been used [12], [13]. Hexavalent chromium may be removed from water using adsorption. Adsorption is regarded as a relatively effective and promising technology with low operational and maintenance cost due to the high capacity toward heavy metals and the regenerability of the most adsorbents. A wide range of adsorbents have been considered for adsorption of chromium

including activated carbon, natural fibers, agricultural and industrial wastes, clays, zerovalent iron, metal oxides and hybrid adsorbents [14]–[20].

Metal oxides such as iron oxides and manganese oxides have been commonly used as effective adsorbents of heavy metals. The heavy metal species can be adsorbed through electrostatic forces or formation of surface complexes or reduction followed by precipitation on the metal oxides [21]–[26]. Nevertheless, the application of pure manganese oxides as viable adsorbents or filter media in a column setting is limited due to that manganese oxides have relatively low hydraulic conductivity and generally exist in colloidal form or nonmaterial form resulting in difficult separation from water body after use [27]. Therefore, manganese oxides have been coated onto various supporting medias such as zeolite, bentonite, alumina and silica sand to improve the mechanical stability [16], [22]–[24]. Manganese-coated sand (MCS) has been used for the removal of a variety of heavy metals either in the formats of cations such as lead ( $\text{Pb}^{2+}$ ), copper ( $\text{Cu}^{2+}$ ), zinc ( $\text{Zn}^{2+}$ ) or in the formats of oxyanions such as arsenic ( $\text{H}_2\text{AsO}_3^-$ ) and uranium [ $\text{UO}_2(\text{CO}_3)_2^{2-}$ ] and has the potential to be an effective adsorbent for the removal of chromium from water [27], [31]–[34]. The effects of various experimental parameters such as MCS dosage, initial chromium concentration, pH of chromium solution, contact time and co-existing ions were evaluated for the removal of chromium using manganese-coated sand (MCS) synthesized in this study. A sorbent can be a sustainable and cost effective sorbent if it can be reused in multiple cycles of operation. The reuse and regeneration of the developed MCS sorbent for chromium removal was also investigated.

## 3.2 Materials and method

### 3.2.1 Chemicals

Potassium dichromate (99.5% purity, ACS grade) and chromium chloride ( $\text{CrCl}_3 \cdot 6\text{H}_2\text{O}$ , 96% purity, ACS grade) were obtained from Fisher Scientific (Fair Lawn, NJ, USA). De-ionized (DI) water was produced inside the laboratory with a resistance of greater than 18 M $\Omega$ . A stock solution of 1000 mg/L Cr(VI) was prepared by mixing potassium dichromate ( $\text{K}_2\text{Cr}_2\text{O}_7$ ) with deionized water. A stock of solution of 1000 mg/L Cr(III) solution was prepared by mixing chromium chloride with deionized water. All other chemicals employed in this study were analytical grade. Sodium hydroxide (NaOH, 99.5% purity, ACS grade), hydrochloric acid (HCl, ACS plus grade) and nitric acid ( $\text{HNO}_3$ , trace metal grade) were obtained from Fisher Scientific (Fair Lawn, NJ, USA). Calcium chloride ( $\text{CaCl}_2$ , 98.8% purity, ACS grade), sodium sulfate ( $\text{Na}_2\text{SO}_4$ , 99.3% purity, ACS grade), sodium bicarbonate ( $\text{NaHCO}_3$ , 100% purity, ACS grade) used for co-existing ion study were purchased from Fisher Scientific (Fair Lawn, NJ, USA).

### 3.2.2 Batch adsorption experiments

Batch adsorption studies were conducted in well-sealed 50-mL high density polyethylene (HDPE) centrifuge tube with MCS. An identical amount of MCS (1g) was mixed with 50mL of Cr(III)/Cr(VI) solution with prescribed concentration of 1mg/L-10mg/L prepared from chromium stock solution. The batch adsorption test was also carried out with different dosage of MCS with 50mL of 1mg/L Cr(III)/Cr(VI) solution from diluting Cr(III)/Cr(VI) stock solution. In order to decide the effect of pH, the initial pH of 50mL 1mg/L Cr(III)/Cr(VI) solution was adjusted (pH =2~10) using 0.1M hydrochloric acid (HCl) and 0.1M sodium hydroxide (NaOH) prior to contact with 1 gram of MCS. Each set of the samples were shaken in a rotary tumbler for a reaction period of 24 hours at 16 rpm to reach equilibrium. To obtain the equilibrium concentration of chromium, all samples were centrifuged at 8000 rpm for 10 minutes to separate the supernatant from adsorbents and a 10-mL sample was taken from each sample

into a test tube that later acidified by adding two drops of concentrated nitric acid (HNO<sub>3</sub>) and analyzed by flame atomic absorption spectroscopy (Perkin-Elmer, Waltham, MA, USA). A chromium hollow cathode lamp (HCL) at 357.9 nm was used to detect chromium. The atomic absorption calibration range was from 0.25 to 1.5 mg/L. The removal efficiency of chromium on MCS was calculated as:

$$Removal(\%) = \frac{(C_0 - C_e)}{C_0} \times 100 \quad (1)$$

The adsorption of chromium onto MCS surface was determined using following equation:

$$q = \frac{(C_0 - C_e)}{m} \times V \quad (2)$$

Where C<sub>0</sub> and C<sub>e</sub> are the initial and equilibrium concentration of chromium in the solution (mg/L), q is the amount of chromium adsorbed per unit weight of the MCS sorbent (mg/kg), m is the weight of the MCS sorbent (kg) and V is the volume of the chromium solution (L).

### 3.2.3 Zeta potential measurement

The net effective charge was determined by measuring the zeta potentials of different MCS suspensions using the Zeta-meter system 3.0 (Zeta meter Inc, Staunton, VA, USA). The 1g/L MCS suspensions were prepared without chromium (Cr), with 1mg/L Cr(III) and with 1mg/L Cr(VI) in 1mM sodium chloride (NaCl) solutions. The pH value of the samples were adjusted from 2 to 12 by adding dropwise 0.1M HCl and 0.1M NaOH.

### 3.2.4 Adsorption kinetics

The adsorption kinetics study were conducted at room temperature by adding a fixed amount of MCS (1g) into 50mL HDPE centrifuge tube containing 50mL of 1mg/L Cr(III)/Cr(VI) solution under varying contact time (30 min to 24 hr) at 16 rpm.

### 3.2.5 Coexisting ions study

In order to determine the effects of ion strength and co-existing ions on chromium adsorption for MCS, different concentrations of CaCl<sub>2</sub>, Na<sub>2</sub>SO<sub>4</sub>, NaHCO<sub>3</sub> or Na<sub>2</sub>(PO<sub>4</sub>)<sub>3</sub> with 1mg/L Cr(III)/Cr(VI) solution were prepared. 50mL of each solution containing the binary system of chromium and selected coexisting ion was mixed with 1 gram of MCS at 16 rpm for a period of 24 hours to reach equilibrium.

### 3.2.6 Sorbent recycling and regeneration experiments

To evaluate the effectiveness of MCS as sorbent for chromium, MCS was used in five consecutive adsorption cycles. One gram of MCS was mixed with 50mL of 1mg/L Cr(III)/Cr(VI) solution in HDPE centrifuge tube for the first adsorption cycle. After 24 hours, the used sorbent was separated from the solution by centrifuging the tube at 8000 rpm for 10 min and supernatant was collected for analysis. This process can be repeated by using the used sorbent from previous cycle with another fresh 50mL of 1mg/L Cr(III)/Cr(VI) solution for the subsequent adsorption cycles. After three adsorption cycles, chromium-loaded MCS sorbent in the centrifuge tube was first washed with 50 mL of DI water, then regenerated by adding 50 mL of 0.001M, 0.01M, and 0.1M of NaOH solution and shaken in a tumbler at 16rpm for 24 hours. The regenerated MCS was extracted from sodium hydroxide solution for another three consecutive adsorption cycles. The regeneration efficiency was calculated by the following equation:

$$\text{Regeneration efficiency (RE\%)} = \left(\frac{q_r}{q_0}\right) \times 100 \quad (1)$$

Where  $q_0$  is the chromium uptake per unit mass of original MCS sorbent and  $q_r$  is the chromium uptake per unit mass of regenerated MCS sorbent.

### 3.2.7 Analytical methods

All the samples were analyzed for chromium or manganese using flame atomic absorption spectroscopy (FAAS) with a Perkin-Elmer AAnalyst 800 system (Perkin-Elmer, Waltham, MA, USA). A chromium hollow cathode lamp (HCL) at wavelength 357.9 nm was used to detect chromium and a manganese hollow cathode lamp (HCL) at wavelength 279.5 nm was used to detect manganese. The atomic absorption calibration range of chromium and manganese were from 0.25 to 1.5 mg/L and from 0.5 to 2 mg/L, respectively. The removal efficiency of chromium on MCS was calculated as:

$$\text{Removal(\%)} = \frac{(C_0 - C_e)}{C_0} \times 100 \quad (2)$$

The adsorption of chromium onto MCS surface was determined using following equation:

$$q = \frac{(C_0 - C_e)}{m} \times V \quad (3)$$

Where  $C_0$  and  $C_e$  are the initial and equilibrium concentration of chromium in the solution (mg/L),  $q$  is the amount of chromium adsorbed per unit weight of the MCS sorbent (mg/kg),  $m$  is the weight of the MCS sorbent (kg) and  $V$  is the volume of the chromium solution (L).

### 3.3 Results and discussion

#### 3.3.1 Effect of MCS dosage

The effect of MCS dosage on Cr(III) and Cr(VI) adsorption was investigated at room temperature in the range of 2 to 30g/L. The result in Figure 3.1 showed that the chromium removal percentage increased from 15% to 98% for Cr(III) and from 11% to 91% for Cr(VI) with MCS dosage from 2 to 30g/L, while the removal of Cr(III) is slightly higher than Cr(VI) at each dosage. The removal of both chromium species experienced a significant continuing increase with the increase of sorbent dosage until the sorbent dosage reached at 20g/L. When MCS sorbent dosage was further increased to 30g/L, the adsorption of Cr(III) and Cr(VI) were merely increased by 4% for both species. The optimum dosage of MCS for chromium adsorption was fixed at 20g/L for all future studies. The increase in adsorption of Cr(III) and Cr(VI) with the increase of MCS dosage can be attributed to more available binding sites for chromium species [35].

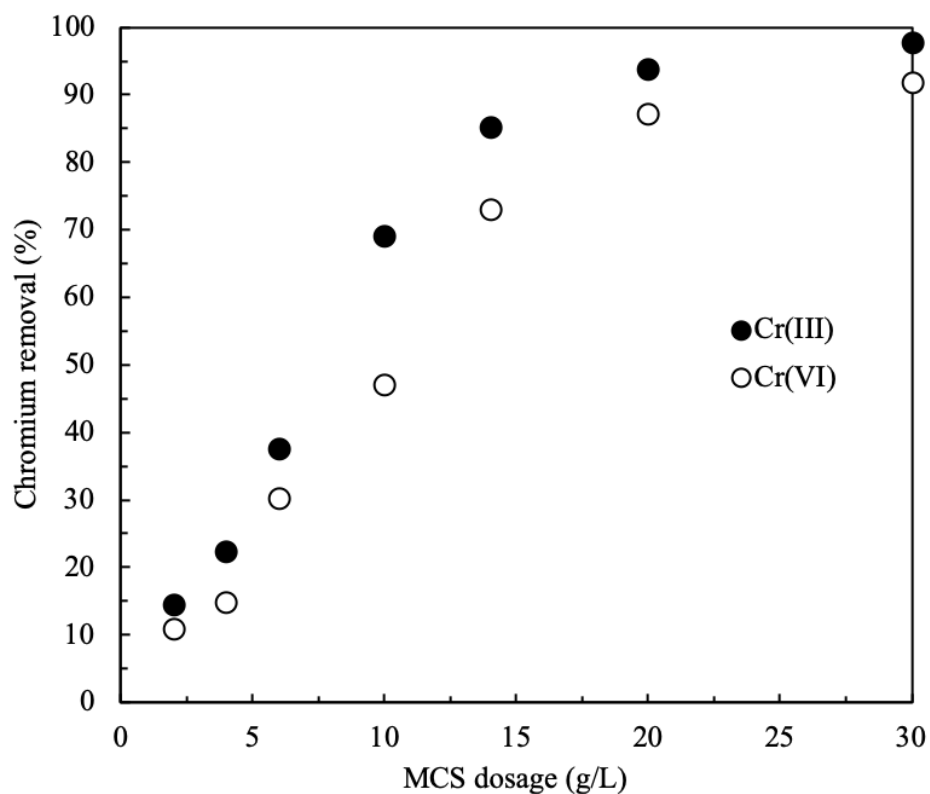


Figure 3. 1 The effect of MCS dosage on chromium removal

### 3.3.2 Isotherm studies

Various equilibrium isotherm models have been developed with different underlying thermodynamic assumptions. By applying these models into adsorption system and further obtaining the physicochemical data, we can gather valuable information in terms of the adsorption mechanism, adsorbent surface properties and adsorption capacity [36]. The Langmuir, Freundlich, Dubinin-Radushkevich (D-R) and Temkin isotherm models were used to describe the adsorption of chromium species onto the MCS sorbent.

The Langmuir empirical model assumes the adsorbent surface consists of identical and equivalent adsorption sites that only allow monolayer adsorption [37]. Moreover, there is no lateral interaction or intermolecular reaction between the adsorbed molecules. The non-linear form of Langmuir can be represented by the following equation:

$$q_e = \frac{q_m K_L C_e}{1 + K_L C_e} \quad (4)$$

Where  $C_e$  is the equilibrium concentration of chromium in solution (mg/L),  $q_e$  is the equilibrium amount of chromium adsorbed per unit weight adsorbent (mg/kg),  $q_m$  is the maximum adsorption capacity of the adsorbent (mg/kg), and  $K_L$  is Langmuir constant that related to the binding energy or affinity parameter of the adsorption system. These parameters can be determined by obtaining slope and intercept from the linear plot  $C_e/q_e$  verse  $C_e$ .

$$\frac{C_e}{q_e} = \frac{C_e}{q_m} + \frac{1}{K_L q_m} \quad (5)$$

The Freundlich isotherm model is presented to describe non-ideal and reversible adsorption process, which can be applied to multilayer adsorption on a heterogeneous adsorbent surface with variations of bonding energies. Freundlich isotherm assumes an exponential decrease of the adsorption energy with the increase of the fraction of occupied sites to account for the interactions between adsorbed molecules and surface sites heterogeneity [38]. The non-linear expression and its corresponding linear form of Freundlich isotherm can be expressed as:

$$q_e = K_F C_e^{1/n} \quad (6)$$

$$\log q_e = \log K_F + \frac{1}{n} \log C_e \quad (7)$$

Where  $K_F$  and  $n$  are Freundlich constants are indicative of adsorption capacity and strength, respectively,  $C_e$  is the equilibrium concentration of chromium in solution (mg/L), and  $q_e$  is the equilibrium amount of chromium adsorbed per unit weight adsorbent (mg/kg).

The assumption that the heat of adsorption of all the adsorbate molecules would decrease linearly with surface coverage rather than exponentially, as implied in Freundlich model, is made in the Temkin

isotherm model to take into account of interactions between adsorbent and adsorbate [39]. The empirical equation of Temkin isotherm can be represented and linearized as:

$$q_e = \frac{RT}{b} \ln (AC_e) \quad (8)$$

$$q_e = \frac{RT}{b} \ln A + \frac{RT}{b} \ln C_e \quad (9)$$

Where A(L/g) is the Temkin isotherm equilibrium binding constant corresponded to the maximum binding energy, b(J/mol) is the heat of adsorption, T is absolute temperature (K) and R is the universal gas constant (8.314J/mol/K).

The Dubinin-Radushkevich (D-R) isotherm is another empirical model which can be fitted with the adsorption equilibrium data to distinguish between the physical and chemical adsorption of metal ions by determining the mean free energy [40]. The non-linear and linear expressions of D-R isotherm model can be illustrated as follows,

$$q_e = q_s \exp(-K_{DR}\varepsilon^2) \quad (10)$$

$$\varepsilon = RT \ln \left(1 + \frac{1}{C_e}\right) \quad (11)$$

$$\ln q_e = \ln q_s - K_{DR}\varepsilon^2 \quad (12)$$

Where  $q_e$  is the equilibrium amount of chromium adsorbed per unit weight adsorbent (mg/kg),  $C_e$  is the equilibrium concentration of chromium in solution (mg/L),  $q_s$  is the theoretical maximum adsorption capacity (mg/kg),  $\varepsilon$  is Polanyi potential,  $K_{DR}$  is a constant related to the mean free energy of adsorption, T is absolute temperature (K) and R is the universal gas constant (8.314J/mol/K). The mean free energy of adsorption can be computed using the following equation,

$$E = \frac{1}{\sqrt{(2K_{DR})}} \quad (13)$$

If a calculated mean free energy (E) is less than 8kJ/mol, it would be indicative of physical sorption; if E value falls into the range of 8 to 16kJ/mol, it would suggest that the sorption process is likely chemisorption.

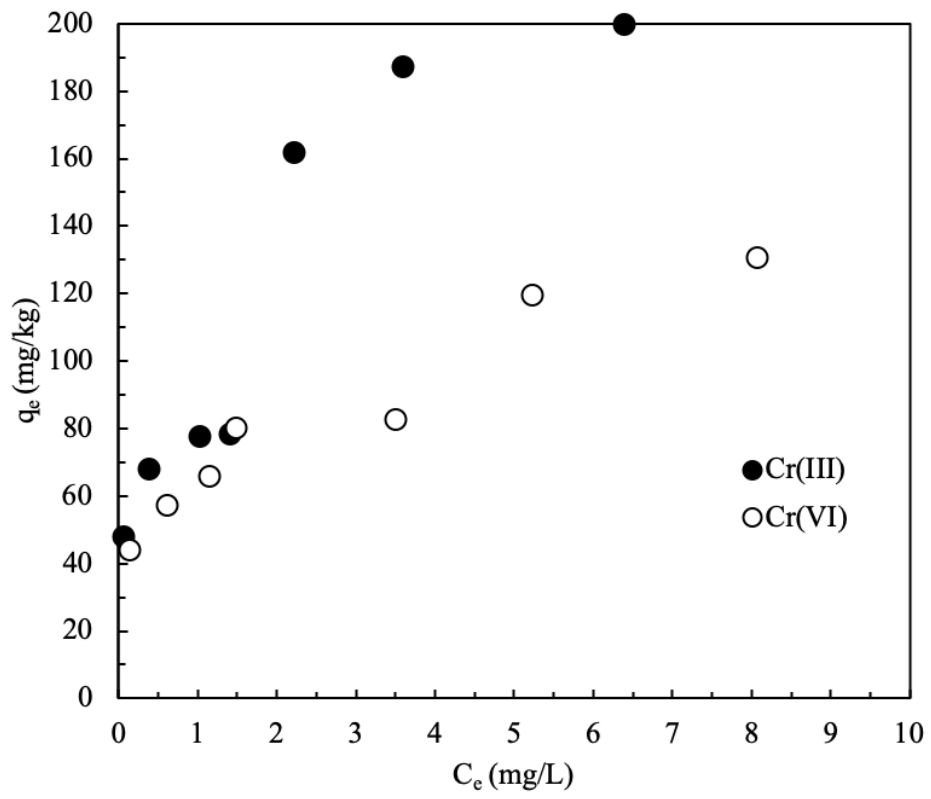


Figure 3. 2 Adsorption equilibrium isotherm data for Cr(III) and Cr(VI)

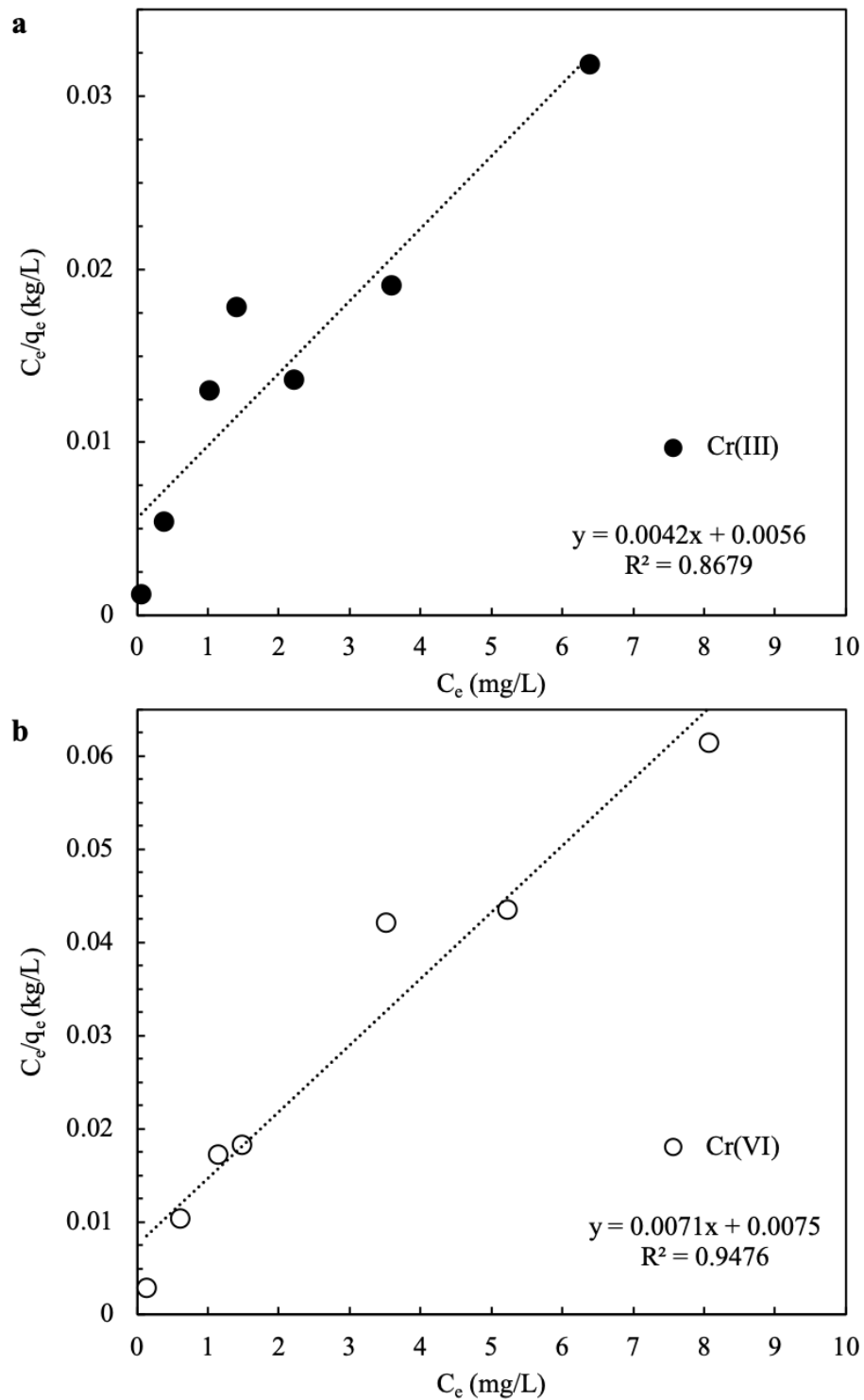


Figure 3. 3 Langmuir isotherm for (a) Cr(III) and (b) Cr(VI) adsorption onto MCS sorbent

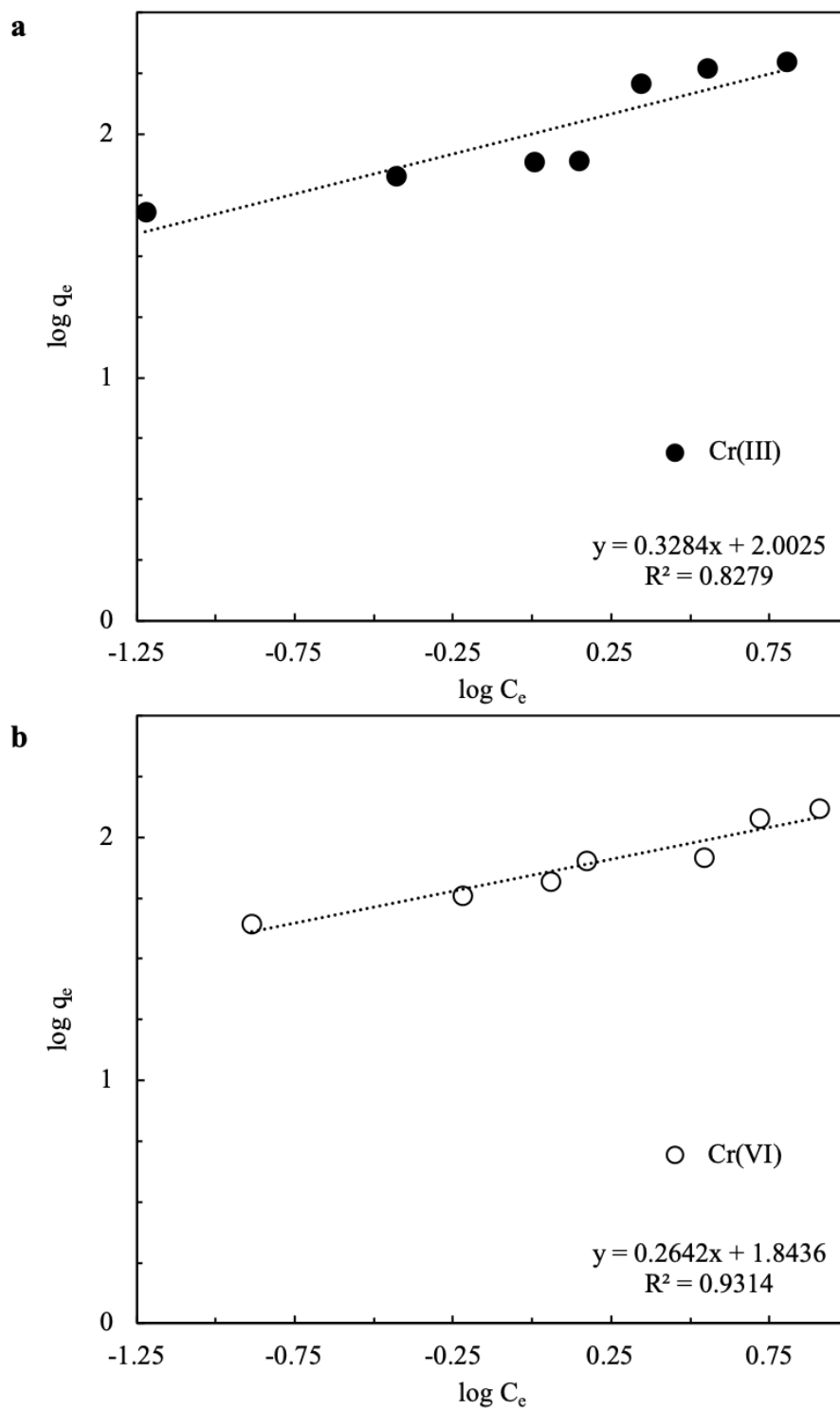


Figure 3. 4 Freundlich isotherm for (a) Cr(III) and (b) Cr(VI) adsorption onto MCS sorbent

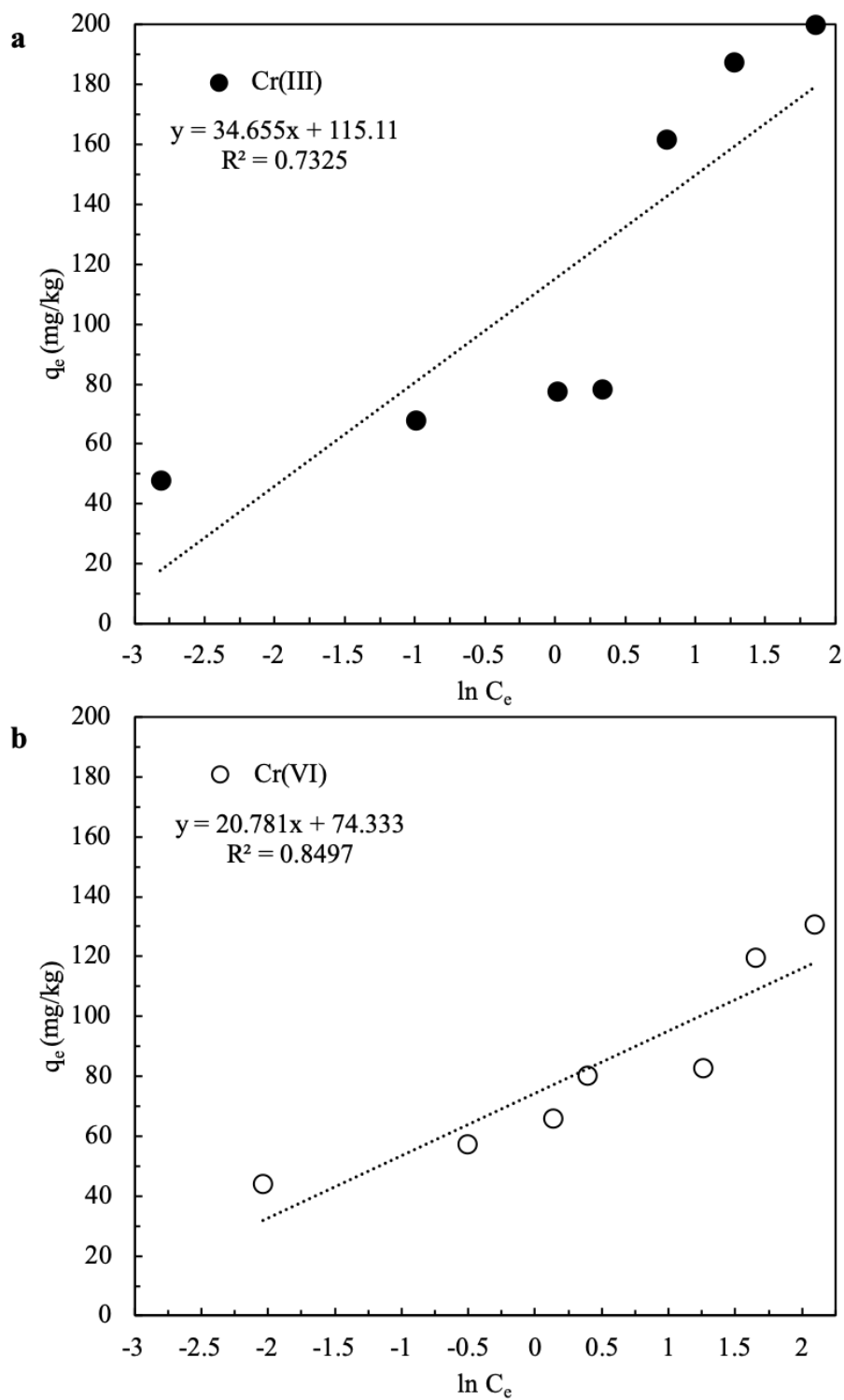


Figure 3. 5 Temkin isotherm for (a) Cr(III) and (b) Cr(VI) adsorption onto MCS sorbent

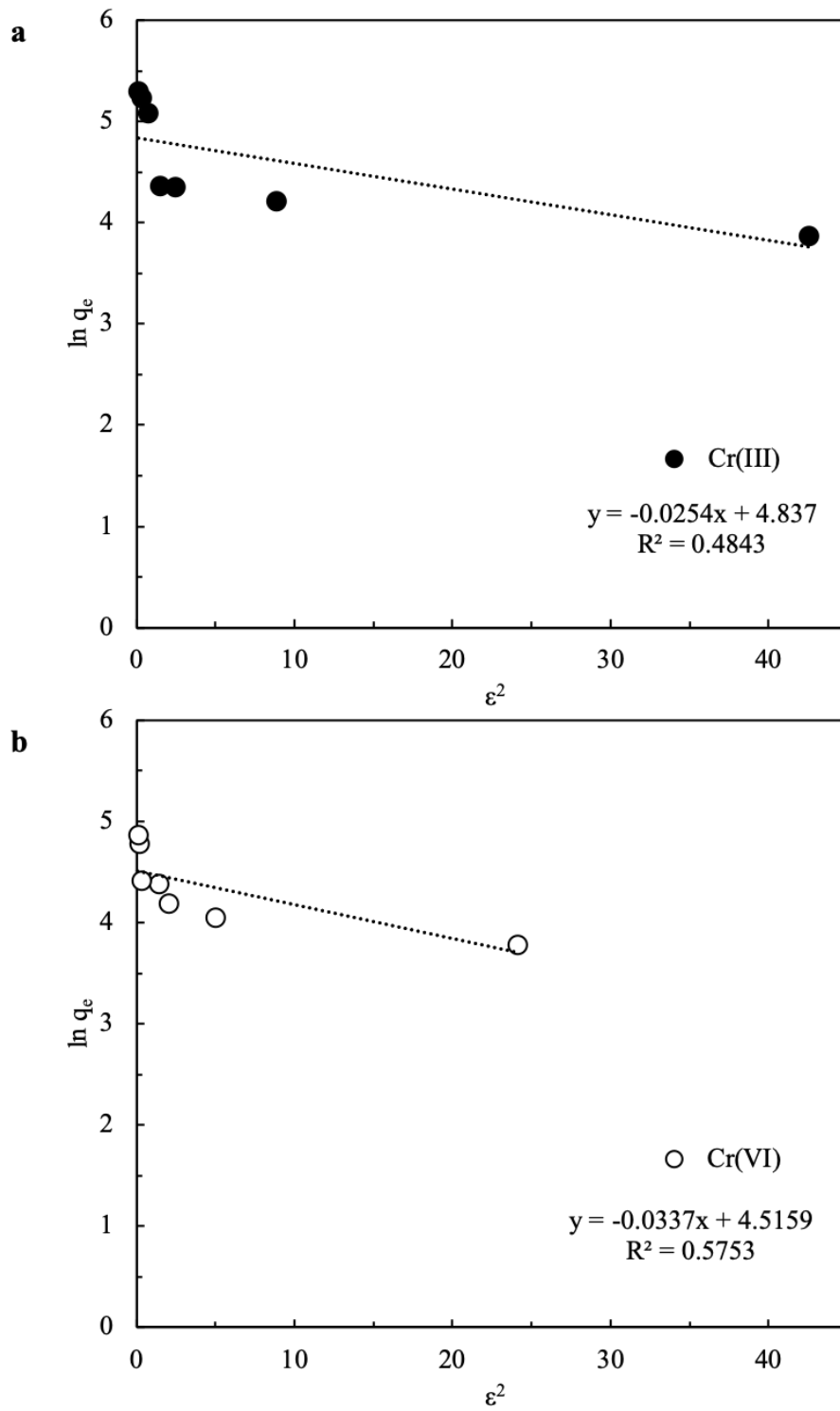


Figure 3. 6 D-R isotherm for (a) Cr(III) and (b) Cr(VI) adsorption onto MCS sorbent

Table 3. 1 Adsorption parameters for chromium adsorption onto MCS

Isotherm	Parameter	Cr(III)	Cr(VI)
Langmuir	$K_L$ (L/mg)	0.75	0.95
	$q_m$ (mg/kg)	238.1	140.85
	$R^2$	0.8679	0.9476
Freundlich	$K_F$	100.58	69.76
	$1/n$	0.3284	0.2642
	$R^2$	0.8279	0.9314
Temkin	$A$ (L/g)	27.7	35.77
	$b$ (J/mol)	65.53	109.28
	$R^2$	0.7325	0.8497
D-R	$E$ (kJ/mol)	3.85	4.43
	$R^2$	0.4843	0.5753

The parameters of the four aforementioned isotherm models obtained from adsorption equilibrium data and isotherm plots for Cr(III) and Cr(VI) onto the MCS sorbent (Figure 3.2-3.6) were presented in Table 3.1. The correlation coefficients ( $R^2$ ) of Langmuir, Freundlich, Temkin and D-R isotherms were found to be 0.8679, 0.8279, 0.7325 and 0.4843 for Cr(III) and 0.9476, 0.9314, 0.8497 and 0.5753 for Cr(VI), respectively. The higher value of  $R^2$  suggests a better fit isotherm model for adsorption of chromium onto MCS, indicating that the application of Langmuir and Freundlich isotherm models provided a more satisfactory fit to the experimental data for adsorption of both chromium species than Temkin and D-R isotherm models. The maximum adsorption capacity ( $q_m$ ) of MCS toward Cr(III) and Cr(VI) were calculated to be 238.1 mg/kg and 140.85 mg/kg according to Langmuir isotherm model, respectively. The Langmuir constant ( $K_L$ ) related to free energy of adsorption was determined to be 0.75 L/mg for Cr(III) and 0.95 L/mg for Cr(VI), respectively, and the greater  $K_L$  value for Cr(VI) indicates that MCS has a relatively stronger binding toward Cr(VI) [41]. The Freundlich parameter  $1/n$  for both chromium species were found to be between 0.1-0.5, 0.3284 for Cr(III) and 0.2642 for Cr(VI), suggesting that adsorption of chromium onto MCS is a favorable adsorption and adsorption of Cr(VI) is slightly more favorable than adsorption of Cr(III) for MCS developed in this study [42]. The similar high  $R^2$  values of adsorption of Cr(III) and Cr(VI) for both Langmuir and Freundlich isotherms could

imply that adsorption of chromium is monolayer on MCS surface and MCS surface is likely a heterogeneous surface [43]. The values of Temkin constant  $A$  and  $b$ , related to binding energy and heat of adsorption, respectively, were both larger for Cr(VI) than Cr(III) which is indicative of a more favorable and stronger binding of Cr(VI) than Cr(III) for the MCS sorbent [41], [44]. The mean free energy for adsorption of Cr(III) and Cr(VI) onto the MCS sorbent calculated based on Dubinin-Radushkevich isotherm were 3.85 kJ/mol and 4.43 kJ/mol, respectively, indicating that the nature of adsorption of chromium onto MCS sorbent is governed by physisorption and MCS shows a stronger binding toward Cr(VI). However, the  $R^2$  values for both chromium species, 0.4843 for Cr(III) and 0.5753 for Cr(VI), are significantly lower than Langmuir, Freundlich and Temkin isotherms, suggesting that the adsorption of chromium onto MCS might not fit to Dubinin-Radushkevich isotherm. While the maximum adsorption capacity ( $q_m$ ) obtained from Langmuir isotherm is in good agreement with the Freundlich parameter  $K_F$  showing that MCS obtains higher adsorption capacity for Cr(III) than Cr(VI), the Langmuir constant ( $K_L$ ), Freundlich parameter ( $1/n$ ), heat of adsorption ( $b$ ) and binding constant ( $A$ ) obtained from Temkin isotherm, and the mean free energy ( $E$ ) calculated from D-R equation suggest that MCS sorbent displays a greater affinity for Cr(VI) than Cr(III).

Table 3.2 and 3.3 summarized the maximum capacity of several other metal oxides based adsorbents for adsorption of Cr(VI) and Cr(III), respectively. The results show that the MCS sorbent developed in this study exhibits comparable or greater adsorption capacity than most of the adsorbents listed when the adsorption capacity is reported based on sorbent area instead of sorbent mass. MCS obtains a relatively lower adsorption capacity per sorbent mass compared to other adsorbents mainly because of the limited surface area. However, the advantages of MCS are low-cost and convenient production process compared to other adsorbents with large surface area and multi-functionality allowing the application of MCS into water treatment system as an affordable and environmental benign filter media [31], [42].

Table 3. 2 Adsorption capacity of different metal oxides based adsorbents for Cr(VI)

Adsorbent	pH	Initial Cr(VI) Concentration (mg/L)	Adsorbent Dosage (g/L)	Specific Surface Area (m <sup>2</sup> /g)	Adsorption Capacity (mg/kg)	Adsorption Capacity per Surface Area(μg/m <sup>2</sup> )	Reference
Manganese dioxide	7.1	520	16.7	15.8	1450	92	[45]
Iron-manganese coated sand	5	10	2	3.06	102	33.3	[42]
Mn nodule leached residue	3	10	2	109.17	25780	236	[46]
Pyrolusite (MnO <sub>2</sub> )	6.9	5	2	7.2	250	34.7	[47]
Anatase (TiO <sub>2</sub> )	2.5	10	1	37.8	7380	195	[48]
Iron oxide (Fe <sub>2</sub> O <sub>3</sub> )	8	1	4	1.7	89	52.4	[49]
Bentonite	2	50	0.52-52	34	570	16.8	[50]
Activated alumina	4	10	10	370	3120	8.4	[51]
Mn-coated sand	6	1	20	3.08	140.85	45.73	This study

Table 3. 3 Adsorption capacity of different metal oxides based adsorbents for Cr(III)

Adsorbent	pH	Initial Cr(III) Concentration (mg/L)	Adsorbent Dosage (g/L)	Specific Surface Area (m <sup>2</sup> /g)	Adsorption Capacity (mg/kg)	Adsorption Capacity per Surface Area(μg/m <sup>2</sup> )	Reference
Bentonite	3.5	52	50	34	1280	37.65	[50]
Iron-oxide nanocomposites (Fe <sub>3</sub> O <sub>4</sub> )	5.4	10	1	970	36920	38.06	[52]
Boehmite nanoplates (γ-AlOOH)	13	10	1	52.22	1250	23.79	[53]
Montmorillonite	5	100	5	240	3600	15	[54]
Mn-coated sand	6	1	20	3.08	238.1	77.31	This study

### 3.3.3 Effect of pH

pH is an important parameter controlling the adsorption process of heavy metal in water body due to that solution pH significantly affects surface protonation process and surface charge of the sorbent, redox potential between sorbent and metal ion species and the extant format of the metal ion species in solution [47], [55]–[57]. Cr(VI) mainly appears as dissolved species bichromate ( $\text{HCrO}_4^-$ ) or chromate ( $\text{CrO}_4^{2-}$ ) when pH is greater than 3, while Cr(III) may precipitate as insoluble species  $\text{Cr}(\text{OH})_3$  at the same pH range or possibly form soluble species such as  $\text{Cr}(\text{OH})^{2+}$  or  $\text{Cr}(\text{OH})_2^+$  at pH range of 4-7.5 or  $\text{Cr}(\text{OH})_4^-$  with excessive presence of hydroxide ions (pH greater than 10) [2].

The pH effect on the adsorption of chromium was investigated with a sorbent dosage of 20g/L at room temperature over the pH range of 2-12. Figure 3.7 demonstrates adsorption of Cr(III) and Cr(VI) onto the MCS sorbent with variation of the solution pH. It can be observed that adsorption for both chromium species initially increased with pH increasing from 2 to 4 and reached a plateau until pH was further increased to 11, after which the adsorption capacity for Cr(III) and Cr(VI) experienced a significant loss. The removal of Cr(III) increased sharply from 60% to 92% at the pH range of 2-4, while the removal of Cr(VI) increased from 50% to 89% at the same pH range. This result may be attributed to the excessive leaching of manganese ion ( $\text{Mn}^{2+}$ ) from MCS sorbent at extremely acid environment (pH less than 3) therefore reducing the available adsorption sites for chromium species [27]. The possible formation of  $\text{Cr}(\text{OH})_4^-$  and the competition between  $\text{Cr}(\text{OH})_4^-$  and  $\text{OH}^-$  for adsorption sites may result in the major loss of adsorption capacity of Cr(III) above pH 10 [2]. Adsorption of Cr(VI), an oxyanion in the studied pH range, decreased drastically from 86% to 35% when pH was increased from 10 to 11, which may result from the reversal of surface charge.

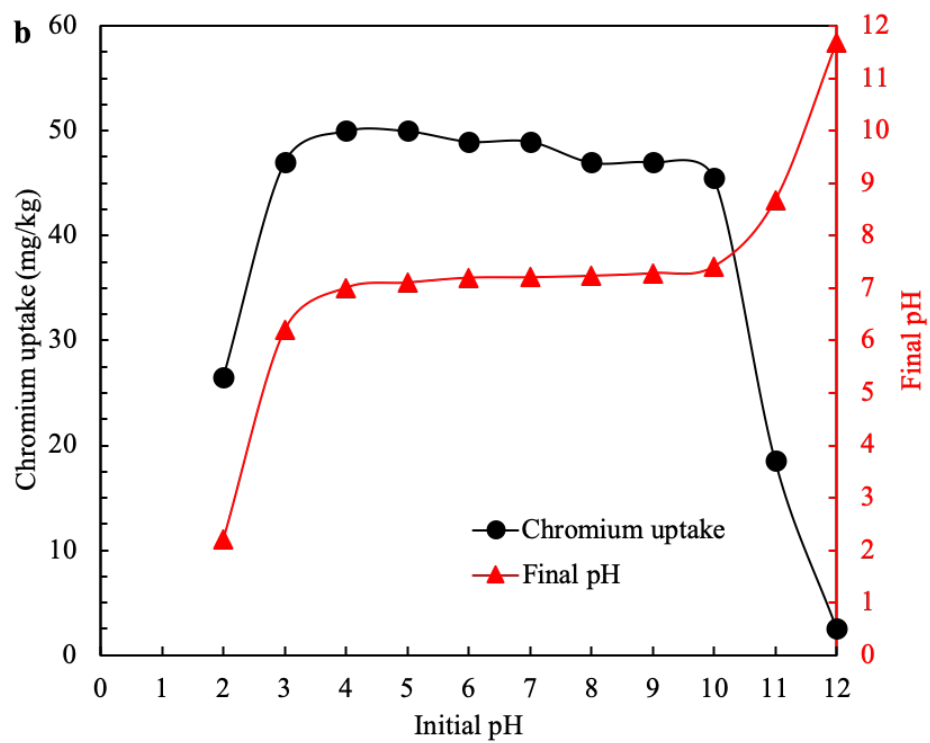
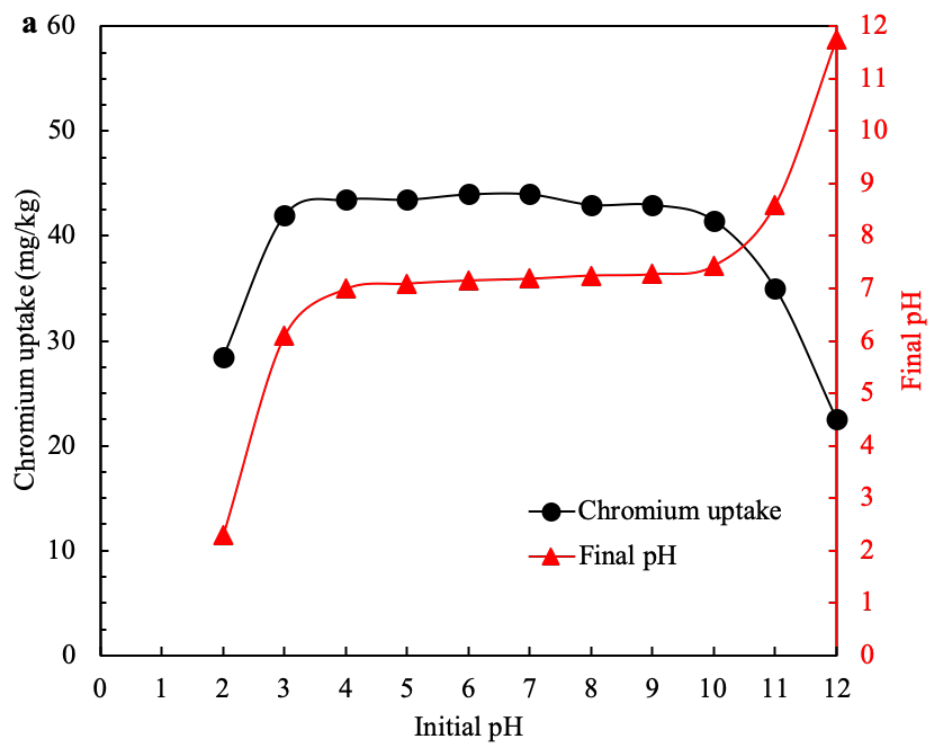


Figure 3. 7 Adsorption of chromium onto MCS as function of pH: (a) Cr(III) and (b) Cr(VI)

### 3.3.4 Effect of surface charge

The pH-dependent behavior of heavy metal adsorption onto metal oxides based adsorbents can be attributed to sorbent surface charge obtained from pH-dependent surface protonation or deprotonation process [58]. The zeta potential ( $\zeta$ ) measurement is a characterization technique to quantify the net surface charge of sorbent surface. The point of zero charge (PZC) is the pH of the solution at which the net charge of sorbent surface is zero [59]. To understand adsorption process between the two chromium species with the surface of the MCS sorbent, the zeta potential of the MCS sorbent was measured using 5g/L MCS in an aqueous solution containing 1mM NaCl with and without the chromium species. As shown in Figure 3.8, the  $\text{pH}_{\text{PZC}}$  of the MCS sorbent was determined to be 7.80 in the absence of chromium, 9.25 in the presence of Cr(III) species and 10.25 in the presence of Cr(V) species. The surface of the MCS sorbent will be positively charged at pH values below  $\text{pH}_{\text{PZC}}$  and negatively charged at pH values above  $\text{pH}_{\text{PZC}}$ . A major shift in PZC of the MCS sorbent can be observed for both chromium species.

Cr(III) can form soluble cationic species such as  $\text{Cr}^{3+}$ ,  $\text{Cr}(\text{OH})^{2+}$  or  $\text{Cr}(\text{OH})_2^+$  at pH range of 2-7.5 or soluble anionic species  $\text{Cr}(\text{OH})_4^-$  with excessive presence of hydroxide ions (pH greater than 10) or as insoluble neutral species  $\text{Cr}(\text{OH})_3$  at pH range of 8-12. Since electrostatic attraction between Cr(III) species and positively charged MCS surface is negligible at the pH range of 2-9.25, the significant shift in the PZC of the MCS sorbent in presence of Cr(III) is indicative of the occurrence of specific adsorption or inner-sphere adsorption because specific adsorbed ions generally reside inside of the shear plane therefore changing the surface charge [60]. The drastic decrease of Cr(III) removal above  $\text{pH}_{\text{pzc}}$  (9.25) observed from the pH study section may result from the occurrence of anionic species  $\text{Cr}(\text{OH})_4^-$  or possible transformation from cationic Cr(III) species to anionic Cr(VI) species. Cr(VI) appears mainly as soluble anionic species chromate ( $\text{CrO}_4^{2-}$ ) or bichromate ( $\text{HCrO}_4^-$ ) at pH from 2 to 12. The significant loss in Cr(VI) adsorption can be observed when pH reached at 11 and this observation is in good agreement with the fact that  $\text{pH}_{\text{pzc}}$  for Cr(VI) is determined to be 10.25, above which the electrostatic

repulsion between negatively charged MCS surface and anionic Cr(VI) species will greatly reduce the adsorption of Cr(VI). Specific adsorption or inner-sphere adsorption can be inferred from the significant shift to the right in PZC of the MCS sorbent for adsorption of Cr(VI). In order to gather more information regarding the adsorption mechanism between the MCS sorbent and chromium species, further surface characterization is necessary to determine the possible redox reaction taken place on the MCS sorbent surface.

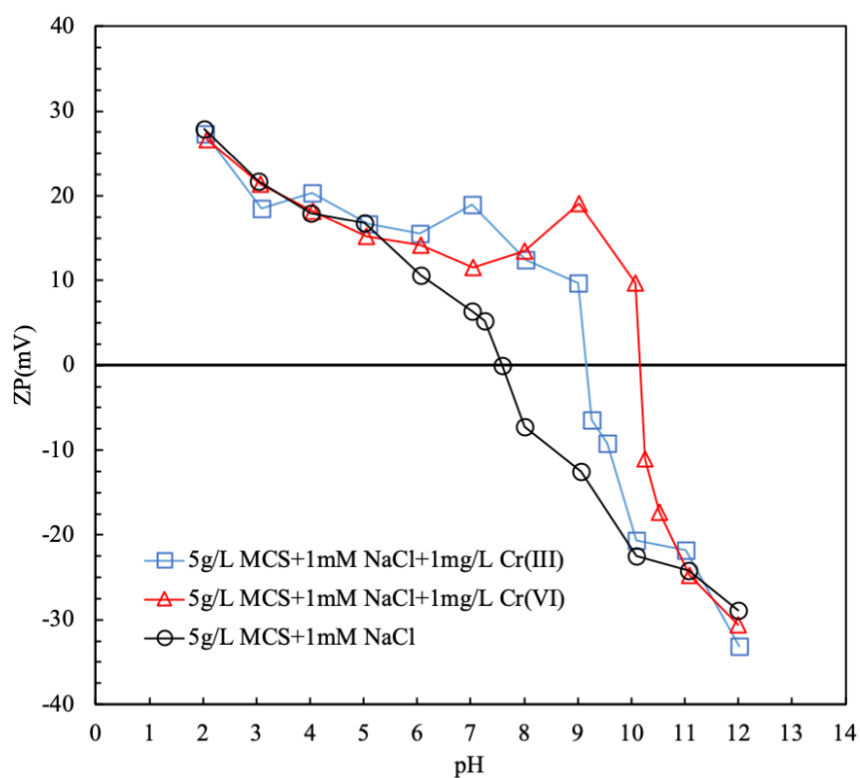


Figure 3. 8 Zeta potential of the MCS sorbent in the presence of Cr(III) and Cr(VI)

### 3.3.5 Effect of contacting time and adsorption kinetic study

Sorption kinetics describes the rate of the adsorption of heavy metal onto adsorbents and can provide crucial information regarding the adsorption mechanism [61]. The rate of chromium adsorption is an important parameter for the application of MCS sorbent as a filter media in practical water treatment operation. The equilibrium time for both Cr(III) and Cr(VI) can be obtained from effect of contact time on adsorption of Cr(III) and Cr(VI) onto MCS sorbent illustrated in Figure 3.9. The results showed that the adsorption for Cr(III) and Cr(VI) rapidly reached at 59% and 50%, respectively, at the first 30 min, then gradually increased from 59% to 90% for Cr(III) and from 50% to 80% when contact time was raised from 30 min to 4 hr. The adsorption equilibrium was approached for both chromium species after contact time further increased to 6 hr. The adsorption for chromium species onto MCS sorbent increased merely 1~2% for additional 18 hr. 91% Cr(VI) was adsorbed at equilibrium and the equilibrium adsorption capacity of MCS sorbent was determined to be 51 mg/kg for Cr(VI), while 94% Cr(III) was adsorbed at equilibrium and the equilibrium adsorption capacity of MCS sorbent was calculated to be 55 mg/kg for Cr(III). All the future experiments were carried out with contact time of 24 hr to ensure the adsorption equilibrium was reached between chromium species and the MCS sorbent.

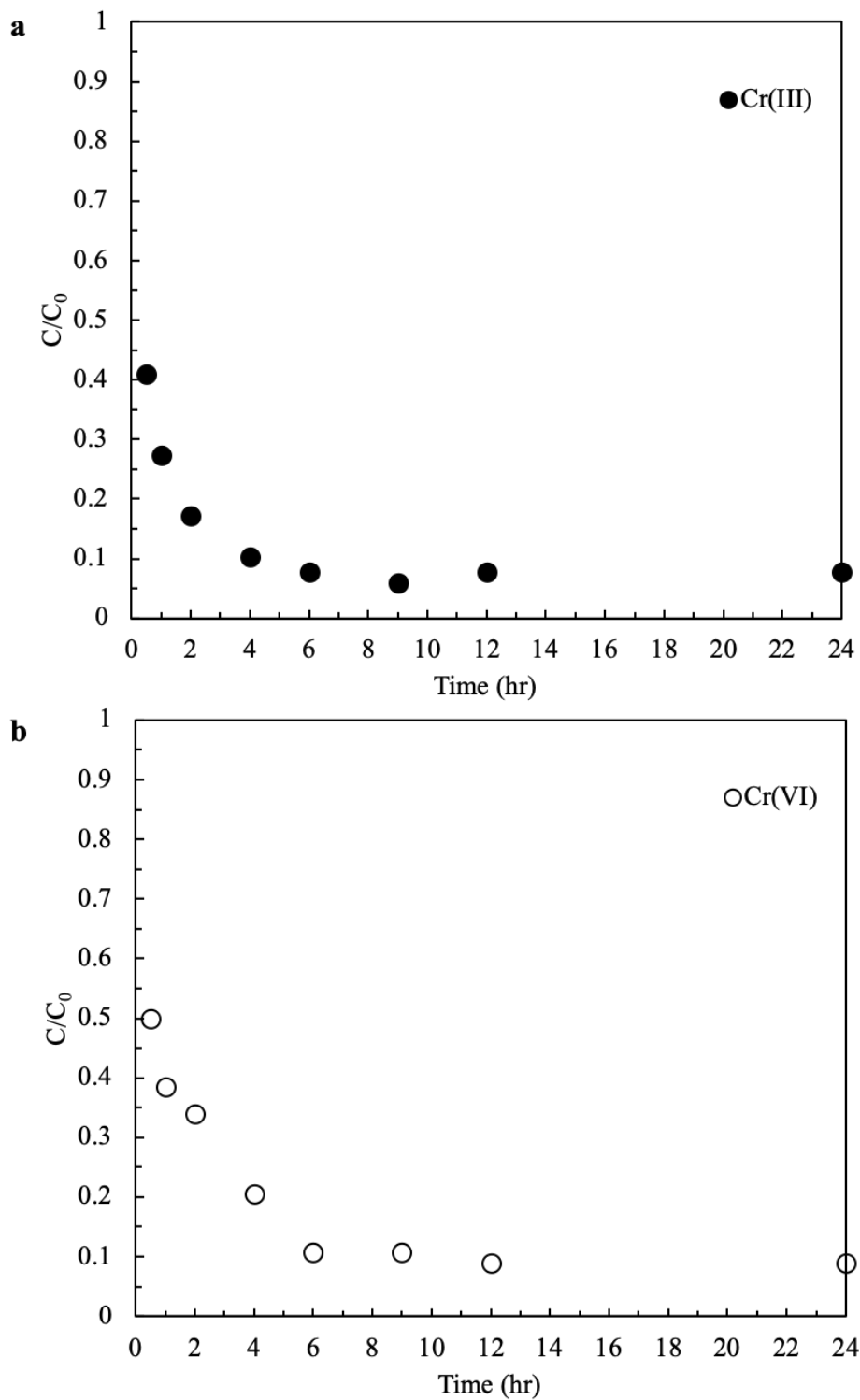


Figure 3. 9 Effect of contact time on adsorption of (a) Cr(III) and (b) Cr(VI) onto MCS sorbent

The experimental data were fitted to three widely used kinetic models: pseudo-first order, pseudo-second order and intraparticle diffusion models to evaluate kinetic mechanism of chromium adsorption onto the MCS sorbent (Figure 3.10-3.12). These kinetic models haven been vastly applied for the adsorption of adsorbates in liquid phase such as heavy metals and organic compounds onto variety of adsorbents including activated carbon, mineral clay, agricultural by-products and metal oxides based adsorbents [62]–[65].

Pseudo-first order model was originally presented by Lagergren to describe the kinetics of the adsorption of adsorbate in aqueous solution onto solid adsorbent surfaces based on adsorbent adsorption capacity [66]. Pseudo-first order equation can be expressed in its differential and integral forms as following,

$$\frac{dq_t}{dt} = k_1(q_e - q_t) \quad (14)$$

$$\ln(q_e - q_t) = \ln q_e - k_1 t \quad (15)$$

Where  $q_e$  is the amount of chromium adsorbed per unit weight adsorbent at equilibrium (mg/kg),  $q_t$  is the amount of chromium adsorbed per unit weight adsorbent at time  $t$  (mg/kg), and  $k_1$  is the rate constant of pseudo-first order adsorption in  $\text{min}^{-1}$ . Studies show that the sorption kinetics of chromium onto adsorbents such as peat, activated carbon, and manganese oxide was better described by the pseudo-second order kinetic model [16], [67]–[69]. The pseudo-second kinetic equation can be written and linearized as follows,

$$\frac{dq_t}{dt} = k_2(q_e - q_t)^2 \quad (16)$$

$$\frac{t}{q_t} = \left(\frac{1}{k_2}\right)\left(\frac{1}{q_e^2}\right) + \frac{t}{q_e} \quad (17)$$

Where  $k_2$  is the rate constant of pseudo-second order adsorption in  $\text{kg}\cdot\text{mg}^{-1}\cdot\text{min}^{-1}$  and can be calculated from the intercept of a linear plot of  $t/q_t$  versus time.

The intraparticle diffusion model was initially proposed by Weber and Morris to describe the adsorption of organic compounds on granular carbon [70]. Sorption process between adsorbate-adsorbent in liquid-solid system generally involves four consecutive steps:

(i) adsorbate transport in bulk solution; (ii) adsorbate diffusion on the liquid film formed around external surface of the adsorbent particles (film diffusion); (iii) adsorbate diffusion on the internal surface of pores and along the pore walls of the adsorbent (intraparticle diffusion); (iv) adsorption on active sites [71]. Single or combination of any of the four aforementioned steps could be the rate-controlling step. The effect of adsorbate transport could be easily eliminated by rapid mixing and adsorption itself generally takes place instantaneously, suggesting that film diffusion and intraparticle diffusion likely control the adsorption rate [72]. If intraparticle diffusion is the rate-limiting step for the adsorption of chromium onto the MCS sorbent, the adsorption data would abide the following equation:

$$q_t = k_{id}t^{\frac{1}{2}} + C \quad (18)$$

Where  $k_{id}$  is the rate constant of intraparticle diffusion in  $\text{mg}\cdot\text{kg}^{-1}\cdot\text{min}^{-1/2}$  and  $C$  represents the thickness of the boundary layer. We can obtain the value of  $k_{id}$  and  $C$  by plotting  $q_t$  against  $t^{1/2}$ .

The kinetic parameters calculated based on these three different kinetic models for adsorption of chromium onto the MCS sorbent were tabulated in Table 3.4. The calculated correlation coefficients ( $R^2$ ) of pseudo-second order kinetics are the highest for both chromium species, 0.9996 for Cr(III) and 0.9984 for Cr(VI). The theoretical  $q_e$  values derived from pseudo-second order kinetics model for Cr(III) and Cr(VI) are 55.87 mg/kg and 53.76 mg/kg, respectively, and these values are extremely close to the experimental values of Cr(III) adsorption capacity of 55 mg/kg and Cr(VI) adsorption capacity of 51mg/kg. The pseudo-first order kinetics model also provides the relatively high values  $R^2$  of 0.9809 for Cr(III) and 0.9773 for Cr(VI). However, the theoretical  $q_e$  values of 23.92 mg/kg for Cr(III) and 25.88 mg/kg for Cr(VI) obtained from pseudo-first order model were significantly different from the

experimental data. Therefore, adsorption of Cr(III) and Cr(VI) onto MCS sorbent can be better described by pseudo-second order kinetics as compared to pseudo-first order kinetics, indicating that there are possibly more than one rate-limiting steps [73]. The  $R^2$  values obtained from intraparticle diffusion model is the lowest among three kinetic models employed in this study, 0.7586 for Cr(III) and 0.9071 for Cr(VI). It can be observe from Figure 3.12 that the straight line plots of  $q_t$  versus  $t^{1/2}$  did not pass through origin for both chromium and have intercept values of 35.752 and 25.341 for Cr(III) and Cr(VI), respectively. This observation can be indicative of that intraparticle diffusion of chromium species into pores of the MCS sorbent is not the only rate-controlling step for this particular adsorption process [32]. The plots of  $q_t$  versus  $t^{1/2}$  can be divided into two distinct portions: the initial steep slope portion that is related to film diffusion and final gradual portion that is related to intraparticle diffusion [74]. Therefore, it can be established that both film diffusion and intraparticle diffusion are involved in the overall adsorption mechanism.

Table 3. 4 Adsorption kinetic parameters of chromium on MCS sorbent

Kinetics Model	Parameter	Cr(III)	Cr(VI)
Pseudo-first order	$k_1$ ( $\text{min}^{-1}$ )	0.0097	0.0057
	$q_e$ (mg/kg)	23.92	25.88
	$R^2$	0.9809	0.9773
Pseudo-second order	$k_2$ ( $\text{kg}\cdot\text{mg}^{-1}\cdot\text{min}^{-1}$ )	0.00107	0.0048
	$q_e$ (mg/kg)	55.87	53.76
	$R^2$	0.9996	0.9984
Intraparticle diffusion	$k_{id}$ ( $\text{mg}\cdot\text{kg}^{-1}\cdot\text{min}^{-1/2}$ )	0.8346	1.0818
	C	35.752	25.341
	$R^2$	0.7586	0.9071

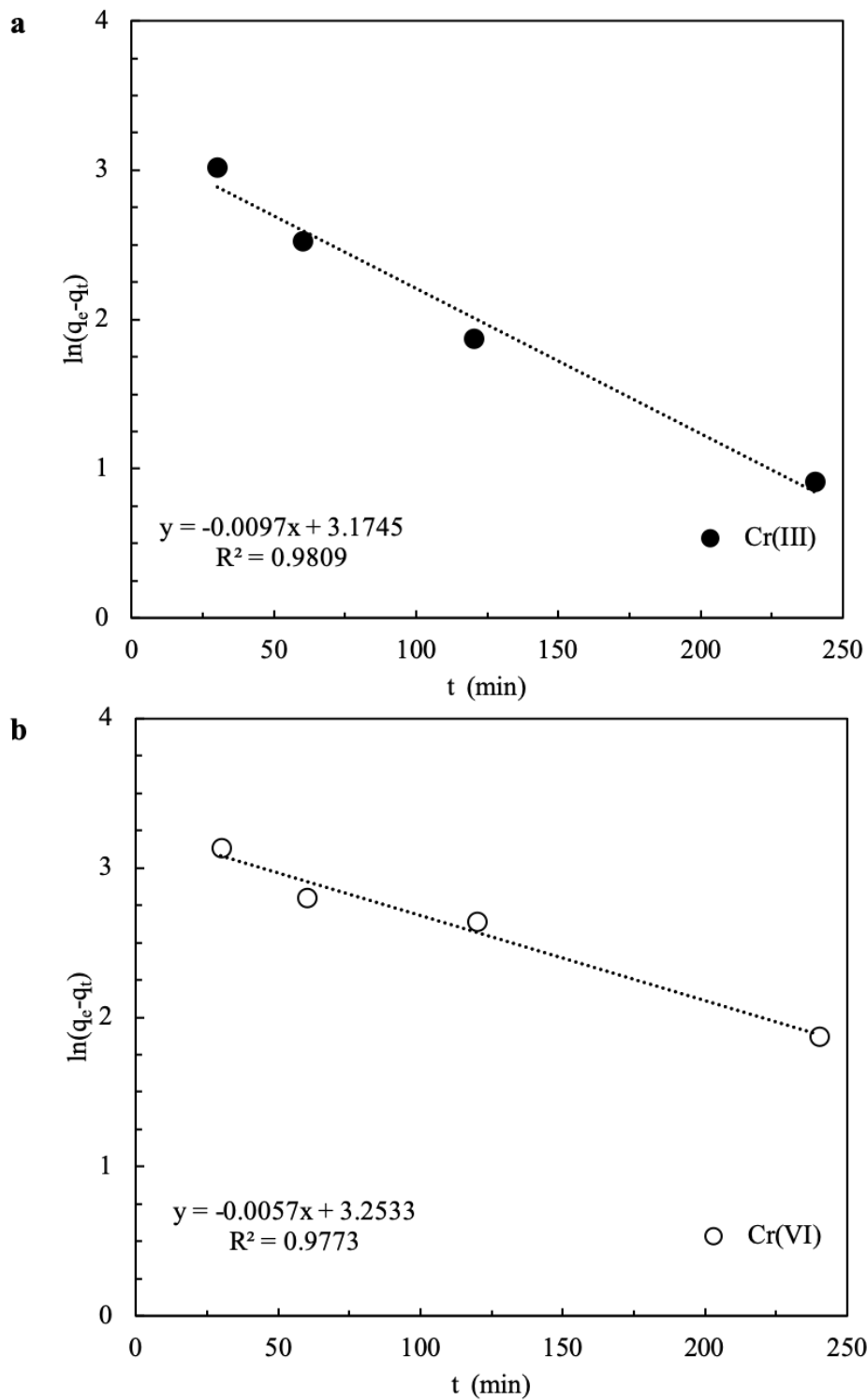


Figure 3. 10 Pseudo-first order kinetic plots for the sorption of (a) Cr(III) and (b) Cr(VI)

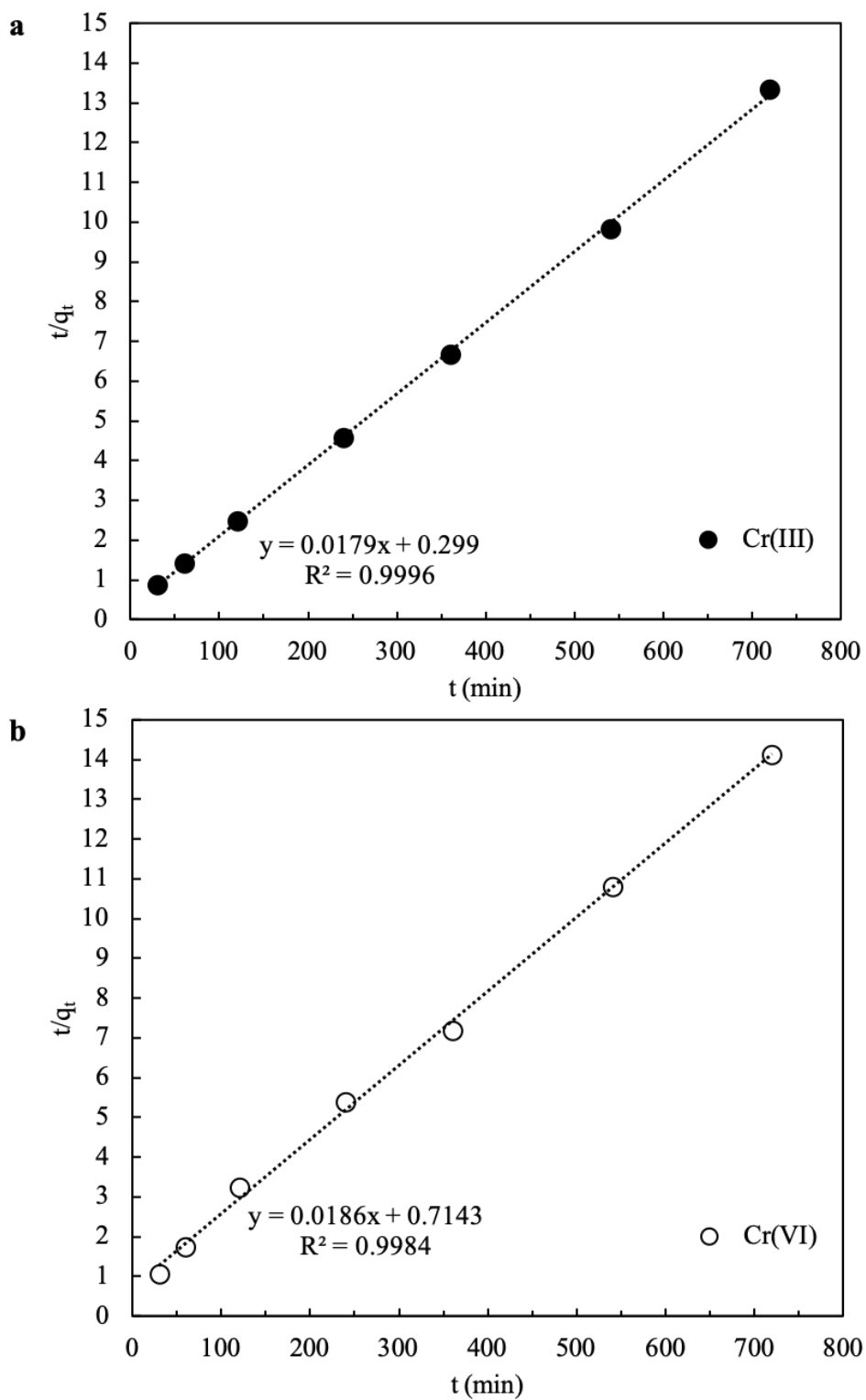


Figure 3. 11 Pseudo-second order kinetic plots for the sorption of (a) Cr(III) and (b) Cr(VI)

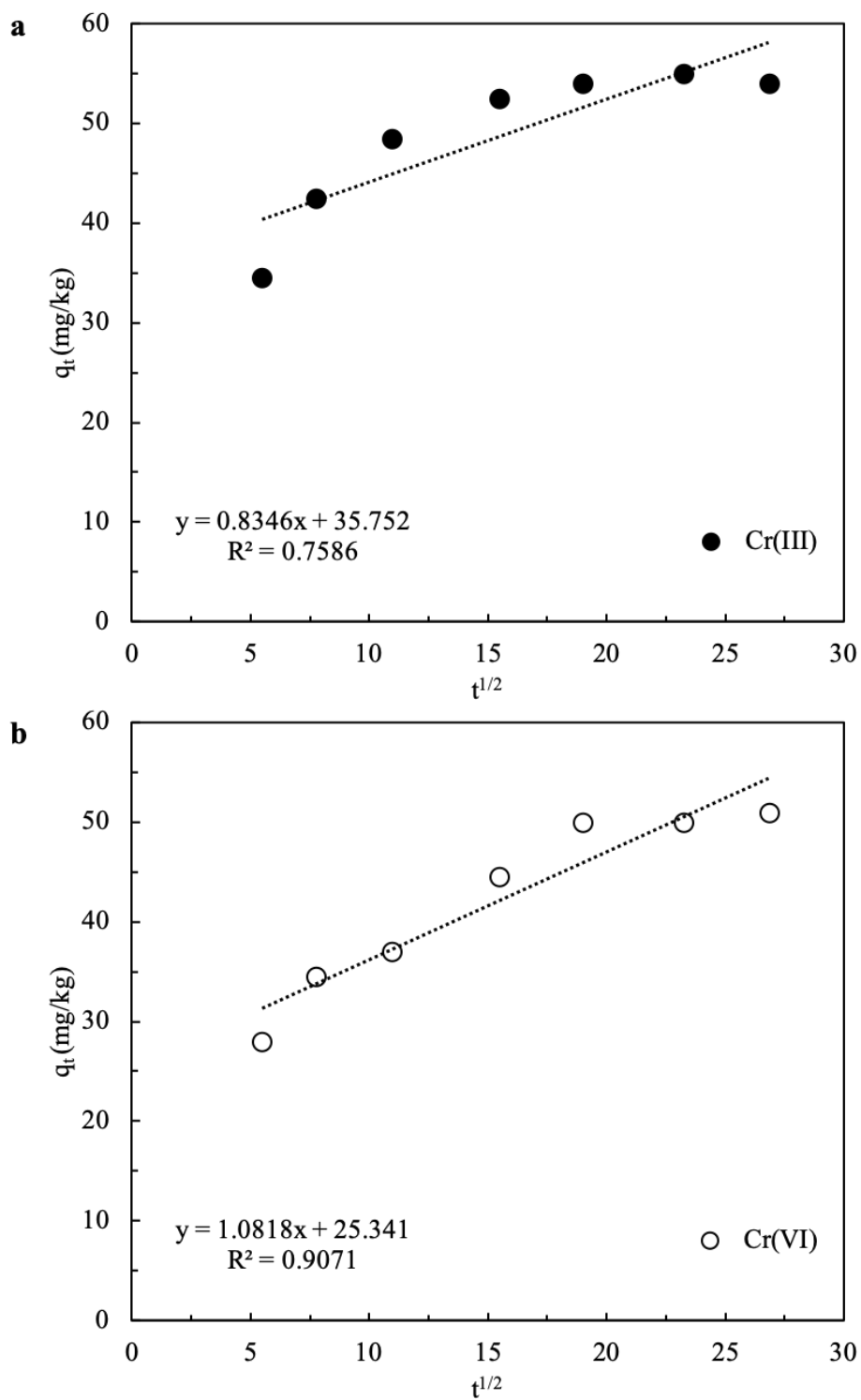


Figure 3. 12 Intraparticle diffusion kinetic plots for the sorption of (a) Cr(III) and (b) Cr(VI)

### 3.3.6 Effect of coexisting ions

In order to investigate the effects of the presence of other cations or anions may accompanying with the appearance of chromium in surface water or industrial wastewater, cation such as calcium ( $\text{Ca}^{2+}$ ) and anions such as bicarbonate ( $\text{HCO}_3^-$ ), sulfate ( $\text{SO}_4^{2-}$ ) and phosphate ( $\text{PO}_4^{3-}$ ) were selected as coexisting ions in this study. Figure 3.13-3.16 illustrate the effects of  $\text{Ca}^{2+}$ ,  $\text{HCO}_3^-$ ,  $\text{SO}_4^{2-}$  and  $\text{PO}_4^{3-}$  at different concentrations on adsorption process of chromium onto MCS. The coexisting ions could have negative influence on the removal of chromium due to the possible competition for available active adsorption sites and the possible alteration of surface charge [75].

The results in Figure 3.13 show that the existence of  $\text{Ca}^{2+}$  has no significant effect on the adsorption of Cr(VI), while the existence of  $\text{Ca}^{2+}$  has significantly negative influence on the adsorption of Cr(III) and with the increasing concentration of  $\text{Ca}^{2+}$  from 0.5 mmol/L to 2mmol/L, the adsorption of Cr(III) decreased sharply from 74% to 52%. Similar results observed from the adsorption of Cr(VI) using chitosan-coated fly ash composite as adsorbent can be attributed to the electrostatic repulsion between cations such as  $\text{Ca}^{2+}$  and  $\text{Mg}^{2+}$  and positively charged sorbent surface, therefore leaving the adsorption sites available for Cr(VI) oxyanions [76]. In contrast to Cr(VI) species, the adsorption of Cr(III), appearing as cationic species at studied pH, could be severely hampered due to that the increasing ionic strength can decrease the electrostatic force between oppositely charged adsorbate-adsorbent and reduce the available sorption sites by inducing the aggregation of the adsorbent [75].

The coexistence of anions ( $\text{HCO}_3^-$ ,  $\text{SO}_4^{2-}$  and  $\text{PO}_4^{3-}$ ) do not have significant effects on the adsorption of Cr(III) onto the MCS sorbent, while the effects on the adsorption of Cr(VI) follow the order:  $\text{PO}_4^{3-} > \text{HCO}_3^- > \text{SO}_4^{2-}$ . Zeng et al [77] reported the same trend of coexisting ions effects for Cr(VI) adsorption on hexadecylpyridinium bromide (HDPB) modified natural zeolites. It can be observed from Figure 3.14 that the increasing concentration of  $\text{HCO}_3^-$  from 0.5 mmol/L to 5.5 mmol/L promoted the adsorption of Cr(III) greatly, while adsorption of Cr(VI) was significantly inhibited. The observation can be related to

the pH effect and competitive adsorption caused by addition of  $\text{HCO}_3^-$ . With the increasing concentration of  $\text{SO}_4^{2-}$  from 0 to 1 and 2 mmol/L and  $\text{PO}_4^{3-}$  from 0 to 1 and 3 mmol/L, the removal of Cr(VI) decreases from 91% to 53% and 44% and from 91% to 43% and 3%, respectively. Sulfate and phosphate ions both share a similar molecular structure with chromate ions as oxyanions resulting in significant competitive effect on Cr(VI) adsorption onto the MCS sorbent. The result that  $\text{PO}_4^{3-}$  had the strongest influence on Cr(VI) adsorption could be explained by that  $\text{PO}_4^{3-}$  ions possess the most negative charge among all the anions selected for this study and become a stronger competing force for sorption sites available on the surface of the MCS sorbent [77].

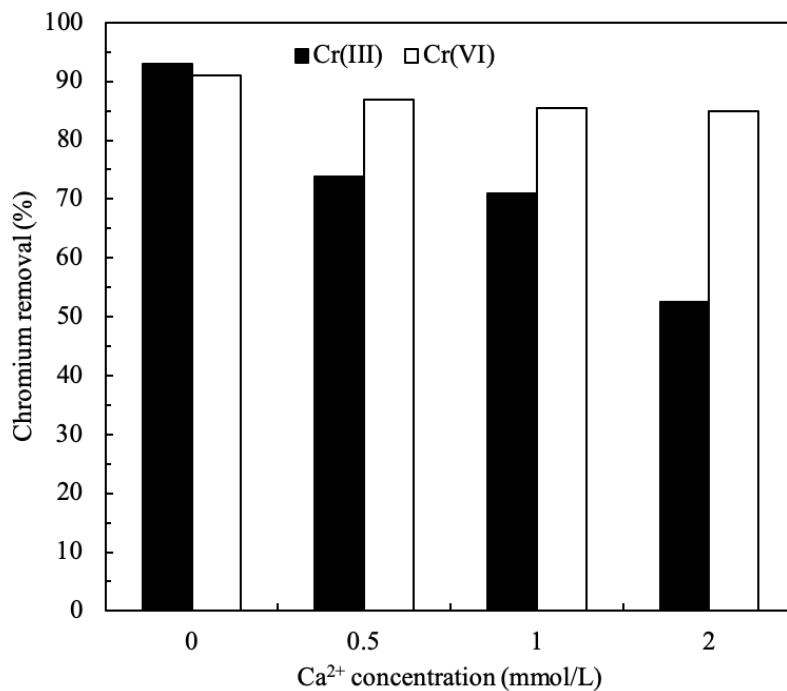


Figure 3. 13 Effect of Ca<sup>2+</sup> ions on the adsorption of chromium onto MCS

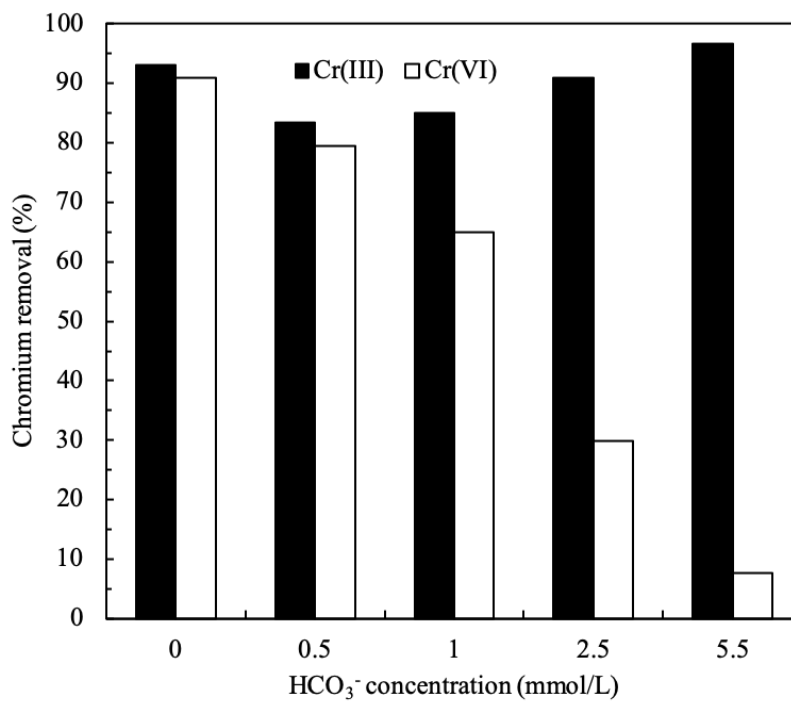


Figure 3. 14 Effect of HCO<sub>3</sub><sup>-</sup> ions on the adsorption of chromium onto MCS

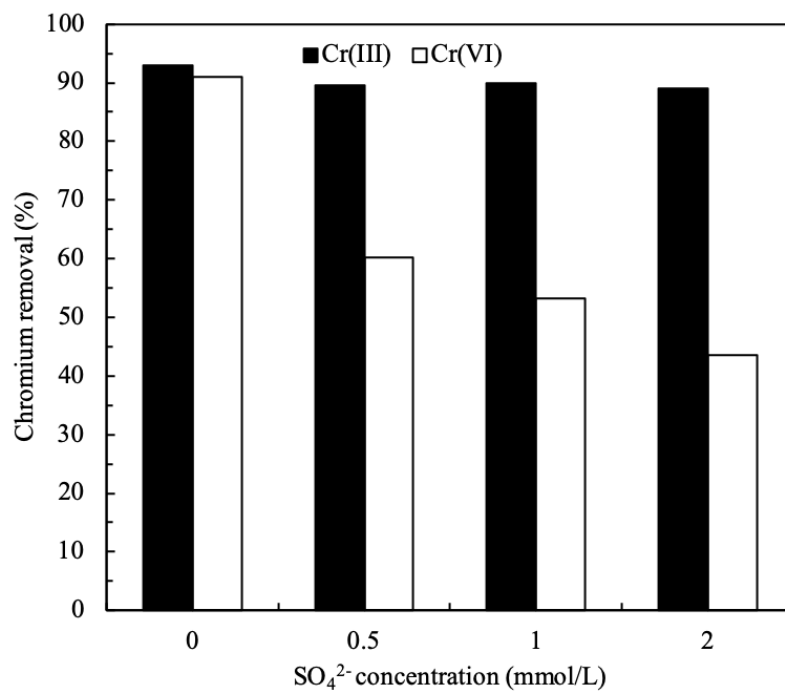


Figure 3. 15 Effect of SO<sub>4</sub><sup>2-</sup> ions on the adsorption of chromium onto MCS

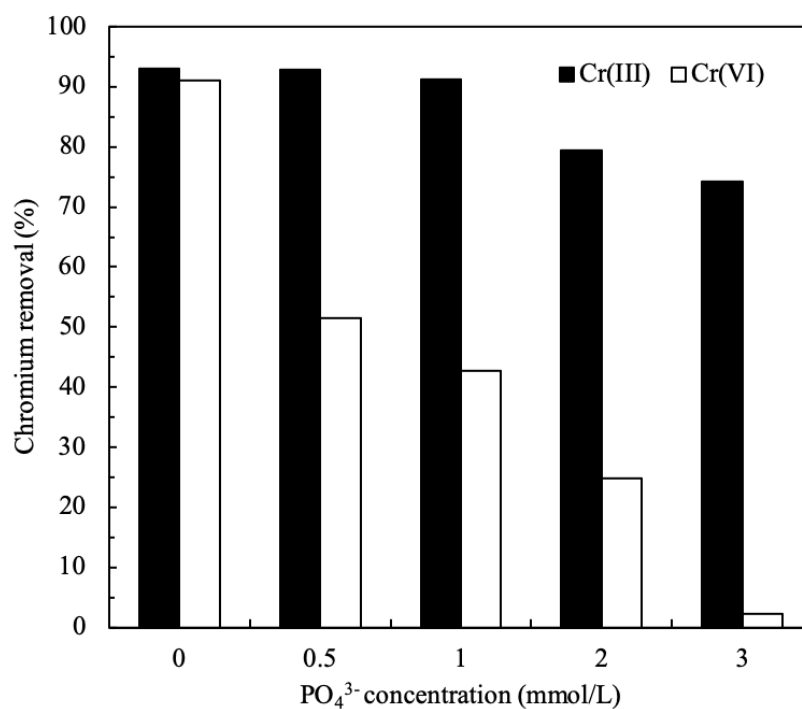


Figure 3. 16 Effect of PO<sub>4</sub><sup>3-</sup> ions on the adsorption of chromium onto MCS

### 3.3.7 Sorbent reuse and regeneration

The reuse of the sorbent is an important factor in determining its potential for practical application since it can reduce the operational cost and make the process economical. After conducting the recycle studies, it shows relatively strong adsorption capacity even after five cycles. The results presented in Figure 3.17 show that greater than 85% removal of Cr(VI) by the MCS sorbent was achieved in the first and second adsorption cycles, while the removal of Cr(VI) gradually decreased in the third, fourth and fifth adsorption cycles. The removal of chromium by the MCS sorbent was 61% and 56% in the fourth and fifth adsorption cycles, respectively.

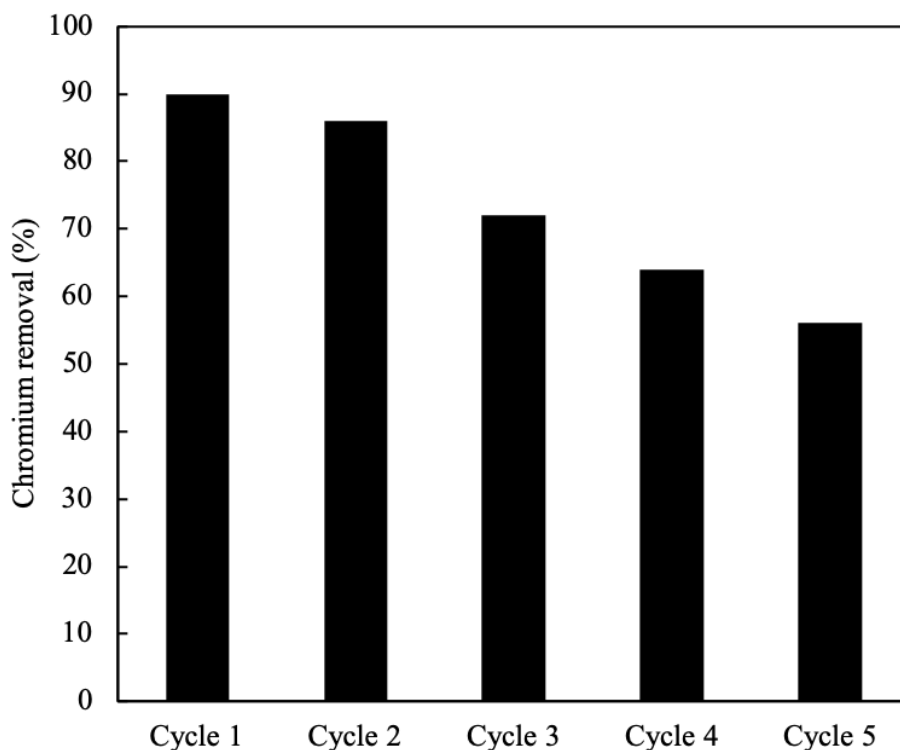


Figure 3. 17 Reuse of MCS sorbent in five adsorption cycles

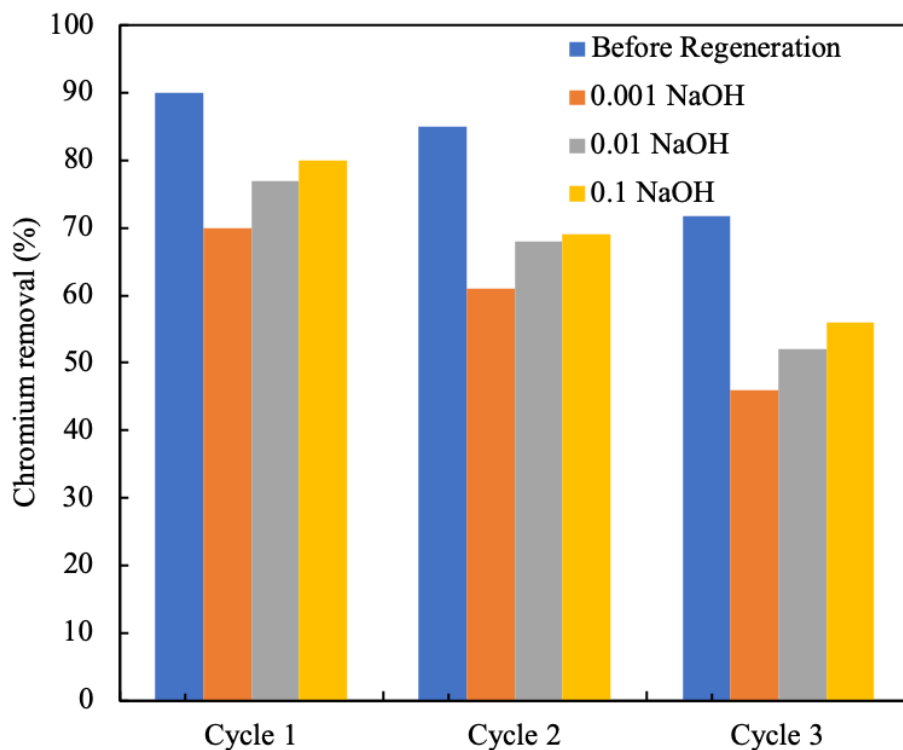


Figure 3. 18 Effect of different NaOH concentrations on regeneration of MCS sorbent

Regeneration of MCS was investigated using different NaOH concentrations of 0.001N, 0.01N and 0.1N and regenerated MCS sorbent was used for three more consecutive adsorption cycles. The regeneration efficiencies of 0.001N, 0.01N, and 0.1N of NaOH for MCS sorbent developed in this study were calculated to 78%, 86% and 89%, respectively. The removal of Cr(VI) increased by 8% when the concentration of NaOH solution increased from 0.001N to 0.01N and by 3% when the concentration of NaOH solution further increased to 0.1N. This result is consistent with suppressed Cr(VI) adsorption under highly alkali environment. The regeneration of the MCS sorbent using 0.01N NaOH is an effective and feasible approach and adsorption of Cr(VI) onto the regenerated MCS sorbent did not decrease significantly for another three adsorption cycles.

### 3.4 Conclusion

The removal of chromium from aqueous systems using the manganese-oxide sand (MCS) developed in former chapter was investigated under different parameters. The adsorption for both chromium species onto MCS sorbent increased significantly with the increasing MCS dosage until it reached 20mg/L. The adsorption equilibrium data of different concentrations of Cr(III) and Cr(VI) solution with constant MCS dosage of 20mg/L were fitted into four widely used isotherm models. Results showed that the Langmuir and Freundlich isotherm models provided better correlation of the experimental data than Temkin and Dubinin-Radushkevich (D-R) isotherm models, suggesting the adsorption of chromium is a monolayer adsorption on the heterogenous MCS surface. While the higher maximum adsorption capacity ( $q_m$ ) obtained from Langmuir isotherm and the higher Freundlich constant ( $K_F$ ) obtained from Freundlich isotherm are indicative of higher adsorption capacity of the MCS sorbent for Cr(III) than Cr(VI), the Langmuir constant ( $K_L$ ), Freundlich parameter ( $1/n$ ), heat of adsorption ( $b$ ) and binding constant ( $A$ ) obtained from Temkin isotherm, and the mean free energy ( $E$ ) calculated from D-R equation suggest that MCS sorbent displays a greater affinity and stronger binding for Cr(VI) than Cr(III). The favorable adsorption of Cr(III) and Cr(VI) onto MCS sorbent at a wide solution pH range of 3-10 makes it a promising adsorbent for practical use. The significant shift in PZC observed from Cr(III) and Cr(VI) adsorption indicated the occurrence of specific adsorption or formation of inner-sphere complexation between chromium species and MCS sorbent.

The adsorption of Cr(III) and Cr(VI) onto MCS can be best described by pseudo-second order model. The coexisting anions such as bicarbonate, sulfate, phosphate reduced the adsorption of Cr(VI) greatly with increasing concentration, while the adsorption of Cr(III) significantly suppressed by the coexisting cation of calcium. The reuse and regeneration study revealed that MCS sorbent can be effective for five consecutive adsorption cycles and can be successfully regenerated by alkali wash using 0.01N sodium hydroxide solution.

### 3.5 Reference

- [1] J. Kotaś and Z. Stasicka, “Chromium occurrence in the environment and methods of its speciation,” *Environ. Pollut.*, vol. 107, no. 3, pp. 263–283, Mar. 2000, doi: 10.1016/S0269-7491(99)00168-2.
- [2] F. C. Richard and A. C. M. Bourg, “Aqueous geochemistry of chromium: A review,” *Water Res.*, vol. 25, no. 7, pp. 807–816, Jul. 1991, doi: 10.1016/0043-1354(91)90160-R.
- [3] D. Rai, L. E. Eary, and J. M. Zachara, “Environmental chemistry of chromium,” *Sci. Total Environ.*, vol. 86, no. 1–2, pp. 15–23, Oct. 1989, doi: 10.1016/0048-9697(89)90189-7.
- [4] S. E. Fendorf, “Surface reactions of chromium in soils and waters,” *Geoderma*, vol. 67, no. 1–2, pp. 55–71, Jun. 1995, doi: 10.1016/0016-7061(94)00062-F.
- [5] S. A. Katz and H. Salem, “The toxicology of chromium with respect to its chemical speciation: A review,” *J. Appl. Toxicol.*, vol. 13, no. 3, pp. 217–224, May 1993, doi: 10.1002/jat.2550130314.
- [6] I. Moffat, N. Martinova, C. Seidel, and C. M. Thompson, “Hexavalent chromium in drinking water,” *J. - AWWA*, vol. 110, no. 5, pp. E22–E35, Apr. 2018, doi: 10.1002/awwa.1044.
- [7] A. H. Smith and C. M. Steinmaus, “Health effects of arsenic and chromium in drinking water: Recent human findings,” *Annu. Rev. Public Health*, vol. 30, no. 1, pp. 107–122, Apr. 2009, doi: 10.1146/annurev.publhealth.031308.100143.
- [8] M. Yoshinaga *et al.*, “A comprehensive study including monitoring, assessment of health effects and development of a remediation method for chromium pollution,” *Chemosphere*, vol. 201, pp. 667–675, Jun. 2018, doi: 10.1016/j.chemosphere.2018.03.026.
- [9] A. Zhitkovich, “Chromium in drinking water: Sources, metabolism, and cancer risks,” *Chem. Res. Toxicol.*, vol. 24, no. 10, pp. 1617–1629, Oct. 2011, doi: 10.1021/tx200251t.
- [10] C.-H. Tseng, C. Lei, and Y.-C. Chen, “Evaluating the health costs of oral hexavalent chromium exposure from water pollution: A case study in Taiwan,” *J. Clean. Prod.*, vol. 172, pp. 819–826, Jan. 2018, doi: 10.1016/j.jclepro.2017.10.177.

- [11] C. Pellerin and S. M. Booker, "Reflections on hexavalent chromium: health hazards of an industrial heavyweight.," *Environ. Health Perspect.*, vol. 108, no. 9, Sep. 2000, doi: 10.1289/ehp.108-a402.
- [12] K. Loska and D. Wiechuła, "Application of principal component analysis for the estimation of source of heavy metal contamination in surface sediments from the Rybnik Reservoir," *Chemosphere*, vol. 51, no. 8, pp. 723–733, Jun. 2003, doi: 10.1016/S0045-6535(03)00187-5.
- [13] R. A. Wuana and F. E. Okieimen, "Heavy metals in contaminated soils: A review of sources, chemistry, risks and best available strategies for remediation," *ISRN Ecol.*, vol. 2011, pp. 1–20, Oct. 2011, doi: 10.5402/2011/402647.
- [14] V. Dimos, K. J. Haralambous, and S. Malamis, "A Review on the Recent Studies for Chromium Species Adsorption on Raw and Modified Natural Minerals," *Crit. Rev. Environ. Sci. Technol.*, vol. 42, no. 19, pp. 1977–2016, Oct. 2012, doi: 10.1080/10643389.2011.574102.
- [15] D. Mohan and C. U. Pittman Jr., "Activated carbons and low cost adsorbents for remediation of tri- and hexavalent chromium from water," *J. Hazard. Mater.*, vol. 137, no. 2, pp. 762–811, Sep. 2006, doi: 10.1016/j.jhazmat.2006.06.060.
- [16] S. Yadav, V. Srivastava, S. Banerjee, C.-H. Weng, and Y. C. Sharma, "Adsorption characteristics of modified sand for the removal of hexavalent chromium ions from aqueous solutions: Kinetic, thermodynamic and equilibrium studies," *CATENA*, vol. 100, pp. 120–127, Jan. 2013, doi: 10.1016/j.catena.2012.08.002.
- [17] M. X. Loukidou, A. I. Zouboulis, T. D. Karapantsios, and K. A. Matis, "Equilibrium and kinetic modeling of chromium(VI) biosorption by *Aeromonas caviae*," *Colloids Surf. Physicochem. Eng. Asp.*, vol. 242, no. 1–3, pp. 93–104, Aug. 2004, doi: 10.1016/j.colsurfa.2004.03.030.
- [18] S. Chen, J. Zhang, H. Zhang, and X. Wang, "Removal of hexavalent chromium from contaminated water by Chinese herb-extraction residues," *Water. Air. Soil Pollut.*, vol. 228, no. 4, p. 145, Apr. 2017, doi: 10.1007/s11270-017-3329-1.

- [19] S. Kuppusamy, P. Thavamani, M. Megharaj, K. Venkateswarlu, Y. B. Lee, and R. Naidu, "Potential of *Melaleuca diosmifolia* leaf as a low-cost adsorbent for hexavalent chromium removal from contaminated water bodies," *Process Saf. Environ. Prot.*, vol. 100, pp. 173–182, Mar. 2016, doi: 10.1016/j.psep.2016.01.009.
- [20] M. Owlad, M. K. Aroua, W. A. W. Daud, and S. Baroutian, "Removal of hexavalent chromium-contaminated water and wastewater: A review," *Water. Air. Soil Pollut.*, vol. 200, no. 1–4, pp. 59–77, Jun. 2009, doi: 10.1007/s11270-008-9893-7.
- [21] K. Babaeivelni and A. P. Khodadoust, "Removal of arsenic from water using manganese (III) oxide: Adsorption of As(III) and As(V)," *J. Environ. Sci. Health Part A*, vol. 51, no. 4, pp. 277–288, Mar. 2016, doi: 10.1080/10934529.2015.1109382.
- [22] B. Sanjeev and C. Malay, "Removal of arsenic from ground water by manganese dioxide-coated sand," *J. Environ. Eng.*, vol. 125, no. 8, pp. 782–784, Aug. 1999, doi: 10.1061/(ASCE)0733-9372(1999)125:8(782).
- [23] F. A. Al-Sagheer and M. I. Zaki, "Synthesis and surface characterization of todorokite-type microporous manganese oxides: implications for shape-selective oxidation catalysts," *Microporous Mesoporous Mater.*, vol. 67, no. 1, pp. 43–52, Jan. 2004, doi: 10.1016/j.micromeso.2003.10.005.
- [24] R. G. Burns, "The uptake of cobalt into ferromanganese nodules, soils, and synthetic manganese (IV) oxides," *Geochim. Cosmochim. Acta*, vol. 40, no. 1, pp. 95–102, Jan. 1976, doi: 10.1016/0016-7037(76)90197-6.
- [25] R. Rao. Gadde and H. A. Laitinen, "Heavy metal adsorption by hydrous iron and manganese oxides," *Anal. Chem.*, vol. 46, no. 13, pp. 2022–2026, Nov. 1974, doi: 10.1021/ac60349a004.
- [26] W. Xu, H. Lan, H. Wang, H. Liu, and J. Qu, "Comparing the adsorption behaviors of Cd, Cu and Pb from water onto Fe-Mn binary oxide, MnO<sub>2</sub> and FeOOH," *Front. Environ. Sci. Eng.*, vol. 9, no. 3, pp. 385–393, Jun. 2015, doi: 10.1007/s11783-014-0648-y.

- [27] S. D. Rachmawati, C. Tizaoui, and N. Hilal, "Manganese coated sand for copper (II) removal from water in batch mode," *Water*, vol. 5, no. 4, pp. 1487–1501, Dec. 2013, doi: 10.3390/w5041487.
- [28] S. M. Maliyekkal, L. Philip, and T. Pradeep, "As(III) removal from drinking water using manganese oxide-coated-alumina: Performance evaluation and mechanistic details of surface binding," *Chem. Eng. J.*, vol. 153, no. 1, pp. 101–107, Nov. 2009, doi: 10.1016/j.cej.2009.06.026.
- [29] S. M. Maliyekkal, A. K. Sharma, and L. Philip, "Manganese-oxide-coated alumina: A promising sorbent for defluoridation of water," *Water Res.*, vol. 40, no. 19, pp. 3497–3506, Nov. 2006, doi: 10.1016/j.watres.2006.08.007.
- [30] E. Eren, B. Afsin, and Y. Onal, "Removal of lead ions by acid activated and manganese oxide-coated bentonite," *J. Hazard. Mater.*, vol. 161, no. 2, pp. 677–685, Jan. 2009, doi: 10.1016/j.jhazmat.2008.04.020.
- [31] N. Boujelben, J. Bouzid, Z. Elouear, and M. Feki, "Retention of nickel from aqueous solutions using iron oxide and manganese oxide coated sand: kinetic and thermodynamic studies," *Environ. Technol.*, vol. 31, no. 14, pp. 1623–1634, Dec. 2010, doi: 10.1080/09593330.2010.482148.
- [32] S. A. Chaudhry, T. A. Khan, and I. Ali, "Adsorptive removal of Pb(II) and Zn(II) from water onto manganese oxide-coated sand: Isotherm, thermodynamic and kinetic studies," *Egypt. J. Basic Appl. Sci.*, vol. 3, no. 3, pp. 287–300, Sep. 2016, doi: 10.1016/j.ejbas.2016.06.002.
- [33] R. Han, W. Zou, Y. Wang, and L. Zhu, "Removal of uranium(VI) from aqueous solutions by manganese oxide coated zeolite: discussion of adsorption isotherms and pH effect," *J. Environ. Radioact.*, vol. 93, no. 3, pp. 127–143, Jan. 2007, doi: 10.1016/j.jenvrad.2006.12.003.
- [34] Y.-Y. Chang, K.-H. Song, M.-R. Yu, and J.-K. Yang, "Removal of arsenic from aqueous solution by iron-coated sand and manganese-coated sand having different mineral types," *Water Sci. Technol.*, vol. 65, no. 4, pp. 683–688, Feb. 2012, doi: 10.2166/wst.2012.910.
- [35] S.-L. Lo, H.-T. Jeng, and C.-H. Lai, "Characteristics and adsorption properties of iron-coated sand," *Water Sci. Technol.*, vol. 35, no. 7, pp. 63–70, Apr. 1997, doi: 10.2166/wst.1997.0261.

- [36] N. Ayawei, A. N. Ebelegi, and D. Wankasi, "Modelling and interpretation of adsorption isotherms," *J. Chem.*, vol. 2017, pp. 1–11, Sep. 2017, doi: 10.1155/2017/3039817.
- [37] Y. S. Ho, J. F. Porter, and G. McKay, "Equilibrium isotherm studies for the sorption of divalent metal ions onto peat: copper, nickel and lead single component systems," *Water. Air. Soil Pollut.*, vol. 141, no. 1, pp. 1-33, Nov. 2002, doi: 10.1016/0009-2541(85)90133-0.
- [38] K. Y. Foo and B. H. Hameed, "Insights into the modeling of adsorption isotherm systems," *Chem. Eng. J.*, vol. 156, no. 1, pp. 2–10, Jan. 2010, doi: 10.1016/j.cej.2009.09.013.
- [39] A. O. Dada, A. P. Olalekan, A. M. Olatunya, and O. Dada, "Langmuir, Freundlich, Temkin and Dubinin–Radushkevich isotherms studies of equilibrium sorption of  $Zn^{2+}$  unto phosphoric acid modified rice husk," *IOSR J. Appl. Chem.*, vol. 3, no. 1, pp. 38–45, Nov. 2012, doi: 10.9790/5736-0313845.
- [40] K. Babaeivelni, A. P. Khodadoust, and D. Bogdan, "Adsorption and removal of arsenic (V) using crystalline manganese (II,III) oxide: Kinetics, equilibrium, effect of pH and ionic strength," *J. Environ. Sci. Health Part A*, vol. 49, no. 13, pp. 1462–1473, Nov. 2014, doi: 10.1080/10934529.2014.937160.
- [41] M. Özacar and İ. A. Şengil, "Adsorption of metal complex dyes from aqueous solutions by pine sawdust," *Bioresour. Technol.*, vol. 96, no. 7, pp. 791–795, May 2005, doi: 10.1016/j.biortech.2004.07.011.
- [42] Y.-Y. Chang, J.-W. Lim, and J.-K. Yang, "Removal of As(V) and Cr(VI) in aqueous solution by sand media simultaneously coated with Fe and Mn oxides," *J. Ind. Eng. Chem.*, vol. 18, no. 1, pp. 188–192, Jan. 2012, doi: 10.1016/j.jiec.2011.11.002.
- [43] C.-C. Kan, M. C. Aganon, C. M. Futralan, and M. L. P. Dalida, "Adsorption of  $Mn^{2+}$  from aqueous solution using Fe and Mn oxide-coated sand," *J. Environ. Sci.*, vol. 25, no. 7, pp. 1483–1491, Jul. 2013, doi: 10.1016/S1001-0742(12)60188-0.
- [44] X. Wang and Y. Qin, "Equilibrium sorption isotherms for of  $Cu^{2+}$  on rice bran," *Process Biochem.*, vol. 40, no. 2, pp. 677–680, Feb. 2005, doi: 10.1016/j.procbio.2004.01.043.

- [45] M. M. Bhutani, A. K. Mitra, and R. Kumari, "Kinetic study of Cr(VI) sorption on MnO<sub>2</sub>," *J. Radioanal. Nucl. Chem.*, vol. 157, no. 1, pp. 75–86, Feb. 1992, doi: 10.1007/BF02039779.
- [46] S. Mallick, S. S. Dash, and K. M. Parida, "Adsorption of hexavalent chromium on manganese nodule leached residue obtained from NH<sub>3</sub>–SO<sub>2</sub> leaching," *J. Colloid Interface Sci.*, vol. 297, no. 2, pp. 419–425, May 2006, doi: 10.1016/j.jcis.2005.11.001.
- [47] M. Gheju, I. Balcu, and G. Mosoarca, "Removal of Cr(VI) from aqueous solutions by adsorption on MnO<sub>2</sub>," *J. Hazard. Mater.*, vol. 310, pp. 270–277, Jun. 2016, doi: 10.1016/j.jhazmat.2016.02.042.
- [48] C. H. Weng, J. H. Wang, and C. P. Huang, "Adsorption of Cr(VI) onto TiO<sub>2</sub> from dilute aqueous solutions," *Water Sci. Technol.*, vol. 35, no. 7, pp. 55–62, Apr. 1997, doi: 10.2166/wst.1997.0260.
- [49] O. Ajouyed, C. Hurel, M. Ammari, L. B. Allal, and N. Marmier, "Sorption of Cr(VI) onto natural iron and aluminum (oxy)hydroxides: Effects of pH, ionic strength and initial concentration," *J. Hazard. Mater.*, vol. 174, no. 1–3, pp. 616–622, Feb. 2010, doi: 10.1016/j.jhazmat.2009.09.096.
- [50] S. A. Khan, Riaz-ur-Rehman, and M. A. Khan, "Adsorption of chromium (III), chromium (VI) and silver (I) on bentonite," *Waste Manag.*, vol. 15, no. 4, pp. 271–282, Jan. 1995, doi: 10.1016/0956-053X(95)00025-U.
- [51] S. Mor, K. Ravindra, and N. R. Bishnoi, "Adsorption of chromium from aqueous solution by activated alumina and activated charcoal," *Bioresour. Technol.*, vol. 98, no. 4, pp. 954–957, Mar. 2007, doi: 10.1016/j.biortech.2006.03.018.
- [52] S. Egodawatte, A. Datt, E. A. Burns, and S. C. Larsen, "Chemical insight into the adsorption of chromium(III) on iron oxide/mesoporous silica nanocomposites," *Langmuir*, vol. 31, no. 27, pp. 7553–7562, Jul. 2015, doi: 10.1021/acs.langmuir.5b01483.
- [53] W. Cui *et al.*, "Cr(III) adsorption by cluster formation on boehmite nanoplates in highly alkaline solution," *Environ. Sci. Technol.*, vol. 53, no. 18, pp. 11043–11055, Sep. 2019, doi: 10.1021/acs.est.9b02693.

- [54] S. Seif, S. Marofi, and S. Mahdavi, "Removal of Cr<sup>3+</sup> ion from aqueous solutions using MgO and montmorillonite nanoparticles," *Environ. Earth Sci.*, vol. 78, no. 13, p. 377, Jun. 2019, doi: 10.1007/s12665-019-8380-3.
- [55] Q. Su, B. Pan, S. Wan, W. Zhang, and L. Lv, "Use of hydrous manganese dioxide as a potential sorbent for selective removal of lead, cadmium, and zinc ions from water," *J. Colloid Interface Sci.*, vol. 349, no. 2, pp. 607–612, Sep. 2010, doi: 10.1016/j.jcis.2010.05.052.
- [56] N. K. Lazaridis and C. Charalambous, "Sorbitive removal of trivalent and hexavalent chromium from binary aqueous solutions by composite alginate–goethite beads," *Water Res.*, vol. 39, no. 18, pp. 4385–4396, Nov. 2005, doi: 10.1016/j.watres.2005.09.013.
- [57] Y. Niu, W. Hu, M. Guo, Y. Wang, J. Jia, and Z. Hu, "Preparation of cotton-based fibrous adsorbents for the removal of heavy metal ions," *Carbohydr. Polym.*, vol. 225, p. UNSP 115218, Dec. 2019, doi: 10.1016/j.carbpol.2019.115218.
- [58] J.-H. An and S. Dultz, "Adsorption of tannic acid on chitosan-montmorillonite as a function of pH and surface charge properties," *Appl. Clay Sci.*, vol. 36, no. 4, pp. 256–264, May 2007, doi: 10.1016/j.clay.2006.11.001.
- [59] R. Sprycha, "Electrical double layer at alumina/electrolyte interface: II. Adsorption of supporting electrolyte ions," *J. Colloid Interface Sci.*, vol. 127, no. 1, pp. 12–25, Jan. 1989, doi: 10.1016/0021-9797(89)90003-9.
- [60] R. J. Hunter, *Zeta potential in colloid science: principles and applications*. Academic Press, 2013.
- [61] P. M. Choksi and V. Y. Joshi, "Adsorption kinetic study for the removal of nickel (II) and aluminum (III) from an aqueous solution by natural adsorbents," *Desalination*, vol. 208, no. 1, pp. 216–231, Apr. 2007, doi: 10.1016/j.desal.2006.04.081.
- [62] V. Vimonses, S. Lei, B. Jin, C. W. K. Chow, and C. Saint, "Kinetic study and equilibrium isotherm analysis of Congo Red adsorption by clay materials," *Chem. Eng. J.*, vol. 148, no. 2, pp. 354–364, May 2009, doi: 10.1016/j.cej.2008.09.009.

- [63] W. Zou, R. Han, Z. Chen, Z. Jinghua, and J. Shi, "Kinetic study of adsorption of Cu(II) and Pb(II) from aqueous solutions using manganese oxide coated zeolite in batch mode," *Colloids Surf. Physicochem. Eng. Asp.*, vol. 279, no. 1, pp. 238–246, May 2006, doi: 10.1016/j.colsurfa.2006.01.008.
- [64] S. Ricordel, S. Taha, I. Cisse, and G. Dorange, "Heavy metals removal by adsorption onto peanut husks carbon: characterization, kinetic study and modeling," *Sep. Purif. Technol.*, vol. 24, no. 3, pp. 389–401, Sep. 2001, doi: 10.1016/S1383-5866(01)00139-3.
- [65] S. Pap *et al.*, "Evaluation of the adsorption potential of eco-friendly activated carbon prepared from cherry kernels for the removal of Pb<sup>2+</sup>, Cd<sup>2+</sup> and Ni<sup>2+</sup> from aqueous wastes," *J. Environ. Manage.*, vol. 184, pp. 297–306, Dec. 2016, doi: 10.1016/j.jenvman.2016.09.089.
- [66] H. Yuh-Shan, "Citation review of Lagergren kinetic rate equation on adsorption reactions," *Scientometrics*, vol. 59, no. 1, pp. 171–177, Jan. 2004, doi: 10.1023/B:SCIE.0000013305.99473.cf.
- [67] D. C. Sharma and C. F. Forster, "Column studies into the adsorption of chromium (VI) using sphagnum moss peat," *Bioresour. Technol.*, vol. 52, no. 3, pp. 261–267, Jan. 1995, doi: 10.1016/0960-8524(95)00035-D.
- [68] K. Henryk, C. Jarosław, and Ż. Witold, "Peat and coconut fiber as biofilters for chromium adsorption from contaminated wastewaters," *Environ. Sci. Pollut. Res.*, vol. 23, no. 1, pp. 527–534, Jan. 2016, doi: 10.1007/s11356-015-5285-x.
- [69] G. M. Ayoub, A. Damaj, H. El-Rassy, M. Al-Hindi, and R. M. Zayyat, "Equilibrium and kinetic studies on adsorption of chromium(VI) onto pine-needle-generated activated carbon," *SN Appl. Sci.*, vol. 1, no. 12, p. 1562, Dec. 2019, doi: 10.1007/s42452-019-1617-7.
- [70] W. J. Weber and J. C. Morris, "Kinetics of adsorption on carbon from solution," *J. Sanit. Eng. Div.*, vol. 89, no. 2, pp. 31–60, 1963.
- [71] Y. Ho, J. Ng, and G. McKay, "Kinetics of pollutant sorption by biosorbents: Review," *Sep. Purif. Methods*, vol. 29, no. 2, p. 189, Jun. 2000, doi: 10.1081/SPM-100100009.

- [72] F.-C. Wu, R.-L. Tseng, and R.-S. Juang, "Initial behavior of intraparticle diffusion model used in the description of adsorption kinetics," *Chem. Eng. J.*, vol. 153, no. 1, pp. 1–8, Nov. 2009, doi: 10.1016/j.cej.2009.04.042.
- [73] K.-Y. Shin, J.-Y. Hong, and J. Jang, "Heavy metal ion adsorption behavior in nitrogen-doped magnetic carbon nanoparticles: Isotherms and kinetic study," *J. Hazard. Mater.*, vol. 190, no. 1, pp. 36–44, Jun. 2011, doi: 10.1016/j.jhazmat.2010.12.102.
- [74] S. A. Chaudhry, T. A. Khan, and I. Ali, "Equilibrium, kinetic and thermodynamic studies of Cr(VI) adsorption from aqueous solution onto manganese oxide coated sand grain (MOCSG)," *J. Mol. Liq.*, vol. 236, pp. 320–330, Jun. 2017, doi: 10.1016/j.molliq.2017.04.029.
- [75] S. He *et al.*, "Competitive adsorption of Cd<sup>2+</sup>, Pb<sup>2+</sup> and Ni<sup>2+</sup> onto Fe<sup>3+</sup>-modified argillaceous limestone: Influence of pH, ionic strength and natural organic matters," *Sci. Total Environ.*, vol. 637–638, pp. 69–78, Oct. 2018, doi: 10.1016/j.scitotenv.2018.04.300.
- [76] Y. Wen, Z. Tang, Y. Chen, and Y. Gu, "Adsorption of Cr(VI) from aqueous solutions using chitosan-coated fly ash composite as biosorbent," *Chem. Eng. J.*, vol. 175, pp. 110–116, Nov. 2011, doi: 10.1016/j.cej.2011.09.066.
- [77] W. Qi, Y. Zhao, X. Zheng, M. Ji, and Z. Zhang, "Adsorption behavior and mechanism of Cr(VI) using Sakura waste from aqueous solution," *Appl. Surf. Sci.*, vol. 360, pp. 470–476, Jan. 2016, doi: 10.1016/j.apsusc.2015.10.088.

## CHAPTER IV

### IV. SURFACE CHARACTERIZATION OF MANGANESE-COATED SAND

#### 4.1 Introduction

Different techniques can be performed to characterize and determine various properties such as size, shape and elemental structure of a material or atoms at the material's surface of particular interest [1]–[3]. Characterization techniques of atomic structure can generally be categorized into nonspecific and element-specific methods. X-ray Diffraction (XRD) and Raman Spectroscopy are both nonspecific methods that can provide information regarding the crystallinity and polymorph type of the material, while X-ray Photoelectron Spectroscopy (XPS) and Scanning Electron Microscopy coupled with Energy Dispersive X-ray Analysis (SEM-EDX) can provide element specific information such as element oxidation states or surface element composition [4]–[6]. The Brunauer-Emmett-Teller (BET) method is commonly used in various studies to decide the specific surface area such as metal oxides, nanomaterials and activated carbon [7]–[10].

In order to accurately characterize the manganese-oxide based adsorbents for the removal of chromium from water, different analytical procedures such as XRD, XPS, SEM-EDX and BET surface analysis were applied to investigate the mineral crystal structure, surface properties and surface phenomena in order to explain the mechanism of adsorption for the adsorption of both chromium species onto the surface of the MCS (manganese-coated sand) sorbent. In the meantime, how these two valence states of chromium (trivalent chromium and hexavalent chromium) species transform and react on the surface of the MCS sorbent were established based on the information gathered from different surface characterization techniques.

## 4.2 Materials and methods

### 4.2.1 Materials

Manganese-coated sand (MCS) developed at different temperatures were investigated with X-ray powder diffraction (XRD) and X-ray Photoelectron Spectroscopy (XPS) directly without further sample preparation. To prepare the samples for XPS and Scanning Electron Microscopy coupled with Energy Dispersive X-ray (SEM-EDX) analysis of the chromium species adsorbed onto the MCS sorbents, we mixed 5 g of the MCS sorbent separately with a 100 mg/L solution of Cr(III) and with a 100 mg/L solution of Cr(VI) in sealed 50mL high density polyethylene (HDPE) inside a rotating tumbler for 24 hours at 16 rpm. After the adsorption reached equilibrium, the MCS sorbent loaded with Cr(III) and Cr(VI) were separated from each bottle by centrifuging at 8500 rpm for 15 minutes. The MCS sorbent samples were dried in an oven for 24 hours and ready for XPS and SEM-EDX analysis.

### 4.2.2 Sorbent characterization

The specific surface area of the MCS sorbent was measured with an Accelerated Surface Area and Porosimeter system (Micromeritics Instrument Corporation, Norcross, GA, USA). The BET surface area of the MCS sorbent was determined to be 3.09 m<sup>2</sup>/g. The X-ray diffraction (XRD-Bruker D8 Discover System, MA, USA) pattern was obtained with Cu K $\alpha$  radiation,  $\lambda=1.5406 \text{ \AA}$ , at 40KV and 30mA. The  $2\theta$  scan range is between 10° to 80°  $2\theta$  with a step size of 0.02°  $2\theta$  and a counting time of 10 s per step. Photomicrography of the external surface and elemental composition information of the MCS sorbent were obtained using Scanning Electron Microscopy coupled with Energy Dispersive X-ray analysis (SEM, TOPCN ABT-150S; EDX, JXA 840, Japan). The oxidation states of both manganese and chromium species on the surface of the MCS sorbent before and after adsorption of chromium were studied by X-ray photoelectron spectrometer (Kratos AXIS-165). The samples were analyzed with Al K $\alpha$  X-ray source at 15kV and 10mA.

## 4.3 Results and discussion

### 4.3.1 X-ray Diffraction

Solid materials can be divided into two main classes: crystalline and amorphous. Unlike amorphous solids lacking of a three-dimensional lattice structure, crystalline solids have an orderly and repeating arrangement formed by their constituent atoms or molecules [11], [12]. X-ray diffraction(XRD) is a powerful nondestructive technique for materials structure determination that can provide valuable geometrical and structural information of a crystalline material [13]. Atoms or molecules in amorphous solids possess no long range order, therefore their X-ray diffraction patterns contain no crystalline diffraction peaks. X-ray diffraction is a well-established and unique analytical method that has been successfully applied to all fields such as pharmaceutical industry, forensic science, geological analysis, microelectronics industry and glass industry because XRD analysis can discover the morphology and the crystallinity degree and identify different polymorphic forms of a variety of materials such as metals, minerals, composites, coatings, thin films, graphite, nanomaterials and pharmaceuticals [1], [14]–[17]. In this study, manganese-coated sand (MCS) was developed under different coating temperature while other coating conditions such as the use of manganese chemicals and pH remained the same. XRD was employed to detect the presence of possible formation of crystalline manganese oxides on the MCS surface.

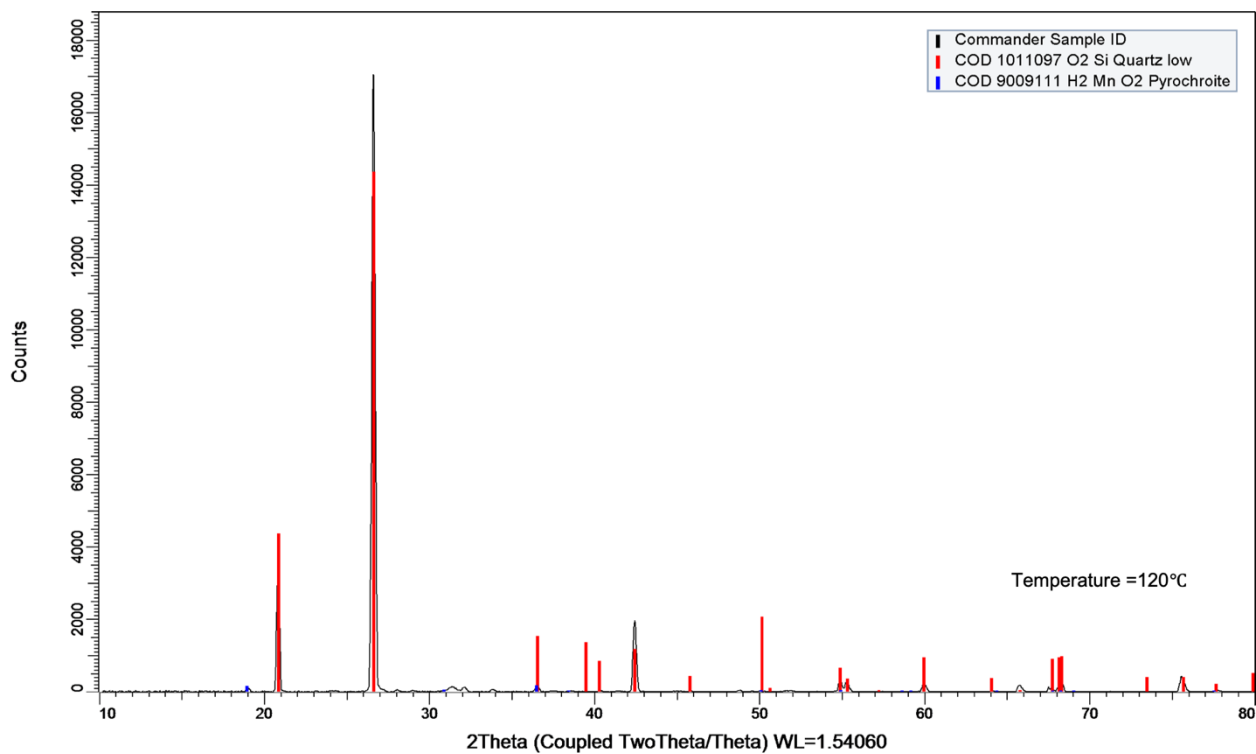


Figure 4. 1 XRD pattern of MCS (Temperature = 120°C)

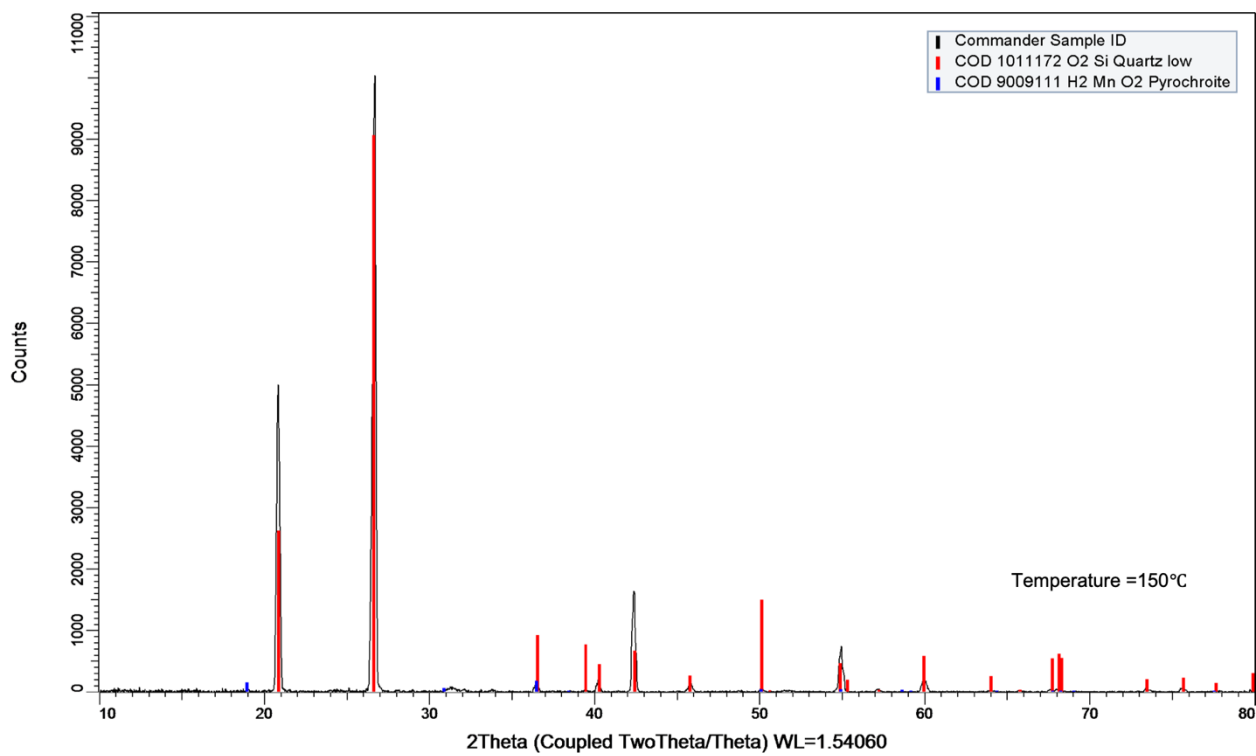


Figure 4. 2 XRD pattern of MCS (Temperature = 150°C)

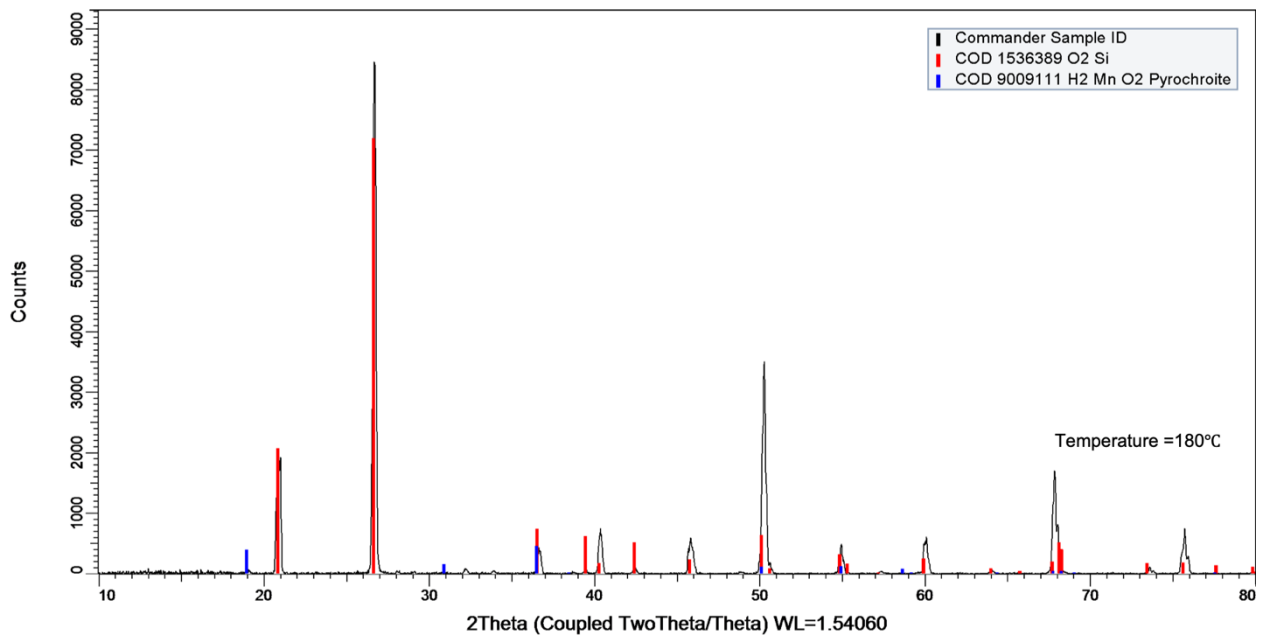


Figure 4. 3 XRD pattern of MCS (Temperature = 180°C)

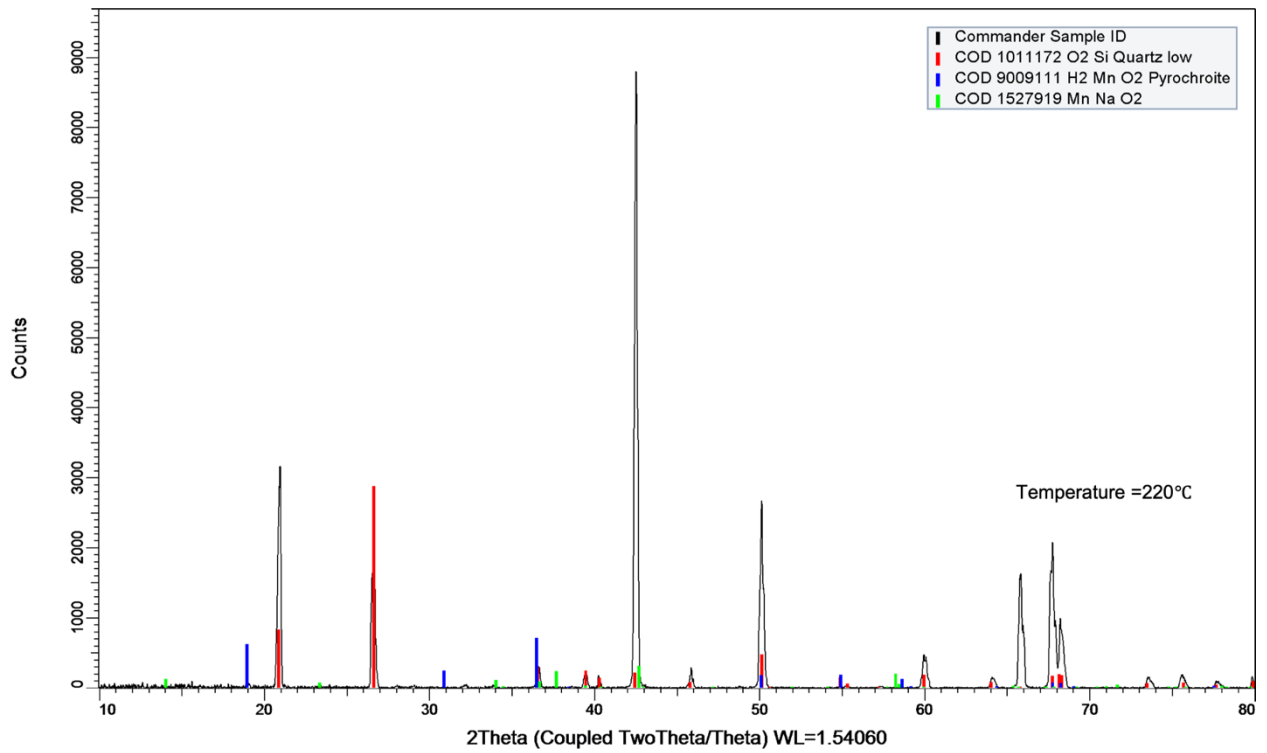


Figure 4. 4 XRD pattern of MCS (Temperature = 220°C)

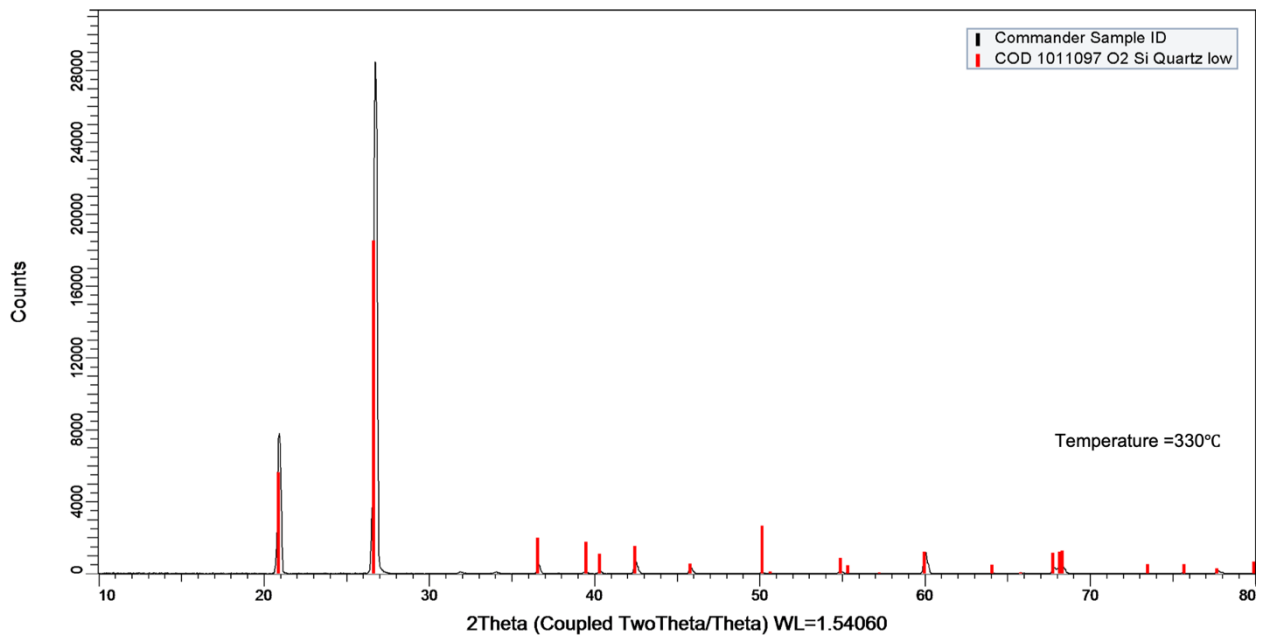


Figure 4. 5 XRD pattern of MCS (Temperature = 330°C)

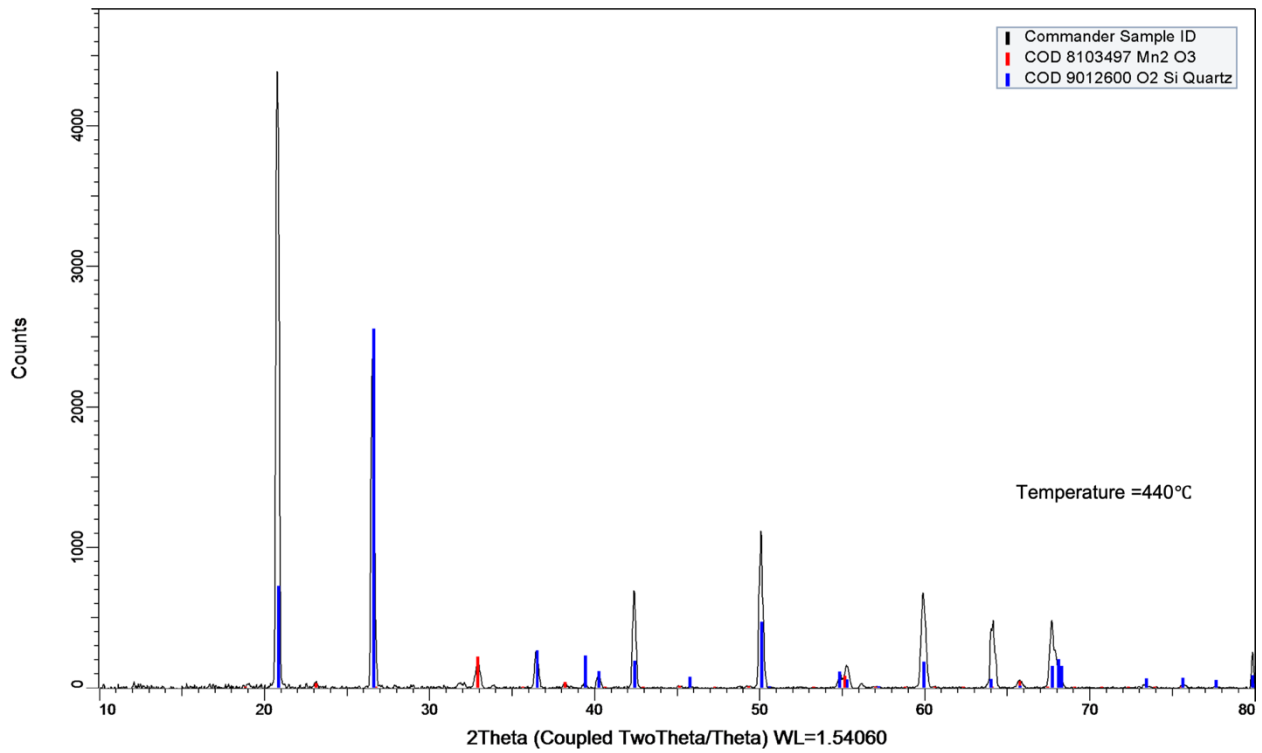


Figure 4. 6 XRD pattern of MCS (Temperature = 440°C)

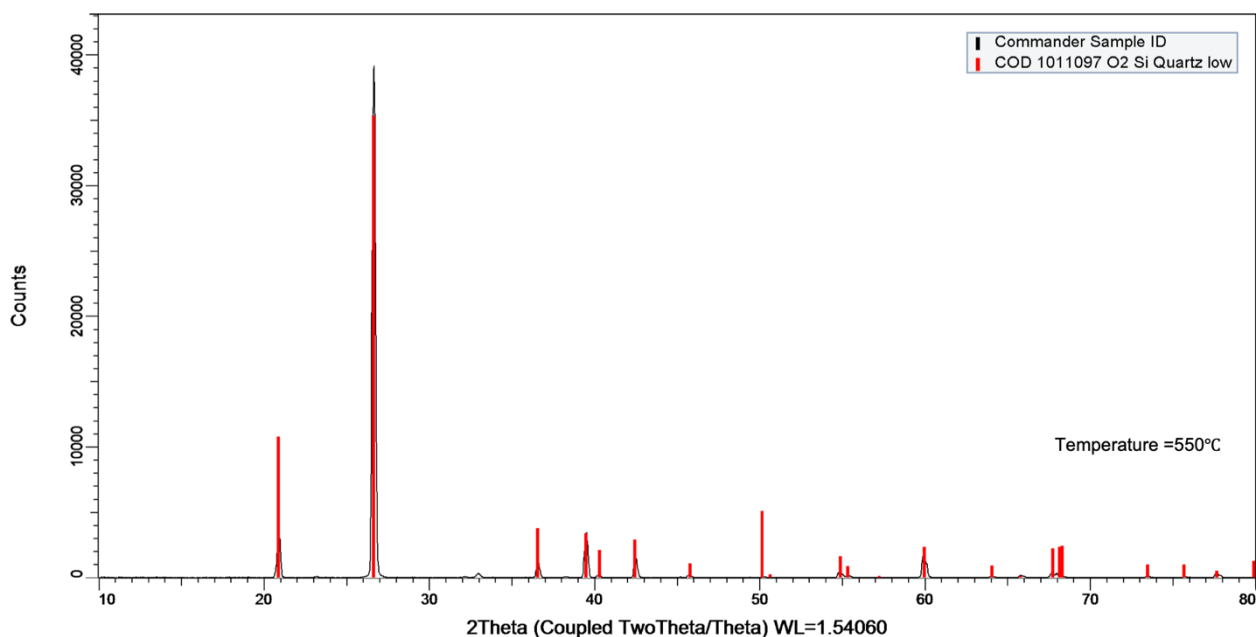


Figure 4. 7 XRD pattern of MCS (Temperature = 550°C)

XRD patterns of all the MCS samples developed under different coating temperature are shown in from Figure 4.1 to Figure 4.7. Crystallography Open Database (COD) was used as diffraction peak reference source to identify the specific crystalline structure of the coated layer. Quartz sand ( $\text{SiO}_2$ ) can be ubiquitously identified in all aforementioned MCS samples due to the fact that quartz sand was selected as supporting material for manganese in this study. Pyrochroite ( $\text{H}_2\text{MnO}_2$ ) was detected in the MCS samples coated at lower furnace temperature ( $120^\circ\text{C}$ ,  $150^\circ\text{C}$ ,  $180^\circ\text{C}$ , and  $220^\circ\text{C}$ ), while only quartz sand can be confirmed in MCS samples coated at higher furnace temperature ( $330^\circ\text{C}$  and  $550^\circ\text{C}$ ) with an exception of MCS sample coated at  $440^\circ\text{C}$  where  $\text{Mn}_2\text{O}_3$  can be identified from matching the XRD peak information with COD. The MCS sample coated at  $220^\circ\text{C}$  is composed of both  $\text{H}_2\text{Mn(II)O}_2$  and  $\text{NaMn(III)O}_2$  as a form of manganese coated onto the sand surface. The mixture of manganese (II, III)

oxides were detected on the MCS sorbent coated at 220°C according to the XRD pattern obtained, while Mn(IV)O<sub>2</sub> were found to be the predominate manganese oxide for the manganese-coated sand developed by other studies for heavy metal removal [18]–[21].

#### 4.3.2 SEM-EDX

Scanning electron microscopy (SEM) is one of the available electron microscopy techniques that allows direct visualization of sample surface and provides information related to surface topography such as morphology and surface condition [22], [23]. SEM has been applied to investigate all types of materials: nanomaterial, biological structure, membrane, and mineral [24]–[29]. When combined with Energy Dispersive X-ray analysis (EDX), SEM-EDX system can provide both surface morphology and elemental distribution on the surface. SEM-EDX is a powerful tool that has been extensively selected in heavy metal adsorption by different adsorbents to visualize the change of surface structure before and after adsorption, confirm appearance of heavy metal on adsorbent surface and quantify specific elemental composition [24], [30]–[33].

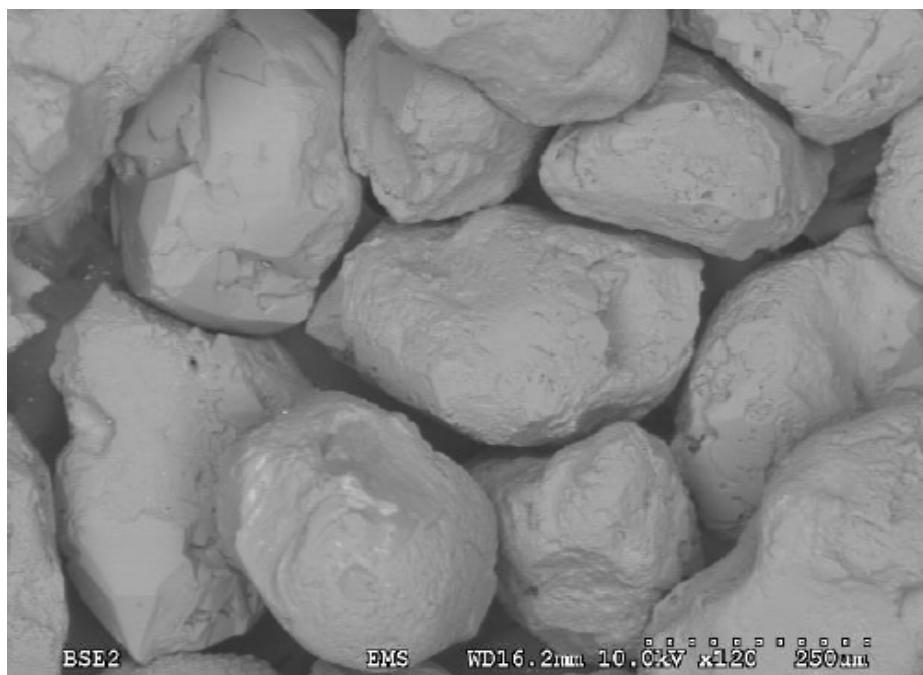


Figure 4. 8 SEM image of virgin silica sand

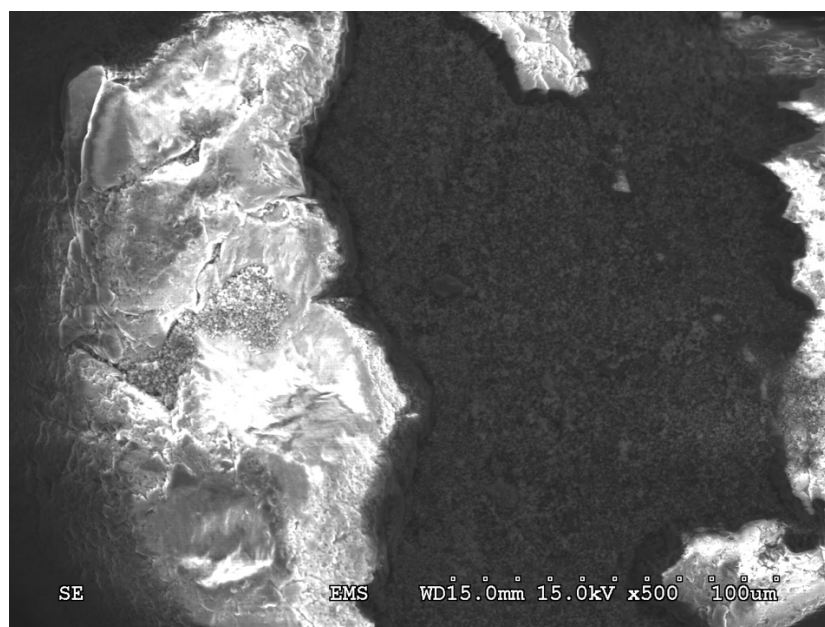
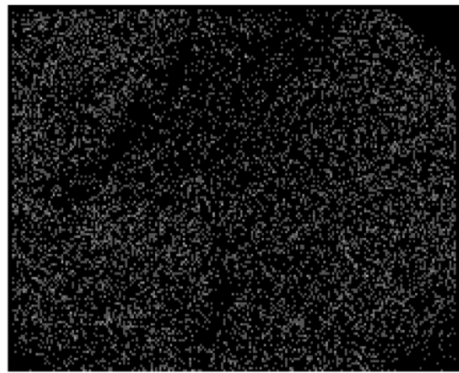
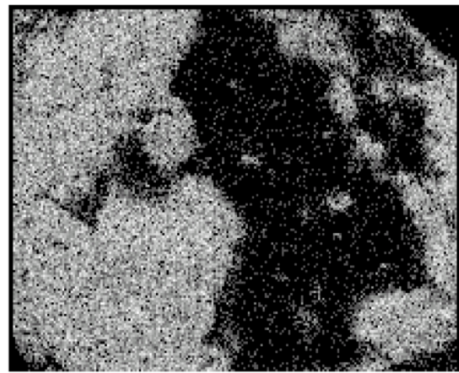


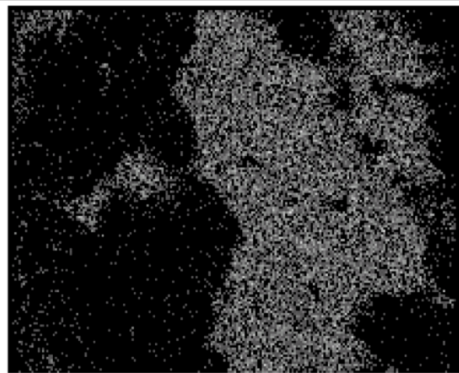
Figure 4. 9 SEM image of MCS overloaded with Cr(III)



Oxygen Ka1\_2



Silicon Ka1



Manganese Ka1



Chromium Ka1

Figure 4. 10 EDX mapping analysis of different elements for MCS overloaded with Cr(III)

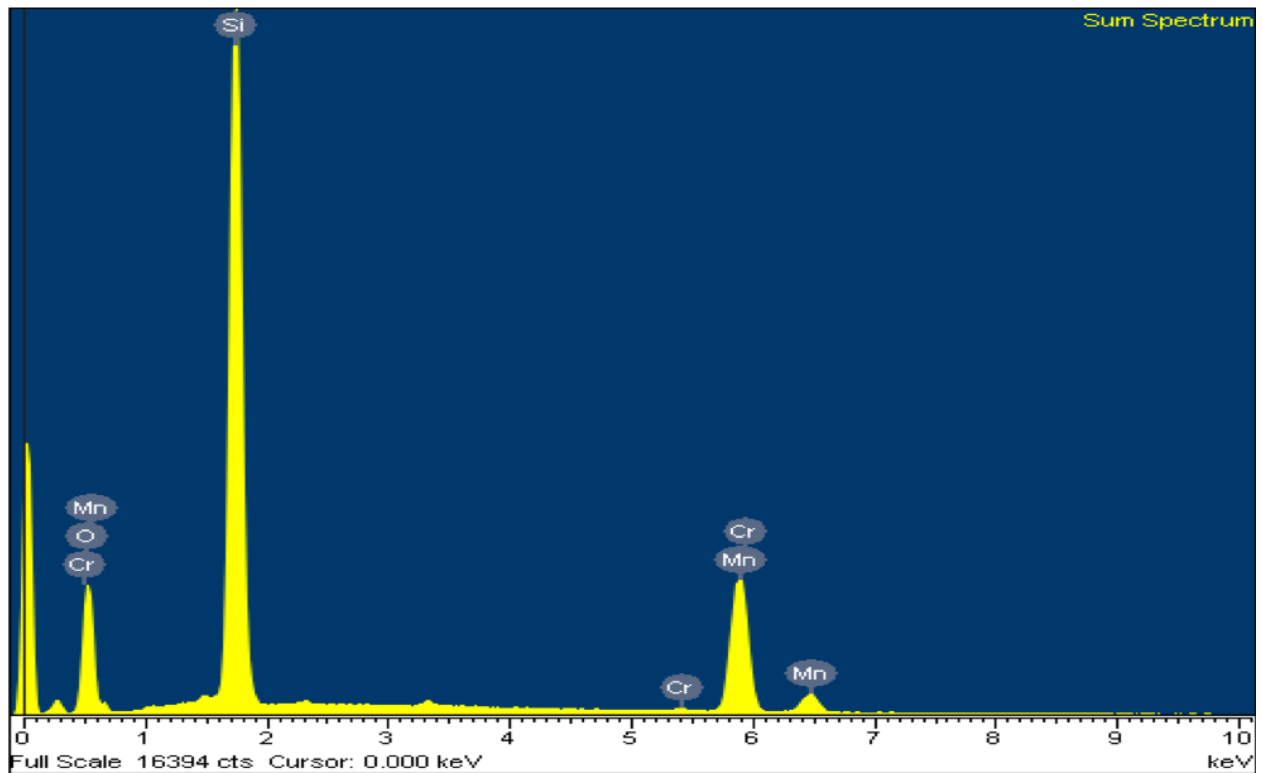


Figure 4. 11 EDX spectrum of MCS overloaded with Cr(III)

Manganese coated sand (MCS) at coating temperature 220°C had the best chromium adsorption performance and therefore was selected as the MCS for all following studies. SEM images of virgin sand in Figure 4.8 and MCS overloaded with Cr(III) and Cr(VI) in Figure 4.9 and 4.11, respectively, showed virgin sand had a relatively smooth surface with rough ridges and small cracks, while the MCS sorbent had a bright rough and irregular silica sand surface and dark area covered by manganese oxides formed during coating process, suggesting surface of the MCS sorbent used in this study is heterogeneous. Manganese oxides were not uniformly or evenly distributed on the sand surface but formed in clusters. The bright points for each element in dot mapping provide the specific elemental distribution on the MCS sorbent surface. The accordance of the appearance of manganese and chromium shown in dot mapping is indicative of that chromium is specifically sorbed onto the MCS sorbent and manganese oxides coated onto the silica sand are the effective surface constituents responsible for chromium removal. Additionally, EDX mapping and spectrum of all elements (Mn, Si, O, Cr) for MCS overloaded with Cr(III) and Cr(VI) (Figure 4.9, Figure 4.10, Figure 4.12 and Figure 4.13) confirmed chromium adsorption onto the surface of the MCS sorbent.

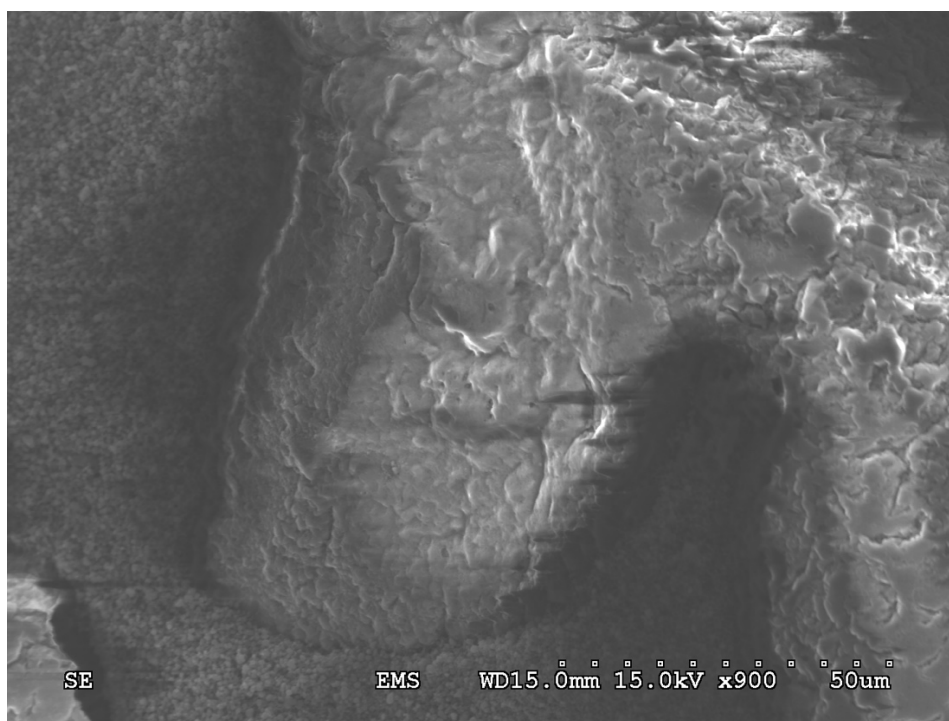


Figure 4. 12 SEM image of MCS overloaded with Cr(VI)

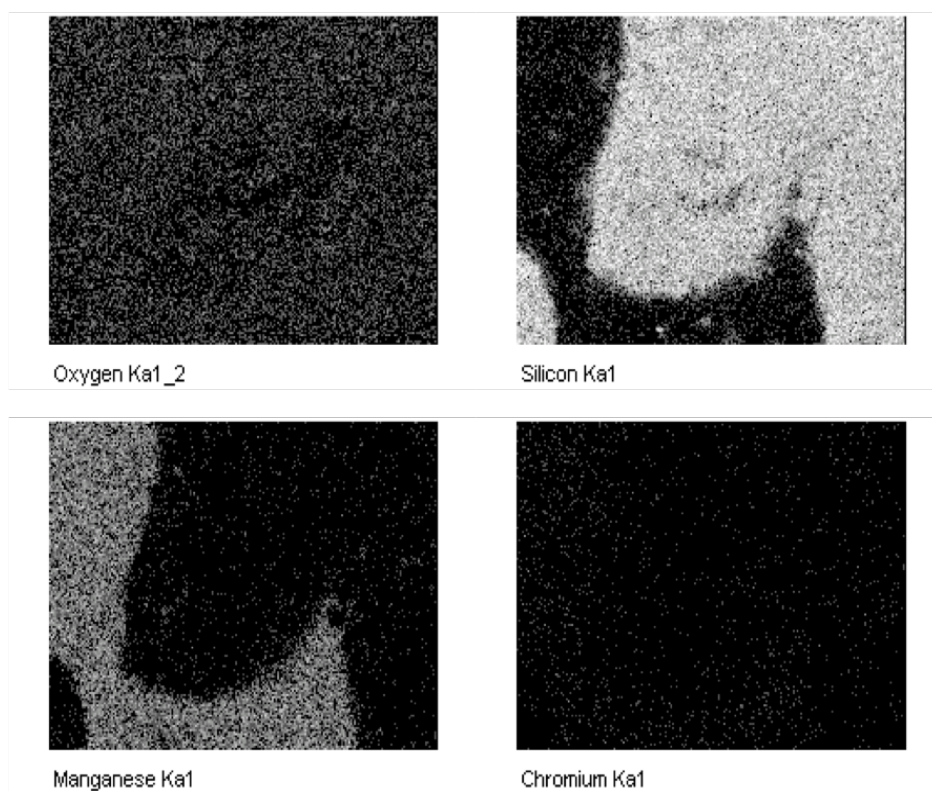


Figure 4. 13 EDX mapping analysis of different elements for MCS overloaded with Cr(VI)

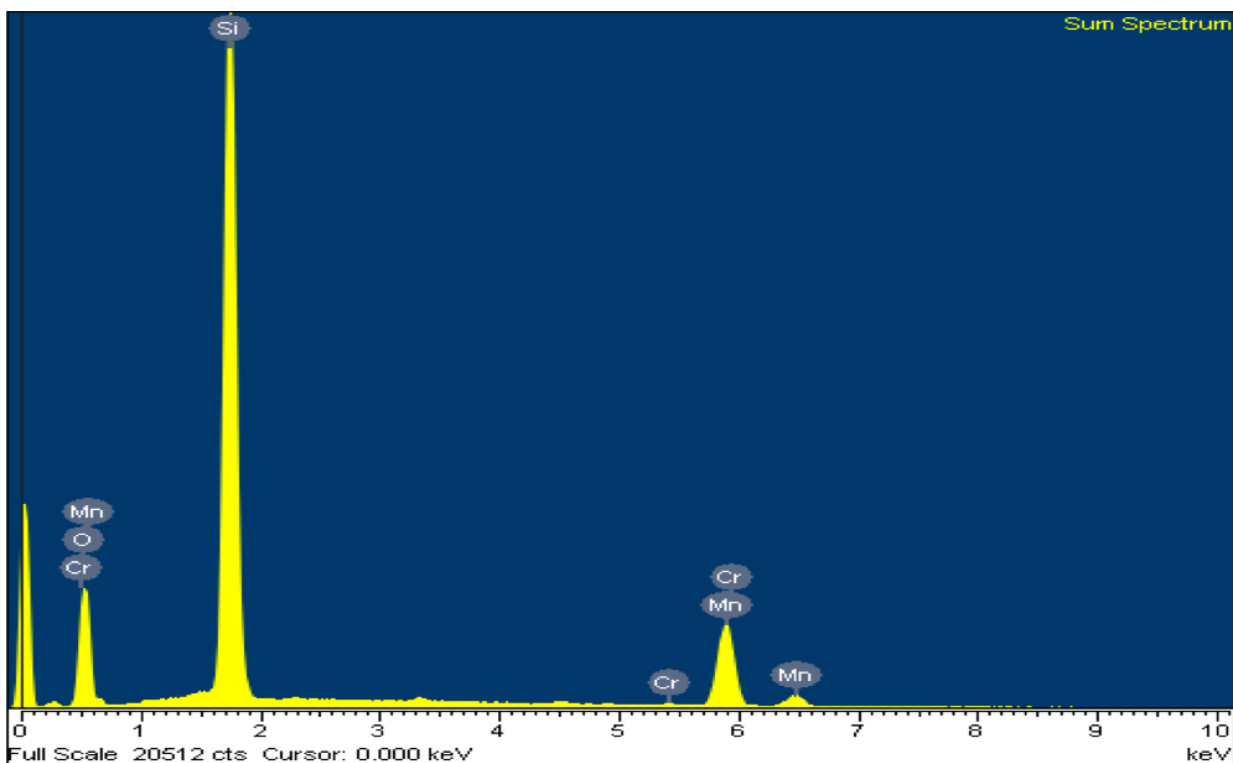


Figure 4. 14 EDX spectrum of MCS overloaded with Cr(VI)

#### 4.3.3 X-ray Photoelectron Spectroscopy

X-ray photoelectron spectroscopy (XPS) is a near-surface sensitive technique that predominately employed in determining the oxidation states of an element [34]. In this study, we overloaded 5g MCS developed at 220°C with of 100mg/L Cr(III) and Cr(VI) solution and analyzed the samples using XPS to identify Mn and Cr oxidation states after the reaction reached equilibrium (24h). The MCS sorbent coated at different temperatures were also investigated by XPS to identify the specific manganese oxides formed on the surface.

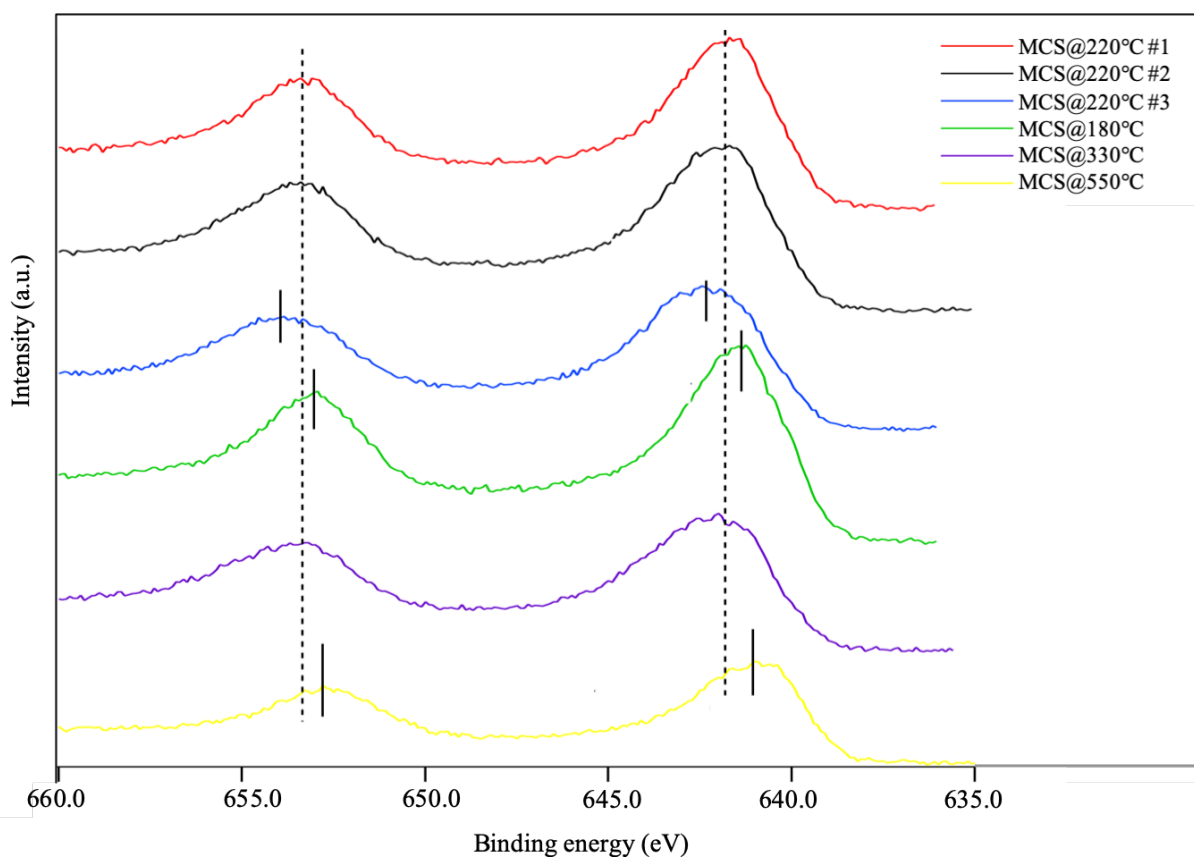


Figure 4. 15 XPS spectra of the MCS sorbent coated at different temperatures

Figure 4.15 showed the XPS spectra of the MCS sorbent developed at different temperature. The binding energy of 641.7 eV for two of the three MCS coated at 220°C and the MCS coated at 330°C is correspond to Mn 2p<sub>3/2</sub> orbitals for MnO or Mn<sub>2</sub>O<sub>3</sub> [35]–[37]. Although one of the three developed MCS at 220°C appeared to have shift to higher energy from 641.7 eV to 642.2 eV, its peak shape is consistent with MnO or Mn<sub>2</sub>O<sub>3</sub>. The Mn 2p<sub>3/2</sub> peaks observed around 641 eV of the MCS sorbent coated at 180°C indicates the manganese oxides formed on the surface of the MCS sorbent are a combination of manganese (II, III) oxides.

The chromium adsorption mechanism onto the MCS sorbent can be investigated by performing XPS analysis on the MCS sorbent after adsorption. To identify the oxidation states of manganese and chromium to determine the possible redox reaction taken place on the sorbent surface, the XPS spectra of all element and chromium were shown in Figure 4.16 and Figure 4.17, respectively. The Cr 2p<sub>3/2</sub> peaks were analyzed for adsorption of both chromium species onto the MCS sorbent and they include three peaks at 576.7 eV, 578 eV and 579.8 eV for Cr(III) adsorption (Figure 4.17a) and two peaks at 579.6 eV and 577.5 eV for Cr(VI) adsorption (Figure 4.17b). The peaks at 576.7 eV, 578 eV and 579.8 eV belonged to the binding energy of 2p<sub>3/2</sub> of Cr(III) as Cr(III) hydroxide [Cr(OH)<sub>3</sub>] or Cr(III) oxide (Cr<sub>2</sub>O<sub>3</sub>) and 2p<sub>3/2</sub> of Cr(VI) as Cr(VI) mixed species, indicating the transformation from Cr(III) to Cr(VI) happened at the surface of the MCS sorbent and the calculation results showed that the mass fraction of Cr(III) and Cr(VI) were 75.29% and 24.71%, respectively [32], [38], [39]. As shown in Figure 4.17b, the two peaks at 579.6 eV and 577.5 eV observed at Cr 2p<sub>3/2</sub> spectra can be assigned to Cr(VI) as chromate ions (CrO<sub>4</sub><sup>2-</sup>) and Cr(III) as Cr(III) hydroxide [Cr(OH)<sub>3</sub>] or Cr(III) oxide (Cr<sub>2</sub>O<sub>3</sub>), suggesting the reduction reaction occurred on the surface of the MCS sorbent [40]–[42]. The mass fraction of Cr(III) and Cr(VI) were determined to be 52.66% and 47.34%, respectively, on the MCS surface after Cr(VI) adsorption. This result can be best explained by that manganese (II, III) oxides coated onto the MCS sorbent can either reduce Cr(VI) to Cr(III) or oxidize Cr(III) to Cr(VI) due to the intermediate oxidation state of Mn(III) can act as either oxidant or reductant in a redox reaction.

The transformation of manganese after adsorption reaction with chromium species were also analyzed by XPS spectra obtained in this study. It can be observed that the peak at 642.8 eV for Mn 2p<sub>3/2</sub> (Figure 4.16b) resulted from the appearance of MnO<sub>2</sub> at the surface of the MCS sorbent after contacting with Cr(VI) solution and the peak at 641 eV for Mn 2p<sub>3/2</sub> (Figure 4.16a) resulted from the appearance of MnOOH or MnO at the surface of the MCS sorbent after contacting with Cr(III) solution [35]–[37].

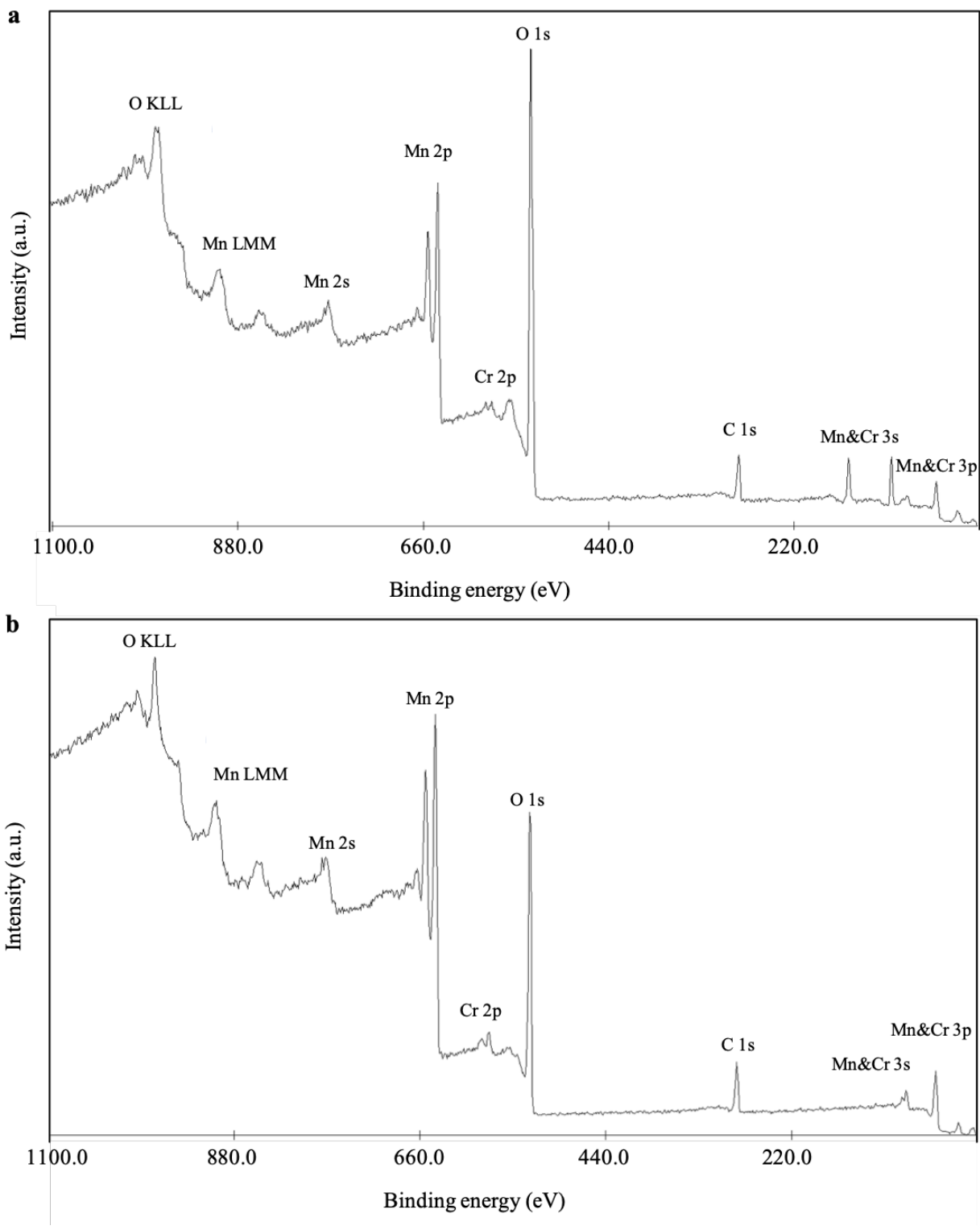


Figure 4. 16 XPS all element spectra of the MCS surface after adsorption of (a) Cr(III) and (b) Cr(VI)

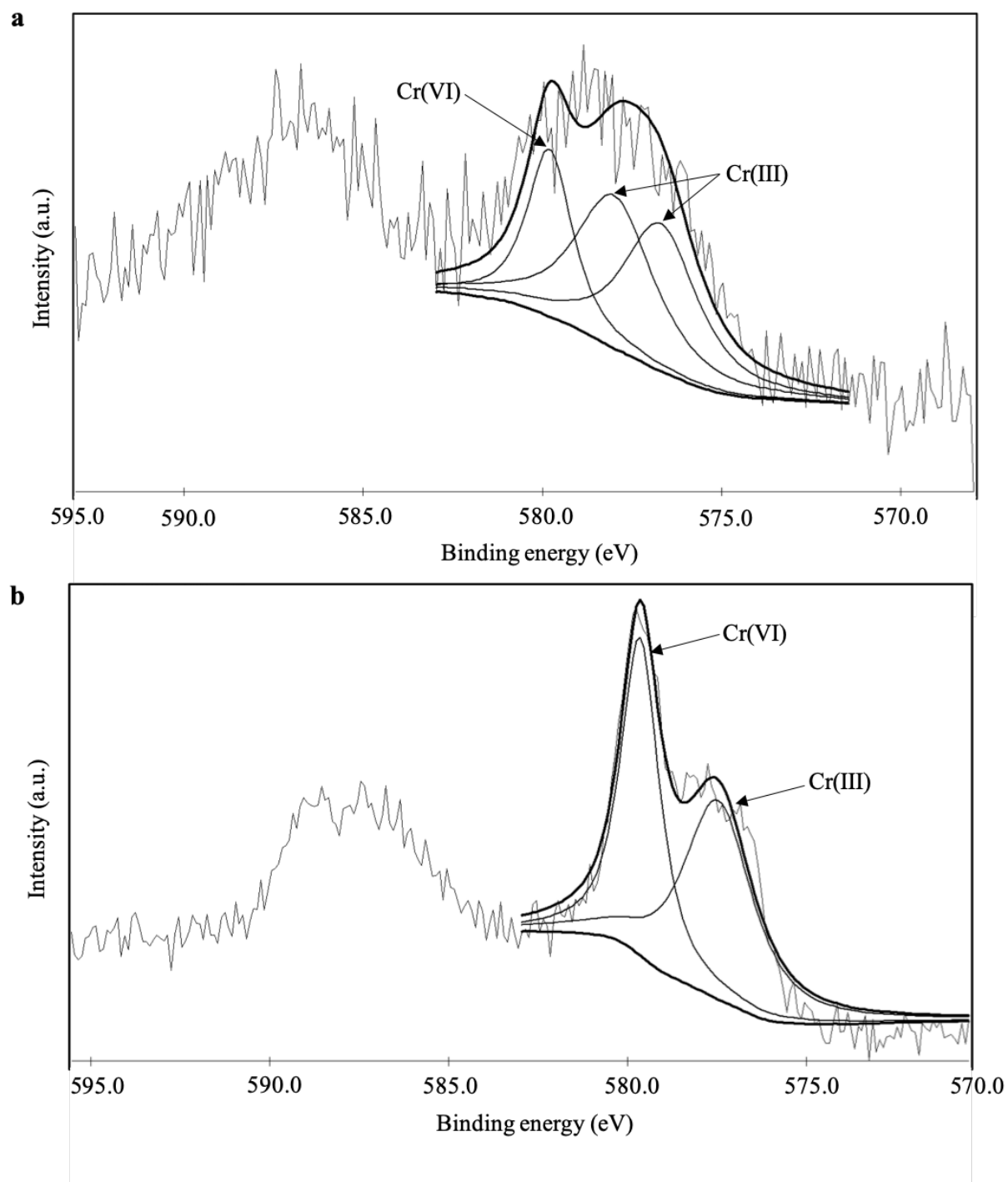


Figure 4. 17 XPS Cr spectra of the MCS sorbent surface after adsorption of (a) Cr(III) and (b) Cr(VI)

#### 4.4 Conclusion

In order to investigate the adsorption mechanism between the MCS sorbent and chromium species, the MCS sorbent was characterized in terms of its material matrix, surface area, crystallinity and oxide constituents, surface elemental composition and surface oxide (groups). The BET surface area of the MCS sorbent was determined to be 3.09 m<sup>2</sup>/g. XRD results combined with XPS spectra showed that the surface manganese oxide of MCS coated at lower temperature (120°C, 150°C, and 180°C) is pyrochroite [Mn(OH)<sub>2</sub>], while NaMn(III)O<sub>2</sub> was the major surface manganese oxide formed at higher temperature (330°C and 550°C). The mixture of manganese (II, III) oxides was detected on the surface of the MCS sorbent coated at 220°C based on the XRD and XPS results. The SEM-EDX analysis indicated that the MCS sorbent employed in this study has a surface heterogeneity with a non-uniform coating of manganese oxides and the appearance of chromium species on the surface of the MCS sorbent is in accordance with the coating of manganese oxides, suggesting that the effective surface component for chromium adsorption is the coated manganese oxides. The surface element composition and their oxidation states can be obtained from XPS spectra results. The occurrence of redox reaction between chromium species and the MCS sorbent was confirmed by Cr(VI) species detected after the adsorption of Cr(III) onto the MCS sorbent and Cr(III) species detected after the adsorption of Cr(VI) onto the MCS sorbent. Partial reduction or oxidation of Cr(III) and Cr(VI) on the surface of the MCS sorbent can be attributed to Mn(II, III) oxides appeared on the MCS surface can act as either a oxidant or a reductant because of its intermediate oxidation state.

#### 4.5 Reference

- [1] J. D. Hanawalt, H. W. Rinn, and L. K. Frevel, “Chemical analysis by X-Ray Diffraction,” *Ind. Eng. Chem. Anal. Ed.*, vol. 10, no. 9, pp. 457–512, Sep. 1938, doi: 10.1021/ac50125a001.
- [2] D. R. Baer *et al.*, “Surface characterization of nanomaterials and nanoparticles: Important needs and challenging opportunities,” *J. Vac. Sci. Technol. Vac. Surf. Films Off. J. Am. Vac. Soc.*, vol. 31, no. 5, p. 50820, Sep. 2013, doi: 10.1116/1.4818423.
- [3] Ž. Mitić *et al.*, “Instrumental methods and techniques for structural and physicochemical characterization of biomaterials and bone tissue: A review,” *Mater. Sci. Eng. C*, vol. 79, pp. 930–949, Oct. 2017, doi: 10.1016/j.msec.2017.05.127.
- [4] A. Gholampour and T. Ozbakkaloglu, “A review of natural fiber composites: properties, modification and processing techniques, characterization, applications,” *J. Mater. Sci.*, vol. 55, no. 3, pp. 829–892, Jan. 2020, doi: 10.1007/s10853-019-03990-y.
- [5] J. Światowska, V. Lair, C. Pereira-Nabais, G. Cote, P. Marcus, and A. Chagnes, “XPS, XRD and SEM characterization of a thin ceria layer deposited onto graphite electrode for application in lithium-ion batteries,” *Appl. Surf. Sci.*, vol. 257, no. 21, pp. 9110–9119, Aug. 2011, doi: 10.1016/j.apsusc.2011.05.108.
- [6] G. Magnacca, G. Cerrato, C. Morterra, M. Signoretto, F. Somma, and F. Pinna, “Structural and surface characterization of pure and sulfated iron oxides,” *Chem. Mater.*, vol. 15, no. 3, pp. 675–687, Feb. 2003, doi: 10.1021/cm021268n.
- [7] M. S. P. Francisco, V. R. Mastelaro, P. A. P. Nascente, and A. O. Florentino, “Activity and characterization by XPS, HR-TEM, Raman Spectroscopy, and BET Surface Area of CuO/CeO<sub>2</sub>-TiO<sub>2</sub> Catalysts,” *J. Phys. Chem. B*, vol. 105, no. 43, pp. 10515–10522, Nov. 2001, doi: 10.1021/jp0109675.
- [8] J. Wang, Y. Xia, Y. Dong, R. Chen, L. Xiang, and S. Komarneni, “Defect-rich ZnO nanosheets of high surface area as an efficient visible-light photocatalyst,” *Appl. Catal. B Environ.*, vol. 192, pp. 8–16, Sep. 2016, doi: 10.1016/j.apcatb.2016.03.040.

- [9] K. Kaneko and C. Ishii, "Superhigh surface area determination of microporous solids," *Colloids Surf.*, vol. 67, pp. 203–212, Nov. 1992, doi: 10.1016/0166-6622(92)80299-H.
- [10] I. Odler, "The BET-specific surface area of hydrated Portland cement and related materials," *Cem. Concr. Res.*, vol. 33, no. 12, pp. 2049–2056, Dec. 2003, doi: 10.1016/S0008-8846(03)00225-4.
- [11] S. Bates, G. Zografii, D. Engers, K. Morris, K. Crowley, and A. Newman, "Analysis of amorphous and nanocrystalline solids from their X-ray diffraction patterns," *Pharm. Res.*, vol. 23, no. 10, pp. 2333–2349, Oct. 2006, doi: 10.1007/s11095-006-9086-2.
- [12] K. Thamaphat, P. Limsuwan, and B. Ngotawornchai, "Phase Characterization of TiO<sub>2</sub> Powder by XRD and TEM," *Kasetsart J. (Nat. Sci.)*, vol. 42, pp. 357-361, 2008.
- [13] E. S. Ameh, "A review of basic crystallography and x-ray diffraction applications," *Int. J. Adv. Manuf. Technol.*, vol. 105, no. 7, pp. 3289–3302, Dec. 2019, doi: 10.1007/s00170-019-04508-1.
- [14] B. Borie, "X-Ray Diffraction in crystals, imperfect crystals, and amorphous bodies.," *J. Am. Chem. Soc.*, vol. 87, no. 1, pp. 140–141, Jan. 1965, doi: 10.1021/ja01079a041.
- [15] R. Sharma, D. P. Bisen, U. Shukla, and B. G. Sharma, "X-ray diffraction: a powerful method of characterizing nanomaterials," *Recent Res. Sci. Technol.*, vol.4, pp. 77-79, Jan. 2012.
- [16] S. D. Wolter, "Materials Science of X-Ray Diffraction," in *X-Ray Diffraction Imaging*, 1st ed., J. Greenberg and K. Iniewski, Eds. Boca Raton : Taylor & Francis, CRC Press, 2018. |
- [17] S. A. Özen, F. Özkalaycı, U. Çevik, and R. V. Grieken, "Investigation of heavy metal distributions along 15 m soil profiles using EDXRF, XRD, SEM-EDX, and ICP-MS techniques," *X-Ray Spectrom.*, vol. 47, no. 3, pp. 231–241, 2018, doi: 10.1002/xrs.2832.
- [18] S. A. Chaudhry, T. A. Khan, and I. Ali, "Adsorptive removal of Pb(II) and Zn(II) from water onto manganese oxide-coated sand: Isotherm, thermodynamic and kinetic studies," *Egypt. J. Basic Appl. Sci.*, vol. 3, no. 3, pp. 287–300, Sep. 2016, doi: 10.1016/j.ejbas.2016.06.002.
- [19] W. Zou, J. Song, K. Li, and R. Han, "Use of manganese oxide-coated sand for the adsorption of uranium(VI) ions from aqueous solution using a column mode," *Adsorpt. Sci. Technol.*, vol. 28, no. 4, pp. 313–325, May 2010, doi: 10.1260/0263-6174.28.4.313.

- [20] R. S. Stahl and B. R. James, "Zinc sorption by manganese-oxide-coated sand as a function of pH," *Soil Sci. Soc. Am. J.*, vol. 55, no. 5, pp. 1291–1294, Oct. 1991, doi: 10.2136/sssaj1991.03615995005500050016x.
- [21] A. S. Tilak, S. Ojewole, C. W. Williford, G. A. Fox, T. M. Sobiecki, and S. L. Larson, "Formation of manganese oxide coatings onto sand for adsorption of trace metals from groundwater," *J. Environ. Qual.*, vol. 42, no. 6, pp. 1743–1751, 2013, doi: 10.2134/jeq2013.04.0142.
- [22] A. Srivastava, V. K. Jain, and A. Srivastava, "SEM-EDX analysis of various sizes aerosols in Delhi India," *Environ. Monit. Assess.*, vol. 150, no. 1, p. 405, Apr. 2008, doi: 10.1007/s10661-008-0239-0.
- [23] S. Rades *et al.*, "High-resolution imaging with SEM/T-SEM, EDX and SAM as a combined methodical approach for morphological and elemental analyses of single engineered nanoparticles," *RSC Adv.*, vol. 4, no. 91, pp. 49577–49587, Oct. 2014, doi: 10.1039/C4RA05092D.
- [24] J. Liu, L. He, F. Dong, and K. A. Hudson-Edwards, "The role of nano-sized manganese coatings on bone char in removing arsenic(V) from solution: Implications for permeable reactive barrier technologies," *Chemosphere*, vol. 153, pp. 146–154, Jun. 2016, doi: 10.1016/j.chemosphere.2016.03.044.
- [25] R. Grissa *et al.*, "XPS and SEM-EDX study of electrolyte nature effect on Li electrode in lithium metal batteries," *ACS Appl. Energy Mater.*, vol. 1, no. 10, pp. 5694–5702, Oct. 2018, doi: 10.1021/acsaem.8b01256.
- [26] I. Michalak, K. Marycz, K. Basińska, and K. Chojnacka, "Using SEM-EDX and ICP-OES to investigate the elemental composition of green Macroalga *Vaucheria sessilis*," *Sci. World J.*, vol. 2014, pp.891928, Aug. 2014, doi: 10.1155/2014/891928.
- [27] C. H. Chia, B. Gong, S. D. Joseph, C. E. Marjo, P. Munroe, and A. M. Rich, "Imaging of mineral-enriched biochar by FTIR, Raman and SEM–EDX," *Vib. Spectrosc.*, vol. 62, pp. 248–257, Sep. 2012, doi: 10.1016/j.vibspec.2012.06.006.

- [28] V. Lynch and L. Miotti, "Introduction to micro-residues analysis: Systematic use of Scanning Electron Microscope and Energy Dispersive X-rays Spectroscopy (SEM-EDX) on Patagonian raw materials," *J. Archaeol. Sci. Rep.*, vol. 16, pp. 299–308, Dec. 2017, doi: 10.1016/j.jasrep.2017.10.020.
- [29] M. Nuspl, W. Wegscheider, J. Angeli, W. Posch, and M. Mayr, "Qualitative and quantitative determination of micro-inclusions by automated SEM/EDX analysis," *Anal. Bioanal. Chem.*, vol. 379, no. 4, pp. 640–645, Jun. 2004, doi: 10.1007/s00216-004-2528-y.
- [30] S. H. Chen, S. L. Ng, Y. L. Cheow, and A. S. Y. Ting, "A novel study based on adaptive metal tolerance behavior in fungi and SEM-EDX analysis," *J. Hazard. Mater.*, vol. 334, pp. 132–141, Jul. 2017, doi: 10.1016/j.jhazmat.2017.04.004.
- [31] V. Murphy, S. A. M. Tofail, H. Hughes, and P. McLoughlin, "A novel study of hexavalent chromium detoxification by selected seaweed species using SEM-EDX and XPS analysis," *Chem. Eng. J.*, vol. 148, no. 2, pp. 425–433, May 2009, doi: 10.1016/j.cej.2008.09.029.
- [32] M. Mende, D. Schwarz, C. Steinbach, R. Boldt, and S. Schwarz, "Simultaneous adsorption of heavy metal ions and anions from aqueous solutions on chitosan—Investigated by spectrophotometry and SEM-EDX analysis," *Colloids Surf. Physicochem. Eng. Asp.*, vol. 510, pp. 275–282, Dec. 2016, doi: 10.1016/j.colsurfa.2016.08.033.
- [33] S. A. Chaudhry, T. A. Khan, and I. Ali, "Equilibrium, kinetic and thermodynamic studies of Cr(VI) adsorption from aqueous solution onto manganese oxide coated sand grain (MOCSG)," *J. Mol. Liq.*, vol. 236, pp. 320–330, Jun. 2017, doi: 10.1016/j.molliq.2017.04.029.
- [34] G. Greczynski and L. Hultman, "X-ray photoelectron spectroscopy: Towards reliable binding energy referencing," *Prog. Mater. Sci.*, vol. 107, p. 100591, Jan. 2020, doi: 10.1016/j.pmatsci.2019.100591.
- [35] J. M. Cerrato, M. F. Hochella, W. R. Knocke, A. M. Dietrich, and T. F. Cromer, "Use of XPS to identify the oxidation state of Mn in solid surfaces of filtration media oxide samples from drinking

- water treatment plants,” *Environ. Sci. Technol.*, vol. 44, no. 15, pp. 5881–5886, Aug. 2010, doi: 10.1021/es100547q.
- [36] M. C. Biesinger, B. P. Payne, A. P. Grosvenor, L. W. M. Lau, A. R. Gerson, and R. St. C. Smart, “Resolving surface chemical states in XPS analysis of first row transition metals, oxides and hydroxides: Cr, Mn, Fe, Co and Ni,” *Appl. Surf. Sci.*, vol. 257, no. 7, pp. 2717–2730, Jan. 2011, doi: 10.1016/j.apsusc.2010.10.051.
- [37] H. W. Nesbitt and D. Banerjee, “Interpretation of XPS Mn(2p) spectra of Mn oxyhydroxides and constraints on the mechanism of MnO<sub>2</sub> precipitation,” *Am. Mineral.*, vol. 83, no. 3–4, pp. 305–315, Apr. 1998, doi: 10.2138/am-1998-3-414.
- [38] N. Fiol, C. Escudero, and I. Villaescusa, “Chromium sorption and Cr(VI) reduction to Cr(III) by grape stalks and yohimbe bark,” *Bioresour. Technol.*, vol. 99, no. 11, pp. 5030–5036, Jul. 2008, doi: 10.1016/j.biortech.2007.09.007.
- [39] S. Boursiquot, M. Mullet, and J.-J. Ehrhardt, “XPS study of the reaction of chromium (VI) with mackinawite (FeS),” *Surf. Interface Anal.*, vol. 34, no. 1, pp. 293–297, Sep. 2002, doi: 10.1002/sia.1303.
- [40] M. Aronniemi, J. Sainio, and J. Lahtinen, “Chemical state quantification of iron and chromium oxides using XPS: The effect of the background subtraction method,” *Surf. Sci.*, vol. 578, no. 1, pp. 108–123, Mar. 2005, doi: 10.1016/j.susc.2005.01.019.
- [41] Y. Wen, Z. Tang, Y. Chen, and Y. Gu, “Adsorption of Cr(VI) from aqueous solutions using chitosan-coated fly ash composite as biosorbent,” *Chem. Eng. J.*, vol. 175, pp. 110–116, Nov. 2011, doi: 10.1016/j.cej.2011.09.066.
- [42] W. Qi, Y. Zhao, X. Zheng, M. Ji, and Z. Zhang, “Adsorption behavior and mechanism of Cr(VI) using Sakura waste from aqueous solution,” *Appl. Surf. Sci.*, vol. 360, pp. 470–476, Jan. 2016, doi: 10.1016/j.apsusc.2015.10.088.

## CHAPTER V

### V. ADSORPTION OF CR(III) AND CR(VI) FROM WATER USING CRYSTALLINE MANGANESE (II, III) OXIDES

#### 5.1 Introduction

Manganese (Mn) can be considered one of the most complex metallic elements due to the fact that as a transition metal, it obtains a series of oxidation states, ranging from -2 to +7. The oxidation states of +2, +3, and +4 are the most stable and common ones [1]. The divalent species of manganese, Mn(II), may be released from a wide range of igneous and metamorphic rocks by the weathering process into various surface waters and into groundwater. Because of the high solubility of Mn(II) in acidic aqueous systems, the ubiquitous presence of manganese deposition in sediments indicates a transformation or oxidation of manganese from highly mobile and more soluble Mn(II) into the less soluble trivalent species of manganese [Mn(III)] and the insoluble tetravalent species of manganese [Mn(IV)] [2]-[3]. The chemical precipitation of manganese is controlled both by the redox potential and the pH of the system, where high pH or high redox potential favors the oxidization of mobile Mn(II), resulting in decreased manganese mobility. Manganese can be readily oxidized by natural oxidizing agents in soil such as hydrogen peroxide (H<sub>2</sub>O<sub>2</sub>) produced by cell metabolism or molecular oxygen (O<sub>2</sub>), forming a wide range of manganese oxide or manganese hydroxide minerals [4]. These manganese minerals may occur as fine-grained aggregates and veins, coatings or dendrites on the rock surfaces, and crusts or nodules in the oceans. Around 90 percent of the current industrial production of manganese is used in the production of steel and cast iron as a deoxidizing and desulfurizing agent or an alloying component. Manganese oxides are commercially important ore minerals that can be used either in production of dry-cell battery, glass, leather and textile or as a starting material for the production of other manganese chemicals [5].

Manganese oxide minerals exhibit an unusually high adsorption capacity for trace metals in soils, and therefore manganese deposits in sediments or soils can significantly alter the mobility and bioavailability

of these metals/metalloids. Manganese oxides have been extensively studied as a potential effective adsorbent of decontamination of a series of heavy metals such as lead, copper, zinc and cadmium, where they exert the highest sorption affinity toward lead [6]–[9]. Except these metal cations, manganese oxides also show adsorption behavior toward the metals and metalloids generally in the form of oxyanions (As, U, Cr, and Se) [10]–[12]. Manganese oxides, including Mn(II)O (manganosite), Mn(III)OOH (manganite), Mn<sub>2</sub>(III)O<sub>3</sub>, and Mn(IV)O<sub>2</sub> (pyrolusite), can form different crystal structures with different oxidation states or within the same oxidation states. MnO<sub>2</sub> (manganese dioxide) is a commonly employed manganese oxide in research with various origins (synthetic or biogenic) or crystal structures.

Chromium (Cr) is a metal that may exist in several oxidation states, ranging from -2 to +6, while it is mostly present in the two oxidation states of trivalent chromium [Cr(III)] and hexavalent chromium [Cr(VI)] in natural waters [13]. Hexavalent chromium compounds are well known as laboratory reagents and manufacturing intermediates. Major sources of hexavalent chromium in drinking water are discharged from steel industry, pulp mills, or metal plating operations [14]. There is strong evidence to consider hexavalent chromium as a carcinogen that may pose serious hazards towards human beings; therefore, the removal of hexavalent chromium from source of drinking water is an important health concern [15]. Only a handful of articles have investigated the adsorption of hexavalent chromium onto manganese oxides, but their experimental conditions are not representative of actual environmental conditions [8], [16]–[21]. The properties of chromium are highly dependent on the oxidation state of chromium. Hexavalent chromium is considerably more mobile and toxic than trivalent chromium, and is more difficult to remove from water due to the fact that Cr(VI) appears mainly as the soluble oxyanionic species of chromate (CrO<sub>4</sub><sup>2-</sup>) from pH 6 to 13.5, whereas the cationic Cr(III) may precipitate as insoluble Cr(OH)<sub>3</sub> in the same pH range. There are several pathways to immobilize the chromate species (CrO<sub>4</sub><sup>2-</sup>) through adsorption by minerals and metal oxides or through reduction of Cr(VI) to Cr(III) followed by precipitation of hydroxide/oxyhydroxide of Cr(III) [22]–[24]. Dissolved Fe(II), minerals

with Fe(II), sulfides, and particular organic matters appear to be the predominant reductants for Cr(VI) [25], [26]. Various studies also investigated the possible oxidation and adsorption of Cr(III) by manganese oxide minerals such as Mn(III,IV) oxide (birnessite) or Mn(IV) oxide (pyrolusite), the most oxidized of the manganese oxides [27]–[32]. Not much research has been carried out on the adsorption and removal of chromium from water by manganese (II, III) oxide, MnO and Mn<sub>2</sub>O<sub>3</sub>, the more reduced forms of the common manganese oxides. Therefore, the aim of this study is to investigate the adsorption and uptake of the two common chromium species [Cr(III) and Cr(VI)] by manganese (II, III) oxide.

## 5.2 Materials and methods

### 5.2.1 Chemicals and reagents

Potassium dichromate (99.5% purity, ACS grade) and chromium chloride ( $\text{CrCl}_3 \cdot 6\text{H}_2\text{O}$ , 96% purity, ACS grade) were obtained from Fisher Scientific (Fair Lawn, NJ, USA). De-ionized (DI) water was produced inside the laboratory with a resistance of greater than  $18 \text{ M}\Omega$ . A stock solution of  $1000 \text{ mg/L}$  Cr(VI) was prepared by mixing potassium dichromate ( $\text{K}_2\text{Cr}_2\text{O}_7$ ) with deionized water. A stock of solution of  $1000 \text{ mg/L}$  Cr(III) solution was prepared by mixing chromium chloride with deionized water. All other chemicals employed in this study were analytical grade. Sodium hydroxide (NaOH, 99.5% purity, ACS grade), hydrochloric acid (HCl, ACS plus grade) and nitric acid ( $\text{HNO}_3$ , trace metal grade) were obtained from Fisher Scientific (Fair Lawn, NJ, USA).

### 5.2.2 Sorbent characterization

The manganese (II) oxide ( $\text{MnO}$ , 99% purity, ACS grade) and manganese (III) oxide ( $\text{Mn}_2\text{O}_3$ , 99% purity, ACS grade) sorbents used in all experiments were obtained from Alfa Aesar (Ward Hill, MA, USA). The specific surface area of the  $\text{MnO}$  and  $\text{Mn}_2\text{O}_3$  sorbents were measured with an Accelerated Surface Area and Porosimeter system (Micromeritics Instrument Corporation, Norcross, GA, USA). The particle size of the  $\text{MnO}$  and  $\text{Mn}_2\text{O}_3$  sorbents were 60 mesh and 325 mesh and the BET surface area of the  $\text{MnO}$  and  $\text{Mn}_2\text{O}_3$  adsorbents were determined to be  $0.47 \text{ m}^2/\text{g}$  and  $2.2 \text{ m}^2/\text{g}$ , respectively. The X-ray diffraction (XRD-Bruker D8 Discover System, MA, USA) pattern was obtained with  $\text{Cu K}\alpha$  radiation at 40KV and 30mA to analyze the structure of the  $\text{MnO}$  and  $\text{Mn}_2\text{O}_3$  sorbents at atomic level. As shown in Figure 5.1 and 5.2, the acquired XRD pattern of the  $\text{MnO}$  sorbent was matched with the Crystallography Open Database which confirmed that the main crystalline phase of the  $\text{MnO}$  sorbent was manganosite ( $\text{Mn}_x\text{O}_y$ ,  $x=1$ ,  $y=1$ ) and the acquired XRD pattern of the  $\text{Mn}_2\text{O}_3$  sorbent was match with Crystallography Open Database which confirmed that the main crystalline phase of the  $\text{Mn}_2\text{O}_3$  sorbent was manganese (III) oxide ( $\text{Mn}_x\text{O}_y$ ,  $x=2$ ,  $y=3$ ).

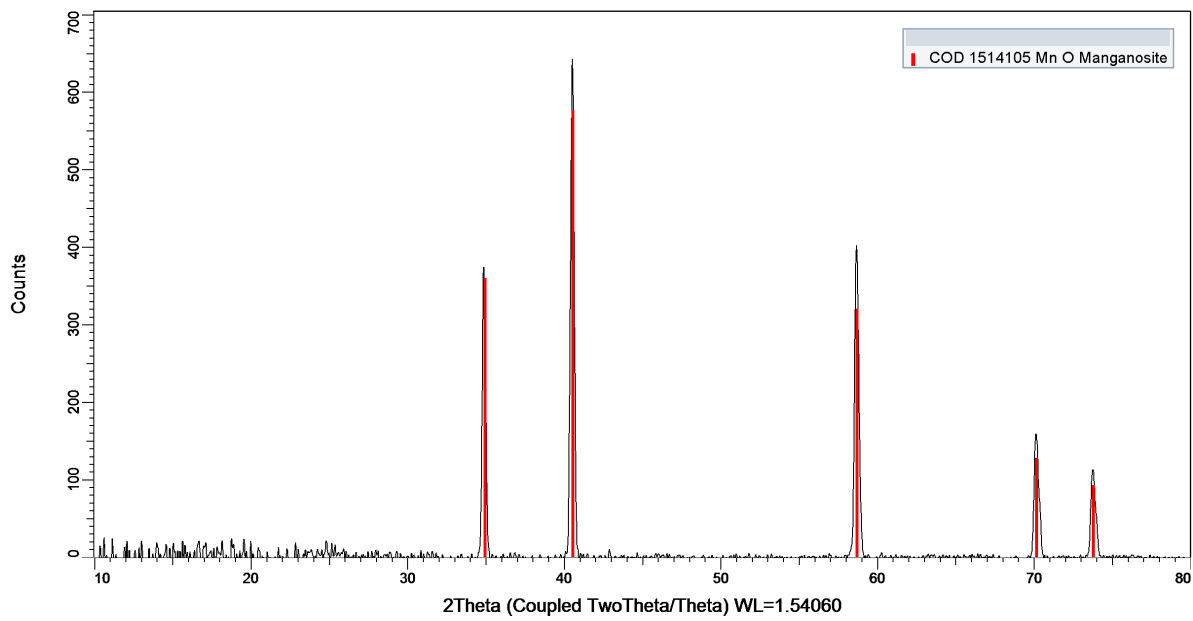


Figure 5. 1 X-ray diffraction pattern of the MnO sorbent

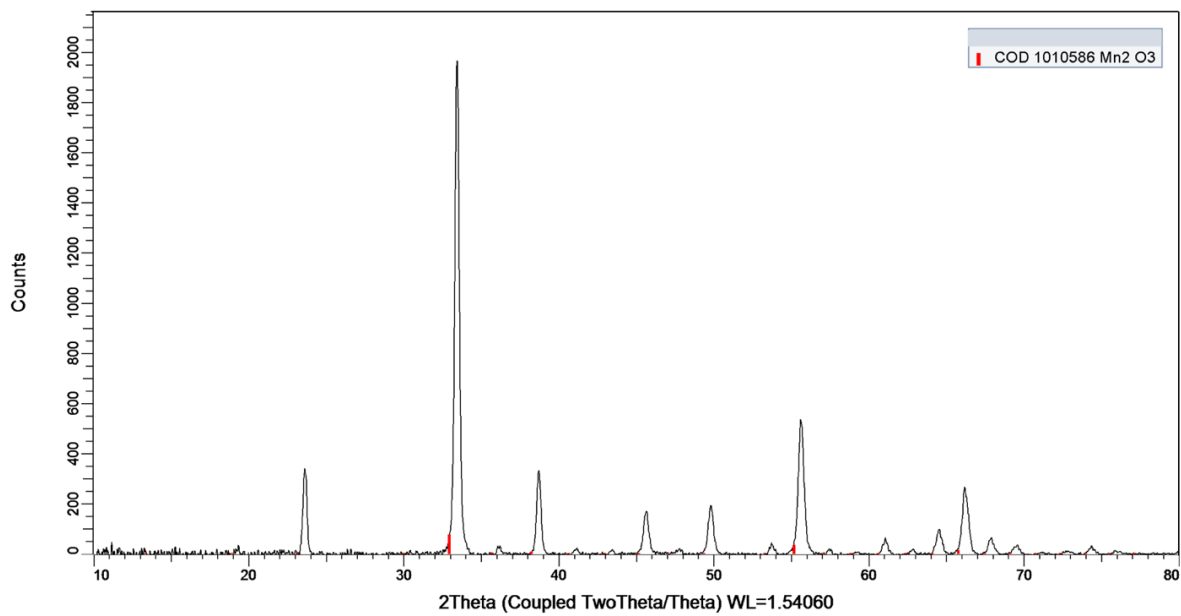


Figure 5. 2 X-ray diffraction pattern of the Mn<sub>2</sub>O<sub>3</sub> sorbent

### 5.2.3 Batch adsorption experiments

Batch adsorption experiments were conducted in sealed 50 mL high density polyethylene (HDPE) bottles. One gram of the MnO or Mn<sub>2</sub>O<sub>3</sub> sorbent (1 g) was placed in each bottle and then 50 mL of the chromium solution was added to the bottle. The 1 g of the MnO or Mn<sub>2</sub>O<sub>3</sub> sorbent was mixed with either 50 mL of a Cr(III) solution or with 50 mL of a Cr(VI) solution with an initial concentration of 1 mg/L to 10 mg/L chromium. The bottles were placed inside a rotating tumbler and shaken for a period of 24 hours at 16 rpm to reach equilibrium. After 24 hours of contact time, the mixture of the MnO or Mn<sub>2</sub>O<sub>3</sub> sorbent and solution from each bottle was removed from the tumbler and the MnO or Mn<sub>2</sub>O<sub>3</sub> sorbent was separated from the supernatant solution using centrifugation at 8000 rpm for 10 minutes. A 10-mL sample of the supernatant was acidified to a pH less than 2 by adding concentrated nitric acid (HNO<sub>3</sub>) and then analyzed for chromium using flame atomic absorption spectroscopy (FAAS) with a Perkin-Elmer AAnalyst 800 system (Perkin-Elmer, Waltham, MA, USA). A chromium hollow cathode lamp (HCL) at 357.9 nm was used to detect chromium. The atomic absorption calibration range was from 0.25 to 1.5 mg/L chromium. The adsorption and uptake of chromium by the MnO or Mn<sub>2</sub>O<sub>3</sub> sorbent was determined using the following equation:

$$q_e = \frac{(C_0 - C_e)}{m} \times V \quad (1)$$

Where  $C_0$  and  $C_e$  are the initial and equilibrium concentration of chromium in the solution (mg/L),  $q_e$  is the uptake of chromium by the MnO or Mn<sub>2</sub>O<sub>3</sub> sorbent (mg/kg),  $m$  is the weight of the MnO or Mn<sub>2</sub>O<sub>3</sub> sorbent (kg) and  $V$  is the volume of solution (L).

### 5.2.4 pH experiments

Mixtures of 1 g of the MnO or Mn<sub>2</sub>O<sub>3</sub> sorbent and 50 mL solutions of either Cr(III) or Cr(VI) with an initial chromium concentration of 1 mg/L were prepared according to the batch adsorption experimental procedure described earlier. The initial pH of the solutions containing either 1 mg/L Cr(III) or 1 mg/L Cr(VI) were adjusted (pH = 2-10) using 0.1 M hydrochloric acid (HCl) and 0.1 M sodium hydroxide (NaOH) prior to contact with the MnO or Mn<sub>2</sub>O<sub>3</sub> sorbent. The pH of all solutions after contact with the

MnO or Mn<sub>2</sub>O<sub>3</sub> sorbent (and adsorption of chromium) were measured and reported as the final pH value (equilibrium pH).

#### 5.2.5 Zeta potential measurements

The net effective charge is determined by measuring the zeta potentials of different suspensions of the MnO or Mn<sub>2</sub>O<sub>3</sub> sorbent using the Zeta-meter system 3.0 (Zeta meter Inc, Staunton, VA, USA). The 1 g/L suspensions of the MnO or Mn<sub>2</sub>O<sub>3</sub> sorbent were prepared without chromium, with 1 mg/L Cr(III), or with 1mg/L Cr(VI) in solutions containing 1 mM sodium chloride (NaCl). The initial pH value of the solutions were adjusted from 2 to 12 by adding 0.1 M HCl and 0.1 M NaOH.

## 5.3 Results and discussion

### 5.3.1 Adsorption isotherm experiments

The Langmuir, the Freundlich, the Dubinin-Radushkevich (D-R) and the Temkin adsorption equations were employed to describe the adsorption of chromium species onto the MnO or Mn<sub>2</sub>O<sub>3</sub> sorbent; valuable information in terms of the adsorption mechanism, adsorbent surface properties and adsorption energy may be gained by applying these adsorption models [33]. The Langmuir empirical adsorption model assumes that the sorbent surface consists of identical and equivalent adsorption sites that only allow monolayer adsorption [34]. The Langmuir adsorption equation is expressed by the following equation:

$$q_e = \frac{q_m K_L C_e}{1 + K_L C_e} \quad (2)$$

where  $C_e$  is the equilibrium concentration of chromium in solution (mg/L),  $q_e$  is the uptake of chromium at equilibrium (mg/kg),  $q_m$  is the (maximum) adsorption capacity of the adsorbent (mg/kg), and  $K_L$  is the Langmuir constant related to the free energy of adsorption which may be referred to as the binding or affinity parameter of the adsorption system. These parameters are determined from a linearized plot of the Langmuir Equation as follows:

$$\frac{C_e}{q_e} = \frac{C_e}{q_m} + \frac{1}{K_L q_m} \quad (3)$$

The Freundlich adsorption equation describes a non-ideal and reversible adsorption process, which can be applied to multilayer adsorption on a heterogeneous adsorbent surface with a range of binding energies [35]. The Freundlich adsorption equation is described in equation (4) and the corresponding linearized form of the Freundlich equation is shown in equation (5):

$$q_e = K_F C_e^{1/n} \quad (4)$$

$$\log q_e = \log K_F + \frac{1}{n} \log C_e \quad (5)$$

where  $K_F$  and  $1/n$  are Freundlich constants indicative of adsorption capacity and adsorption strength (or intensity), respectively,  $C_e$  is the equilibrium concentration of chromium in solution (mg/L), and  $q_e$  is the uptake of chromium at equilibrium (mg/kg).

The Temkin adsorption model takes into account the interactions between adsorbent and adsorbate involving the heat of adsorption [36]. The empirical equation of the Temkin adsorption model is presented in equation (6) and can be shown in the linearized form in equation (7):

$$q_e = \frac{RT}{b} \ln(AC_e) \quad (6)$$

$$q_e = \frac{RT}{b} \ln A + \frac{RT}{b} \ln C_e \quad (7)$$

where  $A$  (L/mg) is the Temkin equilibrium binding constant corresponding to the maximum binding energy,  $b$  (J/mol) is the heat of adsorption,  $T$  is absolute temperature (K) and  $R$  is the universal gas constant (8.314J/mol-K).

The Dubinin-Radushkevich (D-R) adsorption model is another empirical model which can be fitted with the adsorption equilibrium data to distinguish between the physical and chemical adsorption by determining the mean free energy [37]. The D-R adsorption model is described in equations (8) - (9), and can be linearized as shown in equation 10:

$$q_e = q_s \exp(-K_{DR} \varepsilon^2) \quad (8)$$

$$\varepsilon = RT \ln\left(1 + \frac{1}{C_e}\right) \quad (9)$$

$$\ln q_e = \ln q_s - K_{DR} \varepsilon^2 \quad (10)$$

where  $q_e$  is the uptake of chromium at equilibrium (mg/kg),  $C_e$  is the equilibrium concentration of chromium in solution (mg/L),  $q_s$  is the maximum adsorption capacity (mg/kg),  $\varepsilon$  is Polanyi potential,  $K_{DR}$  is a constant related to the mean free energy of adsorption,  $T$  is absolute temperature (K) and  $R$  is the universal gas constant (8.314J/mol-K). The mean free energy of adsorption can be computed using the following equation,

$$E = \frac{1}{\sqrt{(2K_{DR})}} \quad (11)$$

If a calculated mean free energy (E) is less than 8 kJ/mol, it would be indicative of physical sorption; if E value falls into the range of 8 to 16 kJ/mol, it would suggest that the sorption process is likely chemisorption.

The adsorption data for adsorption of chromium onto the MnO or Mn<sub>2</sub>O<sub>3</sub> sorbent obtained from the adsorption isotherm experiments performed for Cr(III) and Cr(V) are presented in Figure 5.3 and 5.4, respectively.

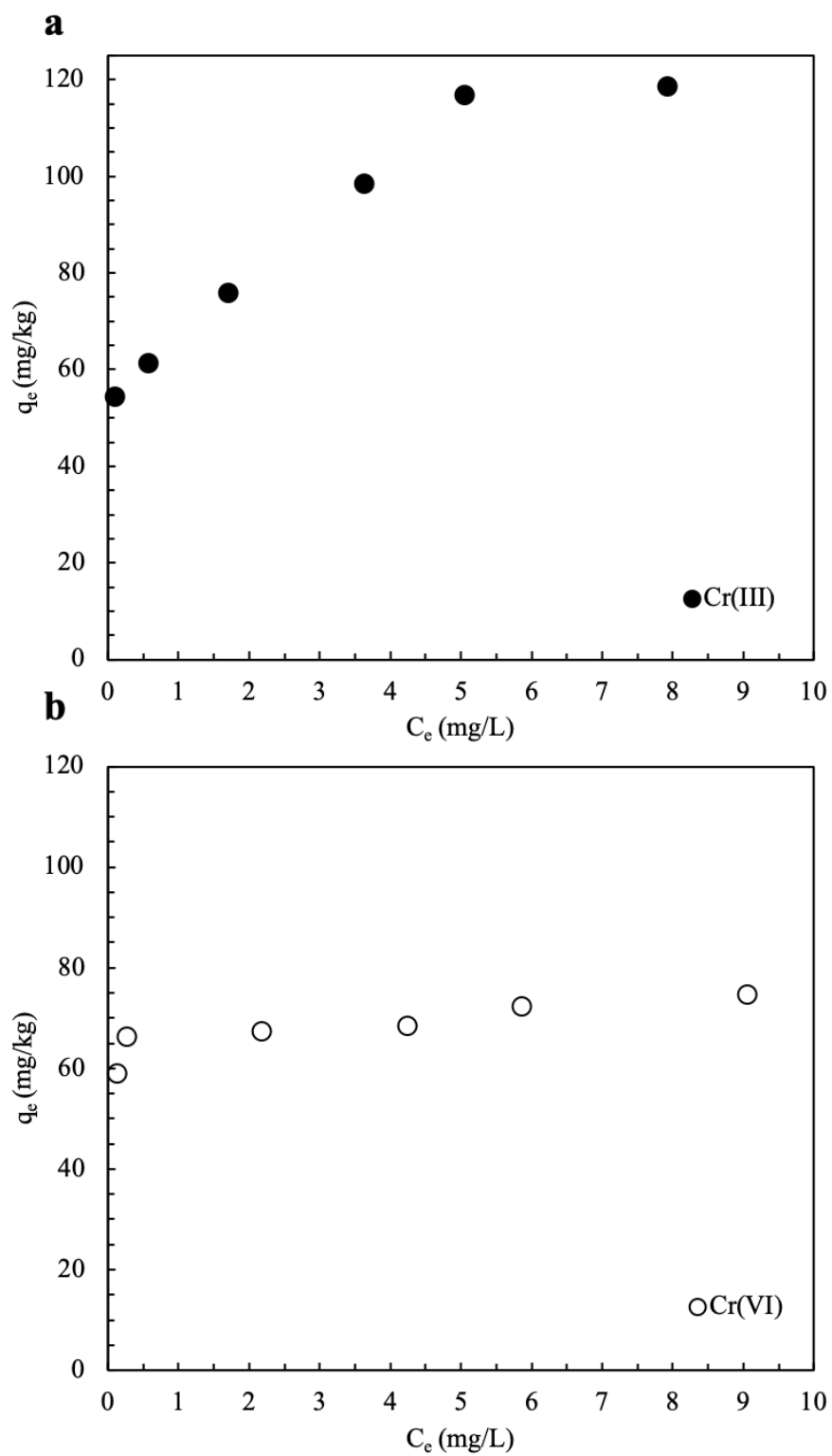


Figure 5. 3 Adsorption isotherm data for chromium: (a) Cr(III) and (b) Cr(VI) onto the MnO sorbent

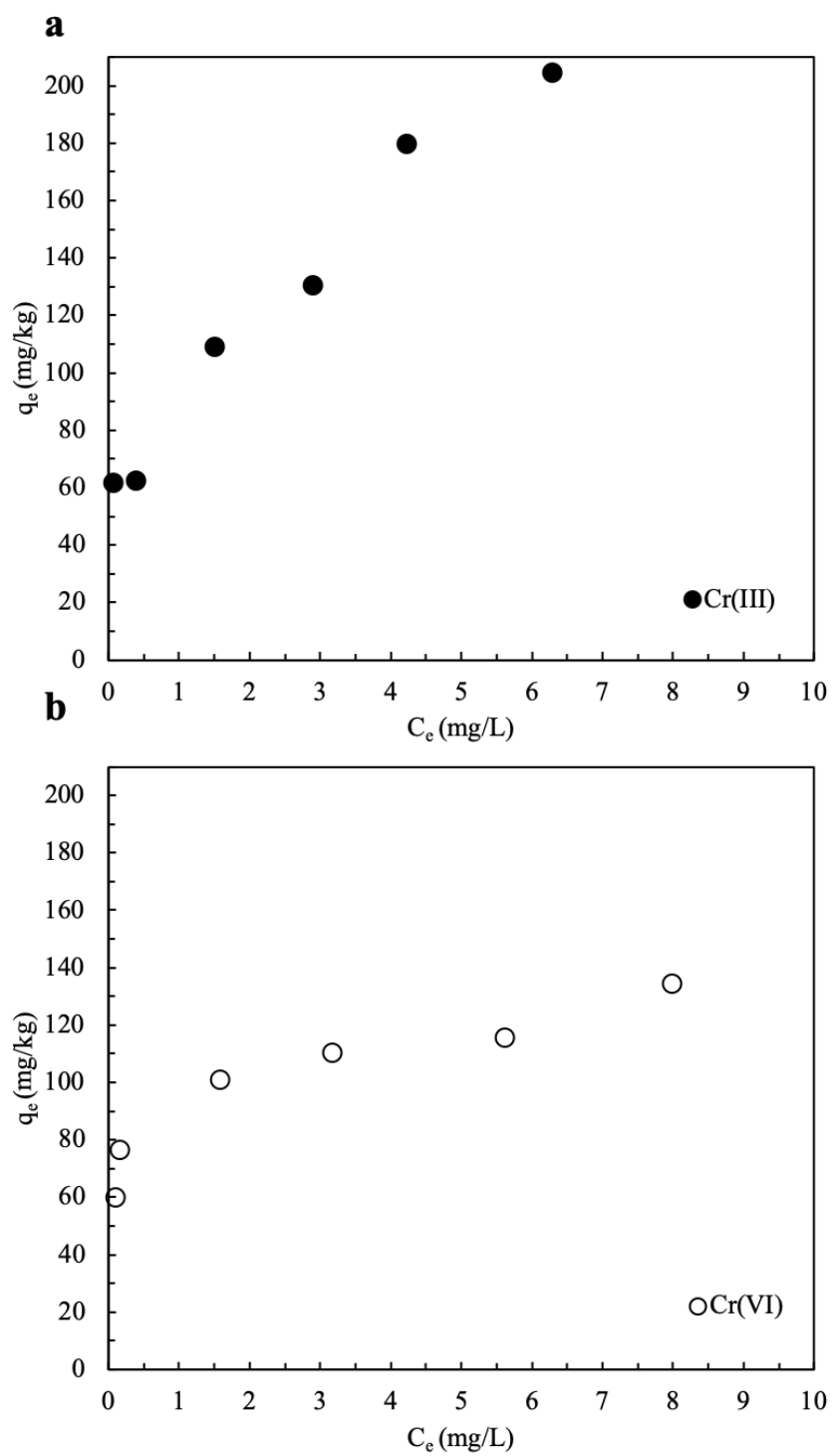


Figure 5. 4 Adsorption isotherm data for chromium: (a) Cr(III) and (b) Cr(VI) onto the  $Mn_2O_3$  sorbent

The adsorption parameters of the four aforementioned adsorption models were determined from the adsorption isotherm data obtained for adsorption of Cr(III) and Cr(VI) onto the MnO or Mn<sub>2</sub>O<sub>3</sub> sorbent are presented in Table 5.1 and 5.2.

Table 5. 1 Adsorption parameters for adsorption of Cr(III) and Cr(VI) onto the MnO sorbent

Isotherm	Parameter	Cr(III)	Cr(VI)
Langmuir	$K_L$ (L/mg)	2.0	6.05
	$q_m$ (mg/kg)	125	78.7
	$R^2$	0.991	0.992
Freundlich	$K_F$	77.5	66.6
	1/n	0.189	0.042
	$R^2$	0.905	0.819
Temkin	A(L/mg)	0.194	603.4
	b(kJ/mol)	0.147	0.479
	$R^2$	0.855	0.896
D-R	E(kJ/mol)	5.09	8.51
	$R^2$	0.543	0.793

Table 5. 2 Adsorption parameters for adsorption of Cr(III) and Cr(VI) onto the Mn<sub>2</sub>O<sub>3</sub> sorbent

Isotherm	Parameter	Cr(III)	Cr(VI)
Langmuir	$K_L$ (L/mg)	1	3.04
	$q_m$ (mg/kg)	222.22	131.58
	$R^2$	0.9207	0.9873
Freundlich	$K_F$	107.920	93.498
	1/n	0.2698	0.1545
	$R^2$	0.866	0.9545
Temkin	A(L/g)	54.93	958.145
	b(J/mol)	75.75	160.73
	$R^2$	0.7945	0.9547
D-R	E(kJ/mol)	4.834	4.857
	$R^2$	0.5	0.9149

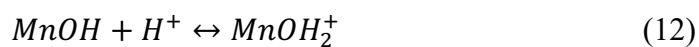
The high value of correlation coefficients ( $R^2$ ) of 0.991 for Cr(III) onto the MnO sorbent and 0.9207 for Cr(III) onto the Mn<sub>2</sub>O<sub>3</sub> sorbent and 0.992 for Cr(VI) onto the MnO sorbent and 0.9873 for Cr(VI) onto the Mn<sub>2</sub>O<sub>3</sub> sorbent indicate that the adsorption data are well fitted to the Langmuir adsorption model, suggesting that the favorable adsorption of Cr(III) and Cr(VI) onto the MnO and Mn<sub>2</sub>O<sub>3</sub> adsorbents. The Langmuir constant related to free energy of adsorption ( $K_L$ ) was determined to be 2.0 L/mg for Cr(III) onto the MnO sorbent and 1.0 L/mg for Cr(III) onto the Mn<sub>2</sub>O<sub>3</sub> sorbent and 6.05 L/mg for Cr(VI) onto the MnO sorbent and 3.04 L/mg for Cr(III) onto the Mn<sub>2</sub>O<sub>3</sub> sorbent, indicating that the MnO and Mn<sub>2</sub>O<sub>3</sub> sorbents adsorbed Cr(VI) more strongly than Cr(III).

The adsorption data were found to be in agreement with the Freundlich adsorption model with  $R^2$  value of 0.819 for Cr(III) onto the MnO sorbent, 0.866 for Cr(III) onto the Mn<sub>2</sub>O<sub>3</sub> sorbent, 0.905 for Cr(VI) onto the MnO sorbent and 0.9545 for Cr(VI) onto the Mn<sub>2</sub>O<sub>3</sub> sorbent. However, a comparison of  $R^2$  values for the Langmuir and the Freundlich models shows that the Langmuir adsorption model provides a better fit for adsorption data of chromium, indicating that the surfaces of the MnO and Mn<sub>2</sub>O<sub>3</sub> sorbents are more likely homogenous and that monolayer adsorption can be assumed for adsorption of both Cr(III) and Cr(VI) onto the surface of the MnO and Mn<sub>2</sub>O<sub>3</sub> sorbents. The Freundlich parameter  $1/n$  for both chromium species is less than 1.0 (0.189 for Cr(III) and 0.042 for Cr(VI) onto the MnO sorbent and 0.27 for Cr(III) and 0.15 for Cr(VI) onto the Mn<sub>2</sub>O<sub>3</sub> sorbent), indicative of favorable adsorption of both Cr(III) and Cr(VI) onto the MnO and Mn<sub>2</sub>O<sub>3</sub> sorbents. For Cr(VI), the larger  $K_L$  from the Langmuir equation and the smaller  $1/n$  from the Freundlich equation are both indicative of a more favorable and stronger binding of Cr(VI) than of Cr(III) with the surface of the MnO and Mn<sub>2</sub>O<sub>3</sub> sorbents [38]. The Temkin constant A related to the binding energy was much larger for Cr(VI) than for Cr(III). The values of the Temkin constant b (indicative of heat of adsorption) were positive for both Cr(III) and Cr(VI), suggesting that the adsorption process of both chromium species were exothermic [39], while the Temkin constant b was several times larger for Cr(VI) than for Cr(III). The mean free energy (E) for uptake of Cr(III) and Cr(VI) by MnO determined from the D-R adsorption equation was found to be 5.1

kJ/mol and 8.5 kJ/mol and the mean free energy (E) for uptake of Cr(III) and Cr(VI) by  $\text{Mn}_2\text{O}_3$  determined from the D-R adsorption equation was found to be 4.834 kJ/mol and 4.857 kJ/mol, respectively. The value of E for Cr(VI) is above 8 kJ/mol which is indicative of the chemisorption of Cr(VI) onto the MnO sorbent, while the E value of Cr(III) adsorption onto the MnO and  $\text{Mn}_2\text{O}_3$  sorbents and Cr(VI) adsorption onto the  $\text{Mn}_2\text{O}_3$  are below 8 kJ/mol which is indicative of physical adsorption [34]. The Langmuir constant  $K_L$ , the Freundlich constant  $1/n$ , the Temkin constants (A and b) and the D-R constant E for adsorption of Cr(III) and Cr(VI) are in good agreement with each other, showing that the MnO and  $\text{Mn}_2\text{O}_3$  sorbents displayed stronger binding and greater affinity for adsorption of Cr(VI) than for adsorption of Cr(III).

### 5.3.2 Effect of pH on adsorption

The pH is an important factor controlling the chromium adsorption process due to the fact that it impacts the extant forms of chromium species, the surface charge of metal oxides and the surface protonation [40]. Cr(III) can be found either as insoluble species such as chromium oxide ( $\text{Cr}_2\text{O}_3$ ) and chromium hydroxide [ $\text{Cr}(\text{OH})_3$ ] or as soluble species such as chromium hydroxide cations or anions at different pH values [41]. Cr(III) generally forms insoluble chromic oxide ( $\text{Cr}_2\text{O}_3$ ) from approximately pH 5.0 to 13.5 or insoluble and amorphous chromium hydroxide  $\text{Cr}(\text{OH})_3$  from approximately pH 8 to 12 [13]. Soluble chromic cations  $\text{Cr}^{3+}$  is generally present in solution at pH range of 2-8, while chromium hydroxide cations  $\text{Cr}(\text{OH})^{2+}$  and  $\text{Cr}(\text{OH})_2^+$  become the main products of dissolution of Cr(III) species at pH greater than 4 to pH 7.5. At extreme pH (pH above 10), soluble chromium hydroxide anion  $\text{Cr}(\text{OH})_4^-$  would be formed with presence of excessive hydroxide ions in solution [42]. Cr(VI) is extensively hydrolyzed and present as soluble oxy-anion species in aqueous environment [13]. The first and second acid dissociation constants ( $\text{pK}_a$ ) for chromic acid ( $\text{H}_2\text{CrO}_4$ ) are 0.74 and 6.49, respectively [43]. Therefore, Cr(VI) generally forms soluble anionic species dichromate ( $\text{HCrO}_4^-$ ) from pH 2 to 6.49 and chromate ( $\text{CrO}_4^{2-}$ ) from pH 6.49 to 14. The formation of surface hydroxyl group on metal oxides (e.g. MnOH) to obtain the more favorable charge distribution may result in surface protonation or deprotonation, which renders the metal oxide surface positively charged or negatively charged [44]:



The Geochemist's Workbench (GWB) 12.0.4 was employed to develop Eh-pH diagram for manganese species (Figure 5.5). The data for the adsorption and uptake of Cr(III) and Cr(VI) by the MnO or Mn<sub>2</sub>O<sub>3</sub> sorbent as function of initial solution pH are presented in Figure 5.6 and 5.7. The results from Figure 6 and 7 show that the adsorption of both Cr(III) and Cr(VI) onto the MnO and Mn<sub>2</sub>O<sub>3</sub> sorbents decreased with increasing pH. The uptake of Cr(VI) decreased gradually from 88% to 78% of the maximum uptake for the MnO sorbent and from 88% to 66% of the maximum uptake for the Mn<sub>2</sub>O<sub>3</sub> sorbent from pH 2 to pH 9, whereas the uptake of Cr(III) decreased sharply from 99% to 52% of the maximum uptake for the MnO sorbent and decreased slightly from 98% to 85% of the maximum uptake for the Mn<sub>2</sub>O<sub>3</sub> sorbent at the same pH range. A significant loss in the adsorption of both Cr(III) and Cr(VI) onto the MnO sorbent was observed at pH greater than 9, with 19% and 23% of the maximum uptake occurring at pH value of 12 for Cr(III) and Cr(VI), respectively. Adsorption of Cr(III) onto the Mn<sub>2</sub>O<sub>3</sub> sorbent experienced a sharp decrease from 61% to 6% of the maximum uptake when pH was raised from 8 to 9, while adsorption of Cr(VI) onto the Mn<sub>2</sub>O<sub>3</sub> sorbent decreased significantly from 66% to 12% with the increasing pH from 9 to 10. As the initial pH increased from 8 to 12, Cr(III) was expected to combine with the hydroxide species (OH<sup>-</sup>) to precipitate as Cr(OH)<sub>3</sub> on the surface of the MnO sorbent [13]. However, it can be seen from Figure 5.6 and 5.7 that the uptake of Cr(III) onto the MnO and Mn<sub>2</sub>O<sub>3</sub> sorbents decreased at pH above 9, which may be attributed to the continued reaction between Cr(III) and OH<sup>-</sup> to form the soluble species of Cr(OH)<sub>4</sub><sup>-</sup> and to the competition between Cr(OH)<sub>4</sub><sup>-</sup> and OH<sup>-</sup> [28]. The final pH values (pH after adsorption) presented in Figure 5.6 show that the final pH increased substantially when the initial pH fell into the range of 2-6 and decreased slightly when initial pH value was above 7 for chromium adsorption onto the MnO sorbent. The dissolution of MnO in acidic solution (pH < 7) was found to be conducive to the release of hydroxide ions in solution which raised the solution pH [45].

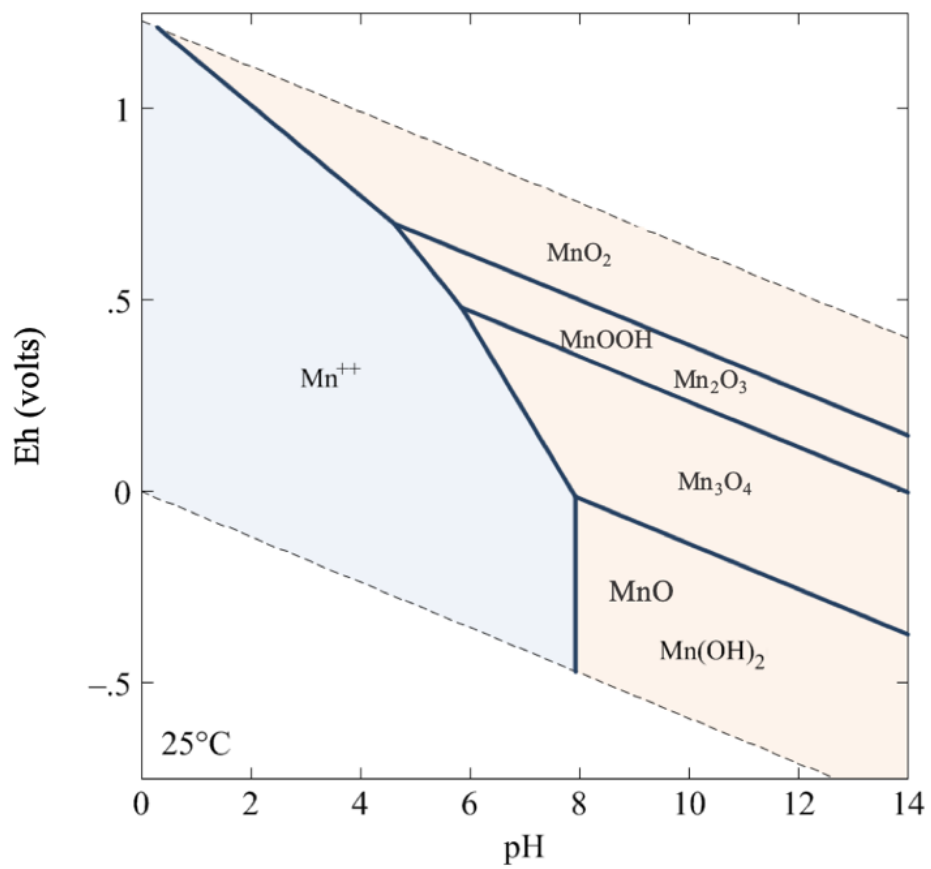


Figure 5. 5 Eh-pH diagram for manganese

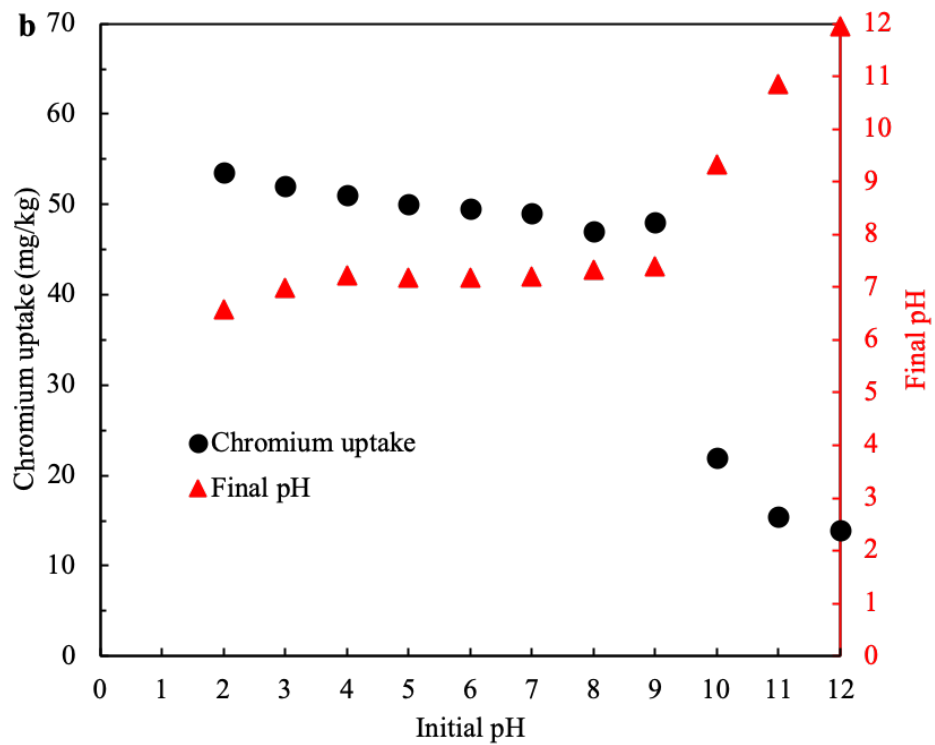
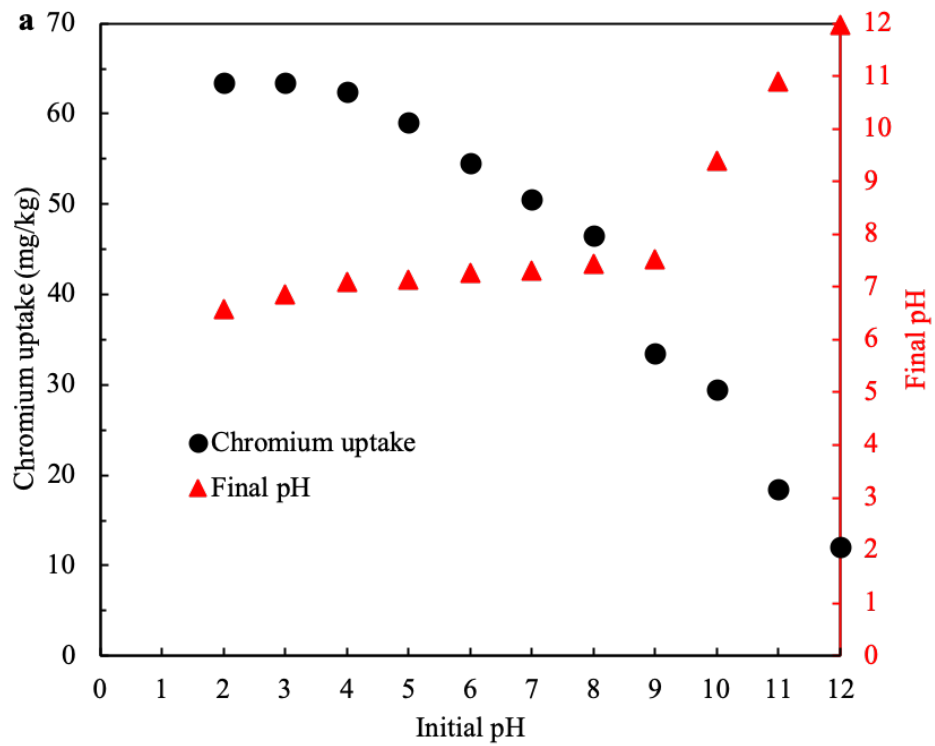


Figure 5. 6 Adsorption of chromium onto the MnO sorbent as function of pH: (a) Cr(III) and (b) Cr(VI)

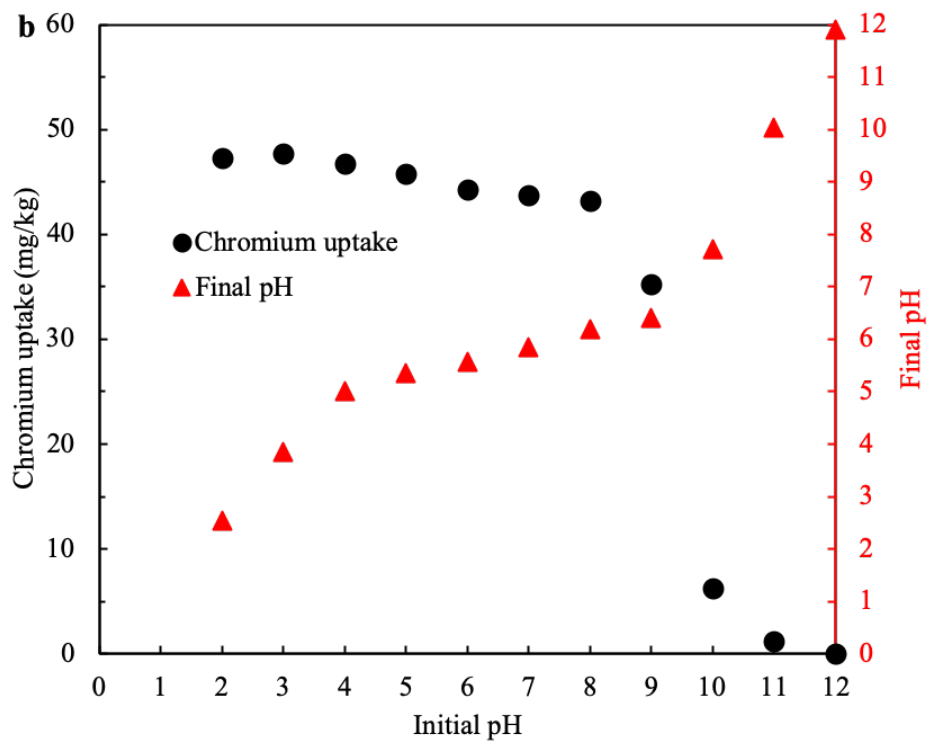
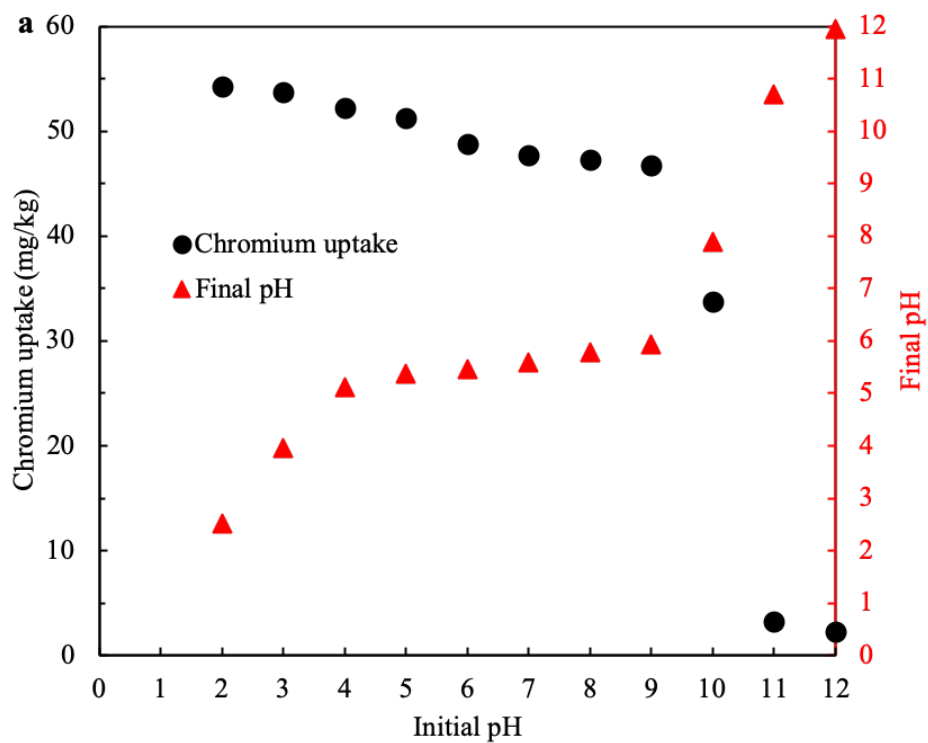


Figure 5. 7 Adsorption of chromium onto the  $Mn_2O_3$  sorbent as function of pH: (a) Cr(III) and (b) Cr(VI)

### 5.3.3 Effect of surface charge on adsorption

The zeta potential ( $\zeta$ ) measurement is a characterization technique to quantify the net surface charge of metal oxides/hydroxides particles in solution. The point of zero charge (PZC) is the pH of the solution at which the net charge of the metal oxides surface is zero [46]. To understand the interactions between the two chromium species when in contact with manganese (II, III) oxide's surface, the zeta potential of the MnO and Mn<sub>2</sub>O<sub>3</sub> sorbents were measured using 1g/L of the adsorbent in an aqueous solution containing 1mM NaCl with and without the chromium species. As shown in Figure 5.8 and 5.9, the pH<sub>PZC</sub> of the MnO sorbent was determined to be 10.39 in the absence of chromium, 10.16 in the presence of Cr(III) species and 10.26 in the presence of Cr(VI) species and the pH<sub>PZC</sub> of the Mn<sub>2</sub>O<sub>3</sub> sorbent was determined to be 6.88 in the absence of chromium, 9.91 in the presence of Cr(III) species and 7.03 in the presence of Cr(VI) species. The surface of the MnO and Mn<sub>2</sub>O<sub>3</sub> sorbents were positively charged at pH values below pH<sub>PZC</sub> and negatively charged at pH values above pH<sub>PZC</sub>. A major shift in PZC of the MnO sorbent was not observed regardless of the presence of chromium or the type of chromium species. A significant shift in PZC of the Mn<sub>2</sub>O<sub>3</sub> sorbent was observed for the Cr(III) adsorption and was not observed for the Cr(VI) adsorption.

Cr(III) may be present in the solution phase as several cationic species (pH 2-7.5), as the neutral species Cr(OH)<sub>3</sub> (pH 8-12) and as the anionic species Cr(OH)<sub>4</sub><sup>-</sup> (pH above 10). There is little electrostatic attraction between the positively charged surface of the MnO sorbent in the pH range of 2-10 and the Mn<sub>2</sub>O<sub>3</sub> sorbent in the pH range of 2-7 and either the cationic or the neutral species of Cr(III). Since the contribution of electrostatic attraction to the adsorption of Cr(III) species onto the MnO sorbent is insignificant in the pH range of 2-10, the adsorption of Cr(III) species in this pH range may therefore be attributed to outer-sphere complexation, which did not result in a significant shift in the PZC of the MnO sorbent in contact with Cr(III) species. A significant increase of PZC from 6.88 to 9.91 indicates that Cr(III) adsorption onto the Mn<sub>2</sub>O<sub>3</sub> sorbent is inner-sphere complexation. Cr(VI) is present in the solution phase as oxy-anionic species (chromate or bichromate). Specific adsorption or inner-sphere

adsorption can be inferred from the occurrence of a shift in the PZC because specific adsorbed ions are considered to reside inside of the shear plane of adsorbent resulting in a significant change of the surface charge [44]-[46]. Since no significant shift in PZC of the MnO and Mn<sub>2</sub>O<sub>3</sub> sorbents occurred after the adsorption of Cr(VI), the adsorption of Cr(VI) was therefore either due to the outer-sphere complexation of Cr(VI) or due to the possible transformation of Cr(VI) species to Cr(III) species.

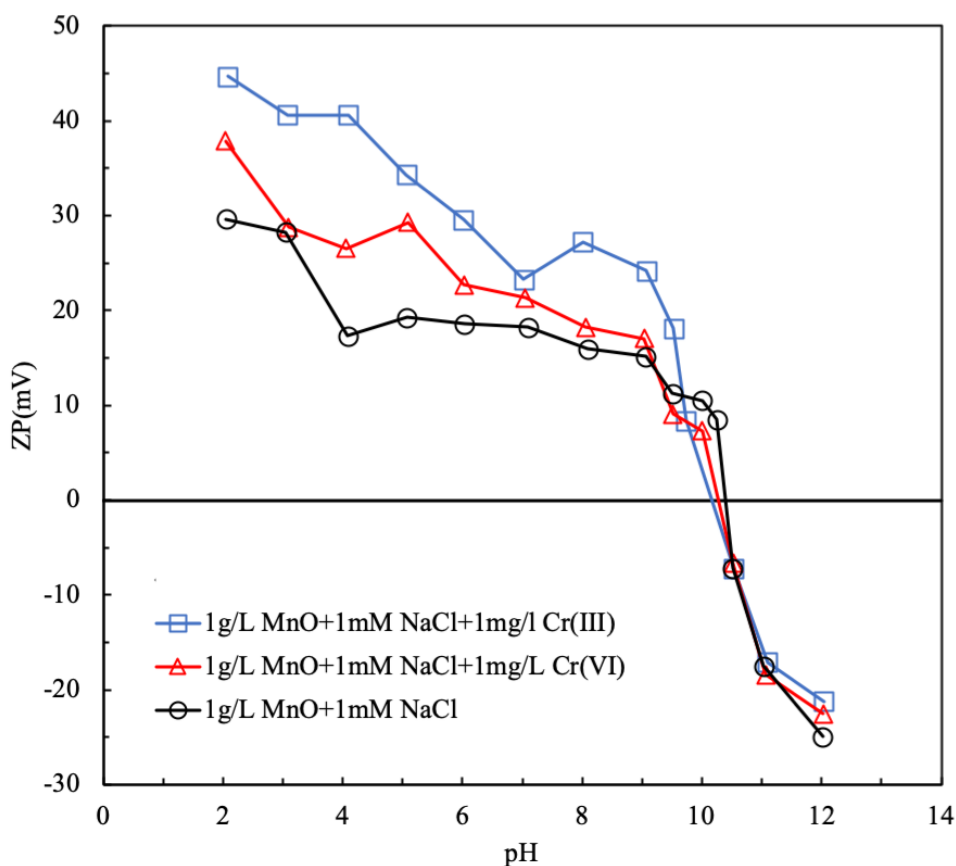


Figure 5. 8 Zeta potential of the MnO sorbent in the presence of Cr(III) and Cr(VI)

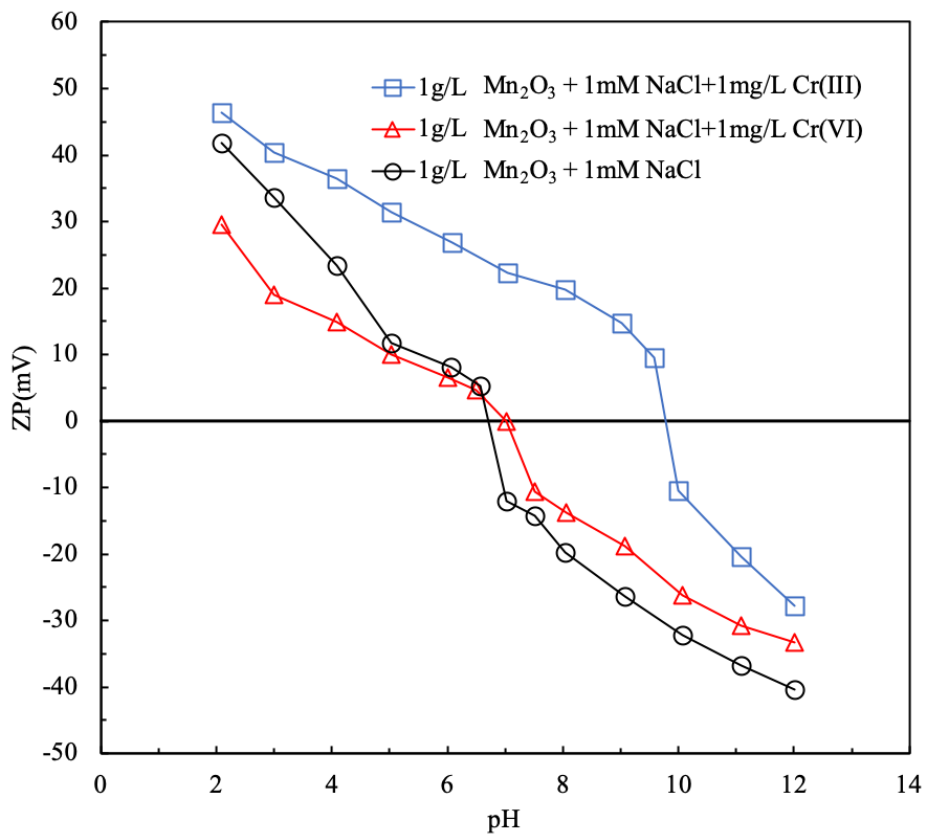


Figure 5. 9 Zeta potential of the  $Mn_2O_3$  sorbent in the presence of Cr(III) and Cr(VI)

#### 5.3.4 Surface characterization

X-ray photoelectron spectroscopy (XPS-Kartos AXIS-165, Manchester, UK) was employed to investigate the chemical oxidation states of manganese and chromium, the structure of the MnO and Mn<sub>2</sub>O<sub>3</sub> sorbents and possible chemical bonds after the adsorption of the chromium species onto the MnO or Mn<sub>2</sub>O<sub>3</sub> sorbent. Spectroscopic investigation is necessary to confirm the aforementioned hypothesis that Cr(VI) can be partially adsorbed onto the manganese (II,III) oxides surface followed by the transformation of Cr(VI) to Cr(III) by direct electron donation of Mn<sup>2+</sup> and Mn<sup>3+</sup> [50]. X-ray photoelectron spectroscopy (XPS) is a near-surface sensitive technique that predominately employed in determining the oxidation states of an element [48]–[50]. In order to prepare samples for XPS analysis of the chromium species adsorbed onto the MnO or Mn<sub>2</sub>O<sub>3</sub> sorbent, we mixed 5 g of the MnO or Mn<sub>2</sub>O<sub>3</sub> sorbent separately with a 100 mg/L solution of Cr(III) and with a 100 mg/L solution of Cr(VI). We analyzed the MnO and Mn<sub>2</sub>O<sub>3</sub> sorbent samples after adsorption using XPS to identify the oxidation states of chromium and manganese on the surface of the MnO or Mn<sub>2</sub>O<sub>3</sub> sorbent. Figure 5.10-13 show the XPS spectra for the MnO or Mn<sub>2</sub>O<sub>3</sub> sorbent after adsorption of Cr(VI) and Cr(III) species.

Figure 5.10 and 5.11 present the XPS spectra of the elements on the surface of the MnO and Mn<sub>2</sub>O<sub>3</sub> sorbents, showing that chromium (Cr) was detected on the surface of the MnO and Mn<sub>2</sub>O<sub>3</sub> sorbents samples exposed to the solution of Cr(III) and to the solution of Cr(VI), respectively. The XPS results from Figure 5.10 and 5.11 indicate that both chromium species were either adsorbed or precipitated onto the surface of the MnO and Mn<sub>2</sub>O<sub>3</sub> sorbents. Figure 5.12 and Figure 5.13 show the XPS spectra for chromium species present on the surface of the MnO or Mn<sub>2</sub>O<sub>3</sub> sorbent samples exposed to solution of Cr(III) and to solution of Cr(VI), respectively. The results from Figure 5.12 and Figure 5.13 show the Cr 2p peaks of chromium adsorbed onto the MnO or Mn<sub>2</sub>O<sub>3</sub> sorbent samples; they include five peaks at 575.9, 576.7, 577.7, 578.7 and 579.1 eV, corresponding to the binding energy of the 2p<sub>3/2</sub> of Cr(III) in Cr<sub>2</sub>O<sub>3</sub> and Cr(OH)<sub>3</sub> for the MnO sorbent sample exposed to the Cr(VI) solution (Figure 5.12b), and one peak at 579.3 eV, corresponding to the binding energy of the 2p<sub>3/2</sub> of Cr(III) in Cr(OH)<sub>3</sub> for the MnO

sorbent sample exposed to the solution of Cr(III) (Figure 5.12a); they include three peaks at 574.5, 575.7, and 577.3 eV, corresponding to the binding energy of the  $2p_{3/2}$  of Cr(III) in  $\text{Cr}_2\text{O}_3$  and  $\text{Cr}(\text{OH})_3$  for the  $\text{Mn}_2\text{O}_3$  sorbent sample exposed to the Cr(III) solution (Figure 5.13a) and one peak at 577.3 eV and one peak at 579.0 eV, corresponding to the binding energy of the  $2p_{3/2}$  of Cr(III) in  $\text{Cr}(\text{OH})_3$  and the  $2p_{3/2}$  of Cr(VI) in chromate ion for the  $\text{Mn}_2\text{O}_3$  sorbent sample exposed to the solution of Cr(VI) [51]–[54]. The results from Figure 5.12 show that there is no contribution of peaks relating to Cr(VI) species on the surface of the MnO sorbent sample exposed to the solution of Cr(VI). Therefore, the XPS analysis indicates that both the adsorption of Cr(VI) and the reduction of Cr(VI) occurred within the MnO sorbent-solution system and that hexavalent chromium [Cr(VI)] was completely reduced to trivalent chromium [Cr(III)] on the surface of the MnO sorbent exposed to the solution of Cr(VI). The appearance of both Cr(III) and Cr(VI) species after the adsorption of Cr(III) or Cr(VI) onto the  $\text{Mn}_2\text{O}_3$  sorbent suggest that  $\text{Mn}_2\text{O}_3$  possesses the ability to either oxidize Cr(III) into Cr(VI) or reduce Cr(VI) into Cr(III) as an intermediate oxidation state for manganese species.

As for the oxidation state of manganese on the MnO sorbent surface after exposure to the solution of Cr(VI), the peak observed at 641.0 eV for Mn  $2p_{3/2}$  (Figure 5.10a) is well compared to the binding energy of Mn(III) in  $\text{MnOOH}$  (manganite) and  $\text{Mn}_2\text{O}_3$ , which indicated that Mn(II) was transformed to Mn(III) [49], [55]. The peak observed at 638.6 eV for Mn  $2p_{3/2}$  (Figure 5.10b) was solely attributed to Mn(II) in the MnO sorbent; this shows that the oxidation state of manganese on the surface of the MnO sorbent after exposure to the solution of Cr(III) remained as Mn(II) with no other (higher) oxidation states of manganese present on the sorbent surface, indicating that no redox reactions involving chromium or manganese were involved in the adsorption of Cr(III) onto the MnO sorbent. Specific change of the oxidation state of manganese on the  $\text{Mn}_2\text{O}_3$  sorbent surface after exposure to the solution of Cr(III) and Cr(VI) can be obtained from the Figure 5.11. It can be observed that the peak at 642.5 eV for Mn  $2p_{3/2}$  (Figure 11b) resulted from the appearance of  $\text{MnO}_2$  at the surface of the  $\text{Mn}_2\text{O}_3$  sorbent after

contacting with Cr(VI) solution and the peak at 641 eV for Mn 2p<sub>3/2</sub> (Figure 5.11a) resulted from the appearance of MnOOH at the surface of the Mn<sub>2</sub>O<sub>3</sub> sorbent after contacting with Cr(III) solution.

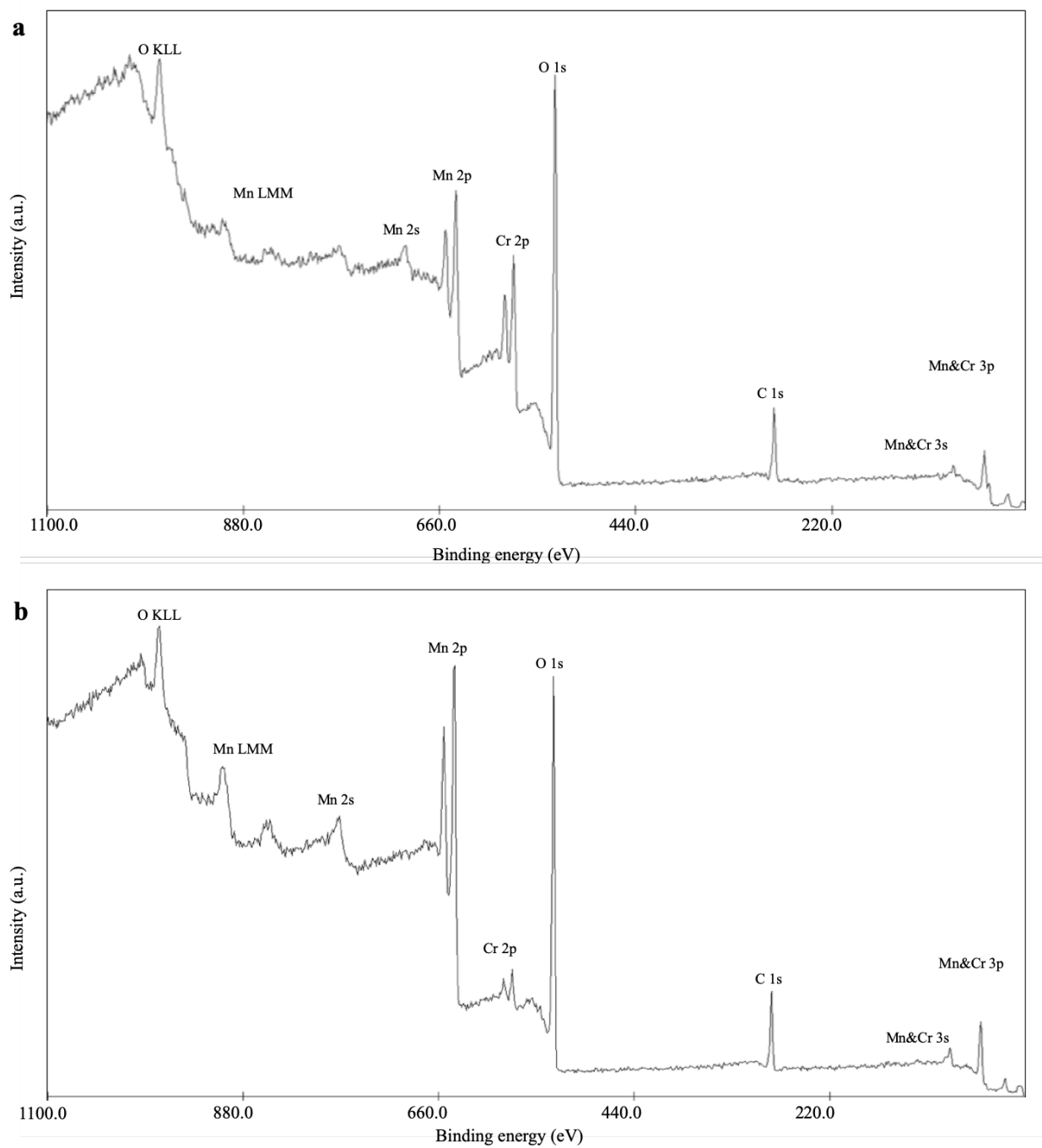


Figure 5. 10 XPS all element spectra of the MnO surface after adsorption of (a) Cr(III) and (b) Cr(VI)

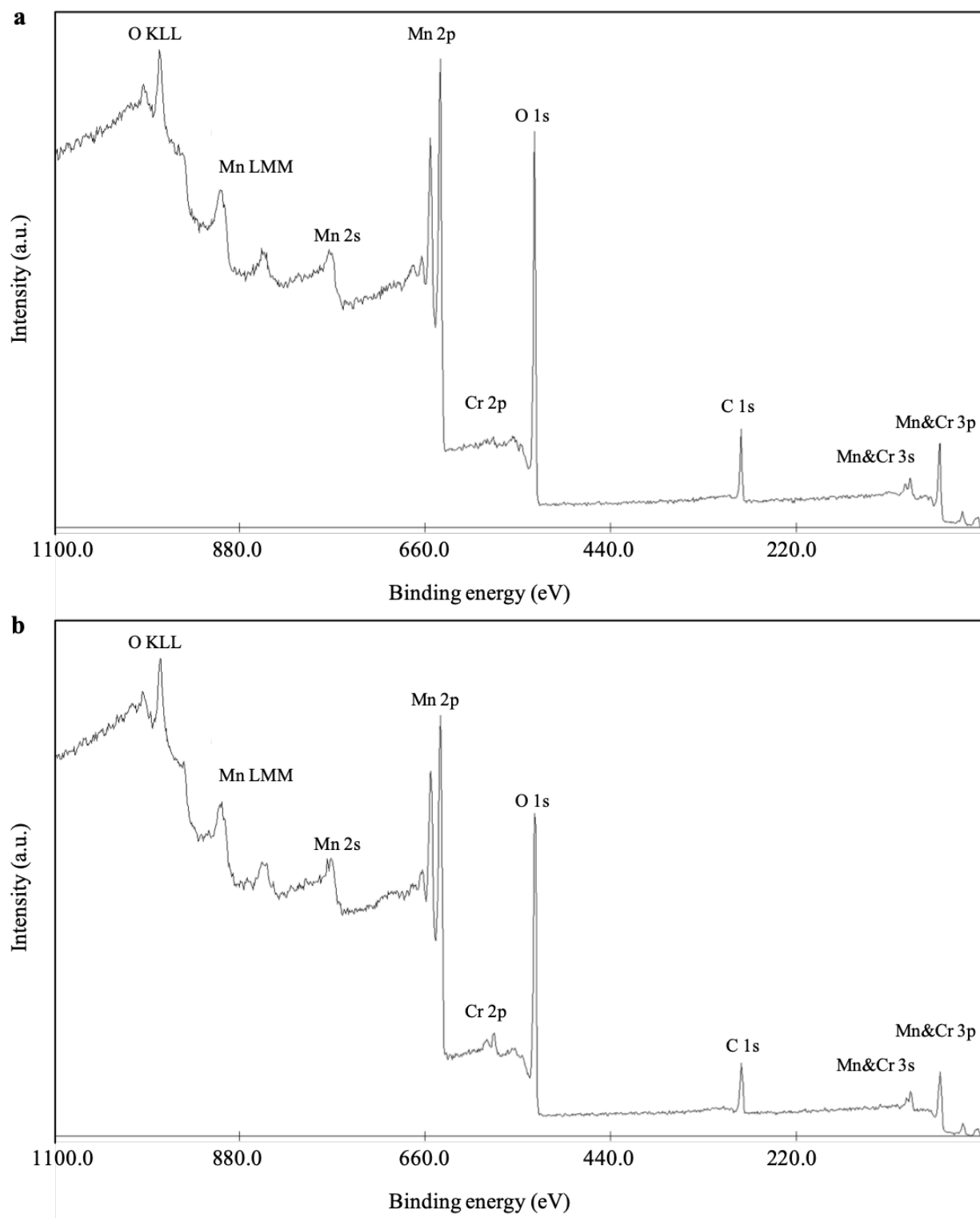


Figure 5. 11 XPS all element spectra of the Mn<sub>2</sub>O<sub>3</sub> surface after adsorption of (a) Cr(III) and (b) Cr(VI)

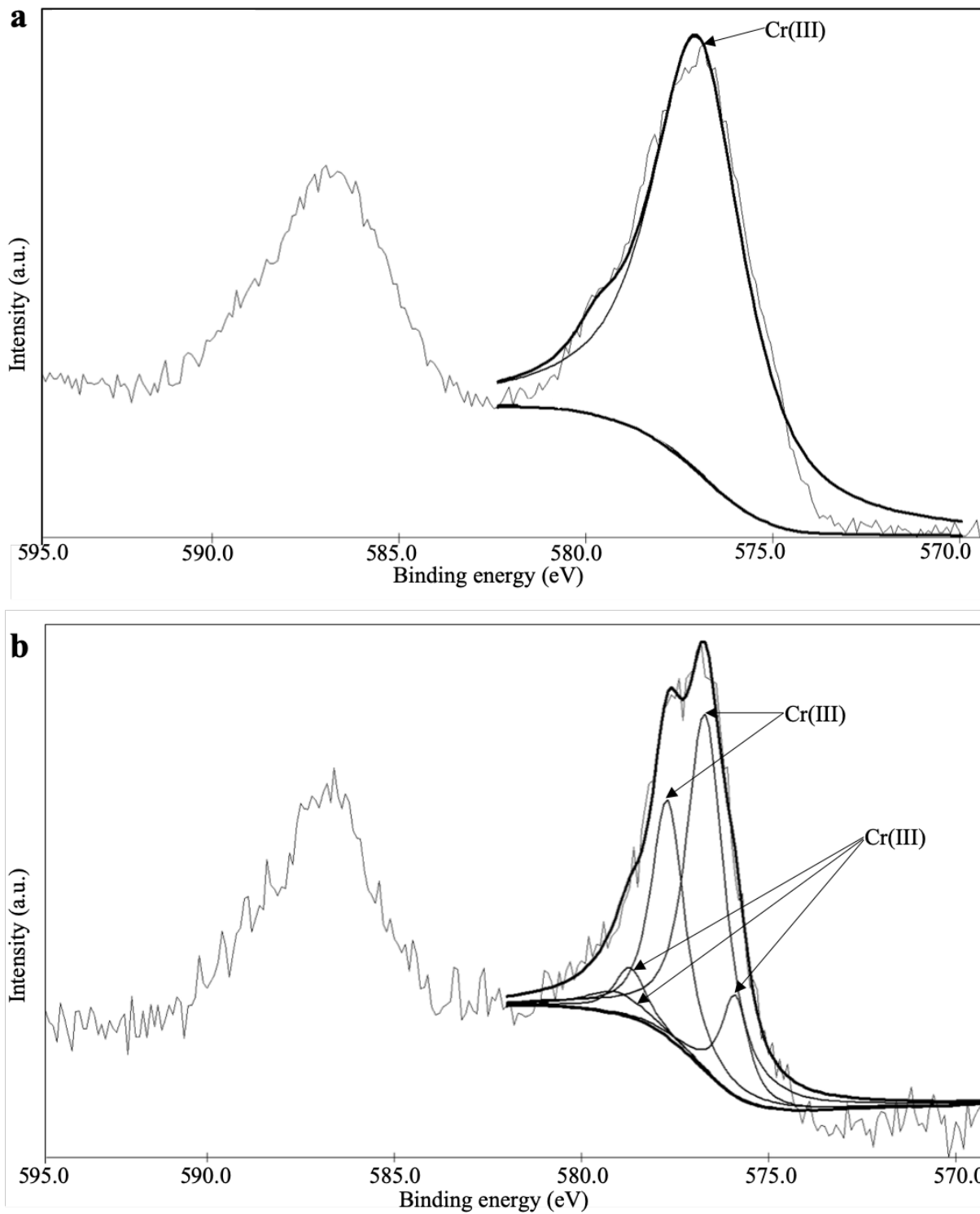


Figure 5. 12 XPS Cr spectra of the MnO sorbent surface after adsorption of (a) Cr(III) and (b) Cr(VI)

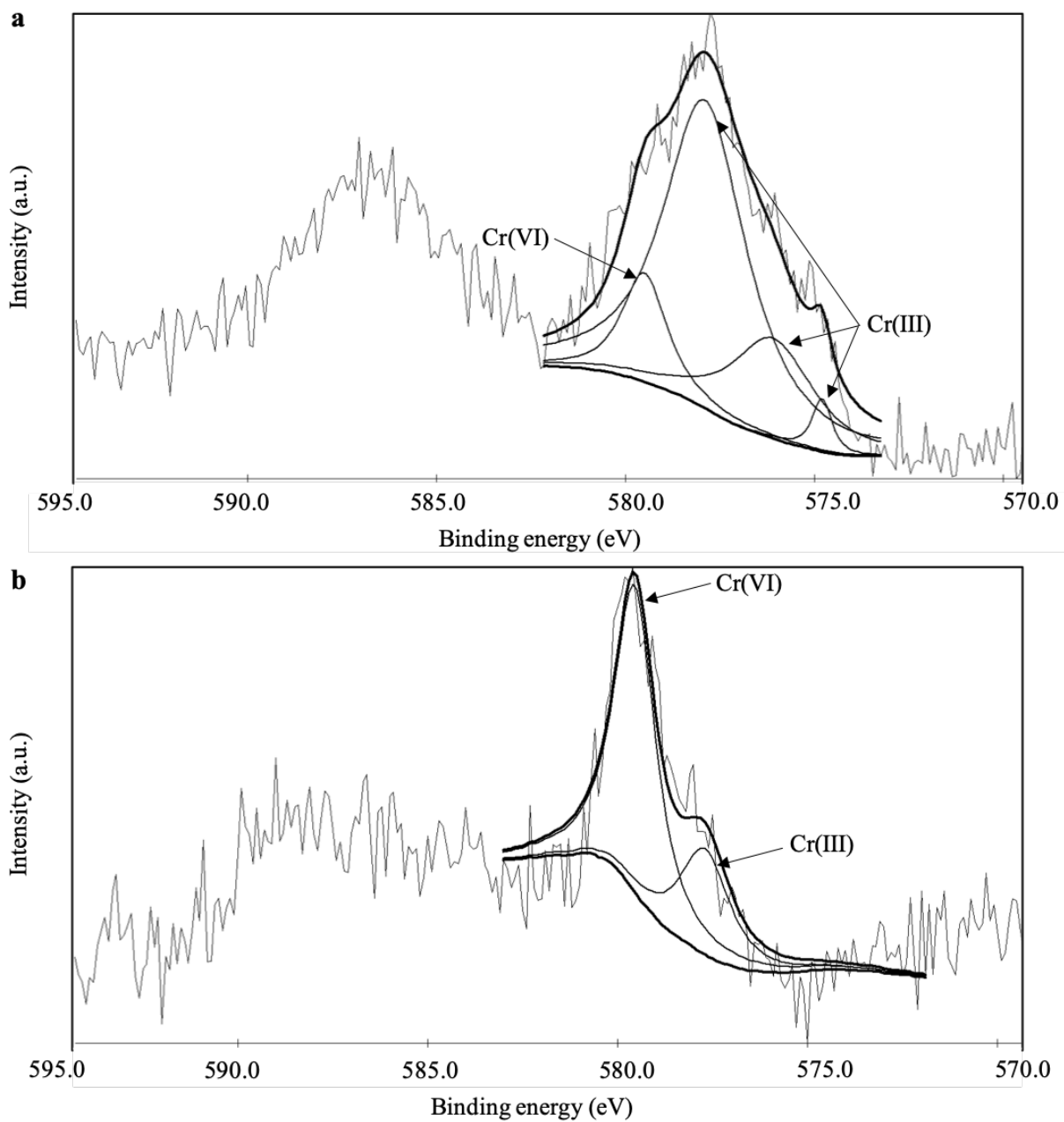


Figure 5. 13 XPS Cr spectra of the  $Mn_2O_3$  sorbent surface after adsorption of (a) Cr(III) and (b) Cr(VI)

## 5.5 Conclusion

This study evaluated the adsorption and uptake of Cr(III) and Cr(VI) from aqueous solutions by the MnO and Mn<sub>2</sub>O<sub>3</sub> sorbents. Based on the adsorption parameters obtained from several adsorption models, the adsorption of Cr(III) and Cr(VI) followed the Langmuir and Freundlich adsorption models with the MnO and Mn<sub>2</sub>O<sub>3</sub> sorbents exhibiting a stronger binding for adsorption of Cr(VI) than for adsorption of Cr(III). The D-R equation parameters were suggestive of adsorption of Cr(III) onto the MnO sorbent and both Cr(III) and Cr(VI) onto the Mn<sub>2</sub>O<sub>3</sub> sorbent as physisorption and adsorption of Cr(VI) onto the MnO sorbent as chemisorption. The adsorption of both chromium species decreased appreciably for pH values greater than 9 due to the fact that the MnO sorbent obtained a PZC of about 10 in the absence of or in the presence of chromium species, while the adsorption of Cr(III) and Cr(VI) onto the Mn<sub>2</sub>O<sub>3</sub> sorbent experience a drastic drop with increasing pH from 9 to 10 and from 8 to 9, respectively, due to the reversal of the surface charge. The XPS spectra combined with the results from the adsorption parameters, the effect of pH and the effect of surface charge indicate that the mechanism of adsorption of Cr(VI) onto the MnO sorbent surface was likely through the adsorption of oxy-anionic species of Cr(VI) followed by the reduction of Cr(VI) to Cr(III) on the surface of the MnO sorbent. The reduction of Cr(VI) to Cr(III) occurred through either the oxidation of Mn(II) to Mn(III) in solution or the oxidation of Mn(II) to Mn(III) on the surface of the MnO sorbent, followed by the subsequent precipitation of chromium and manganese onto the MnO sorbent surface as Cr(OH)<sub>3</sub> and MnOOH, respectively, or that the Cr(VI) is directly reduced to Cr<sub>2</sub>O<sub>3</sub> and the MnO is oxidized to Mn<sub>2</sub>O<sub>3</sub>. The appearance of both Cr(III) and Cr(VI) species on the Mn<sub>2</sub>O<sub>3</sub> sorbent surface after chromium adsorption can be explained by that Mn<sub>2</sub>O<sub>3</sub>, as intermediate oxidation state, has the potential to either reduce Cr(VI) into Cr(III) or oxidize Cr(III) into Cr(VI).

## 5.5 Reference

- [1] J. E. Johnson, S. M. Webb, C. Ma, and W. W. Fischer, “Manganese mineralogy and diagenesis in the sedimentary rock record,” *Geochim. Cosmochim. Acta*, vol. 173, pp. 210–231, Jan. 2016, doi: 10.1016/j.gca.2015.10.027.
- [2] J. E. Post, “Manganese oxide minerals: Crystal structures and economic and environmental significance,” *Proc. Natl. Acad. Sci.*, vol. 96, no. 7, pp. 3447–3454, Mar. 1999, doi: 10.1073/pnas.96.7.3447.
- [3] K. Nicholson and M. Eley, “Geochemistry of manganese oxides: metal adsorption in freshwater and marine environments,” *Geol. Soc. Lond. Spec. Publ.*, vol. 119, no. 1, pp. 309–326, 1997, doi: 10.1144/GSL.SP.1997.119.01.20.
- [4] D. J. Burdige, S. P. Dhakar, and K. H. Nealson, “Effects of manganese oxide mineralogy on microbial and chemical manganese reduction,” *Geomicrobiol. J.*, vol. 10, no. 1, pp. 27–48, Jan. 1992, doi: 10.1080/01490459209377902.
- [5] Yu. N. Vodyanitskii, “Mineralogy and geochemistry of manganese: a review of publications,” *Eurasian Soil Sci.*, vol. 42, no. 10, pp. 1170–1178, Oct. 2009, doi: 10.1134/S1064229309100123.
- [6] L. Della Puppa, M. Komárek, F. Bordas, J.-C. Bollinger, and E. Joussein, “Adsorption of copper, cadmium, lead and zinc onto a synthetic manganese oxide,” *J. Colloid Interface Sci.*, vol. 399, pp. 99–106, Jun. 2013, doi: 10.1016/j.jcis.2013.02.029.
- [7] J. Slavek and W. F. Pici, “Chemical leaching of metal ions sorbed on hydrous manganese oxide,” *Chem. Geol.*, vol. 51, no. 3–4, pp. 213–223, Oct. 1985, doi: 10.1016/00092541(85)90133-0.
- [8] R. Rao. Gadde and H. A. Laitinen, “Heavy metal adsorption by hydrous iron and manganese oxides,” *Anal. Chem.*, vol. 46, no. 13, pp. 2022–2026, Nov. 1974, doi: 10.1021/ac60349a004.
- [9] Y. Wang, X. Feng, M. Villalobos, W. Tan, and F. Liu, “Sorption behavior of heavy metals on birnessite: Relationship with its Mn average oxidation state and implications for types of sorption sites,” *Chem. Geol.*, vol. 292–293, pp. 25–34, Jan. 2012, doi: 10.1016/j.chemgeo.2011.11.001.

- [10] J. C. J. Gude, L. C. Rietveld, and D. van Halem, "As(III) oxidation by MnO<sub>2</sub> during groundwater treatment," *Water Res.*, vol. 111, pp. 41–51, Mar. 2017, doi: 10.1016/j.watres.2016.12.041.
- [11] Z. Wang *et al.*, "Adsorption of uranium(VI) to manganese oxides: X-ray absorption spectroscopy and surface complexation modeling," *Environ. Sci. Technol.*, vol. 47, no. 2, pp. 850–858, Jan. 2013, doi: 10.1021/es304454g.
- [12] M. M. Wiatros-Motyka, C. Sun, L. A. Stevens, and C. E. Snape, "High capacity co-precipitated manganese oxides sorbents for oxidative mercury capture," *Fuel*, vol. 109, pp. 559–562, Jul. 2013, doi: 10.1016/j.fuel.2013.03.019.
- [13] F. C. Richard and A. C. M. Bourg, "Aqueous geochemistry of chromium: A review," *Water Res.*, vol. 25, no. 7, pp. 807–816, Jul. 1991, doi: 10.1016/0043-1354(91)90160-R.
- [14] J. Barnhart, "Occurrences, uses, and properties of chromium," *Regul. Toxicol. Pharmacol.*, vol. 26, no. 1, pp. S3–S7, Aug. 1997, doi: 10.1006/rtph.1997.1132.
- [15] Ş. Uluçınar and A. Nur Onar, "Effect of organic Cr(III) complexes on chromium speciation," *Chem. Speciat. Bioavailab.*, vol. 17, no. 2, pp. 31–39, Jan. 2005, doi: 10.3184/095422905782774955.
- [16] M. B. Desta, "Batch sorption experiments: Langmuir and Freundlich isotherm studies for the adsorption of textile metal ions onto teff straw (*Eragrostis tef*) agricultural waste," *J. Thermodyn.*, vol. 2013, pp. 1–6, 2013, doi: 10.1155/2013/375830.
- [17] X. Du, Z. Yu, and Y. Zhu, "Cr(VI) adsorption from aqueous solution and its reactions behavior on the surfaces of granular Fe-Mn binary oxides," *Environ. Prog. Sustain. Energy*, vol. 38, pp. S176–S184, Mar. 2019, doi: 10.1002/ep.12968.
- [18] S. A. Chaudhry, T. A. Khan, and I. Ali, "Equilibrium, kinetic and thermodynamic studies of Cr(VI) adsorption from aqueous solution onto manganese oxide coated sand grain (MOCSG)," *J. Mol. Liq.*, vol. 236, pp. 320–330, Jun. 2017, doi: 10.1016/j.molliq.2017.04.029.

- [19] C. Pan, H. Liu, J. G. Catalano, A. Qian, Z. Wang, and D. E. Giammar, "Rates of Cr(VI) Generation from  $\text{Cr}_x\text{Fe}_{1-x}(\text{OH})_3$  Solids upon Reaction with Manganese Oxide," *Environ. Sci. Technol.*, vol. 51, no. 21, pp. 12416–12423, Nov. 2017, doi: 10.1021/acs.est.7b04097.
- [20] M. Gheju, I. Balcu, and G. Mosoarca, "Removal of Cr(VI) from aqueous solutions by adsorption on  $\text{MnO}_2$ ," *J. Hazard. Mater.*, vol. 310, pp. 270–277, Jun. 2016, doi: 10.1016/j.jhazmat.2016.02.042.
- [21] S. Kwak, J.-C. Yoo, and K. Baek, "Synergistic and inhibitory reduction of Cr(VI) by montmorillonite, citric acid, and Mn(II)," *J. Soils Sediments*, vol. 18, no. 1, pp. 205–210, Jan. 2018, doi: 10.1007/s11368-017-1748-7.
- [22] W. Zhang, L. Qian, D. Ouyang, Y. Chen, L. Han, and M. Chen, "Effective removal of Cr(VI) by attapulgite-supported nanoscale zero-valent iron from aqueous solution: Enhanced adsorption and crystallization," *Chemosphere*, vol. 221, pp. 683–692, Apr. 2019, doi: 10.1016/j.chemosphere.2019.01.070.
- [23] P. Li *et al.*, "Adsorption and reduction transformation behaviors of Cr(VI) on mesoporous polydopamine/titanium dioxide composite nanospheres," *J. Chem. Eng. Data*, vol. 64, no. 6, pp. 2686–2696, Jun. 2019, doi: 10.1021/acs.jced.9b00111.
- [24] N. Fiol, C. Escudero, and I. Villaescusa, "Chromium sorption and Cr(VI) reduction to Cr(III) by grape stalks and yohimbe bark," *Bioresour. Technol.*, vol. 99, no. 11, pp. 5030–5036, Jul. 2008, doi: 10.1016/j.biortech.2007.09.007.
- [25] H.-B. Kim, J.-G. Kim, S.-H. Kim, E. E. Kwon, and K. Baek, "Consecutive reduction of Cr(VI) by Fe(II) formed through photo-reaction of iron-dissolved organic matter originated from biochar," *Environ. Pollut.*, vol. 253, pp. 231–238, Oct. 2019, doi: 10.1016/j.envpol.2019.07.026.
- [26] J. Nelson, C. Joe-Wong, and K. Maher, "Cr(VI) reduction by Fe(II) sorbed to silica surfaces," *Chemosphere*, vol. 234, pp. 98–107, Nov. 2019, doi: 10.1016/j.chemosphere.2019.06.039.

- [27] H. Guha, J. E. Saiers, S. Brooks, P. Jardine, and K. Jayachandran, "Chromium transport, oxidation, and adsorption in manganese-coated sand," *J. Contam. Hydrol.*, vol. 49, no. 3, pp. 311–334, Jun. 2001, doi: 10.1016/S0169-7722(00)00199-6.
- [28] E. Li, X. Zeng, and Y. Fan, "Removal of chromium ion (III) from aqueous solution by manganese oxide and microemulsion modified diatomite," *Desalination*, vol. 238, no. 1, pp. 158–165, Mar. 2009, doi: 10.1016/j.desal.2007.11.062.
- [29] L. Wang *et al.*, "Study on the removal of chromium(III) from leather waste by a two-step method," *J. Ind. Eng. Chem.*, vol. 79, pp. 172–180, Nov. 2019, doi: 10.1016/j.jiec.2019.06.030.
- [30] X. H. Feng, L. M. Zhai, W. F. Tan, W. Zhao, F. Liu, and J. Z. He, "The controlling effect of pH on oxidation of Cr(III) by manganese oxide minerals," *J. Colloid Interface Sci.*, vol. 298, no. 1, pp. 258–266, Jun. 2006, doi: 10.1016/j.jcis.2005.12.012.
- [31] Z. Stepniewska, K. Bucior, and R. P. Bennicelli, "The effects of MnO<sub>2</sub> on sorption and oxidation of Cr(III) by soils," *Geoderma*, vol. 122, no. 2–4, pp. 291–296, Oct. 2004, doi: 10.1016/j.geoderma.2004.01.015.
- [32] C. A. Johnson and A. G. Xyla, "The oxidation of chromium(III) to chromium(VI) on the surface of manganite ( $\gamma$ -MnOOH)," *Geochim. Cosmochim. Acta*, vol. 55, no. 10, pp. 2861–2866, Oct. 1991, doi: 10.1016/0016-7037(91)90451-A.
- [33] N. Ayawei, A. N. Ebelegi, and D. Wankasi, "Modelling and interpretation of adsorption isotherms," *J. Chem.*, vol. 2017, pp. 1–11, Sep. 2017, doi: 10.1155/2017/3039817.
- [34] Y. S. Ho, J. F. Porter, and G. Mckay, "Equilibrium isotherm studies for the sorption of divalent metal ions onto peat: copper, nickel and lead single component systems," *Water. Air. Soil Pollut.*, vol. 141, no. 1–4, pp. 1–33, Nov. 2002, doi: 10.1023/A:1021304828010.
- [35] K. Y. Foo and B. H. Hameed, "Insights into the modeling of adsorption isotherm systems," *Chem. Eng. J.*, vol. 156, no. 1, pp. 2–10, Jan. 2010, doi: 10.1016/j.cej.2009.09.013.
- [36] A. O. Dada, A. P. Olalekan, A. M. Olatunya, and O. Dada, "Langmuir, Freundlich, Temkin and Dubinin–Radushkevich isotherms studies of equilibrium sorption of Zn<sup>2+</sup> unto phosphoric acid

- modified rice husk,” *IOSR J. Appl. Chem.*, vol. 3, no. 1, pp. 38–45, Nov. 2012, doi: 10.9790/5736-0313845.
- [37] B. Rand, “On the empirical nature of the Dubinin—Radushkevich equation of adsorption,” *J. Colloid Interface Sci.*, vol. 56, no. 2, pp. 337–346, Aug. 1976, doi: 10.1016/0021-9797(76)90259-9.
- [38] K. Babaeivelni, A. P. Khodadoust, and D. Bogdan, “Adsorption and removal of arsenic (V) using crystalline manganese (II,III) oxide: Kinetics, equilibrium, effect of pH and ionic strength,” *J. Environ. Sci. Health Part A*, vol. 49, no. 13, pp. 1462–1473, Nov. 2014, doi: 10.1080/10934529.2014.937160.
- [39] B. Nagy, C. Mânzatu, A. Măicăneanu, C. Indolean, L. Barbu-Tudoran, and C. Majdik, “Linear and nonlinear regression analysis for heavy metals removal using *Agaricus bisporus* macrofungus,” *Arab. J. Chem.*, vol. 10, pp. S3569–S3579, May 2017, doi: 10.1016/j.arabjc.2014.03.004.
- [40] M. Kosmulski and E. Mączka, “Surface charging and points of zero charge of less common oxides: Beryllium oxide,” *Colloids Surf. Physicochem. Eng. Asp.*, vol. 575, pp. 140–143, Aug. 2019, doi: 10.1016/j.colsurfa.2019.05.024.
- [41] B. Beverskog and I. Puigdomenech, “Revised pourbaix diagrams for chromium at 25–300 °C,” *Corros. Sci.*, vol. 39, no. 1, pp. 43–57, Jan. 1997, doi: 10.1016/S0010-938X(97)89244-X.
- [42] J. D. Hem, “Reactions of metal ions at surfaces of hydrous iron oxide,” *Geochim. Cosmochim. Acta*, vol. 41, no. 4, pp. 527–538, Apr. 1977, doi: 10.1016/0016-7037(77)90290-3.
- [43] Z. Khan, Md. Z. A. Rafiquee, and K.- Din, “Oxidation of l-methionine with aqueous chromic acid: a kinetic study,” *Transit. Met. Chem.*, vol. 22, no. 4, pp. 350–355, Jul. 1997, doi: 10.1023/A:1018457701269.
- [44] T. Cosgrove and P. T. Cosgrove, *Colloid science: principles, methods and applications*. John Wiley & Sons, Incorporated, 2010.

- [45] C. F. Jones, R. S. C. Smart, and P. S. Turner, "Dissolution kinetics of manganese oxides. Effects of preparation conditions, pH and oxidation/reduction from solution," *J. Chem. Soc. Faraday Trans.*, vol. 86, no. 6, pp. 947–953, Jan. 1990, doi: 10.1039/FT9908600947.
- [46] R. Spryca, "Electrical double layer at alumina/electrolyte interface: II. Adsorption of supporting electrolyte ions," *J. Colloid Interface Sci.*, vol. 127, no. 1, pp. 12–25, Jan. 1989, doi: 10.1016/0021-9797(89)90003-9.
- [47] D. L. Sparks and T. J. Grundl, *Mineral-Water Interfacial Reactions*. American Chemical Society, 1999.
- [48] R. J. Hunter, *Zeta potential in colloid science: principles and applications*. Academic Press, 2013.
- [49] R. M. Ali, H. A. Hamad, M. M. Hussein, and G. F. Malash, "Potential of using green adsorbent of heavy metal removal from aqueous solutions: Adsorption kinetics, isotherm, thermodynamic, mechanism and economic analysis," *Ecol. Eng.*, vol. 91, pp. 317–332, Jun. 2016, doi: 10.1016/j.ecoleng.2016.03.015.
- [50] E. Smith and K. Ghiassi, "Chromate removal by an iron sorbent: mechanism and modeling," *Water Environ. Res.*, vol. 78, no. 1, pp. 84–93, Jan. 2006, doi: 10.2175/106143005X84558.
- [51] N. C. Saha and H. G. Tompkins, "Titanium nitride oxidation chemistry: An x-ray photoelectron spectroscopy study," *J. Appl. Phys.*, vol. 72, no. 7, pp. 3072–3079, Oct. 1992, doi: 10.1063/1.351465.
- [52] J. M. Cerrato, M. F. Hochella, W. R. Knocke, A. M. Dietrich, and T. F. Cromer, "Use of XPS to identify the oxidation state of Mn in solid surfaces of filtration media oxide samples from drinking water treatment plants," *Environ. Sci. Technol.*, vol. 44, no. 15, pp. 5881–5886, Aug. 2010, doi: 10.1021/es100547q.
- [53] D. Yang *et al.*, "Chemical analysis of graphene oxide films after heat and chemical treatments by X-ray photoelectron and Micro-Raman spectroscopy," *Carbon*, vol. 47, no. 1, pp. 145–152, Jan. 2009, doi: 10.1016/j.carbon.2008.09.045.

- [54] A. Manceau and L. Charlet, "X-ray absorption spectroscopic study of the sorption of Cr(III) at the oxide-water interface: I. Molecular mechanism of Cr(III) oxidation on Mn oxides," *J. Colloid Interface Sci.*, vol. 148, no. 2, pp. 425-442, Feb. 1992, doi: 10.1016/0021-9797(92)90181-K.
- [55] S. Boursiquot, M. Mullet, and J.-J. Ehrhardt, "XPS study of the reaction of chromium (VI) with mackinawite (FeS)," *Surf. Interface Anal.*, vol. 34, no. 1, pp. 293-297, Sep. 2002, doi: 10.1002/sia.1303.
- [56] Y. Zhang *et al.*, "Enhancing surface gully erosion of micron-sized zero-valent aluminum (mZVAL) for Cr(VI) removal: Performance and mechanism in the presence of carbonate buffer," *J. Clean. Prod.*, vol. 238, pp. 117943, Nov. 2019, doi: 10.1016/j.jclepro.2019.117943.
- [57] L. Qian *et al.*, "Enhanced reduction and adsorption of hexavalent chromium by palladium and silicon rich biochar supported nanoscale zero-valent iron," *J. Colloid Interface Sci.*, vol. 533, pp. 428-436, Jan. 2019, doi: 10.1016/j.jcis.2018.08.075.
- [58] M. C. Biesinger, B. P. Payne, A. P. Grosvenor, L. W. M. Lau, A. R. Gerson, and R. St. C. Smart, "Resolving surface chemical states in XPS analysis of first row transition metals, oxides and hydroxides: Cr, Mn, Fe, Co and Ni," *Appl. Surf. Sci.*, vol. 257, no. 7, pp. 2717-2730, Jan. 2011, doi: 10.1016/j.apsusc.2010.10.051.

## CHAPTER VI

### VI. SURFACE COMPLEXATION MODELING OF CHROMATE ADSORPTION ON MANGANESE OXIDES

#### 6.1 Introduction

Chromium is a metal that exists in several oxidation states, ranging from chromium (-II) to chromium (+VI), whereas it is mostly present in two valence states of trivalent chromium and hexavalent chromium in natural water [1], [2]. Chromium compounds are most stable in the trivalent oxidation state and can be found in the nature as trivalent chromium compounds or ores. The hexavalent state, on the other hand, rarely occurs naturally. Hexavalent chromium compounds are well known as laboratory reagents and manufacturing intermediates. Major sources of hexavalent chromium in drinking water are discharged from steel and pulp mills, metal plating operations and erosion of natural deposits of trivalent chromium that can be oxidized into hexavalent chromium [3], [4]. There is strong evidence to consider hexavalent chromium as carcinogen that can pose serious hazards towards human beings; therefore the removal of hexavalent chromium from source of drinking water is an important health concern [5]–[8]. Adsorption is considered to be an effective, economic, eco-friendly technology for the removal of heavy metal contaminants from drinking water [9]–[11]. Hydrated manganese oxides are mostly found in forms of discrete particles or coating on other mineral grains [12], [13]. They have been found to be potential effective adsorbents to remove hexavalent chromium because of its high exchange capacity and selectivity towards toxic heavy metal ions [14]–[18].

Manganese can be considered one of the most complex metallic elements due to the fact that as a transition metal, it obtains a series of oxidation states, ranging from -2 to +7, and +2, +3, +4 are the most stable and common ones. Surface complexation modeling has been applied to simulate the interactions between aqueous species and mineral surface at solid/solution interfaces and predict the fate and transport process of certain concerned toxic species such as hexavalent chromium when they appear in natural water systems [19]. Each SCM model describes the structure of the electrical double layer

differently in terms of the relationships between charge and potential and the position of surface complexes relative to mineral surfaces [20], [21]. These models can be divided into sorption taking place at surface binding sites and sorption simply following mass law equations. Manganese oxides mineral has been intensively investigated and developed an internally consistent sorption database that contains a series of cations such as  $\text{Co}^{2+}$ ,  $\text{Cu}^{2+}$ ,  $\text{Mg}^{2+}$ ,  $\text{Ni}^{2+}$  and  $\text{Zn}^{2+}$  [14], [22]. However, data sets of chromium and other anion adsorption on Mn oxides were hardly developed. In previous spectroscopy studies, we discovered the mechanism of adsorption of chromate ions onto manganese oxides is surface complexation accompanying with reduction of solution-phase chromate ions into Cr(III) later on precipitated onto solid surface. The possible reduction of Cr(VI) into Cr(III) in presence of relatively more reduced form of Mn, Mn(II) or Mn(III), is an essential element when modeling the adsorption process between chromate ions with manganese oxides. In this chapter, based on the information gathered from previous studies and literatures, we developed a surface complexation model to specifically describe the system under study. It is of critical importance to obtain consistent model parameters such as specific surface area, site densities, surface complexes and their stability constants. The evaluation of chromate reduction incorporated in the model is necessary to accurately depict the specific adsorption reaction between different manganese oxides in solid phase and Cr(VI) in solution phase. The goal of this chapter is to develop a robust model to describe adsorption of chromate ion as oxyanion onto manganese oxides surface under wide reaction conditions that can be suitable for modeling Cr(VI) fate and transport in real life scenario without major revisions.

## 6.2 Materials and methods

### 6.2.1 Description of SCM model

Two-pK triple layer surface complexation model (TLM) is employed in our study to accurately describe chromate adsorption on manganese oxides [23]. Titration data previously published were used to obtain the optimal values of model parameters including adsorption stability constants, site density and the linear charge-potential coefficients [21]. The surface area of sorbent was characterized by N<sub>2</sub>-Brunauer-Emmett-Teller adsorption method. The model parameters were then included into Visual Minteq program to assess and predict the adsorption between chromate with manganese oxides. The reduction potential was also specified in Visual Minteq program to account for the possible reduction reaction.

### 6.2.2 Adsorption studies

Batch adsorption studies were conducted in well-sealed 50-mL high density polyethylene (HDPE) centrifuge tube with different adsorbents (MnO and Mn<sub>2</sub>O<sub>3</sub>). An identical amount of each adsorbent (1g) was mixed with 50mL of Cr(VI) solution with prescribed concentration of 1mg/L prepared from potassium dichromate (K<sub>2</sub>Cr<sub>2</sub>O<sub>7</sub>). The initial pH of 1mg/L Cr(VI) stock solutions were adjusted (pH =2~10) using 0.1M hydrochloric acid (HCl) and 0.1M sodium hydroxide (NaOH) prior to contact with different adsorbents. A series of samples were shaken in a rotary tumbler for a reaction period of 24 hours at 16 rpm to reach equilibrium. To obtain the equilibrium concentration of chromium, all samples were centrifuged at 8000 rpm for 10 minutes to separate the supernatant from adsorbents and a 10-mL sample was taken from each sample into a test tube that later acidified by adding two drops of concentrated nitric acid (HNO<sub>3</sub>) and analyzed by flame atomic absorption spectroscopy.

### 6.3 Results and discussion

The formation of hydroxyl group on metal oxides to obtain the more favorable charge distribution can result in surface protonation or deprotonation which renders a solid surface positive or negative charged [24], [25].



Various surface complexation models depict different surface configuration and location of adsorbed ions. The constant capacitance model (CCM) or diffuse layer model (DLM) are indicative of formation of inner-sphere complexes located at a single surface plane, while a diffuse layer (d-plane) further extended to solution phase is included into the DLM. The triple layer model (TLM) adds another surface plane ( $\beta$ -plane) between surface o-plane (inner-sphere complexes) and d-plane (diffuse layer) to account for the possible formation of outer-sphere complexes (Figure 6.1) [19].

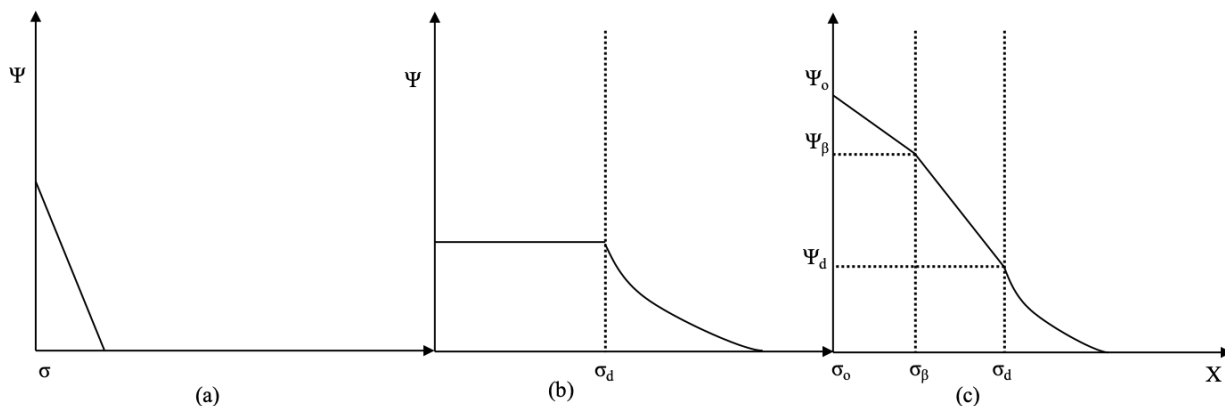


Figure 6. 1 Different surface planes in SCM models (a) constant capacitance model; (b) diffuse layer model; (c) triple layer model.

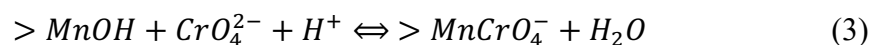
The spectroscopic studies accompanying with zeta potential data sets of chromate adsorption onto manganese oxides have suggested adsorbed chromate ions forming both inner-sphere complexes and outer-sphere complexes. Therefore, TLM is specifically selected for our study due to the inclusion of both surface complexes. In order to accurately modeling the adsorption process under our study, it is reasonable to separate surface complexation and redox reaction and fit them with different reaction models, respectively. We introduced the electrical potential values under different system conditions to evaluate the degree of reduction of Cr(VI) into Cr(III).

### 6.3.1 Surface complexation modeling

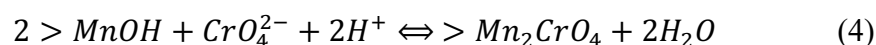
Specific surface area (SSA) is the total reactive surface area for solutes per unit weight of the sorbent that most commonly determined by N<sub>2</sub>-Brunauer-Emmett-Teller adsorption method. The input value for SSA in this study is derived from a collection of literature values. The spectroscopic results of Mn<sub>2</sub>O<sub>3</sub> overloaded with Cr(VI) solution show that 70% of adsorbed chromium remains at hexavalent, while 30% of adsorbed chromium is reduced into trivalent (Figure 6.2). There are two possible mechanisms of this redox reaction: (1) chromate ions are directly adsorbed onto surface of Mn<sub>2</sub>O<sub>3</sub> and then reduced on the solid surface; (2) hexavalent ions are reduced into trivalent in the solution phase and subsequently precipitated onto solid phase. Pervious research on chromate removal by reduction suggests the high probability of initial reduction in solution followed by precipitation as Cr(OH)<sub>3</sub> [26]–[30].

For the TLM, site density, stability constant, and inner-layer/outer-layer capacitance are derived from previously published titration data and tested with possible reaction stoichiometries [31], [32].

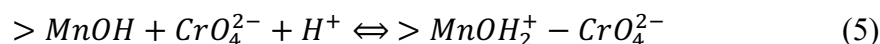
Monodentate, inner-sphere complexes:



Bidentate, inner-sphere complexes:



Monodentate, outer-sphere complexes:



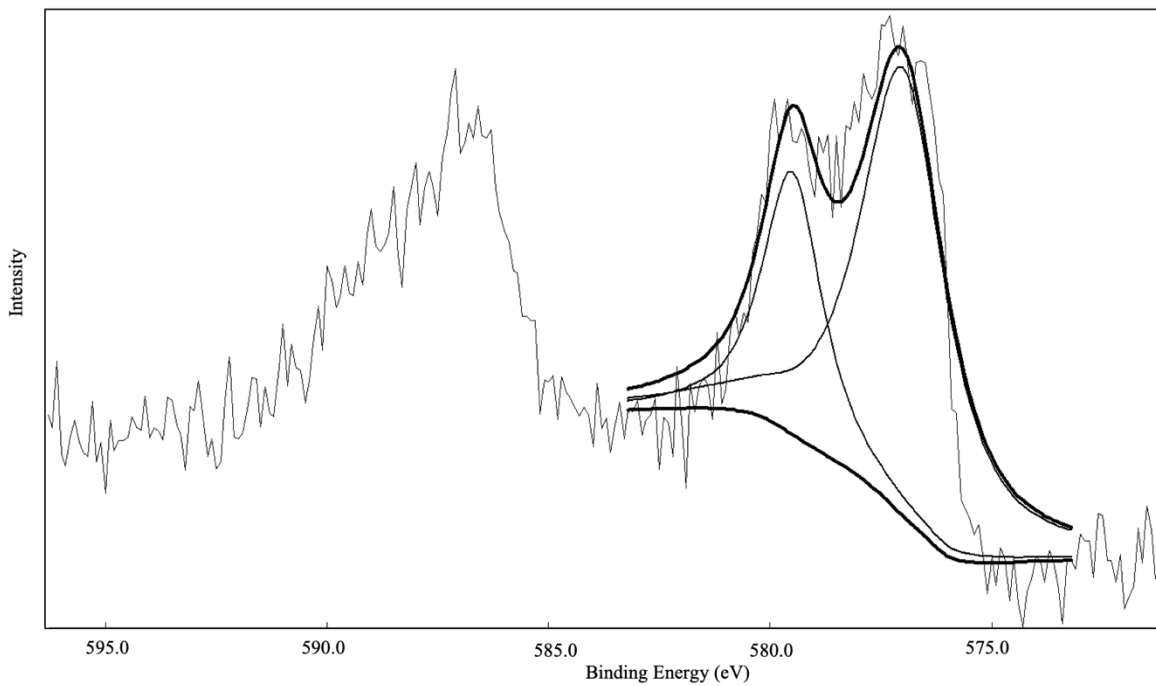


Figure 6. 2 Cr photoemission spectra of  $Mn_2O_3$

All the site density data with correspondent equilibrium constants of surface complexation reactions and the linear charge-potential coefficients are shown in Table 6.1. Redox reaction can be included into TLM model by introducing redox potential (Eh) into Visual Minteq 3.1. Redox potential (Eh) is the indicator of reducing or oxidizing ability and directly related to pH value. The relatively low pH favors the reduction of chromate in solution. We specified the Eh value in the program and add the Cr(III)/Cr(VI) redox couple into modeling system to account for the redox reaction taken place.

Table 6. 1 The Input Values for TLM model

Inner-layer capacitance (F/m <sup>2</sup> )	C <sub>1</sub>	Outer-layer capacitance (F/m <sup>2</sup> )	C <sub>2</sub>	Site density (mmol/m <sup>2</sup> )	SSA (m <sup>2</sup> /g)
1.8		0.3		2.6	120

Table 6. 2 Stability Constants for TLM model

Surface reactions	Log Stability constants (Log K)
$> MnOH + CrO_4^{2-} + H^+ \Leftrightarrow > MnCrO_4^- + H_2O$	9.4
$2 > MnOH + CrO_4^{2-} + 2H^+ \Leftrightarrow > Mn_2CrO_4 + 2H_2O$	10.6
$> MnOH + CrO_4^{2-} + H^+ \Leftrightarrow > MnOH_2^+ - CrO_4^{2-}$	8.57

To understand the possibility of chromium reduction when in contact with manganese oxides surface, the Geochemist's Workbench (GWB) 12.0.4 is employed to develop Eh-pH diagram on chromium and manganese species (Figure 6.2). Chromium appears mainly as dissolved species bichromate ( $HCrO_4^-$ ) or chromate ( $CrO_4^{2-}$ ) with pH more than 3, while trivalent chromium precipitates at the same pH range unless when under extremely acidic condition (pH less than 3), it appears as  $Cr^{3+}$  ion in solution phase. The Eh-pH diagrams for Cr and Mn can suggest the high probability of reduction of Cr(VI) by Mn(II) or Mn(III) in solution into Cr(III) from thermodynamic perspective. Reducing environment and relatively acidic pH are generally necessary for the reduction of hexavalent chromium to take place in solution [33]–[35]. Therefore, at lower pH values, chromium removal can be dominated more by Cr(VI) reduction.

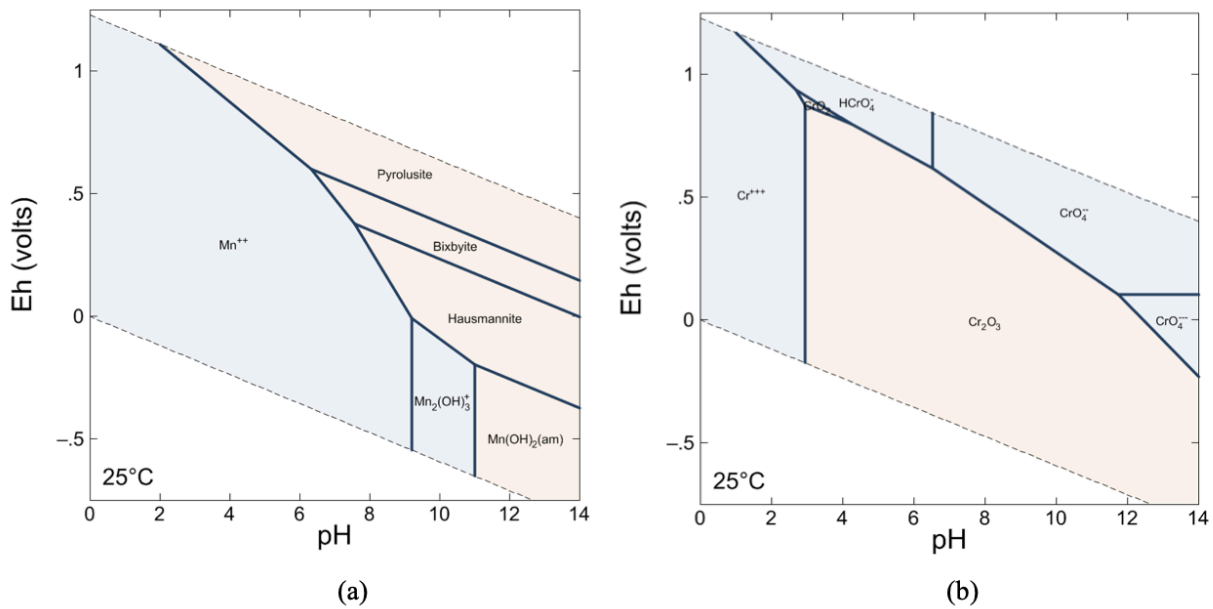


Figure 6. 3 (a) Eh-pH diagram of manganese species; (b) Eh-pH diagram of chromium species.

After inputting all the model parameters into Visual Minteq 3.1, we can plot the model results with experimental data of chromium adsorption on Mn<sub>2</sub>O<sub>3</sub> (Figure 6.4). The model results adequately capture the shape of the adsorption envelope under pH less than 5 or pH more than 10 but underestimate the amount of Cr adsorbed between pH 5 to 10. The poor fit of the TLM model at this particular pH range (5-10) can be result from multiple reasons. The model fails to include the possible partial dissolution of Mn<sub>2</sub>O<sub>3</sub> above pH 5, which can release Mn<sup>2+</sup> into the solution by disproportionation side reaction and later reduce hexavalent chromium into trivalent chromium [36], [37]. The data set used to derived all the model parameters could be another cause of this trend. Inner-sphere complexes are the dominant format of this TLM model with possible lesser amount of outer-sphere complexes, while the ZP study suggest that the chromate adsorption on Mn<sub>2</sub>O<sub>3</sub> contains the formation of a similar amount of inner-sphere complexes and out-sphere complexes.



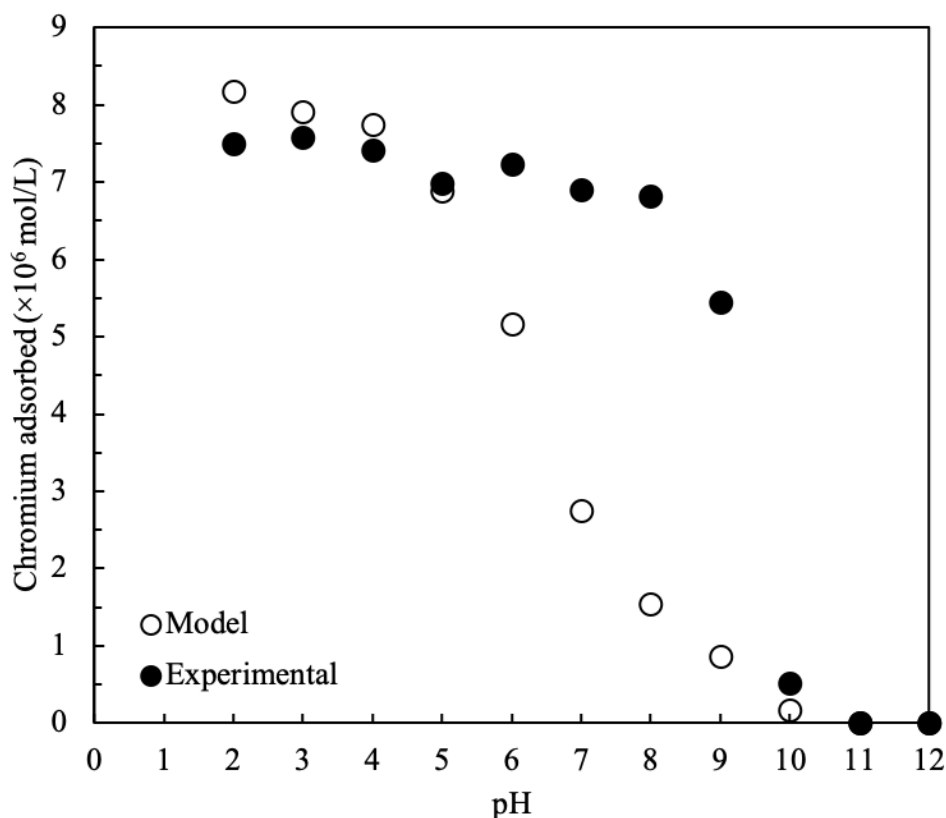


Figure 6. 4 The experimental and model data of adsorption of at  $8 \times 10^{-6}$  M Cr(VI) on  $Mn_2O_3$

### 6.3.2 Reduction modeling

XPS data showed that 100% of adsorbed Cr on MnO is Cr(III), which contributes at the lower binding energy (577.0-578.5eV) (Figure 6.5) [33], [38], [39]. The total reduction of Cr(VI) into Cr(III) indicates the reducing ability of  $Mn^{2+}$  is relatively strong. Comparison of Cr spectra with MnO and  $Mn_2O_3$  suggests that when manganese oxides obtains the valence state of +2 and +3, they are potential strong reductants for chromate in natural water system (pH=6-10) without promoting the anoxic condition. The spectroscopic evidence suggests that Cr(VI) is 100% reduced into Cr(III) and subsequently followed precipitation or adsorption. In this scenario, we consider reduction is the predominant reaction between chromate and  $Mn^{2+}$  present in solution phase. In order to model this redox reaction, we specified the Eh

values based on system conditions in Visual Minteq program without including surface complexation reaction. The results in Figure 6.6 accurately predict the reduction rate of chromate at lower pH range and underestimate the Cr(VI) reduction above pH 6. The assumption that reduction of chromate is strictly restricted to the solution phase can result in underestimation in the model due to the negligence of possible reduction at solid phase.

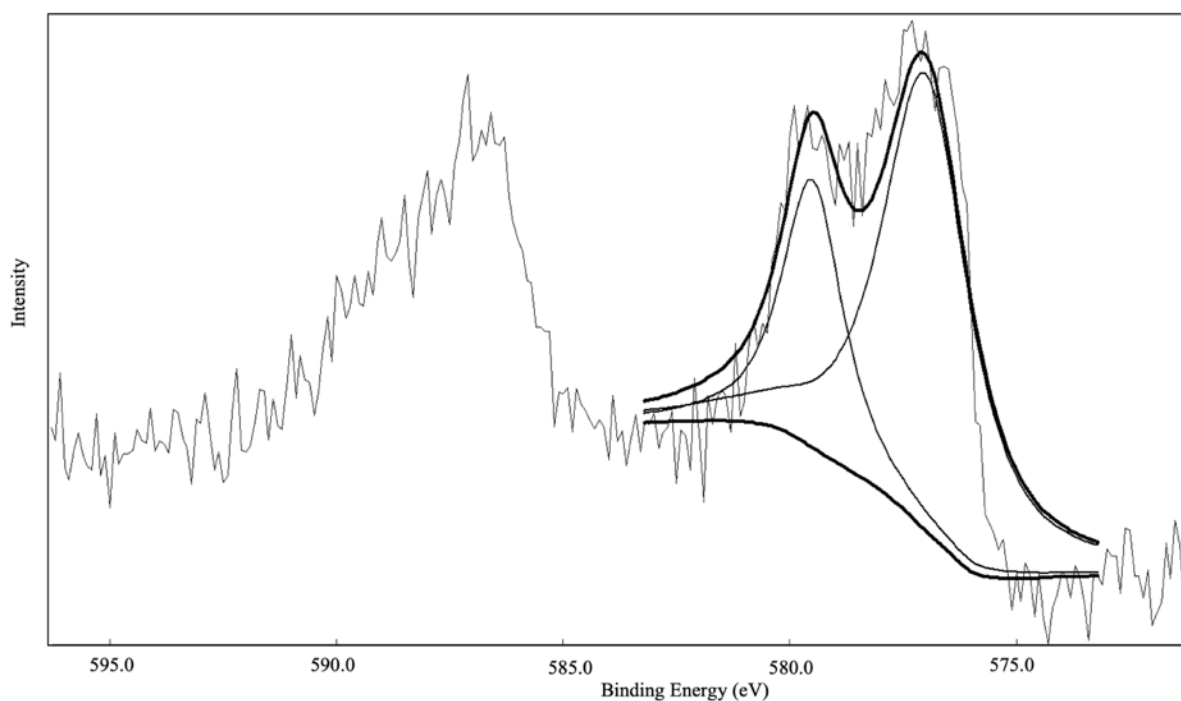


Figure 6. 5 Cr photoemission spectra of MnO

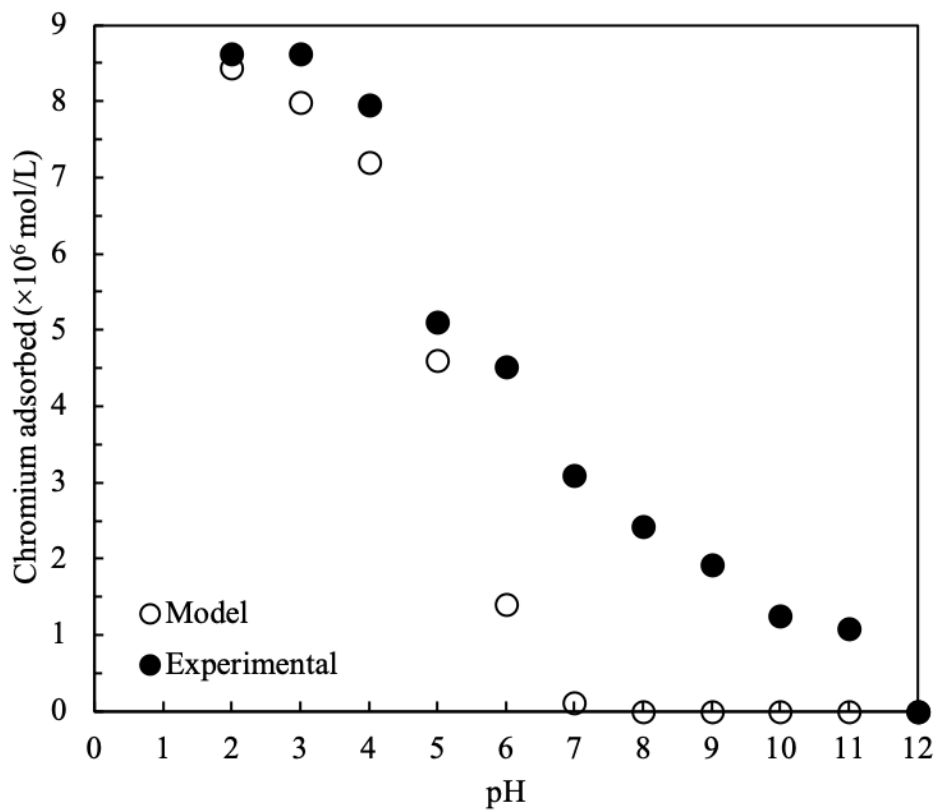


Figure 6. 6 The experimental and model data of adsorption of at  $8 \times 10^{-6}$  M Cr(VI) on MnO

#### 6.4 Conclusion

When in contact with chromate solution, manganese oxides such as MnO or Mn<sub>2</sub>O<sub>3</sub> can remove Cr(VI) by reduction-precipitation/adsorption. The involvement of redox reaction raises problems in employing pre-existed SCM models to predict this specific system. TLM is selected as an accurate model to model the system under study because chromate adsorption onto Mn<sub>2</sub>O<sub>3</sub> includes the formation of both inner-sphere complexes and outer-sphere complexes. After incorporation of the redox potential into the Visual Minteq program, the results perfectly capture the adsorption envelop of chromate adsorption onto Mn<sub>2</sub>O<sub>3</sub> from pH 2 to pH 5 and pH 10 to 12. The model failed to predict at pH range from 5 to 10 mainly due to the failure to consider the dissolution of Mn<sub>2</sub>O<sub>3</sub>, which contributes the higher concentration of Mn<sup>2+</sup> in liquid phase. MnO can be an extremely strong reductant for chromate because it can fully convert Cr(VI) into Cr(III). The underestimation of Cr(VI) adsorption on MnO above pH 6 suggests the primary mechanism of chromium removal is no longer purely reduction but reduction accompanying with surface complexation.

## 6.5 Reference

- [1] J. Barnhart, "Occurrences, uses, and properties of chromium," *Regul. Toxicol. Pharmacol.*, vol. 26, no. 1, pp. S3–S7, Aug. 1997, doi: 10.1006/rtph.1997.1132.
- [2] F. C. Richard and A. C. M. Bourg, "Aqueous geochemistry of chromium: A review," *Water Res.*, vol. 25, no. 7, pp. 807–816, Jul. 1991, doi: 10.1016/0043-1354(91)90160-R.
- [3] C.-C. Kan, A. H. Ibe, K. K. P. Rivera, R. O. Arazo, and M. D. G. de Luna, "Hexavalent chromium removal from aqueous solution by adsorbents synthesized from groundwater treatment residuals," *Sustain. Environ. Res.*, vol. 27, no. 4, pp. 163–171, Jul. 2017, doi: 10.1016/j.serj.2017.04.001.
- [4] M. Owlad, M. K. Aroua, W. A. W. Daud, and S. Baroutian, "Removal of hexavalent chromium-contaminated water and wastewater: A review," *Water. Air. Soil Pollut.*, vol. 200, no. 1–4, pp. 59–77, Jun. 2009, doi: 10.1007/s11270-008-9893-7.
- [5] A. H. Smith and C. M. Steinmaus, "Health effects of arsenic and chromium in drinking water: Recent human findings," *Annu. Rev. Public Health*, vol. 30, no. 1, pp. 107–122, Apr. 2009, doi: 10.1146/annurev.publhealth.031308.100143.
- [6] A. Zhitkovich, "Chromium in drinking water: Sources, metabolism, and cancer risks," *Chem. Res. Toxicol.*, vol. 24, no. 10, pp. 1617–1629, Oct. 2011, doi: 10.1021/tx200251t.
- [7] S. A. Katz and H. Salem, "The toxicology of chromium with respect to its chemical speciation: A review," *J. Appl. Toxicol.*, vol. 13, no. 3, pp. 217–224, May 1993, doi: 10.1002/jat.2550130314.
- [8] G. Quievryn, E. Peterson, J. Messer, and A. Zhitkovich, "Genotoxicity and Mutagenicity of Chromium(VI)/Ascorbate-Generated DNA Adducts in Human and Bacterial Cells," *Biochemistry*, vol. 42, no. 4, pp. 1062–1070, Feb. 2003, doi: 10.1021/bi0271547.
- [9] G. M. Ayoub, A. Damaj, H. El-Rassy, M. Al-Hindi, and R. M. Zayyat, "Equilibrium and kinetic studies on adsorption of chromium(VI) onto pine-needle-generated activated carbon," *SN Appl. Sci.*, vol. 1, no. 12, p. 1562, Dec. 2019, doi: 10.1007/s42452-019-1617-7.

- [10] V. Dimos, K. J. Haralambous, and S. Malamis, “A Review on the recent studies for chromium species adsorption on raw and modified natural minerals,” *Crit. Rev. Environ. Sci. Technol.*, vol. 42, no. 19, pp. 1977–2016, Oct. 2012, doi: 10.1080/10643389.2011.574102.
- [11] H. N. Tran *et al.*, “Adsorption mechanism of hexavalent chromium onto layered double hydroxides-based adsorbents: A systematic in-depth review,” *J. Hazard. Mater.*, vol. 373, pp. 258–270, Jul. 2019, doi: 10.1016/j.jhazmat.2019.03.018.
- [12] J. E. Johnson, S. M. Webb, C. Ma, and W. W. Fischer, “Manganese mineralogy and diagenesis in the sedimentary rock record,” *Geochim. Cosmochim. Acta*, vol. 173, pp. 210–231, Jan. 2016, doi: 10.1016/j.gca.2015.10.027.
- [13] K. Nicholson and M. Eley, “Geochemistry of manganese oxides: Metal adsorption in freshwater and marine environments,” *Geol. Soc. Lond. Spec. Publ.*, vol. 119, no. 1, pp. 309–326, 1997, doi: 10.1144/GSL.SP.1997.119.01.20.
- [14] L. Della Puppa, M. Komárek, F. Bordas, J.-C. Bollinger, and E. Joussein, “Adsorption of copper, cadmium, lead and zinc onto a synthetic manganese oxide,” *J. Colloid Interface Sci.*, vol. 399, pp. 99–106, Jun. 2013, doi: 10.1016/j.jcis.2013.02.029.
- [15] R. Han, W. Zou, Y. Wang, and L. Zhu, “Removal of uranium(VI) from aqueous solutions by manganese oxide coated zeolite: Discussion of adsorption isotherms and pH effect,” *J. Environ. Radioact.*, vol. 93, no. 3, pp. 127–143, Jan. 2007, doi: 10.1016/j.jenvrad.2006.12.003.
- [16] R. G. Burns, “The uptake of cobalt into ferromanganese nodules, soils, and synthetic manganese (IV) oxides,” *Geochim. Cosmochim. Acta*, vol. 40, no. 1, pp. 95–102, Jan. 1976, doi: 10.1016/0016-7037(76)90197-6.
- [17] K. D. Kwon, K. Refson, and G. Sposito, “Understanding the trends in transition metal sorption by vacancy sites in birnessite,” *Geochim. Cosmochim. Acta*, vol. 101, pp. 222–232, Jan. 2013, doi: 10.1016/j.gca.2012.08.038.

- [18] Q. Su, B. Pan, S. Wan, W. Zhang, and L. Lv, "Use of hydrous manganese dioxide as a potential sorbent for selective removal of lead, cadmium, and zinc ions from water," *J. Colloid Interface Sci.*, vol. 349, no. 2, pp. 607–612, Sep. 2010, doi: 10.1016/j.jcis.2010.05.052.
- [19] J. Xie, X. Gu, F. Tong, Y. Zhao, and Y. Tan, "Surface complexation modeling of Cr(VI) adsorption at the goethite–water interface," *J. Colloid Interface Sci.*, vol. 455, pp. 55–62, Oct. 2015, doi: 10.1016/j.jcis.2015.05.041.
- [20] K. Mesuere and W. Fish, "Chromate and oxalate adsorption on goethite. 2. Surface complexation modeling of competitive adsorption," *Environ. Sci. Technol.*, vol. 26, no. 12, pp. 2365–2370, Dec. 1992, doi: 10.1021/es00036a005.
- [21] Z. Wang *et al.*, "Adsorption of Uranium(VI) to manganese oxides: X-ray absorption spectroscopy and surface complexation modeling," *Environ. Sci. Technol.*, vol. 47, no. 2, pp. 850–858, Jan. 2013, doi: 10.1021/es304454g.
- [22] R. Han, Z. Lu, W. Zou, W. Daotong, J. Shi, and Y. Jiujun, "Removal of copper(II) and lead(II) from aqueous solution by manganese oxide coated sand: II. Equilibrium study and competitive adsorption," *J. Hazard. Mater.*, vol. 137, no. 1, pp. 480–488, Sep. 2006, doi: 10.1016/j.jhazmat.2006.02.018.
- [23] K. Mesuere and W. Fish, "Chromate and oxalate adsorption on goethite. 1. Calibration of surface complexation models," *Environ. Sci. Technol.*, vol. 26, no. 12, pp. 2357–2364, Dec. 1992, doi: 10.1021/es00036a004.
- [24] J.-H. An and S. Dultz, "Adsorption of tannic acid on chitosan-montmorillonite as a function of pH and surface charge properties," *Appl. Clay Sci.*, vol. 36, no. 4, pp. 256–264, May 2007, doi: 10.1016/j.clay.2006.11.001.
- [25] A. Degen and M. Kosec, "Effect of pH and impurities on the surface charge of zinc oxide in aqueous solution," *J. Eur. Ceram. Soc.*, p. 7, 2000.

- [26] M. F. Brigatti, "Reduction and sorption of chromium by Fe(II)-bearing phyllosilicates: chemical treatments and X-Ray Absorption Spectroscopy (XAS) studies," *Clays Clay Miner.*, vol. 48, no. 2, pp. 272–281, 2000, doi: 10.1346/CCMN.2000.0480214.
- [27] I. J. Buerge and S. J. Hug, "Influence of mineral surfaces on chromium(VI) reduction by iron(II)," *Environ. Sci. Technol.*, vol. 33, no. 23, pp. 4285–4291, Dec. 1999, doi: 10.1021/es981297s.
- [28] R. R. Patterson, S. Fendorf, and M. Fendorf, "Reduction of hexavalent chromium by amorphous iron sulfide," *Environ. Sci. Technol.*, vol. 31, no. 7, pp. 2039–2044, Jul. 1997, doi: 10.1021/es960836v.
- [29] D. Pradhan, L. B. Sukla, M. Sawyer, and P. K. S. M. Rahman, "Recent bioreduction of hexavalent chromium in wastewater treatment: A review," *J. Ind. Eng. Chem.*, vol. 55, pp. 1–20, Nov. 2017, doi: 10.1016/j.jiec.2017.06.040.
- [30] L. Di Palma, M. T. Gueye, and E. Petrucci, "Hexavalent chromium reduction in contaminated soil: A comparison between ferrous sulphate and nanoscale zero-valent iron," *J. Hazard. Mater.*, vol. 281, pp. 70–76, Jan. 2015, doi: 10.1016/j.jhazmat.2014.07.058.
- [31] M. Hua, S. Zhang, B. Pan, W. Zhang, L. Lv, and Q. Zhang, "Heavy metal removal from water/wastewater by nanosized metal oxides: A review," *J. Hazard. Mater.*, vol. 211–212, pp. 317–331, Apr. 2012, doi: 10.1016/j.jhazmat.2011.10.016.
- [32] M. Villalobos, J. Bargar, and G. Sposito, "Mechanisms of Pb(II) sorption on a biogenic manganese oxide," *Environ. Sci. Technol.*, vol. 39, no. 2, pp. 569–576, Jan. 2005, doi: 10.1021/es049434a.
- [33] L. Tang *et al.*, "Synergistic adsorption and reduction of hexavalent chromium using highly uniform polyaniline–magnetic mesoporous silica composite," *Chem. Eng. J.*, vol. 254, pp. 302–312, Oct. 2014, doi: 10.1016/j.cej.2014.05.119.
- [34] N. Fiol, C. Escudero, and I. Villaescusa, "Chromium sorption and Cr(VI) reduction to Cr(III) by grape stalks and yohimbe bark," *Bioresour. Technol.*, vol. 99, no. 11, pp. 5030–5036, Jul. 2008, doi: 10.1016/j.biortech.2007.09.007.

- [35] C. Zheng *et al.*, “Simultaneous adsorption and reduction of hexavalent chromium on the poly(4-vinyl pyridine) decorated magnetic chitosan biopolymer in aqueous solution,” *Bioresour. Technol.*, vol. 293, p. 122038, Dec. 2019, doi: 10.1016/j.biortech.2019.122038.
- [36] C. F. Jones, R. S. C. Smart, and P. S. Turner, “Dissolution kinetics of manganese oxides. Effects of preparation conditions, pH and oxidation/reduction from solution,” *J. Chem. Soc. Faraday Trans.*, vol. 86, no. 6, pp. 947–953, Jan. 1990, doi: 10.1039/FT9908600947.
- [37] Y. Luo, W. Tan, S. L. Suib, G. Qiu, and F. Liu, “Dissolution and phase transformation processes of hausmannite in acidic aqueous systems under anoxic conditions,” *Chem. Geol.*, vol. 487, pp. 54–62, May 2018, doi: 10.1016/j.chemgeo.2018.04.016.
- [38] S. Boursiquot, M. Mullet, and J.-J. Ehrhardt, “XPS study of the reaction of chromium (VI) with mackinawite (FeS),” *Surf. Interface Anal.*, vol. 34, no. 1, pp. 293–297, Sep. 2002, doi: 10.1002/sia.1303.
- [39] V. Murphy, S. A. M. Tofail, H. Hughes, and P. McLoughlin, “A novel study of hexavalent chromium detoxification by selected seaweed species using SEM-EDX and XPS analysis,” *Chem. Eng. J.*, vol. 148, no. 2, pp. 425–433, May 2009, doi: 10.1016/j.cej.2008.09.029.

## CHAPTER VII

### VII. SUSTAINABILITY ASSESSMENT OF DIFFERENT CR(VI) REMOVAL TECHNOLOGIES: ADSORPTION, ION-EXCHANGE, AND REDUCTION-COAGULATION-FILTRATION

#### 7.1 Introduction

The national primary drinking water regulation has established the maximum contaminant level (MCL) for total chromium of 100 parts per billion in 1991. In September, 2010, a draft of toxicological review of hexavalent chromium was released by EPA for public comment and external peer review and further determining if current chromium regulation should be revised [1], [2]. California EPA conducted an extensive literature review and concluded that Cr(VI) exposure via ingestion in drinking water can be linked to increased incidences of tumor in experimental animals and human [3]–[5]. Their results included in the report California Public Health Goal published in July, 2011 to justify the development of a more cautious PHG for Cr(VI) in drinking water. The Environmental Working Group conducted a study of U.S. tap water and Cr(VI) was detected in 31 of 35 cities tap water tested in 2010 (Figure 7.1).

Due to the limitation of conventional water treatment process on Cr(VI) decontamination, an enhanced treatment process targeted Cr(VI) is needed to meet the standard for drinking purpose. A broad range of Cr(VI) removal technologies are reported in the literature including adsorption, ion-exchange, membrane filtration, electrocoagulation, and reduction-coagulation-filtration [6]–[10]. Among all the techniques mentioned above, adsorption is considered more economically and operationally feasible when compared to technologies like membrane filtration or ion exchange. There are extensive investigations regarding the technical performance of ion exchange, adsorption and reduction-coagulation-filtration systems. However, the environmental impacts of operating different treatment systems are rarely reported. To compare the implementation of these three different system into a real-life scenario, a holistic analysis using life cycle assessment(LCA) is necessary to decide which technology is more environmental friendly, economically feasible and socially equitable. LCA is a



produced in this process must be disposed of. Reduction-coagulation-filtration is a multi-step unit process that is comprising of reduction of soluble Cr(VI) into insoluble Cr(III) using ferrous ion in reduction tank, and coagulation of Cr(III) and Fe(III) particles and filtration of precipitates in dual-media filter unit. As a result, RCF technology requires a larger footprint owing to a series of processes to remove hexavalent chromium compared to adsorption or ion-exchange unit, hence it may be difficult to utilize at relatively small treatment plant. The high frequency of backwashing can result in large quantity of waste water to dispose. The purpose of this chapter focuses on the Environmental Sustainability Assessment of adsorption system using MCS adsorbent developed in this study, ion-exchange system using commercial anion exchange resin, and reduction-coagulation-filtration using ferrous ion to remove hexavalent chromium in water body. Additionally, the economic and social aspects of these three technologies are compared.

## 7.2 Method

### 7.2.1 Goal and scope

This chapter is intended to quantify and compare the removal of Cr(VI) from water using adsorption system with MCS, ion-exchange system with commercial resin and RCF system with ferrous iron in three different aspects: environmental, economic and social. The results provide an understanding to the feasibility and sustainability of adsorption system utilizing MCS as adsorbent in operation scenario in contrast to ion-exchange technology and RCF technology. The product life cycle can be divided into three stages: “cradle to gate”, including raw materials extraction and water and energy acquisition for manufacture process, “gate to gate”, where the use of the product and water or energy needed in the operation were considered, and “gate to grave”, consisted of waste management and disposal options [15]–[17]. The scope of this assessment was limited to “cradle to gate” life cycle of the treatment process and entailed chemicals, water and energy usage. Disposal of spent adsorbent, resin or filter media was not considered in this assessment.

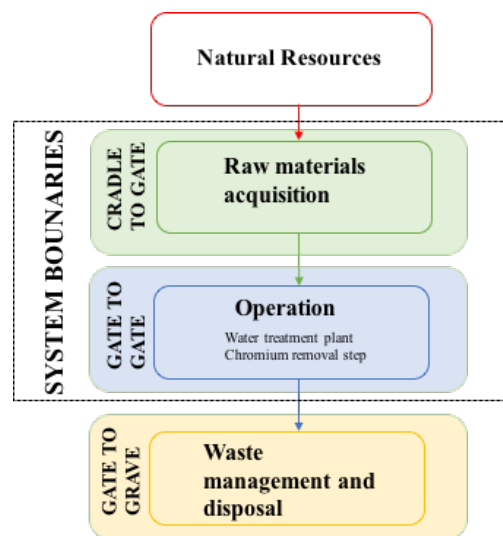


Figure 7. 2 Block diagram of boundaries of the system under study

### 7.2.2 Functional unit selection

In this work, the functional unit (FU) is related to remove hexavalent chromium from water. Therefore, the functional unit was chosen as 100 million gallons (MG) per year of drinking water treated with 25 $\mu$ g/L Cr(VI) removal over the course of 20 years (average design life of most water treatment plant). The purpose of this study is comparing three different systems abilities to achieve the desired chromium level under operational condition. Therefore, the FU chosen in this study is not restricted to water quantity treated but the water quality is incorporated in the meantime. The volume of 100MG per year represented the domestic use for a small drinking water treatment plant supplying about 2500 people (150 gallons per capita per day). In addition, raw water quality may vary regarding the water source and series of different pretreatment processes or post-treatments could be necessary. The focus of this study is on Cr(VI) removal; thus any materials or energy input related to pretreatment or post-treatment was not considered.

### 7.2.3 Technical design

Ion exchange resins fall into four categories in terms of their functional groups: strong acid and weak acid cation exchange resin; strong base and weak base anion exchange resin [9], [18], [19]. Cr(VI) exists in aqueous media in the form of oxyanion: chromate ( $\text{CrO}_4^{2-}$ ), bichromate ( $\text{HCrO}_4^-$ ) or dichromate ( $\text{Cr}_2\text{O}_7^{2-}$ ) depend on pH value of the media [2], [20], [21]. The two primary types of resins for the removal of Cr(VI) is strong base anion (SBA) exchange resin and weak base anion (WBA) exchange resin. SBA resins typically contain quaternary amine functional group that exists as permanent cation and readily ionizes regardless of pH values, whereas WBA resins typically contain secondary or tertiary amine functional group that ionizes only in the acidic pH region [11], [16], [19], [22]. Therefore, SBA resin can be regenerated with salt solution and WBA resin requires acids and/or bases to regenerate[22]. SBA system is selected in this study due to challenges in regenerating spent WBA resin. 10% sodium chloride (NaCl) is used to regenerate exhausted SBA resin by replacing chromate ions with chloride ions to restore the exchange capacity. Regeneration of MCS in the adsorber unit is accomplished by

employing 0.01M sodium hydroxide (NaOH) solution to dissociate chromate ions to regain the adsorption active sites.

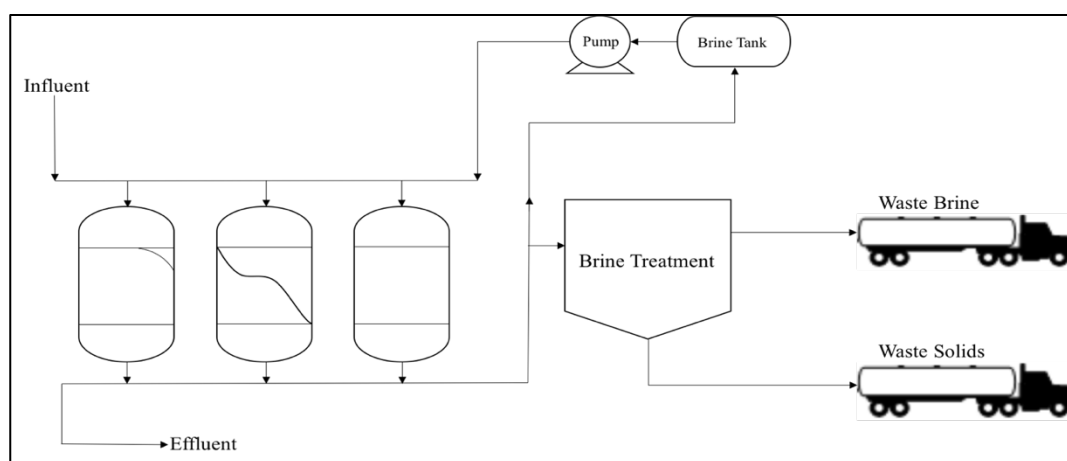


Figure 7. 3 Diagram for an SBA treatment system

Reduction/coagulation/filtration (RCF) process for chromium removal from water is comparable to the process of coagulation and filtration for heavy metal removal with pretreatment of reducing hexavalent chromium. Cr(VI) is first reduced by selected reductant (ferrous sulfate) into Cr(III) in a reduction contactor or column before pumping the contaminated water into coagulation tank [23]–[27]. The addition of reduction contactor unit is essential and mandatory for RCF system due to the fact that the reduction of Cr(VI) into Cr(III) is not an instantaneous reaction. Therefore, reduction contactor

unit can provide necessary time for maximum reduction of Cr(VI) by ferrous ions. After reduction reaction completed, the water stream will be introduced into coagulation unit. An optimum type and dosage of coagulant is added into coagulation unit to facilitate the precipitation process of Cr(III), rendering more effective filtration of the Cr(III) precipitates. Filtered water is discharged into a clear well and used as filter backwash water. All the design parameters for SBA, adsorber and RCF System are tabulated in Table 7.1 and Table 7.2.

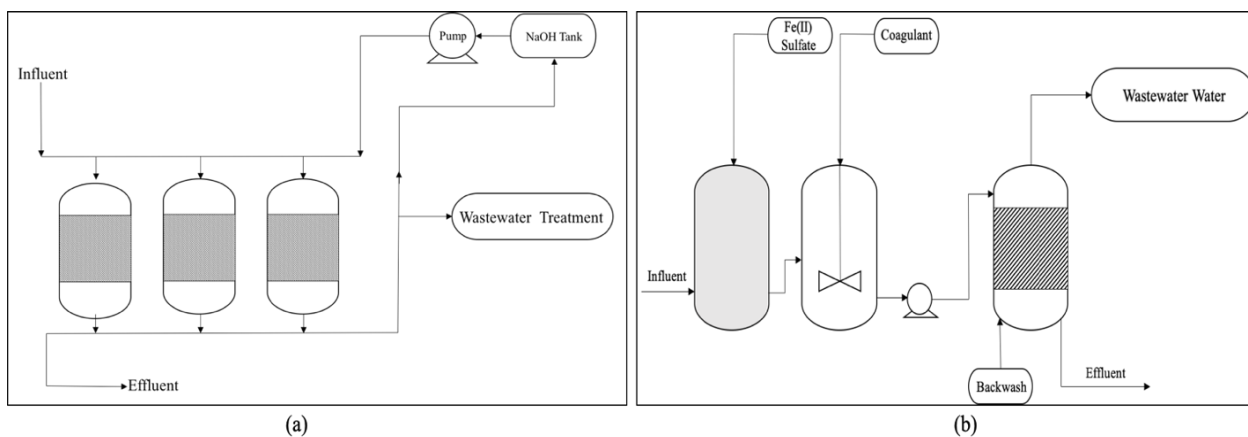


Figure 7. 4 (a)Diagram for an adsorber system; (b)diagram for an RCF system

Table 7. 1 Design parameters in SBA and adsorber system

Purolite A600E/9149	SBA System	MCS	Adsorber System
IX Vessel Configuration	One unit, plus one standby	Adsorber Configuration	Two in parallel, plus one standby
Design flow rate	35ft <sup>3</sup> /min	Design flow rate	35ft <sup>3</sup> /min
Resin depth	6ft	MCS depth	6ft
Resin per Vessel	80ft <sup>3</sup>	Adsorbent per Adsorber	80ft <sup>3</sup>
HLR	5ft <sup>3</sup> /min·ft <sup>2</sup>	HLR	2.6ft <sup>3</sup> /min·ft <sup>2</sup>
EBCT per Vessel	5min	EBCT per Adsorber	10min

Table 7. 2 Design parameters in RCF system

Design parameters	RCF system
Reduction contact time(min)	15
Filter units	2 units, 1 unit standby for backwash period
Silica sand depth (m)	0.3
Anthracite depth (m)	0.6
Filter loading rate (gpm/ft <sup>2</sup> )	4.1
Design flow rate (ft <sup>3</sup> /min)	35
Ferrous sulfate (mg/L)	2.25
Aluminum sulfate (mg/L)	3

## 7.3 Results and discussion

### 7.3.1 LCA inventory

In order to determine the overall environmental impacts, the adsorption, ion-exchange and RCF processes were designed to accommodate the hexavalent chromium removal demand of a small water treatment plant. Based on the scope and functional unit selected in this study, the life cycle inventory was estimated for each process comprising of the raw materials acquisition for each media, regeneration and backwash processes, the energy required for pumping, and transportation of materials. Calculation process of all selected parameters and the results of simulation are provided in the appendix with full details. The input quantities for Simapro 8.4.0.0 LCA software are summarized in Table 7.3 below.

Table 7. 3 LCA inventory of adsorber, ion-exchange and RCF

Adsorber	Materials	Total demand(kg)	Transportation(tkm)	Energy(kW·h)
Adsorbent	silica sand	77540.9	89973.8	
	MnSO <sub>4</sub> ·H <sub>2</sub> O	16384.4	8411.5	
	Na <sub>2</sub> CO <sub>3</sub>	10274.2	5820.2	
Regeneration	NaOH	4652.5	2635.6	
Total (20 yrs)			106941.1	99864

Ion-exchange unit	Materials	Total demand(kg)	Transportation(tkm)	Energy(kW·h)
Resin	A600E/9149	17159.9	21264.4	
Regeneration	NaCl	16473.5	9332.1	
Total (20 yrs)			30596.5	133152

RCF unit	Materials	Total demand(kg)	Transportation(tkm)	Energy(kW·h)
Reduction	FeSO <sub>4</sub>	11200	21448	
Coagulant	Al <sub>2</sub> (SO <sub>4</sub> ) <sub>3</sub>	31200	59748	
Filter media	silica sand	9075	10530.1	
	anthracite	9762	10745.9	
Total (20 yrs)			102472	71902

The tool for the reduction and assessment of chemical and other environmental impacts (TRACI) was employed as major impact assessment method for our study because TRACI was specifically designed by U.S. EPA as a comprehensive and applicable to the United States tool to conduct impact assessment [28]. The impact categories selected in this tool are ozone depletion, global warming, smog, acidification, eutrophication, carcinogenics, non carcinogenics, respiratory effects, ecotoxicity and fossil fuel depletion.

### 7.3.2 Environmental sustainability

The environmental impacts for adsorption, ion-exchange and RCF system were calculated and normalized by TRACI (U.S. 2008) method, as shown in Figure 7.5. Ion-exchange system tends to have higher impacts for the categories of ozone depletion, global warming, and fossil fuel depletion. However, adsorption system obtains higher impacts in other categories such as smog, acidification, eutrophication, and respiratory effects, whereas RCF exhibits higher impacts in categories such as carcinogenics, non carcinogenics and ecotoxicity. The main electricity consumers in all three systems are the pumping required for water flowing through the treatment systems which are designed as fixed bed columns in adsorber and ion exchange unit, dual-media filtration unit, adsorbent/resin regeneration and filter backwash process. The electricity in the regeneration step is considered negligible compared to the electricity used to overcome pressure drop. The assumption of different pressure drops in adsorber and ion-exchange units due to different particle sizes results in different amount of electricity consumption. As for RCF system, electricity consumed by the relatively high frequency of backwash is necessary to be considered in total electricity usage. Therefore, the environmental impacts of these three systems mostly depend on primary resources to produce resin, adsorbent, reductant and coagulant and transportation of the chemicals and materials involved in the production process. The normalization of the environmental impacts indicates that adsorption, ion-exchange and RCF systems have highest impact in the category of carcinogenics that contributes to 39%, 36.31% and 66.70% of total impacts for ion-exchange, adsorption, and RCF respectively. The chemicals used in production and regeneration of adsorbent, resin, reductant, and coagulant are expected to mainly affect the categories of carcinogenics,

non carcinogenics, and ecotoxicity. RCF shows the highest impacts in these categories indicating that the production of reductant and coagulant are chemical intensive processes and severely damaging the environment. The trichloromethane used in production of anionic resin is directly related to 10.8% effect on ozone depletion for ion exchange system, whereas there is merely 0.09% effect on ozone depletion for adsorption system and 0.02% for RCF system [18].

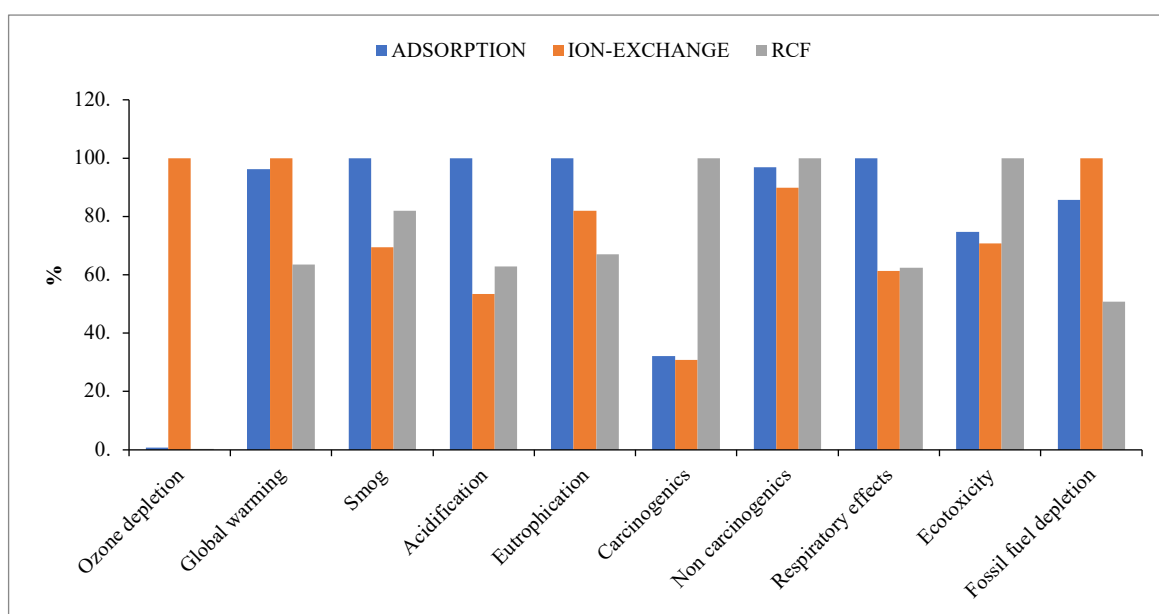


Figure 7. 5 Characterization of environmental impacts using TRACI 2.1 method: adsorption, ion-exchange and RCF system

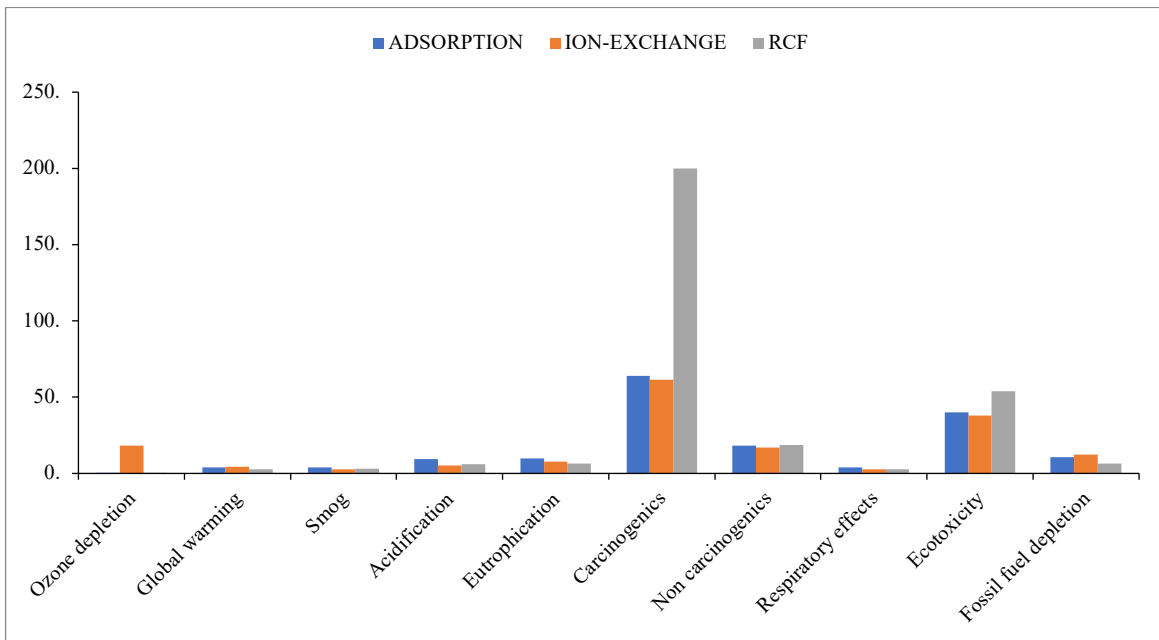
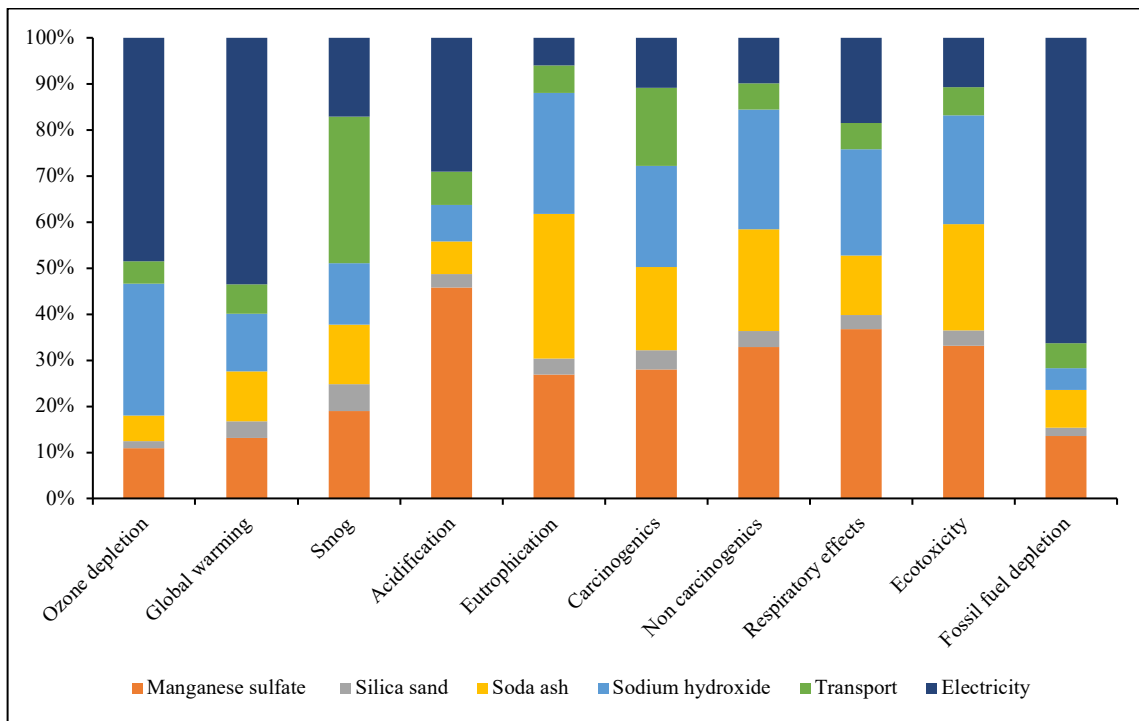


Figure 7. 6 Normalization of environmental impacts using TRACI 2.1 method: adsorption, ion-exchange and RCF system



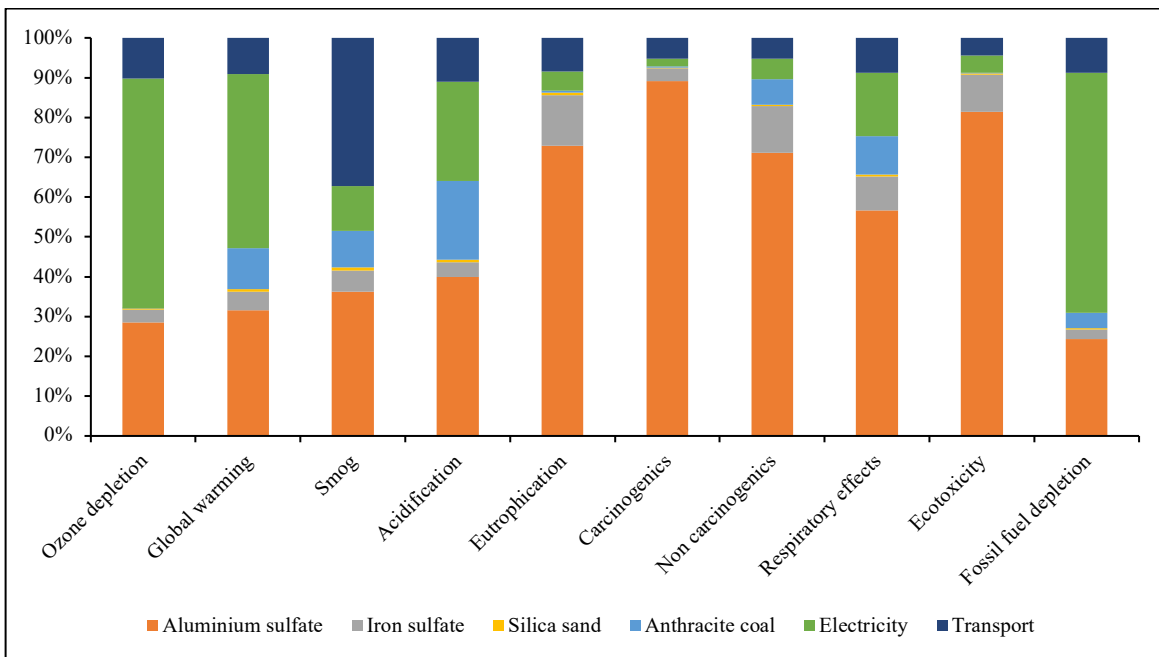
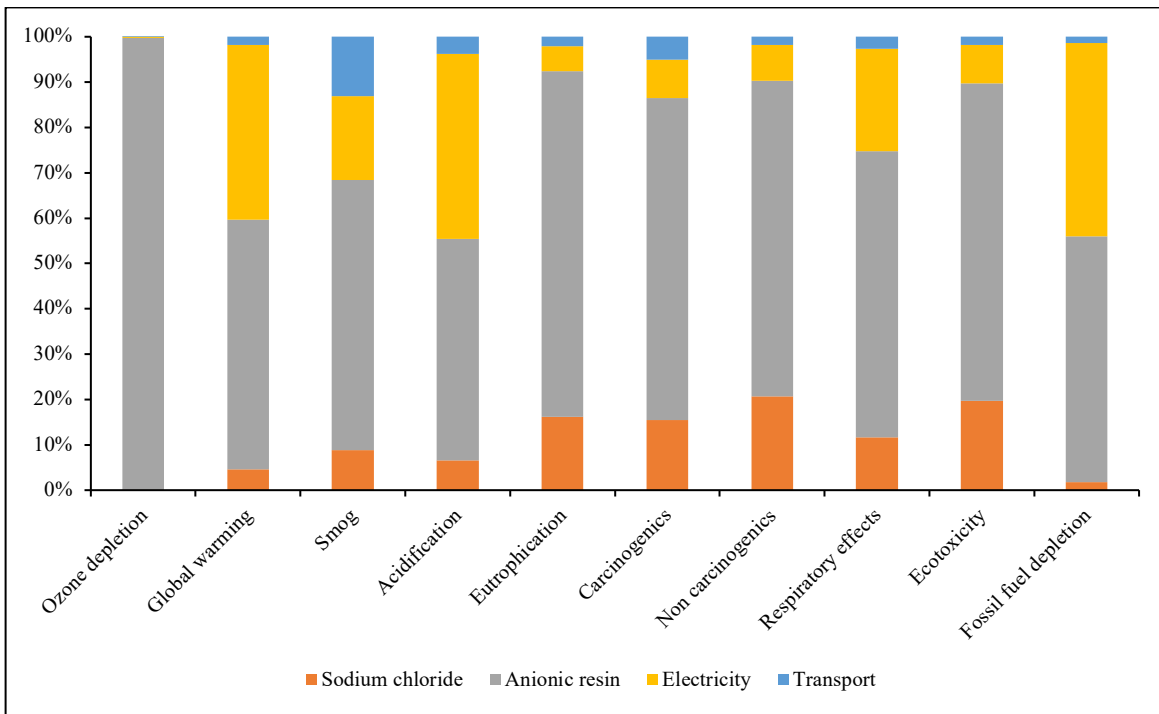


Figure 7.7 Characterization of environmental impacts for adsorption, ion-exchange and RCF systems of different input materials and processes

For adsorption system, the production and regeneration of adsorbent (MCS) has the most contribution to the environmental impacts, which is expected because of the intensive use chemicals in these process. For ion exchange system, the environmental impacts are linked closely to production of anionic resin. For RCF system, the usage of coagulant accounting for the most of environmental impacts are indicative of that the production of aluminum sulfate is substantially detrimental to natural environment. In all three systems, electricity is an essential contributor for various environmental damages. Thus, it is promising to modify the process and decrease the total environmental impacts by switching power sources to renewable energy such as biomass or biofuel.

### 7.3.3 Economic sustainability

The cost-effectiveness of the technologies was determined using the cost information (including equipment selection, site design and planning, installation of units, operation and maintenance costs) quoted by the vendors, distributor or manufacturer and collected from the demonstration studies [29]. The economic estimates were performed under two different scenarios: 1. The waste brine is discharged to the sewer without treatment; 2. The waste brine is treated and then returned to the head of the plant or hauled off-site for disposal. Detailed calculation and assumption are showed in appendix. Results in Table 7.4 show that adsorber system is the most cost-effective system compared to ion-exchange system and RCF system under two different scenarios. The high salt content of the waste brine from ion-exchange treatment system is relatively difficult to handle. The backwash water from RCF treatment system can be directly released into waste stream if considered as non-hazardous. The relatively high capital costs associated with ion-exchange system is because of the expense of resin.

Table 7. 4 Overall costs for adsorber, ion-exchange and RCF systems

	Scenario 1		Scenario 2	
	Capital Costs (\$/year)	O&M Costs (\$/year)	Capital Costs (\$/year)	O&M Costs (\$/year)
Adsorption	8,308	30,000	8,308	36,000
Ion-exchange	50,105	28,000	50,105	48,000
RCF	16,092	32,000	16,092	56,000

#### 7.3.4 Social sustainability

The indicator chosen to evaluate the social impacts is gleaned from a variety of literatures under three different life stages: construction, operation, and waste disposal. The indicators are listed below: local capacity, within local capacity to operate and maintain; community acceptance, acknowledged by the community in which the treatment unit is installed in, satisfactory results to meet with the water quality demands of the community, accepted by the community in which the treatment unit is installed in and minimize impacts of system failure; economic development, contributing to economic development; community development, providing a stable and reliable quality control for the water supply, selected by people aware of the impact of the decision and provided with other potentially effective alternatives, contributing to community development, and incorporating plans for improvement of the quality of life; equity, contributing to inter-generational and intra-generational equity and providing water to all members of the community; health, providing a safe source of water, ensuring the safety and health of operation and maintenance personnel; cultural, supporting the community cultural traditions and rituals [15], [30]–[33].

The social matrix scoring is given from 0 to 4, where 0-highes impact, 1-substantial impact, 2-moderate impact, 3-minimum impact, and 4-no impact. Adsorber system exhibits more superiority and more socially sustainability than ion-exchange and RCF system (Table 7.5).

Table 7. 5 Social sustainability matrix for adsorber, ion-exchange and RCF systems

Life stage		Local capacity	Community acceptance	Economic development	Community development	Equity	Health	Cultural	Recreational
Construction	Adsorber	3	2	4	4	3	3	3	3
	IX	3	3	3	4	4	2	3	3
	RCF	3	2	3	4	3	2	3	3
Operation	Adsorber	3	3	3	3	3	3	3	4
	IX	2	3	3	3	4	2	3	3
	RCF	2	2	4	3	3	2	3	4
Waste	Adsorber	2	3	3	3	2	3	3	4
	IX	3	1	2	3	2	1	3	2
	RCF	2	2	2	4	3	2	3	2
Overall	Adsorber	73/96							
	IX	64/96							
	RCF	66/96							

## 7.4 Conclusion

This study conducted a holistic sustainability assessment of three different Cr(VI) removal systems: strong base anion exchange system (SBA), adsorption system using manganese-coated sand and reduction-coagulation-filtration system. Triple bottom line concept is applied to this study to evaluate environmental, economic and social aspects of sustainability. Environmental sustainability was assessed by life cycle analysis using SimaPro 8.4.0.0. In conclusion, ion-exchange system displays to be slightly more environmental friendly, except the impact of ozone depletion caused by manufacturing of resin, global warming and fossil fuel depletion, while RCF system displays to obtain the highest impact of carcinogenics, non carcinogenics, and ecotoxicity. Adsorption system is more economic than ion-exchange and RCF system under two different waste brine disposal scenarios owing to the low-cost developed adsorbent and employment of single unit process to remove chromium. After all, employing the indicators from different resources, adsorption indicates to be more social viable due to the fact that the waste brine of SBA system contains high salt and manufacture of strong anion resin and the disposal of the solid and liquid waste from backwash process in RCF system. With all aspects considered, adsorption system is a relatively more promising and sustainable technology to remove hexavalent chromium from water.

## 7.5 Reference

- [1] J. Barnhart, “Occurrences, uses, and properties of chromium,” *Regul. Toxicol. Pharmacol.*, vol. 26, no. 1, pp. S3–S7, Aug. 1997, doi: 10.1006/rtph.1997.1132.
- [2] J. Kotaś and Z. Stasicka, “Chromium occurrence in the environment and methods of its speciation,” *Environ. Pollut.*, vol. 107, no. 3, pp. 263–283, Mar. 2000, doi: 10.1016/S0269-7491(99)00168-2.
- [3] A. Zhitkovich, “Chromium in drinking water: Sources, metabolism, and cancer risks,” *Chem. Res. Toxicol.*, vol. 24, no. 10, pp. 1617–1629, Oct. 2011, doi: 10.1021/tx200251t.
- [4] G. Quievryn, E. Peterson, J. Messer, and A. Zhitkovich, “Genotoxicity and mutagenicity of chromium(VI)/ascorbate-generated DNA adducts in human and bacterial cells,” *Biochemistry*, vol. 42, no. 4, pp. 1062–1070, Feb. 2003, doi: 10.1021/bi0271547.
- [5] C.-H. Tseng, C. Lei, and Y.-C. Chen, “Evaluating the health costs of oral hexavalent chromium exposure from water pollution: A case study in Taiwan,” *J. Clean. Prod.*, vol. 172, pp. 819–826, Jan. 2018, doi: 10.1016/j.jclepro.2017.10.177.
- [6] C. E. Barrera-Díaz, V. Lugo-Lugo, and B. Bilyeu, “A review of chemical, electrochemical and biological methods for aqueous Cr(VI) reduction,” *J. Hazard. Mater.*, vol. 223–224, pp. 1–12, Jul. 2012, doi: 10.1016/j.jhazmat.2012.04.054.
- [7] J. Bohdziewicz, “Removal of chromium ions (VI) from underground water in the hybrid complexation-ultrafiltration process,” *Desalination*, vol. 129, no. 3, pp. 227–235, Aug. 2000, doi: 10.1016/S0011-9164(00)00063-1.
- [8] N. K. Lazaridis and Ch. Charalambous, “Sorptive removal of trivalent and hexavalent chromium from binary aqueous solutions by composite alginate–goethite beads,” *Water Res.*, vol. 39, no. 18, pp. 4385–4396, Nov. 2005, doi: 10.1016/j.watres.2005.09.013.
- [9] J. A. Korak, R. Huggins, and M. Arias-Paic, “Regeneration of pilot-scale ion exchange columns for hexavalent chromium removal,” *Water Res.*, vol. 118, pp. 141–151, Jul. 2017, doi: 10.1016/j.watres.2017.03.018.

- [10] L. Rafati, A. H. Mahvi, A. R. Asgari, and S. S. Hosseini, "Removal of chromium (VI) from aqueous solutions using Lewatit FO36 nano ion exchange resin," *Int. J. Environ. Sci. Technol.*, vol. 7, no. 1, pp. 147–156, Dec. 2010, doi: 10.1007/BF03326126.
- [11] G. A. Maul, Y. Kim, A. Amini, Q. Zhang, and T. H. Boyer, "Efficiency and life cycle environmental impacts of ion-exchange regeneration using sodium, potassium, chloride, and bicarbonate salts," *Chem. Eng. J.*, vol. 254, pp. 198–209, Oct. 2014, doi: 10.1016/j.cej.2014.05.086.
- [12] L. Høiby, J. Clauson-Kaas, H. Wenzel, H. F. Larsen, B. N. Jacobsen, and O. Dalgaard, "Sustainability assessment of advanced wastewater treatment technologies," *Water Sci. Technol.*, vol. 58, no. 5, pp. 963–968, Sep. 2008, doi: 10.2166/wst.2008.450.
- [13] H. A. Alhashimi and C. B. Aktas, "Life cycle environmental and economic performance of biochar compared with activated carbon: A meta-analysis," *Resour. Conserv. Recycl.*, vol. 118, pp. 13–26, Mar. 2017, doi: 10.1016/j.resconrec.2016.11.016.
- [14] D. Mohan and C. U. Pittman Jr., "Activated carbons and low cost adsorbents for remediation of tri- and hexavalent chromium from water," *J. Hazard. Mater.*, vol. 137, no. 2, pp. 762–811, Sep. 2006, doi: 10.1016/j.jhazmat.2006.06.060.
- [15] A. Amini, Y. Kim, J. Zhang, T. Boyer, and Q. Zhang, "Environmental and economic sustainability of ion exchange drinking water treatment for organics removal," *J. Clean. Prod.*, vol. 104, pp. 413–421, Oct. 2015, doi: 10.1016/j.jclepro.2015.05.056.
- [16] M. Gifford, M. Chester, K. Hristovski, and P. Westerhoff, "Reducing environmental impacts of metal (hydr)oxide nanoparticle embedded anion exchange resins using anticipatory life cycle assessment," *Environ. Sci. Nano*, vol. 3, no. 6, pp. 1351–1360, 2016, doi: 10.1039/C6EN00191B.
- [17] G. Finnveden *et al.*, "Recent developments in Life Cycle Assessment," *J. Environ. Manage.*, vol. 91, no. 1, pp. 1–21, Oct. 2009, doi: 10.1016/j.jenvman.2009.06.018.

- [18] A. Dominguez-Ramos *et al.*, “Arsenic Removal from Natural Waters by Adsorption or Ion Exchange: An Environmental Sustainability Assessment,” *Ind. Eng. Chem. Res.*, vol. 53, no. 49, pp. 18920–18927, Dec. 2014, doi: 10.1021/ie4044345.
- [19] K. Kadirvelu and J. Goel, “Ion Exchange and Inorganic Adsorption,” in *Water Encyclopedia*, J. H. Lehr and J. Keeley, Eds. Hoboken, NJ, USA: John Wiley & Sons, Inc., 2005.
- [20] F. C. Richard and A. C. M. Bourg, “Aqueous geochemistry of chromium: A review,” *Water Res.*, vol. 25, no. 7, pp. 807–816, Jul. 1991, doi: 10.1016/0043-1354(91)90160-R.
- [21] S. Boursiquot, M. Mullet, and J.-J. Ehrhardt, “XPS study of the reaction of chromium (VI) with mackinawite (FeS),” *Surf. Interface Anal.*, vol. 34, no. 1, pp. 293–297, Sep. 2002, doi: 10.1002/sia.1303.
- [22] X. Li, P. G. Green, C. Seidel, C. Gorman, and J. L. Darby, “Meeting California’s hexavalent chromium MCL using strong base anion exchange resin,” *J. - Am. Water Works Assoc.*, vol. 108, pp. E474–E481, Sep. 2016, doi: 10.5942/jawwa.2016.108.0112.
- [23] I. J. Buerge and S. J. Hug, “Influence of mineral surfaces on chromium(VI) Reduction by Iron(II),” *Environ. Sci. Technol.*, vol. 33, no. 23, pp. 4285–4291, Dec. 1999, doi: 10.1021/es981297s.
- [24] I. J. Buerge and S. J. Hug, “Kinetics and pH dependence of chromium(VI) reduction by Iron(II),” *Environ. Sci. Technol.*, vol. 31, no. 5, pp. 1426–1432, May 1997, doi: 10.1021/es960672i.
- [25] R. R. Patterson, S. Fendorf, and M. Fendorf, “Reduction of hexavalent chromium by amorphous iron sulfide,” *Environ. Sci. Technol.*, vol. 31, no. 7, pp. 2039–2044, Jul. 1997, doi: 10.1021/es960836v.
- [26] L. Di Palma, M. T. Gueye, and E. Petrucci, “Hexavalent chromium reduction in contaminated soil: A comparison between ferrous sulphate and nanoscale zero-valent iron,” *J. Hazard. Mater.*, vol. 281, pp. 70–76, Jan. 2015, doi: 10.1016/j.jhazmat.2014.07.058.
- [27] G. Qin, M. J. McGuire, N. K. Blute, C. Seidel, and L. Fong, “Hexavalent chromium removal by reduction with ferrous sulfate, coagulation, and filtration: A pilot-scale study,” *Environ. Sci. Technol.*, vol. 39, no. 16, pp. 6321–6327, Aug. 2005, doi: 10.1021/es050486p.

- [28] J. C. Bare, “Traci.: The Tool for the reduction and assessment of chemical and other environmental impacts,” *J. Ind. Ecol.*, vol. 6, no. 3–4, pp. 49–78, Jun. 2002, doi: 10.1162/108819802766269539.
- [29] “Impact of Water Quality on Hexavalent Chromium Removal Efficiency and Cost,” *The Water Research Foundation*.
- [30] J. Zhang *et al.*, “Life cycle assessment of a microbial desalination cell for sustainable wastewater treatment and saline water desalination,” *J. Clean. Prod.*, vol. 200, pp. 900–910, Nov. 2018, doi: 10.1016/j.jclepro.2018.07.197.
- [31] H. E. Muga and J. R. Mihelcic, “Sustainability of wastewater treatment technologies,” *J. Environ. Manage.*, vol. 88, no. 3, pp. 437–447, Aug. 2008, doi: 10.1016/j.jenvman.2007.03.008.
- [32] S. Foteinis, A. G. L. Borthwick, Z. Frontistis, D. Mantzavinos, and E. Chatzisyneon, “Environmental sustainability of light-driven processes for wastewater treatment applications,” *J. Clean. Prod.*, vol. 182, pp. 8–15, May 2018, doi: 10.1016/j.jclepro.2018.02.038.
- [33] M. Schulz, M. D. Short, and G. M. Peters, “A streamlined sustainability assessment tool for improved decision making in the urban water industry,” *Integr. Environ. Assess. Manag.*, vol. 8, no. 1, pp. 183–193, Jan. 2012, doi: 10.1002/ieam.247.
- [34] A. J. Balkema, H. A. Preisig, R. Otterpohl, and F. J. D. Lambert, “Indicators for the sustainability assessment of wastewater treatment systems,” *Urban Water*, vol. 4, no. 2, pp. 153–161, Jun. 2002, doi: 10.1016/S1462-0758(02)00014-6.
- [35] Ll. Corominas *et al.*, “Life cycle assessment applied to wastewater treatment: State of the art,” *Water Res.*, vol. 47, no. 15, pp. 5480–5492, Oct. 2013, doi: 10.1016/j.watres.2013.06.049.

## CHAPTER VIII

### VIII. CONCLUSIONS

#### 8. Conclusion

This dissertation aims to synthesize a novel manganese-coated sand (MCS) for the removal of chromium from water. In order to obtain an efficient, applicable and inexpensive sorbent, various coating parameters such as the source of manganese, coating temperature and coating pH were adjusted. The optimum MCS was obtained at coating temperature 220°C using manganese sulfate as manganese source without adjusting the pH of the coating solution. Adsorption capacity of MCS synthesized in this study was evaluated as function of MCS dosage, initial chromium concentration, pH, contact time, and co-existing ions. Adsorption equilibrium data were fitted into four different isotherms including Langmuir, Freundlich, Temkin and Dubinin-Radushkevich. The parameters obtained from aforementioned isotherms were indicative of that MCS sorbent displays a greater affinity and stronger binding for Cr(VI) than Cr(III), despite the higher adsorption capacity of MCS sorbent for Cr(III). They also suggest adsorption of chromium onto MCS sorbent is monolayer adsorption on a heterogeneous surface. The effective adsorption over a wide range of from pH 3 to 10 for both chromium species makes the MCS sorbent as a desirable sorbent for practical use. Specific adsorption can be inferred from the significant shift observed from surface charge measurements of the MCS sorbent with or without chromium species. The adsorption of Cr(III) and Cr(VI) can be better explained by pseudo-second order kinetics and the rate-limiting step was decided to be a combination of film diffusion and intraparticle diffusion. MCS sorbent can be successfully regenerated with 0.01 N NaOH without significant loss in chromium adsorption capacity.

Different surface characterization procedures such as XRD, XPS, SEM-EDX and BET surface analysis were applied to investigate the mineral crystal structure, surface properties and surface phenomena in order to explain the mechanism of adsorption for the adsorption of both chromium species onto the surface of the MCS. The BET surface area was determined to be 3.09 m<sup>2</sup>/g. The surface

crystalline structures formed at different temperatures were analyzed by XRD and identified by matching the obtained XRD patterns with Crystallography Open Database (COD). Pyrochroite ( $\text{H}_2\text{MnO}_2$ ) was the main and more reduced form of manganese oxide detected on the surface of the MCS sorbents developed at temperature lower than  $220^\circ\text{C}$ , while  $\text{NaMn(III)O}_2$  was the main and more oxidized form of manganese oxide detected on the surface of the MCS sorbents coated at temperature higher than  $220^\circ\text{C}$ . Both manganese oxides were detected on the optimum MCS selected for this study. XPS spectra confirmed the oxidation states of surface manganese oxides as Mn(II) and Mn(III) without the appearance of Mn(IV). SEM image showed manganese oxides was not uniformly coated on the silica sand and EDM spectrum confirmed the adsorption of chromium onto the MCS sorbent. The distribution of chromium species on the surface appeared in the dot mapping is in good accordance with the coating of manganese oxides on the surface, therefore suggesting surface manganese oxides are responsible for chromium adsorption. The transformation of Cr(III) to Cr(VI) or Cr(VI) to Cr(III) accompanying with the transformation of Mn(III) to Mn(II) or Mn(III) to Mn(IV) were the results of occurrence of redox reactions between chromium species and surface oxides.

The mixture of Mn(II,III) oxides found on the surface of the selected MCS sorbent made it necessary to study the chromium removal with pure manganese oxides to further elucidate the adsorption mechanism. The adsorption and uptake of Cr(III) and Cr(VI) by the MnO and  $\text{Mn}_2\text{O}_3$  sorbents were investigated under different experimental conditions. Based on the adsorption parameters obtained from several adsorption models, the adsorption of Cr(III) and Cr(VI) followed the Langmuir and Freundlich adsorption models with the MnO and  $\text{Mn}_2\text{O}_3$  sorbents exhibiting a stronger binding for adsorption of Cr(VI) than for adsorption of Cr(III). The D-R equation parameters were suggestive of adsorption of Cr(III) onto the MnO sorbent and both Cr(III) and Cr(VI) onto the  $\text{Mn}_2\text{O}_3$  sorbent as physisorption and adsorption of Cr(VI) onto the MnO sorbent as chemisorption. The adsorption of both chromium species decreased appreciably for pH values greater than 9 due to the fact that the MnO sorbent obtained a PZC of about 10 in the absence of or in the presence of chromium species, while the adsorption of Cr(III) and

Cr(VI) onto the  $\text{Mn}_2\text{O}_3$  sorbent experience a drastic drop with increasing pH from 9 to 10 and from 8 to 9, respectively, due to the reversal of the surface charge. The XPS results showed that Cr(VI) was fully reduced by the MnO sorbent and partially reduced by the  $\text{Mn}_2\text{O}_3$  sorbent.

Two-pK triple layer surface complexation model (TLM) was used to describe the adsorption of chromate ion as oxyanion onto manganese(II,III) oxides surface. Specific surface area, site density, stability constants and redox potential were included in the model to predict possible outcome. The model results have some discrepancies with the actual experimental data due to the failure to consider the dissolution of  $\text{Mn}_2\text{O}_3$ , which may produce more  $\text{Mn}^{2+}$  in solution and enhance the adsorption of chromium.

Sustainability assessment of adsorber system using MCS adsorbent developed in this study, ion-exchange system using commercial anion exchange resin, and reduction-coagulation-filtration using ferrous ion to remove hexavalent chromium in water body were evaluated and compared from environmental, economic and social perspectives. Ion-exchange system displays to be slightly more environmental friendly, except the impact of ozone depletion caused by manufacturing of resin, global warming and fossil fuel depletion, while RCF system display to obtain the highest impact of carcinogenics, non carcinogenics, and ecotoxicity. Adsorption system is more economic than ion-exchange and RCF system under two different waste brine disposal scenarios owing to the low-cost developed adsorbent and employment of single unit process to remove chromium. Adsorber system is a relatively more promising and sustainable technology to remove chromium from water.

## CITED LITERATURE

- [1] J. Barnhart, "Occurrences, uses, and properties of chromium," *Regul. Toxicol. Pharmacol.*, vol. 26, no. 1, pp. S3–S7, Aug. 1997, doi: 10.1006/rtph.1997.1132.
- [2] J. Kotaś and Z. Stasicka, "Chromium occurrence in the environment and methods of its speciation," *Environ. Pollut.*, vol. 107, no. 3, pp. 263–283, Mar. 2000, doi: 10.1016/S0269-7491(99)00168-2.
- [3] R. E. Cranston and J. W. Murray, "The determination of chromium species in natural waters," *Anal. Chim. Acta*, vol. 99, no. 2, pp. 275–282, Aug. 1978, doi: 10.1016/S0003-2670(01)83568-6.
- [4] S. A. Katz and H. Salem, "The toxicology of chromium with respect to its chemical speciation: A review," *J. Appl. Toxicol.*, vol. 13, no. 3, pp. 217–224, May 1993, doi: 10.1002/jat.2550130314.
- [5] I. Moffat, N. Martinova, C. Seidel, and C. M. Thompson, "Hexavalent chromium in drinking water," *J. - AWWA*, vol. 110, no. 5, pp. E22–E35, Apr. 2018, doi: 10.1002/awwa.1044.
- [6] S. E. Fendorf, "Surface reactions of chromium in soils and waters," *Geoderma*, vol. 67, no. 1–2, pp. 55–71, Jun. 1995, doi: 10.1016/0016-7061(94)00062-F.
- [7] F. M. G. Tack and M. G. Verloo, "Chemical speciation and fractionation in soil and sediment heavy metal analysis: A review," *Int. J. Environ. Anal. Chem.*, vol. 59, no. 2–4, pp. 225–238, Apr. 1995, doi: 10.1080/03067319508041330.
- [8] D. C. Schroeder and G. F. Lee, "Potential transformations of chromium in natural waters," *Water. Air. Soil Pollut.*, vol. 4, no. 3, pp. 355–365, Sep. 1975, doi: 10.1007/BF00280721.
- [9] S. E. Fendorf and G. Li, "Kinetics of chromate reduction by ferrous iron," *Environ. Sci. Technol.*, vol. 30, no. 5, pp. 1614–1617, Jan. 1996, doi: 10.1021/es950618m.
- [10] P. M. Jardine, S. E. Fendorf, M. A. Mayes, I. L. Larsen, S. C. Brooks, and W. B. Bailey, "Fate and transport of hexavalent chromium in undisturbed heterogeneous soil," *Environ. Sci. Technol.*, vol. 33, no. 17, pp. 2939–2944, Sep. 1999, doi: 10.1021/es981211v.
- [11] F. Y. Salem, T. F. Parkerton, R. V. Lewis, J. H. Huang, and K. L. Dickson, "Kinetics of chromium transformations in the environment," *Sci. Total Environ.*, vol. 86, no. 1, pp. 25–41, Oct. 1989, doi: 10.1016/0048-9697(89)90190-3.

- [12] W. Cui *et al.*, “Cr(III) adsorption by cluster formation on boehmite nanoplates in highly alkaline solution,” *Environ. Sci. Technol.*, vol. 53, no. 18, pp. 11043–11055, Sep. 2019, doi: 10.1021/acs.est.9b02693.
- [13] C. Oze, D. K. Bird, and S. Fendorf, “Genesis of hexavalent chromium from natural sources in soil and groundwater,” *Proc. Natl. Acad. Sci.*, vol. 104, no. 16, pp. 6544–6549, Apr. 2007, doi: 10.1073/pnas.0701085104.
- [14] S. Egodawatte, A. Datt, E. A. Burns, and S. C. Larsen, “Chemical insight into the adsorption of chromium(III) on iron oxide/mesoporous silica nanocomposites,” *Langmuir*, vol. 31, no. 27, pp. 7553–7562, Jul. 2015, doi: 10.1021/acs.langmuir.5b01483.
- [15] M. Tuzen and M. Soylak, “Multiwalled carbon nanotubes for speciation of chromium in environmental samples,” *J. Hazard. Mater.*, vol. 147, no. 1, pp. 219–225, Aug. 2007, doi: 10.1016/j.jhazmat.2006.12.069.
- [16] Y. Li *et al.*, “Hexavalent chromium removal from aqueous solution by adsorption on aluminum magnesium mixed hydroxide,” *Water Res.*, vol. 43, no. 12, pp. 3067–3075, Jul. 2009, doi: 10.1016/j.watres.2009.04.008.
- [17] F. C. Richard and A. C. M. Bourg, “Aqueous geochemistry of chromium: A review,” *Water Res.*, vol. 25, no. 7, pp. 807–816, Jul. 1991, doi: 10.1016/0043-1354(91)90160-R.
- [18] A. C. M. Bourg and J. P. G. Loch, “Mobilization of heavy metals as affected by pH and redox conditions,” in *Biogeochemistry of Pollutants in Soils and Sediments: Risk Assessment of Delayed and Non-Linear Responses*, W. Salomons and W. M. Stigliani, Eds. Berlin, Heidelberg: Springer, 1995, pp. 87–102.
- [19] M. L. Peterson, G. E. Brown, G. A. Parks, and C. L. Stein, “Differential redox and sorption of Cr (III/VI) on natural silicate and oxide minerals: EXAFS and XANES results,” *Geochim. Cosmochim. Acta*, vol. 61, no. 16, pp. 3399–3412, Aug. 1997, doi: 10.1016/S0016-7037(97)00165-8.

- [20] G. Choppala, N. Bolan, and J. H. Park, "Chromium contamination and its risk management in complex environmental settings," in *Advances in Agronomy*, vol. 120, Elsevier, 2013, pp. 129–172.
- [21] J. Gorny, G. Billon, C. Noiriél, D. Dumoulin, L. Lesven, and B. Madé, "Chromium behavior in aquatic environments: a review," *Environ. Rev.*, vol. 24, no. 4, pp. 503–516, Dec. 2016, doi: 10.1139/er-2016-0012.
- [22] J. Wu, J. Zhang, and C. Xiao, "Focus on factors affecting pH, flow of Cr and transformation between Cr(VI) and Cr(III) in the soil with different electrolytes," *Electrochimica Acta*, vol. 211, pp. 652–662, Sep. 2016, doi: 10.1016/j.electacta.2016.06.048.
- [23] J. E. Johnson, S. M. Webb, C. Ma, and W. W. Fischer, "Manganese mineralogy and diagenesis in the sedimentary rock record," *Geochim. Cosmochim. Acta*, vol. 173, pp. 210–231, Jan. 2016, doi: 10.1016/j.gca.2015.10.027.
- [24] X. H. Feng, L. M. Zhai, W. F. Tan, W. Zhao, F. Liu, and J. Z. He, "The controlling effect of pH on oxidation of Cr(III) by manganese oxide minerals," *J. Colloid Interface Sci.*, vol. 298, no. 1, pp. 258–266, Jun. 2006, doi: 10.1016/j.jcis.2005.12.012.
- [25] I. J. Buerge and S. J. Hug, "Kinetics and pH Dependence of Chromium(VI) Reduction by Iron(II)," *Environ. Sci. Technol.*, vol. 31, no. 5, pp. 1426–1432, May 1997, doi: 10.1021/es960672i.
- [26] L. Di Palma, M. T. Gueye, and E. Petrucci, "Hexavalent chromium reduction in contaminated soil: A comparison between ferrous sulphate and nanoscale zero-valent iron," *J. Hazard. Mater.*, vol. 281, pp. 70–76, Jan. 2015, doi: 10.1016/j.jhazmat.2014.07.058.
- [27] L. E. Eary and Dhanpat. Rai, "Chromate removal from aqueous wastes by reduction with ferrous ion," *Environ. Sci. Technol.*, vol. 22, no. 8, pp. 972–977, Aug. 1988, doi: 10.1021/es00173a018.
- [28] J. D. Hem, "Reactions of metal ions at surfaces of hydrous iron oxide," *Geochim. Cosmochim. Acta*, vol. 41, no. 4, pp. 527–538, Apr. 1977, doi: 10.1016/0016-7037(77)90290-3.

- [29] H.-B. Kim, J.-G. Kim, S.-H. Kim, E. E. Kwon, and K. Baek, "Consecutive reduction of Cr(VI) by Fe(II) formed through photo-reaction of iron-dissolved organic matter originated from biochar," *Environ. Pollut.*, vol. 253, pp. 231–238, Oct. 2019, doi: 10.1016/j.envpol.2019.07.026.
- [30] K. H. Shah *et al.*, "Native and magnetic oxide nanoparticles (Fe<sub>3</sub>O<sub>4</sub>) impregnated bentonite clays as economic adsorbents for Cr(III) removal," *J. Solut. Chem.*, vol. 48, no. 11, pp. 1640–1656, Dec. 2019, doi: 10.1007/s10953-019-00912-z.
- [31] R. A. Griffin, A. K. Au, and R. R. Frost, "Effect of pH on adsorption of chromium from landfill-leachate by clay minerals," *J. Environ. Sci. Health Part Environ. Sci. Eng.*, vol. 12, no. 8, pp. 431–449, Jan. 1977, doi: 10.1080/10934527709374769.
- [32] M. Hua, S. Zhang, B. Pan, W. Zhang, L. Lv, and Q. Zhang, "Heavy metal removal from water/wastewater by nanosized metal oxides: A review," *J. Hazard. Mater.*, vol. 211–212, pp. 317–331, Apr. 2012, doi: 10.1016/j.jhazmat.2011.10.016.
- [33] K. Mesuere and W. Fish, "Chromate and oxalate adsorption on goethite. 2. Surface complexation modeling of competitive adsorption," *Environ. Sci. Technol.*, vol. 26, no. 12, pp. 2365–2370, Dec. 1992, doi: 10.1021/es00036a005.
- [34] A. B. Mukherjee, "Chromium in the environment of Finland," *Sci. Total Environ.*, vol. 217, no. 1, pp. 9–19, Jun. 1998, doi: 10.1016/S0048-9697(98)00163-6.
- [35] B. M. Sass and D. Rai, "Solubility of amorphous chromium(III)-iron(III) hydroxide solid solutions," *Inorg. Chem.*, vol. 26, no. 14, pp. 2228–2232, Jul. 1987, doi: 10.1021/ic00261a013.
- [36] R. Mattuck and N. P. Nikolaidis, "Chromium mobility in freshwater wetlands," *J. Contam. Hydrol.*, vol. 23, no. 3, pp. 213–232, Jul. 1996, doi: 10.1016/0169-7722(95)00097-6.
- [37] G. Godgul and K. C. Sahu, "Chromium contamination from chromite mine," *Environ. Geol.*, vol. 25, no. 4, pp. 251–257, Jun. 1995, doi: 10.1007/BF00766754.
- [38] J. Robles-Camacho and M. A. Armienta, "Natural chromium contamination of groundwater at León Valley, México," *J. Geochem. Explor.*, vol. 68, no. 3, pp. 167–181, Apr. 2000, doi: 10.1016/S0375-6742(99)00083-7.

- [39] R. Saha, R. Nandi, and B. Saha, "Sources and toxicity of hexavalent chromium," *J. Coord. Chem.*, vol. 64, no. 10, pp. 1782–1806, May 2011, doi: 10.1080/00958972.2011.583646.
- [40] Burke T, Fagliano J, Goldoft M, Hazen R E, Iglewicz R, and McKee T, "Chromite ore processing residue in Hudson County, New Jersey.," *Environ. Health Perspect.*, vol. 92, pp. 131–137, May 1991, doi: 10.1289/ehp.9192131.
- [41] C. P. Jordão, J. L. Pereira, and G. N. Jham, "Chromium contamination in sediment, vegetation and fish caused by tanneries in the State of Minas Gerais, Brazil," *Sci. Total Environ.*, vol. 207, no. 1, pp. 1–11, Nov. 1997, doi: 10.1016/S0048-9697(97)00232-5.
- [42] S. G. Sturges, P. McBeth, and R. C. Pratt, "Performance of soil flushing and groundwater extraction at the United Chrome Superfund site," *J. Hazard. Mater.*, vol. 29, no. 1, pp. 59–78, Dec. 1991, doi: 10.1016/0304-3894(91)87074-C.
- [43] Z. Stępniewska and K. Bucior, "Chromium contamination of soils, waters, and plants in the vicinity of a tannery waste lagoon," *Environ. Geochem. Health*, vol. 23, no. 3, pp. 241–245, Sep. 2001, doi: 10.1023/A:1012247230682.
- [44] A. Zahoor and A. Rehman, "Isolation of Cr(VI) reducing bacteria from industrial effluents and their potential use in bioremediation of chromium containing wastewater," *J. Environ. Sci.*, vol. 21, no. 6, pp. 814–820, Jan. 2009, doi: 10.1016/S1001-0742(08)62346-3.
- [45] W. Mertz, "Chromium in human nutrition: A review," *J. Nutr.*, vol. 123, no. 4, pp. 626–633, Apr. 1993, doi: 10.1093/jn/123.4.626.
- [46] R. A. Anderson, "Chromium as an essential nutrient for humans," *Regul. Toxicol. Pharmacol.*, vol. 26, no. 1, pp. S35–S41, Aug. 1997, doi: 10.1006/rtph.1997.1136.
- [47] A. Zhitkovich, "Importance of chromium–DNA adducts in mutagenicity and toxicity of chromium(VI)," *Chem. Res. Toxicol.*, vol. 18, no. 1, pp. 3–11, Jan. 2005, doi: 10.1021/tx049774+.
- [48] C.-H. Tseng, C. Lei, and Y.-C. Chen, "Evaluating the health costs of oral hexavalent chromium exposure from water pollution: A case study in Taiwan," *J. Clean. Prod.*, vol. 172, pp. 819–826, Jan. 2018, doi: 10.1016/j.jclepro.2017.10.177.

- [49] G. Quievryn, E. Peterson, J. Messer, and A. Zhitkovich, "Genotoxicity and mutagenicity of chromium(VI)/ascorbate-generated DNA adducts in human and bacterial cells," *Biochemistry*, vol. 42, no. 4, pp. 1062–1070, Feb. 2003, doi: 10.1021/bi0271547.
- [50] G. Quievryn, J. Messer, and A. Zhitkovich, "Carcinogenic chromium(VI) induces cross-linking of vitamin C to DNA in vitro and in human lung A549 cells," *Biochemistry*, vol. 41, no. 9, pp. 3156–3167, Mar. 2002, doi: 10.1021/bi011942z.
- [51] P. A. Lay and A. Levina, "Activation of molecular oxygen during the reactions of chromium(VI/V/IV) with biological reductants: Implications for chromium-induced genotoxicities<sup>1</sup>," *J. Am. Chem. Soc.*, vol. 120, no. 27, pp. 6704–6714, Jun. 1998, doi: 10.1021/ja974240z.
- [52] J. D. Zhang and X. L. Li, "Chromium pollution of soil and water in Jinzhou," *Zhonghua Yu Fang Yi Xue Za Zhi*, vol. 21, no. 5, pp. 262–264, Sep. 1987.
- [53] C. E. Barrera-Díaz, V. Lugo-Lugo, and B. Bilyeu, "A review of chemical, electrochemical and biological methods for aqueous Cr(VI) reduction," *J. Hazard. Mater.*, vol. 223–224, pp. 1–12, Jul. 2012, doi: 10.1016/j.jhazmat.2012.04.054.
- [54] M. J. Alowitz and M. M. Scherer, "Kinetics of nitrate, nitrite, and Cr(VI) reduction by iron metal," *Environ. Sci. Technol.*, vol. 36, no. 3, pp. 299–306, Feb. 2002, doi: 10.1021/es011000h.
- [55] J. B. Fein, D. A. Fowle, J. Cahill, K. Kemner, M. Boyanov, and B. Bunker, "Nonmetabolic reduction of Cr(VI) by bacterial surfaces under nutrient-absent conditions," *Geomicrobiol. J.*, vol. 19, no. 3, pp. 369–382, May 2002, doi: 10.1080/01490450290098423.
- [56] R. M. Powell, R. W. Puls, S. K. Hightower, and D. A. Sabatini, "Coupled iron corrosion and chromate reduction: Mechanisms for subsurface remediation," *Environ. Sci. Technol.*, vol. 29, no. 8, pp. 1913–1922, Aug. 1995, doi: 10.1021/es00008a008.
- [57] S. M. Ponder, J. G. Darab, and T. E. Mallouk, "Remediation of Cr(VI) and Pb(II) aqueous solutions using supported, nanoscale zero-valent iron," *Environ. Sci. Technol.*, vol. 34, no. 12, pp. 2564–2569, Jun. 2000, doi: 10.1021/es9911420.

- [58] X. Cheng *et al.*, “Electrochemical behaviour of chromium in acid solutions with H<sub>2</sub>S,” *Corros. Sci.*, vol. 41, no. 4, pp. 773–788, Apr. 1999, doi: 10.1016/S0010-938X(98)00150-4.
- [59] H. Shen and Y. T. Wang, “Characterization of enzymatic reduction of hexavalent chromium by *Escherichia coli* ATCC 33456,” *Appl. Environ. Microbiol.*, vol. 59, no. 11, pp. 3771–3777, Nov. 1993.
- [60] C. Cervantes *et al.*, “Interactions of chromium with microorganisms and plants,” *FEMS Microbiol. Rev.*, vol. 25, no. 3, pp. 335–347, May 2001, doi: 10.1111/j.1574-6976.2001.tb00581.x.
- [61] S.-Y. Kang, J.-U. Lee, and K.-W. Kim, “Biosorption of Cr(III) and Cr(VI) onto the cell surface of *Pseudomonas aeruginosa*,” *Biochem. Eng. J.*, vol. 36, no. 1, pp. 54–58, Aug. 2007, doi: 10.1016/j.bej.2006.06.005.
- [62] M. X. Loukidou, A. I. Zouboulis, T. D. Karapantsios, and K. A. Matis, “Equilibrium and kinetic modeling of chromium(VI) biosorption by *Aeromonas caviae*,” *Colloids Surf. Physicochem. Eng. Asp.*, vol. 242, no. 1–3, pp. 93–104, Aug. 2004, doi: 10.1016/j.colsurfa.2004.03.030.
- [63] N. Sapari, A. Idris, and N. H. Ab. Hamid, “Total removal of heavy metal from mixed plating rinse wastewater,” *Desalination*, vol. 106, no. 1, pp. 419–422, Aug. 1996, doi: 10.1016/S0011-9164(96)00139-7.
- [64] S. H. Lin and C. D. Kiang, “Chromic acid recovery from waste acid solution by an ion exchange process: equilibrium and column ion exchange modeling,” *Chem. Eng. J.*, vol. 92, no. 1, pp. 193–199, Apr. 2003, doi: 10.1016/S1385-8947(02)00140-7.
- [65] N. Kabay *et al.*, “Packed column study of the sorption of hexavalent chromium by novel solvent impregnated resins containing aliquat 336: Effect of chloride and sulfate ions,” *React. Funct. Polym.*, vol. 64, no. 2, pp. 75–82, Aug. 2005, doi: 10.1016/j.reactfunctpolym.2005.05.002.
- [66] J. Sánchez and B. L. Rivas, “Cationic hydrophilic polymers coupled to ultrafiltration membranes to remove chromium (VI) from aqueous solution,” *Desalination*, vol. 279, no. 1, pp. 338–343, Sep. 2011, doi: 10.1016/j.desal.2011.06.029.

- [67] S. Nosrati, N. S. Jayakumar, and M. A. Hashim, "Extraction performance of chromium (VI) with emulsion liquid membrane by Cyanex 923 as carrier using response surface methodology," *Desalination*, vol. 266, no. 1, pp. 286–290, Jan. 2011, doi: 10.1016/j.desal.2010.08.023.
- [68] M. Soylak, U. Divrikli, S. Saracoglu, and L. Elci, "Membrane filtration – atomic absorption spectrometry combination for copper, cobalt, cadmium, lead and chromium in environmental samples," *Environ. Monit. Assess.*, vol. 127, no. 1, pp. 169–176, Apr. 2007, doi: 10.1007/s10661-006-9271-0.
- [69] G.-R. Xu, J.-N. Wang, and C.-J. Li, "Preparation of hierarchically nanofibrous membrane and its high adaptability in hexavalent chromium removal from water," *Chem. Eng. J.*, vol. 198–199, pp. 310–317, Aug. 2012, doi: 10.1016/j.cej.2012.05.104.
- [70] R. Yang *et al.*, "Thiol-modified cellulose nanofibrous composite membranes for chromium (VI) and lead (II) adsorption," *Polymer*, vol. 55, no. 5, pp. 1167–1176, Mar. 2014, doi: 10.1016/j.polymer.2014.01.043.
- [71] Yu. S. Dzyazko, A. Mahmoud, F. Lapique, and V. N. Belyakov, "Cr(VI) transport through ceramic ion-exchange membranes for treatment of industrial wastewaters," *J. Appl. Electrochem.*, vol. 37, no. 2, pp. 209–217, Feb. 2007, doi: 10.1007/s10800-006-9243-7.
- [72] J. Bohdziewicz, "Removal of chromium ions (VI) from underground water in the hybrid complexation-ultrafiltration process," *Desalination*, vol. 129, no. 3, pp. 227–235, Aug. 2000, doi: 10.1016/S0011-9164(00)00063-1.
- [73] D. Mohan and C. U. Pittman Jr., "Activated carbons and low cost adsorbents for remediation of tri- and hexavalent chromium from water," *J. Hazard. Mater.*, vol. 137, no. 2, pp. 762–811, Sep. 2006, doi: 10.1016/j.jhazmat.2006.06.060.
- [74] S. Kuppusamy, P. Thavamani, M. Megharaj, K. Venkateswarlu, Y. B. Lee, and R. Naidu, "Potential of *Melaleuca diosmifolia* leaf as a low-cost adsorbent for hexavalent chromium removal from contaminated water bodies," *Process Saf. Environ. Prot.*, vol. 100, pp. 173–182, Mar. 2016, doi: 10.1016/j.psep.2016.01.009.

- [75] M. Owlad, M. K. Aroua, W. A. W. Daud, and S. Baroutian, "Removal of hexavalent chromium-contaminated water and wastewater: A review," *Water. Air. Soil Pollut.*, vol. 200, no. 1–4, pp. 59–77, Jun. 2009, doi: 10.1007/s11270-008-9893-7.
- [76] D. Pradhan, L. B. Sukla, M. Sawyer, and P. K. S. M. Rahman, "Recent bioreduction of hexavalent chromium in wastewater treatment: A review," *J. Ind. Eng. Chem.*, vol. 55, pp. 1–20, Nov. 2017, doi: 10.1016/j.jiec.2017.06.040.
- [77] M. Pérez-Candela, JoséM. Martín-Martínez, and R. Torregrosa-Maciá, "Chromium(VI) removal with activated carbons," *Water Res.*, vol. 29, no. 9, pp. 2174–2180, Sep. 1995, doi: 10.1016/0043-1354(95)00035-J.
- [78] A. S. Thajeel, "Modeling and optimization of adsorption of heavy metal ions onto local activated carbon," *Aquat. Sci. Technol.*, vol. 1, no. 2, pp. 108–134, Jun. 2013, doi: 10.5296/ast.v1i2.3890.
- [79] G. M. Ayoub, A. Damaj, H. El-Rassy, M. Al-Hindi, and R. M. Zayyat, "Equilibrium and kinetic studies on adsorption of chromium(VI) onto pine-needle-generated activated carbon," *SN Appl. Sci.*, vol. 1, no. 12, p. 1562, Dec. 2019, doi: 10.1007/s42452-019-1617-7.
- [80] J. Fang, Z. Gu, D. Gang, C. Liu, E. S. Ilton, and B. Deng, "Cr(VI) removal from aqueous solution by activated carbon coated with quaternized poly(4-vinylpyridine)," *Environ. Sci. Technol.*, vol. 41, no. 13, pp. 4748–4753, Jul. 2007, doi: 10.1021/es061969b.
- [81] S. Pap *et al.*, "Evaluation of the adsorption potential of eco-friendly activated carbon prepared from cherry kernels for the removal of  $Pb^{2+}$ ,  $Cd^{2+}$  and  $Ni^{2+}$  from aqueous wastes," *J. Environ. Manage.*, vol. 184, pp. 297–306, Dec. 2016, doi: 10.1016/j.jenvman.2016.09.089.
- [82] J. Acharya, J. N. Sahu, B. K. Sahoo, C. R. Mohanty, and B. C. Meikap, "Removal of chromium(VI) from wastewater by activated carbon developed from Tamarind wood activated with zinc chloride," *Chem. Eng. J.*, vol. 150, no. 1, pp. 25–39, Jul. 2009, doi: 10.1016/j.cej.2008.11.035.
- [83] N. F. Fahim, B. N. Barsoum, A. E. Eid, and M. S. Khalil, "Removal of chromium(III) from tannery wastewater using activated carbon from sugar industrial waste," *J. Hazard. Mater.*, vol. 136, no. 2, pp. 303–309, Aug. 2006, doi: 10.1016/j.jhazmat.2005.12.014.

- [84] M. Owlad, M. K. Aroua, and W. M. A. Wan Daud, "Hexavalent chromium adsorption on impregnated palm shell activated carbon with polyethyleneimine," *Bioresour. Technol.*, vol. 101, no. 14, pp. 5098–5103, Jul. 2010, doi: 10.1016/j.biortech.2010.01.135.
- [85] M. K. Rai *et al.*, "Removal of hexavalent chromium Cr (VI) using activated carbon prepared from mango kernel activated with H<sub>3</sub>PO<sub>4</sub>," *Resour.-Effic. Technol.*, vol. 2, pp. S63–S70, Dec. 2016, doi: 10.1016/j.reffit.2016.11.011.
- [86] N. K. Hamadi, X. D. Chen, M. M. Farid, and M. G. Q. Lu, "Adsorption kinetics for the removal of chromium(VI) from aqueous solution by adsorbents derived from used tyres and sawdust," *Chem. Eng. J.*, vol. 84, no. 2, pp. 95–105, Oct. 2001, doi: 10.1016/S1385-8947(01)00194-2.
- [87] S.-J. Park and W.-Y. Jung, "Adsorption behaviors of chromium(III) and (VI) on electroless Cu-plated activated carbon fibers," *J. Colloid Interface Sci.*, vol. 243, no. 2, pp. 316–320, Nov. 2001, doi: 10.1006/jcis.2001.7910.
- [88] S. Ricordel, S. Taha, I. Cisse, and G. Dorange, "Heavy metals removal by adsorption onto peanut husks carbon: characterization, kinetic study and modeling," *Sep. Purif. Technol.*, vol. 24, no. 3, pp. 389–401, Sep. 2001, doi: 10.1016/S1383-5866(01)00139-3.
- [89] V. M. Boddu, K. Abburi, J. L. Talbott, and E. D. Smith, "Removal of hexavalent chromium from wastewater using a new composite chitosan biosorbent," *Environ. Sci. Technol.*, vol. 37, no. 19, pp. 4449–4456, Oct. 2003, doi: 10.1021/es021013a.
- [90] Y.-Y. Deng, X.-F. Xiao, D. Wang, B. Han, Y. Gao, and J.-L. Xue, "Adsorption of Cr(VI) from aqueous solution by ethylenediaminetetraacetic acid-chitosan-modified metal-organic framework," *J. Nanosci. Nanotechnol.*, vol. 20, no. 3, pp. 1660–1669, Mar. 2020, doi: 10.1166/jnn.2020.17157.
- [91] E. Rosales, J. Meijide, T. Tavares, M. Pazos, and M. A. Sanromán, "Grapefruit peelings as a promising biosorbent for the removal of leather dyes and hexavalent chromium," *Process Saf. Environ. Prot.*, vol. 101, pp. 61–71, May 2016, doi: 10.1016/j.psep.2016.03.006.

- [92] R. Saha *et al.*, “Application of Chattim tree (devil tree, *Alstonia scholaris*) saw dust as a biosorbent for removal of hexavalent chromium from contaminated water,” *Can. J. Chem. Eng.*, vol. 91, no. 5, pp. 814–821, 2013, doi: 10.1002/cjce.21703.
- [93] G.-R. R. Bernardo, R.-M. J. Rene, and A.-D. la T. Ma. Catalina, “Chromium (III) uptake by agro-waste biosorbents: Chemical characterization, sorption–desorption studies, and mechanism,” *J. Hazard. Mater.*, vol. 170, no. 2, pp. 845–854, Oct. 2009, doi: 10.1016/j.jhazmat.2009.05.046.
- [94] D. Kratochvil, P. Pimentel, and B. Volesky, “Removal of trivalent and hexavalent chromium by seaweed biosorbent,” *Environ. Sci. Technol.*, vol. 32, no. 18, pp. 2693–2698, Sep. 1998, doi: 10.1021/es971073u.
- [95] N. K. Akunwa, M. N. Muhammad, and J. C. Akunna, “Treatment of metal-contaminated wastewater: A comparison of low-cost biosorbents,” *J. Environ. Manage.*, vol. 146, pp. 517–523, Dec. 2014, doi: 10.1016/j.jenvman.2014.08.014.
- [96] V. A. Spinelli, M. C. M. Laranjeira, and V. T. Fávere, “Preparation and characterization of quaternary chitosan salt: adsorption equilibrium of chromium(VI) ion,” *React. Funct. Polym.*, vol. 61, no. 3, pp. 347–352, Nov. 2004, doi: 10.1016/j.reactfunctpolym.2004.06.010.
- [97] A. S. K. Kumar, S. Kalidhasan, V. Rajesh, and N. Rajesh, “Application of cellulose-clay composite biosorbent toward the effective adsorption and removal of chromium from industrial wastewater,” *Ind. Eng. Chem. Res.*, vol. 51, no. 1, pp. 58–69, Jan. 2012, doi: 10.1021/ie201349h.
- [98] S. Hena, “Removal of chromium hexavalent ion from aqueous solutions using biopolymer chitosan coated with poly 3-methyl thiophene polymer,” *J. Hazard. Mater.*, vol. 181, no. 1, pp. 474–479, Sep. 2010, doi: 10.1016/j.jhazmat.2010.05.037.
- [99] V. Dimos, K. J. Haralambous, and S. Malamis, “A review on the recent studies for chromium species adsorption on raw and modified natural minerals,” *Crit. Rev. Environ. Sci. Technol.*, vol. 42, no. 19, pp. 1977–2016, Oct. 2012, doi: 10.1080/10643389.2011.574102.

- [100] M. Gürü, D. Venedik, and A. Murathan, "Removal of trivalent chromium from water using low-cost natural diatomite," *J. Hazard. Mater.*, vol. 160, no. 2, pp. 318–323, Dec. 2008, doi: 10.1016/j.jhazmat.2008.03.002.
- [101] A. B. Albadarin, C. Mangwandi, A. H. Al-Muhtaseb, G. M. Walker, S. J. Allen, and M. N. M. Ahmad, "Kinetic and thermodynamics of chromium ions adsorption onto low-cost dolomite adsorbent," *Chem. Eng. J.*, vol. 179, pp. 193–202, Jan. 2012, doi: 10.1016/j.cej.2011.10.080.
- [102] S. A. Khan, Riaz-ur-Rehman, and M. A. Khan, "Adsorption of chromium (III), chromium (VI) and silver (I) on bentonite," *Waste Manag.*, vol. 15, no. 4, pp. 271–282, Jan. 1995, doi: 10.1016/0956-053X(95)00025-U.
- [103] A. A. El-Bayaa, N. A. Badawy, and E. A. AlKhalik, "Effect of ionic strength on the adsorption of copper and chromium ions by vermiculite pure clay mineral," *J. Hazard. Mater.*, vol. 170, no. 2, pp. 1204–1209, Oct. 2009, doi: 10.1016/j.jhazmat.2009.05.100.
- [104] S. S. Tahir and R. Naseem, "Removal of Cr(III) from tannery wastewater by adsorption onto bentonite clay," *Sep. Purif. Technol.*, vol. 53, no. 3, pp. 312–321, Mar. 2007, doi: 10.1016/j.seppur.2006.08.008.
- [105] M. C. Brum, J. L. Capitaneo, and J. F. Oliveira, "Removal of hexavalent chromium from water by adsorption onto surfactant modified montmorillonite," *Miner. Eng.*, vol. 23, no. 3, pp. 270–272, Feb. 2010, doi: 10.1016/j.mineng.2009.10.008.
- [106] X. Jin, M. Jiang, J. Du, and Z. Chen, "Removal of Cr(VI) from aqueous solution by surfactant-modified kaolinite," *J. Ind. Eng. Chem.*, vol. 20, no. 5, pp. 3025–3032, Sep. 2014, doi: 10.1016/j.jiec.2013.11.038.
- [107] J. Hu, G. Chen, and I. M. C. Lo, "Removal and recovery of Cr(VI) from wastewater by maghemite nanoparticles," *Water Res.*, vol. 39, no. 18, pp. 4528–4536, Nov. 2005, doi: 10.1016/j.watres.2005.05.051.

- [108] M. G. da Fonseca, M. M. de Oliveira, and L. N. H. Arakaki, "Removal of cadmium, zinc, manganese and chromium cations from aqueous solution by a clay mineral," *J. Hazard. Mater.*, vol. 137, no. 1, pp. 288–292, Sep. 2006, doi: 10.1016/j.jhazmat.2006.02.001.
- [109] K. Babaeivelni and A. P. Khodadoust, "Removal of arsenic from water using manganese (III) oxide: Adsorption of As(III) and As(V)," *J. Environ. Sci. Health Part A*, vol. 51, no. 4, pp. 277–288, Mar. 2016, doi: 10.1080/10934529.2015.1109382.
- [110] Bajpai Sanjeev and Chaudhuri Malay, "Removal of arsenic from ground water by manganese dioxide-coated sand," *J. Environ. Eng.*, vol. 125, no. 8, pp. 782–784, Aug. 1999, doi: 10.1061/(ASCE)0733-9372(1999)125:8(782).
- [111] F. A. Al-Sagheer and M. I. Zaki, "Synthesis and surface characterization of todorokite-type microporous manganese oxides: implications for shape-selective oxidation catalysts," *Microporous Mesoporous Mater.*, vol. 67, no. 1, pp. 43–52, Jan. 2004, doi: 10.1016/j.micromeso.2003.10.005.
- [112] R. G. Burns, "The uptake of cobalt into ferromanganese nodules, soils, and synthetic manganese (IV) oxides," *Geochim. Cosmochim. Acta*, vol. 40, no. 1, pp. 95–102, Jan. 1976, doi: 10.1016/0016-7037(76)90197-6.
- [113] R. Rao. Gadde and H. A. Laitinen, "Heavy metal adsorption by hydrous iron and manganese oxides," *Anal. Chem.*, vol. 46, no. 13, pp. 2022–2026, Nov. 1974, doi: 10.1021/ac60349a004.
- [114] W. Xu, H. Lan, H. Wang, H. Liu, and J. Qu, "Comparing the adsorption behaviors of Cd, Cu and Pb from water onto Fe-Mn binary oxide, MnO<sub>2</sub> and FeOOH," *Front. Environ. Sci. Eng.*, vol. 9, no. 3, pp. 385–393, Jun. 2015, doi: 10.1007/s11783-014-0648-y.
- [115] S. D. Rachmawati, C. Tizaoui, and N. Hilal, "Manganese coated sand for copper (II) removal from water in batch mode," *Water*, vol. 5, no. 4, pp. 1487–1501, Dec. 2013, doi: 10.3390/w5041487.

- [116] S. M. Maliyekkal, L. Philip, and T. Pradeep, "As(III) removal from drinking water using manganese oxide-coated-alumina: Performance evaluation and mechanistic details of surface binding," *Chem. Eng. J.*, vol. 153, no. 1, pp. 101–107, Nov. 2009, doi: 10.1016/j.cej.2009.06.026.
- [117] S. M. Maliyekkal, A. K. Sharma, and L. Philip, "Manganese-oxide-coated alumina: A promising sorbent for defluoridation of water," *Water Res.*, vol. 40, no. 19, pp. 3497–3506, Nov. 2006, doi: 10.1016/j.watres.2006.08.007.
- [118] E. Eren, B. Afsin, and Y. Onal, "Removal of lead ions by acid activated and manganese oxide-coated bentonite," *J. Hazard. Mater.*, vol. 161, no. 2, pp. 677–685, Jan. 2009, doi: 10.1016/j.jhazmat.2008.04.020.
- [119] N. Boujelben, J. Bouzid, Z. Elouear, and M. Feki, "Retention of nickel from aqueous solutions using iron oxide and manganese oxide coated sand: kinetic and thermodynamic studies," *Environ. Technol.*, vol. 31, no. 14, pp. 1623–1634, Dec. 2010, doi: 10.1080/09593330.2010.482148.
- [120] S. A. Chaudhry, T. A. Khan, and I. Ali, "Adsorptive removal of Pb(II) and Zn(II) from water onto manganese oxide-coated sand: Isotherm, thermodynamic and kinetic studies," *Egypt. J. Basic Appl. Sci.*, vol. 3, no. 3, pp. 287–300, Sep. 2016, doi: 10.1016/j.ejbas.2016.06.002.
- [121] R. Han, W. Zou, Y. Wang, and L. Zhu, "Removal of uranium(VI) from aqueous solutions by manganese oxide coated zeolite: discussion of adsorption isotherms and pH effect," *J. Environ. Radioact.*, vol. 93, no. 3, pp. 127–143, Jan. 2007, doi: 10.1016/j.jenvrad.2006.12.003.
- [122] Y.-Y. Chang, K.-H. Song, M.-R. Yu, and J.-K. Yang, "Removal of arsenic from aqueous solution by iron-coated sand and manganese-coated sand having different mineral types," *Water Sci. Technol.*, vol. 65, no. 4, pp. 683–688, Feb. 2012, doi: 10.2166/wst.2012.910.
- [123] J. Kotaś and Z. Stasicka, "Chromium occurrence in the environment and methods of its speciation," *Environ. Pollut.*, vol. 107, no. 3, pp. 263–283, Mar. 2000, doi: 10.1016/S0269-7491(99)00168-2.
- [124] S. A. Katz and H. Salem, "The toxicology of chromium with respect to its chemical speciation: A review," *J. Appl. Toxicol.*, vol. 13, no. 3, pp. 217–224, May 1993, doi: 10.1002/jat.2550130314.

- [125] I. Moffat, N. Martinova, C. Seidel, and C. M. Thompson, “Hexavalent chromium in drinking water,” *J. - AWWA*, vol. 110, no. 5, pp. E22–E35, Apr. 2018, doi: 10.1002/awwa.1044.
- [126] A. H. Smith and C. M. Steinmaus, “Health effects of arsenic and chromium in drinking water: Recent human findings,” *Annu. Rev. Public Health*, vol. 30, no. 1, pp. 107–122, Apr. 2009, doi: 10.1146/annurev.publhealth.031308.100143.
- [127] M. Yoshinaga *et al.*, “A comprehensive study including monitoring, assessment of health effects and development of a remediation method for chromium pollution,” *Chemosphere*, vol. 201, pp. 667–675, Jun. 2018, doi: 10.1016/j.chemosphere.2018.03.026.
- [128] A. Zhitkovich, “Chromium in drinking water: Sources, metabolism, and cancer risks,” *Chem. Res. Toxicol.*, vol. 24, no. 10, pp. 1617–1629, Oct. 2011, doi: 10.1021/tx200251t.
- [129] C.-H. Tseng, C. Lei, and Y.-C. Chen, “Evaluating the health costs of oral hexavalent chromium exposure from water pollution: A case study in Taiwan,” *J. Clean. Prod.*, vol. 172, pp. 819–826, Jan. 2018, doi: 10.1016/j.jclepro.2017.10.177.
- [130] C. Pellerin and S. M. Booker, “Reflections on hexavalent chromium: health hazards of an industrial heavyweight,” *Environ. Health Perspect.*, vol. 108, no. 9, Sep. 2000, doi: 10.1289/ehp.108-a402.
- [131] K. Loska and D. Wiechuła, “Application of principal component analysis for the estimation of source of heavy metal contamination in surface sediments from the Rybnik Reservoir,” *Chemosphere*, vol. 51, no. 8, pp. 723–733, Jun. 2003, doi: 10.1016/S0045-6535(03)00187-5.
- [132] R. A. Wuana and F. E. Okieimen, “Heavy metals in contaminated soils: A review of sources, chemistry, risks and best available strategies for remediation,” *ISRN Ecol.*, vol. 2011, pp. 1–20, Oct. 2011, doi: 10.5402/2011/402647.
- [133] V. Dimos, K. J. Haralambous, and S. Malamis, “A Review on the Recent Studies for Chromium Species Adsorption on Raw and Modified Natural Minerals,” *Crit. Rev. Environ. Sci. Technol.*, vol. 42, no. 19, pp. 1977–2016, Oct. 2012, doi: 10.1080/10643389.2011.574102.

- [134] D. Mohan and C. U. Pittman Jr., “Activated carbons and low cost adsorbents for remediation of tri- and hexavalent chromium from water,” *J. Hazard. Mater.*, vol. 137, no. 2, pp. 762–811, Sep. 2006, doi: 10.1016/j.jhazmat.2006.06.060.
- [135] S. Yadav, V. Srivastava, S. Banerjee, C.-H. Weng, and Y. C. Sharma, “Adsorption characteristics of modified sand for the removal of hexavalent chromium ions from aqueous solutions: Kinetic, thermodynamic and equilibrium studies,” *CATENA*, vol. 100, pp. 120–127, Jan. 2013, doi: 10.1016/j.catena.2012.08.002.
- [136] M. X. Loukidou, A. I. Zouboulis, T. D. Karapantsios, and K. A. Matis, “Equilibrium and kinetic modeling of chromium(VI) biosorption by *Aeromonas caviae*,” *Colloids Surf. Physicochem. Eng. Asp.*, vol. 242, no. 1–3, pp. 93–104, Aug. 2004, doi: 10.1016/j.colsurfa.2004.03.030.
- [137] S. Chen, J. Zhang, H. Zhang, and X. Wang, “Removal of hexavalent chromium from contaminated water by Chinese herb-extraction residues,” *Water. Air. Soil Pollut.*, vol. 228, no. 4, p. 145, Apr. 2017, doi: 10.1007/s11270-017-3329-1.
- [138] S. Kuppusamy, P. Thavamani, M. Megharaj, K. Venkateswarlu, Y. B. Lee, and R. Naidu, “Potential of *Melaleuca diosmifolia* leaf as a low-cost adsorbent for hexavalent chromium removal from contaminated water bodies,” *Process Saf. Environ. Prot.*, vol. 100, pp. 173–182, Mar. 2016, doi: 10.1016/j.psep.2016.01.009.
- [139] M. Owlad, M. K. Aroua, W. A. W. Daud, and S. Baroutian, “Removal of hexavalent chromium-contaminated water and wastewater: A review,” *Water. Air. Soil Pollut.*, vol. 200, no. 1–4, pp. 59–77, Jun. 2009, doi: 10.1007/s11270-008-9893-7.
- [140] K. Babaeivelni and A. P. Khodadoust, “Removal of arsenic from water using manganese (III) oxide: Adsorption of As(III) and As(V),” *J. Environ. Sci. Health Part A*, vol. 51, no. 4, pp. 277–288, Mar. 2016, doi: 10.1080/10934529.2015.1109382.
- [141] B. Sanjeev and C. Malay, “Removal of arsenic from ground water by manganese dioxide-coated sand,” *J. Environ. Eng.*, vol. 125, no. 8, pp. 782–784, Aug. 1999, doi: 10.1061/(ASCE)0733-9372(1999)125:8(782).

- [142] F. A. Al-Sagheer and M. I. Zaki, "Synthesis and surface characterization of todorokite-type microporous manganese oxides: implications for shape-selective oxidation catalysts," *Microporous Mesoporous Mater.*, vol. 67, no. 1, pp. 43–52, Jan. 2004, doi: 10.1016/j.micromeso.2003.10.005.
- [143] R. G. Burns, "The uptake of cobalt into ferromanganese nodules, soils, and synthetic manganese (IV) oxides," *Geochim. Cosmochim. Acta*, vol. 40, no. 1, pp. 95–102, Jan. 1976, doi: 10.1016/0016-7037(76)90197-6.
- [144] R. Rao. Gadde and H. A. Laitinen, "Heavy metal adsorption by hydrous iron and manganese oxides," *Anal. Chem.*, vol. 46, no. 13, pp. 2022–2026, Nov. 1974, doi: 10.1021/ac60349a004.
- [145] W. Xu, H. Lan, H. Wang, H. Liu, and J. Qu, "Comparing the adsorption behaviors of Cd, Cu and Pb from water onto Fe-Mn binary oxide, MnO<sub>2</sub> and FeOOH," *Front. Environ. Sci. Eng.*, vol. 9, no. 3, pp. 385–393, Jun. 2015, doi: 10.1007/s11783-014-0648-y.
- [146] S. D. Rachmawati, C. Tizaoui, and N. Hilal, "Manganese coated sand for copper (II) removal from water in batch mode," *Water*, vol. 5, no. 4, pp. 1487–1501, Dec. 2013, doi: 10.3390/w5041487.
- [147] S. M. Maliyekkal, L. Philip, and T. Pradeep, "As(III) removal from drinking water using manganese oxide-coated-alumina: Performance evaluation and mechanistic details of surface binding," *Chem. Eng. J.*, vol. 153, no. 1, pp. 101–107, Nov. 2009, doi: 10.1016/j.cej.2009.06.026.
- [148] S. M. Maliyekkal, A. K. Sharma, and L. Philip, "Manganese-oxide-coated alumina: A promising sorbent for defluoridation of water," *Water Res.*, vol. 40, no. 19, pp. 3497–3506, Nov. 2006, doi: 10.1016/j.watres.2006.08.007.
- [149] E. Eren, B. Afsin, and Y. Onal, "Removal of lead ions by acid activated and manganese oxide-coated bentonite," *J. Hazard. Mater.*, vol. 161, no. 2, pp. 677–685, Jan. 2009, doi: 10.1016/j.jhazmat.2008.04.020.

- [150] N. Boujelben, J. Bouzid, Z. Elouear, and M. Feki, "Retention of nickel from aqueous solutions using iron oxide and manganese oxide coated sand: kinetic and thermodynamic studies," *Environ. Technol.*, vol. 31, no. 14, pp. 1623–1634, Dec. 2010, doi: 10.1080/09593330.2010.482148.
- [151] S. A. Chaudhry, T. A. Khan, and I. Ali, "Adsorptive removal of Pb(II) and Zn(II) from water onto manganese oxide-coated sand: Isotherm, thermodynamic and kinetic studies," *Egypt. J. Basic Appl. Sci.*, vol. 3, no. 3, pp. 287–300, Sep. 2016, doi: 10.1016/j.ejbas.2016.06.002.
- [152] R. Han, W. Zou, Y. Wang, and L. Zhu, "Removal of uranium(VI) from aqueous solutions by manganese oxide coated zeolite: discussion of adsorption isotherms and pH effect," *J. Environ. Radioact.*, vol. 93, no. 3, pp. 127–143, Jan. 2007, doi: 10.1016/j.jenvrad.2006.12.003.
- [153] Y.-Y. Chang, K.-H. Song, M.-R. Yu, and J.-K. Yang, "Removal of arsenic from aqueous solution by iron-coated sand and manganese-coated sand having different mineral types," *Water Sci. Technol.*, vol. 65, no. 4, pp. 683–688, Feb. 2012, doi: 10.2166/wst.2012.910.
- [154] S.-L. Lo, H.-T. Jeng, and C.-H. Lai, "Characteristics and adsorption properties of iron-coated sand," *Water Sci. Technol.*, vol. 35, no. 7, pp. 63–70, Apr. 1997, doi: 10.2166/wst.1997.0261.
- [155] N. Ayawei, A. N. Ebelegi, and D. Wankasi, "Modelling and interpretation of adsorption isotherms," *J. Chem.*, vol. 2017, pp. 1–11, Sep. 2017, doi: 10.1155/2017/3039817.
- [156] Y. S. Ho, J. F. Porter, and G. McKay, "Equilibrium isotherm studies for the sorption of divalent metal ions onto peat: copper, nickel and lead single component systems," *Water. Air. Soil Pollut.*, vol. 141, no. 1, pp. 1-33, Nov. 2002, doi: 10.1016/0009-2541(85)90133-0.
- [157] K. Y. Foo and B. H. Hameed, "Insights into the modeling of adsorption isotherm systems," *Chem. Eng. J.*, vol. 156, no. 1, pp. 2–10, Jan. 2010, doi: 10.1016/j.cej.2009.09.013.
- [158] A. O. Dada, A. P. Olalekan, A. M. Olatunya, and O. Dada, "Langmuir, Freundlich, Temkin and Dubinin–Radushkevich isotherms studies of equilibrium sorption of Zn<sup>2+</sup> unto phosphoric acid modified rice husk," *IOSR J. Appl. Chem.*, vol. 3, no. 1, pp. 38–45, Nov. 2012, doi: 10.9790/5736-0313845.

- [159] K. Babaeivelni, A. P. Khodadoust, and D. Bogdan, "Adsorption and removal of arsenic (V) using crystalline manganese (II,III) oxide: Kinetics, equilibrium, effect of pH and ionic strength," *J. Environ. Sci. Health Part A*, vol. 49, no. 13, pp. 1462–1473, Nov. 2014, doi: 10.1080/10934529.2014.937160.
- [160] M. Özacar and İ. A. Şengil, "Adsorption of metal complex dyes from aqueous solutions by pine sawdust," *Bioresour. Technol.*, vol. 96, no. 7, pp. 791–795, May 2005, doi: 10.1016/j.biortech.2004.07.011.
- [161] Y.-Y. Chang, J.-W. Lim, and J.-K. Yang, "Removal of As(V) and Cr(VI) in aqueous solution by sand media simultaneously coated with Fe and Mn oxides," *J. Ind. Eng. Chem.*, vol. 18, no. 1, pp. 188–192, Jan. 2012, doi: 10.1016/j.jiec.2011.11.002.
- [162] C.-C. Kan, M. C. Aganon, C. M. Futalan, and M. L. P. Dalida, "Adsorption of  $Mn^{2+}$  from aqueous solution using Fe and Mn oxide-coated sand," *J. Environ. Sci.*, vol. 25, no. 7, pp. 1483–1491, Jul. 2013, doi: 10.1016/S1001-0742(12)60188-0.
- [163] X. Wang and Y. Qin, "Equilibrium sorption isotherms for of  $Cu^{2+}$  on rice bran," *Process Biochem.*, vol. 40, no. 2, pp. 677–680, Feb. 2005, doi: 10.1016/j.procbio.2004.01.043.
- [164] M. M. Bhutani, A. K. Mitra, and R. Kumari, "Kinetic study of Cr(VI) sorption on  $MnO_2$ ," *J. Radioanal. Nucl. Chem.*, vol. 157, no. 1, pp. 75–86, Feb. 1992, doi: 10.1007/BF02039779.
- [165] S. Mallick, S. S. Dash, and K. M. Parida, "Adsorption of hexavalent chromium on manganese nodule leached residue obtained from  $NH_3$ – $SO_2$  leaching," *J. Colloid Interface Sci.*, vol. 297, no. 2, pp. 419–425, May 2006, doi: 10.1016/j.jcis.2005.11.001.
- [166] M. Gheju, I. Balcu, and G. Mosoarca, "Removal of Cr(VI) from aqueous solutions by adsorption on  $MnO_2$ ," *J. Hazard. Mater.*, vol. 310, pp. 270–277, Jun. 2016, doi: 10.1016/j.jhazmat.2016.02.042.
- [167] C. H. Weng, J. H. Wang, and C. P. Huang, "Adsorption of Cr(VI) onto  $TiO_2$  from dilute aqueous solutions," *Water Sci. Technol.*, vol. 35, no. 7, pp. 55–62, Apr. 1997, doi: 10.2166/wst.1997.0260.

- [168] O. Ajouyed, C. Hurel, M. Ammari, L. B. Allal, and N. Marmier, "Sorption of Cr(VI) onto natural iron and aluminum (oxy)hydroxides: Effects of pH, ionic strength and initial concentration," *J. Hazard. Mater.*, vol. 174, no. 1–3, pp. 616–622, Feb. 2010, doi: 10.1016/j.jhazmat.2009.09.096.
- [169] S. A. Khan, Riaz-ur-Rehman, and M. A. Khan, "Adsorption of chromium (III), chromium (VI) and silver (I) on bentonite," *Waste Manag.*, vol. 15, no. 4, pp. 271–282, Jan. 1995, doi: 10.1016/0956-053X(95)00025-U.
- [170] S. Mor, K. Ravindra, and N. R. Bishnoi, "Adsorption of chromium from aqueous solution by activated alumina and activated charcoal," *Bioresour. Technol.*, vol. 98, no. 4, pp. 954–957, Mar. 2007, doi: 10.1016/j.biortech.2006.03.018.
- [171] S. Egodawatte, A. Datt, E. A. Burns, and S. C. Larsen, "Chemical insight into the adsorption of chromium(III) on iron oxide/mesoporous silica nanocomposites," *Langmuir*, vol. 31, no. 27, pp. 7553–7562, Jul. 2015, doi: 10.1021/acs.langmuir.5b01483.
- [172] W. Cui *et al.*, "Cr(III) adsorption by cluster formation on boehmite nanoplates in highly alkaline solution," *Environ. Sci. Technol.*, vol. 53, no. 18, pp. 11043–11055, Sep. 2019, doi: 10.1021/acs.est.9b02693.
- [173] S. Seif, S. Marofi, and S. Mahdavi, "Removal of Cr<sup>3+</sup> ion from aqueous solutions using MgO and montmorillonite nanoparticles," *Environ. Earth Sci.*, vol. 78, no. 13, p. 377, Jun. 2019, doi: 10.1007/s12665-019-8380-3.
- [174] Q. Su, B. Pan, S. Wan, W. Zhang, and L. Lv, "Use of hydrous manganese dioxide as a potential sorbent for selective removal of lead, cadmium, and zinc ions from water," *J. Colloid Interface Sci.*, vol. 349, no. 2, pp. 607–612, Sep. 2010, doi: 10.1016/j.jcis.2010.05.052.
- [175] N. K. Lazaridis and C. Charalambous, "Sorption removal of trivalent and hexavalent chromium from binary aqueous solutions by composite alginate–goethite beads," *Water Res.*, vol. 39, no. 18, pp. 4385–4396, Nov. 2005, doi: 10.1016/j.watres.2005.09.013.

- [176] Y. Niu, W. Hu, M. Guo, Y. Wang, J. Jia, and Z. Hu, "Preparation of cotton-based fibrous adsorbents for the removal of heavy metal ions," *Carbohydr. Polym.*, vol. 225, p. UNSP 115218, Dec. 2019, doi: 10.1016/j.carbpol.2019.115218.
- [177] J.-H. An and S. Dultz, "Adsorption of tannic acid on chitosan-montmorillonite as a function of pH and surface charge properties," *Appl. Clay Sci.*, vol. 36, no. 4, pp. 256–264, May 2007, doi: 10.1016/j.clay.2006.11.001.
- [178] R. Sprycha, "Electrical double layer at alumina/electrolyte interface: II. Adsorption of supporting electrolyte ions," *J. Colloid Interface Sci.*, vol. 127, no. 1, pp. 12–25, Jan. 1989, doi: 10.1016/0021-9797(89)90003-9.
- [179] R. J. Hunter, *Zeta potential in colloid science: principles and applications*. Academic Press, 2013.
- [180] P. M. Choksi and V. Y. Joshi, "Adsorption kinetic study for the removal of nickel (II) and aluminum (III) from an aqueous solution by natural adsorbents," *Desalination*, vol. 208, no. 1, pp. 216–231, Apr. 2007, doi: 10.1016/j.desal.2006.04.081.
- [181] V. Vimonses, S. Lei, B. Jin, C. W. K. Chow, and C. Saint, "Kinetic study and equilibrium isotherm analysis of Congo Red adsorption by clay materials," *Chem. Eng. J.*, vol. 148, no. 2, pp. 354–364, May 2009, doi: 10.1016/j.cej.2008.09.009.
- [182] W. Zou, R. Han, Z. Chen, Z. Jinghua, and J. Shi, "Kinetic study of adsorption of Cu(II) and Pb(II) from aqueous solutions using manganese oxide coated zeolite in batch mode," *Colloids Surf. Physicochem. Eng. Asp.*, vol. 279, no. 1, pp. 238–246, May 2006, doi: 10.1016/j.colsurfa.2006.01.008.
- [183] S. Ricordel, S. Taha, I. Cisse, and G. Dorange, "Heavy metals removal by adsorption onto peanut husks carbon: characterization, kinetic study and modeling," *Sep. Purif. Technol.*, vol. 24, no. 3, pp. 389–401, Sep. 2001, doi: 10.1016/S1383-5866(01)00139-3.
- [184] S. Pap *et al.*, "Evaluation of the adsorption potential of eco-friendly activated carbon prepared from cherry kernels for the removal of Pb<sup>2+</sup>, Cd<sup>2+</sup> and Ni<sup>2+</sup> from aqueous wastes," *J. Environ. Manage.*, vol. 184, pp. 297–306, Dec. 2016, doi: 10.1016/j.jenvman.2016.09.089.

- [185] H. Yuh-Shan, "Citation review of Lagergren kinetic rate equation on adsorption reactions," *Scientometrics*, vol. 59, no. 1, pp. 171–177, Jan. 2004, doi: 10.1023/B:SCIE.0000013305.99473.cf.
- [186] D. C. Sharma and C. F. Forster, "Column studies into the adsorption of chromium (VI) using sphagnum moss peat," *Bioresour. Technol.*, vol. 52, no. 3, pp. 261–267, Jan. 1995, doi: 10.1016/0960-8524(95)00035-D.
- [187] K. Henryk, C. Jarosław, and Ż. Witold, "Peat and coconut fiber as biofilters for chromium adsorption from contaminated wastewaters," *Environ. Sci. Pollut. Res.*, vol. 23, no. 1, pp. 527–534, Jan. 2016, doi: 10.1007/s11356-015-5285-x.
- [188] G. M. Ayoub, A. Damaj, H. El-Rassy, M. Al-Hindi, and R. M. Zayyat, "Equilibrium and kinetic studies on adsorption of chromium(VI) onto pine-needle-generated activated carbon," *SN Appl. Sci.*, vol. 1, no. 12, p. 1562, Dec. 2019, doi: 10.1007/s42452-019-1617-7.
- [189] W. J. Weber and J. C. Morris, "Kinetics of adsorption on carbon from solution," *J. Sanit. Eng. Div.*, vol. 89, no. 2, pp. 31–60, 1963.
- [190] Y. Ho, J. Ng, and G. McKay, "Kinetics of pollutant sorption by biosorbents: Review," *Sep. Purif. Methods*, vol. 29, no. 2, p. 189, Jun. 2000, doi: 10.1081/SPM-100100009.
- [191] F.-C. Wu, R.-L. Tseng, and R.-S. Juang, "Initial behavior of intraparticle diffusion model used in the description of adsorption kinetics," *Chem. Eng. J.*, vol. 153, no. 1, pp. 1–8, Nov. 2009, doi: 10.1016/j.cej.2009.04.042.
- [192] K.-Y. Shin, J.-Y. Hong, and J. Jang, "Heavy metal ion adsorption behavior in nitrogen-doped magnetic carbon nanoparticles: Isotherms and kinetic study," *J. Hazard. Mater.*, vol. 190, no. 1, pp. 36–44, Jun. 2011, doi: 10.1016/j.jhazmat.2010.12.102.
- [193] S. A. Chaudhry, T. A. Khan, and I. Ali, "Equilibrium, kinetic and thermodynamic studies of Cr(VI) adsorption from aqueous solution onto manganese oxide coated sand grain (MOCSG)," *J. Mol. Liq.*, vol. 236, pp. 320–330, Jun. 2017, doi: 10.1016/j.molliq.2017.04.029.

- [194] S. He *et al.*, “Competitive adsorption of Cd<sup>2+</sup>, Pb<sup>2+</sup> and Ni<sup>2+</sup> onto Fe<sup>3+</sup>-modified argillaceous limestone: Influence of pH, ionic strength and natural organic matters,” *Sci. Total Environ.*, vol. 637–638, pp. 69–78, Oct. 2018, doi: 10.1016/j.scitotenv.2018.04.300.
- [195] Y. Wen, Z. Tang, Y. Chen, and Y. Gu, “Adsorption of Cr(VI) from aqueous solutions using chitosan-coated fly ash composite as biosorbent,” *Chem. Eng. J.*, vol. 175, pp. 110–116, Nov. 2011, doi: 10.1016/j.cej.2011.09.066.
- [196] W. Qi, Y. Zhao, X. Zheng, M. Ji, and Z. Zhang, “Adsorption behavior and mechanism of Cr(VI) using Sakura waste from aqueous solution,” *Appl. Surf. Sci.*, vol. 360, pp. 470–476, Jan. 2016, doi: 10.1016/j.apsusc.2015.10.088.
- [197] J. D. Hanawalt, H. W. Rinn, and L. K. Frevel, “Chemical analysis by X-Ray Diffraction,” *Ind. Eng. Chem. Anal. Ed.*, vol. 10, no. 9, pp. 457–512, Sep. 1938, doi: 10.1021/ac50125a001.
- [198] D. R. Baer *et al.*, “Surface characterization of nanomaterials and nanoparticles: Important needs and challenging opportunities,” *J. Vac. Sci. Technol. Vac. Surf. Films Off. J. Am. Vac. Soc.*, vol. 31, no. 5, p. 50820, Sep. 2013, doi: 10.1116/1.4818423.
- [199] Ž. Mitić *et al.*, “Instrumental methods and techniques for structural and physicochemical characterization of biomaterials and bone tissue: A review,” *Mater. Sci. Eng. C*, vol. 79, pp. 930–949, Oct. 2017, doi: 10.1016/j.msec.2017.05.127.
- [200] A. Gholampour and T. Ozbakkaloglu, “A review of natural fiber composites: properties, modification and processing techniques, characterization, applications,” *J. Mater. Sci.*, vol. 55, no. 3, pp. 829–892, Jan. 2020, doi: 10.1007/s10853-019-03990-y.
- [201] J. Światowska, V. Lair, C. Pereira-Nabais, G. Cote, P. Marcus, and A. Chagnes, “XPS, XRD and SEM characterization of a thin ceria layer deposited onto graphite electrode for application in lithium-ion batteries,” *Appl. Surf. Sci.*, vol. 257, no. 21, pp. 9110–9119, Aug. 2011, doi: 10.1016/j.apsusc.2011.05.108.

- [202] G. Magnacca, G. Cerrato, C. Morterra, M. Signoretto, F. Somma, and F. Pinna, "Structural and surface characterization of pure and sulfated iron oxides," *Chem. Mater.*, vol. 15, no. 3, pp. 675–687, Feb. 2003, doi: 10.1021/cm021268n.
- [203] M. S. P. Francisco, V. R. Mastelaro, P. A. P. Nascente, and A. O. Florentino, "Activity and characterization by XPS, HR-TEM, Raman Spectroscopy, and BET Surface Area of CuO/CeO<sub>2</sub>-TiO<sub>2</sub> Catalysts," *J. Phys. Chem. B*, vol. 105, no. 43, pp. 10515–10522, Nov. 2001, doi: 10.1021/jp0109675.
- [204] J. Wang, Y. Xia, Y. Dong, R. Chen, L. Xiang, and S. Komarneni, "Defect-rich ZnO nanosheets of high surface area as an efficient visible-light photocatalyst," *Appl. Catal. B Environ.*, vol. 192, pp. 8–16, Sep. 2016, doi: 10.1016/j.apcatb.2016.03.040.
- [205] K. Kaneko and C. Ishii, "Superhigh surface area determination of microporous solids," *Colloids Surf.*, vol. 67, pp. 203–212, Nov. 1992, doi: 10.1016/0166-6622(92)80299-H.
- [206] I. Odler, "The BET-specific surface area of hydrated Portland cement and related materials," *Cem. Concr. Res.*, vol. 33, no. 12, pp. 2049–2056, Dec. 2003, doi: 10.1016/S0008-8846(03)00225-4.
- [207] S. Bates, G. Zografis, D. Engers, K. Morris, K. Crowley, and A. Newman, "Analysis of amorphous and nanocrystalline solids from their X-ray diffraction patterns," *Pharm. Res.*, vol. 23, no. 10, pp. 2333–2349, Oct. 2006, doi: 10.1007/s11095-006-9086-2.
- [208] K. Thamaphat, P. Limsuwan, and B. Ngotawornchai, "Phase Characterization of TiO<sub>2</sub> Powder by XRD and TEM," *Kasetsart J. (Nat. Sci.)*, vol. 42, pp. 357-361, 2008.
- [209] E. S. Ameh, "A review of basic crystallography and x-ray diffraction applications," *Int. J. Adv. Manuf. Technol.*, vol. 105, no. 7, pp. 3289–3302, Dec. 2019, doi: 10.1007/s00170-019-04508-1.
- [210] B. Borie, "X-Ray Diffraction in crystals, imperfect crystals, and amorphous bodies.," *J. Am. Chem. Soc.*, vol. 87, no. 1, pp. 140–141, Jan. 1965, doi: 10.1021/ja01079a041.
- [211] R. Sharma, D. P. Bisen, U. Shukla, and B. G. Sharma, "X-ray diffraction: a powerful method of characterizing nanomaterials," *Recent Res. Sci. Technol.*, vol.4, pp. 77-79, Jan. 2012.

- [212] S. D. Wolter, “Materials Science of X-Ray Diffraction,” in *X-Ray Diffraction Imaging*, 1st ed., J. Greenberg and K. Iniewski, Eds. Boca Raton : Taylor & Francis, CRC Press, 2018. |
- [213] S. A. Özen, F. Özkalaycı, U. Çevik, and R. V. Grieken, “Investigation of heavy metal distributions along 15 m soil profiles using EDXRF, XRD, SEM-EDX, and ICP-MS techniques,” *X-Ray Spectrom.*, vol. 47, no. 3, pp. 231–241, 2018, doi: 10.1002/xrs.2832.
- [214] A. Srivastava, V. K. Jain, and A. Srivastava, “SEM-EDX analysis of various sizes aerosols in Delhi India,” *Environ. Monit. Assess.*, vol. 150, no. 1, p. 405, Apr. 2008, doi: 10.1007/s10661-008-0239-0.
- [215] S. Rades *et al.*, “High-resolution imaging with SEM/T-SEM, EDX and SAM as a combined methodical approach for morphological and elemental analyses of single engineered nanoparticles,” *RSC Adv.*, vol. 4, no. 91, pp. 49577–49587, Oct. 2014, doi: 10.1039/C4RA05092D.
- [216] J. Liu, L. He, F. Dong, and K. A. Hudson-Edwards, “The role of nano-sized manganese coatings on bone char in removing arsenic(V) from solution: Implications for permeable reactive barrier technologies,” *Chemosphere*, vol. 153, pp. 146–154, Jun. 2016, doi: 10.1016/j.chemosphere.2016.03.044.
- [217] R. Grissa *et al.*, “XPS and SEM-EDX study of electrolyte nature effect on Li electrode in lithium metal batteries,” *ACS Appl. Energy Mater.*, vol. 1, no. 10, pp. 5694–5702, Oct. 2018, doi: 10.1021/acsaem.8b01256.
- [218] I. Michalak, K. Marycz, K. Basińska, and K. Chojnacka, “Using SEM-EDX and ICP-OES to investigate the elemental composition of green Macroalga *Vaucheria sessilis*,” *Sci. World J.*, vol. 2014, pp.891928, Aug. 2014, doi: 10.1155/2014/891928.
- [219] C. H. Chia, B. Gong, S. D. Joseph, C. E. Marjo, P. Munroe, and A. M. Rich, “Imaging of mineral-enriched biochar by FTIR, Raman and SEM–EDX,” *Vib. Spectrosc.*, vol. 62, pp. 248–257, Sep. 2012, doi: 10.1016/j.vibspec.2012.06.006.
- [220] V. Lynch and L. Miotti, “Introduction to micro-residues analysis: Systematic use of Scanning Electron Microscope and Energy Dispersive X-rays Spectroscopy (SEM-EDX) on Patagonian

- raw materials,” *J. Archaeol. Sci. Rep.*, vol. 16, pp. 299–308, Dec. 2017, doi: 10.1016/j.jasrep.2017.10.020.
- [221] M. Nuspl, W. Wegscheider, J. Angeli, W. Posch, and M. Mayr, “Qualitative and quantitative determination of micro-inclusions by automated SEM/EDX analysis,” *Anal. Bioanal. Chem.*, vol. 379, no. 4, pp. 640–645, Jun. 2004, doi: 10.1007/s00216-004-2528-y.
- [222] S. H. Chen, S. L. Ng, Y. L. Cheow, and A. S. Y. Ting, “A novel study based on adaptive metal tolerance behavior in fungi and SEM-EDX analysis,” *J. Hazard. Mater.*, vol. 334, pp. 132–141, Jul. 2017, doi: 10.1016/j.jhazmat.2017.04.004.
- [223] V. Murphy, S. A. M. Tofail, H. Hughes, and P. McLoughlin, “A novel study of hexavalent chromium detoxification by selected seaweed species using SEM-EDX and XPS analysis,” *Chem. Eng. J.*, vol. 148, no. 2, pp. 425–433, May 2009, doi: 10.1016/j.cej.2008.09.029.
- [224] M. Mende, D. Schwarz, C. Steinbach, R. Boldt, and S. Schwarz, “Simultaneous adsorption of heavy metal ions and anions from aqueous solutions on chitosan—Investigated by spectrophotometry and SEM-EDX analysis,” *Colloids Surf. Physicochem. Eng. Asp.*, vol. 510, pp. 275–282, Dec. 2016, doi: 10.1016/j.colsurfa.2016.08.033.
- [225] G. Greczynski and L. Hultman, “X-ray photoelectron spectroscopy: Towards reliable binding energy referencing,” *Prog. Mater. Sci.*, vol. 107, p. 100591, Jan. 2020, doi: 10.1016/j.pmatsci.2019.100591.
- [226] J. M. Cerrato, M. F. Hochella, W. R. Knocke, A. M. Dietrich, and T. F. Cromer, “Use of XPS to identify the oxidation state of Mn in solid surfaces of filtration media oxide samples from drinking water treatment plants,” *Environ. Sci. Technol.*, vol. 44, no. 15, pp. 5881–5886, Aug. 2010, doi: 10.1021/es100547q.
- [227] M. C. Biesinger, B. P. Payne, A. P. Grosvenor, L. W. M. Lau, A. R. Gerson, and R. St. C. Smart, “Resolving surface chemical states in XPS analysis of first row transition metals, oxides and hydroxides: Cr, Mn, Fe, Co and Ni,” *Appl. Surf. Sci.*, vol. 257, no. 7, pp. 2717–2730, Jan. 2011, doi: 10.1016/j.apsusc.2010.10.051.

- [228] H. W. Nesbitt and D. Banerjee, "Interpretation of XPS Mn(2p) spectra of Mn oxyhydroxides and constraints on the mechanism of MnO<sub>2</sub> precipitation," *Am. Mineral.*, vol. 83, no. 3–4, pp. 305–315, Apr. 1998, doi: 10.2138/am-1998-3-414.
- [229] N. Fiol, C. Escudero, and I. Villaescusa, "Chromium sorption and Cr(VI) reduction to Cr(III) by grape stalks and yohimbe bark," *Bioresour. Technol.*, vol. 99, no. 11, pp. 5030–5036, Jul. 2008, doi: 10.1016/j.biortech.2007.09.007.
- [230] S. Boursiquot, M. Mullet, and J.-J. Ehrhardt, "XPS study of the reaction of chromium (VI) with mackinawite (FeS)," *Surf. Interface Anal.*, vol. 34, no. 1, pp. 293–297, Sep. 2002, doi: 10.1002/sia.1303.
- [231] M. Aronniemi, J. Sainio, and J. Lahtinen, "Chemical state quantification of iron and chromium oxides using XPS: The effect of the background subtraction method," *Surf. Sci.*, vol. 578, no. 1, pp. 108–123, Mar. 2005, doi: 10.1016/j.susc.2005.01.019.
- [232] Y. Wen, Z. Tang, Y. Chen, and Y. Gu, "Adsorption of Cr(VI) from aqueous solutions using chitosan-coated fly ash composite as biosorbent," *Chem. Eng. J.*, vol. 175, pp. 110–116, Nov. 2011, doi: 10.1016/j.cej.2011.09.066.
- [233] W. Qi, Y. Zhao, X. Zheng, M. Ji, and Z. Zhang, "Adsorption behavior and mechanism of Cr(VI) using Sakura waste from aqueous solution," *Appl. Surf. Sci.*, vol. 360, pp. 470–476, Jan. 2016, doi: 10.1016/j.apsusc.2015.10.088.
- [234] L. Høiby, J. Clauson-Kaas, H. Wenzel, H. F. Larsen, B. N. Jacobsen, and O. Dalgaard, "Sustainability assessment of advanced wastewater treatment technologies," *Water Sci. Technol.*, vol. 58, no. 5, pp. 963–968, Sep. 2008, doi: 10.2166/wst.2008.450.
- [235] H. A. Alhashimi and C. B. Aktas, "Life cycle environmental and economic performance of biochar compared with activated carbon: A meta-analysis," *Resour. Conserv. Recycl.*, vol. 118, pp. 13–26, Mar. 2017, doi: 10.1016/j.resconrec.2016.11.016.

- [236] D. Mohan and C. U. Pittman Jr., “Activated carbons and low cost adsorbents for remediation of tri- and hexavalent chromium from water,” *J. Hazard. Mater.*, vol. 137, no. 2, pp. 762–811, Sep. 2006, doi: 10.1016/j.jhazmat.2006.06.060.
- [237] A. Amini, Y. Kim, J. Zhang, T. Boyer, and Q. Zhang, “Environmental and economic sustainability of ion exchange drinking water treatment for organics removal,” *J. Clean. Prod.*, vol. 104, pp. 413–421, Oct. 2015, doi: 10.1016/j.jclepro.2015.05.056.
- [238] M. Gifford, M. Chester, K. Hristovski, and P. Westerhoff, “Reducing environmental impacts of metal (hydr)oxide nanoparticle embedded anion exchange resins using anticipatory life cycle assessment,” *Environ. Sci. Nano*, vol. 3, no. 6, pp. 1351–1360, 2016, doi: 10.1039/C6EN00191B.
- [239] G. Finnveden *et al.*, “Recent developments in Life Cycle Assessment,” *J. Environ. Manage.*, vol. 91, no. 1, pp. 1–21, Oct. 2009, doi: 10.1016/j.jenvman.2009.06.018.
- [240] A. Dominguez-Ramos *et al.*, “Arsenic Removal from Natural Waters by Adsorption or Ion Exchange: An Environmental Sustainability Assessment,” *Ind. Eng. Chem. Res.*, vol. 53, no. 49, pp. 18920–18927, Dec. 2014, doi: 10.1021/ie4044345.
- [241] K. Kadirvelu and J. Goel, “Ion Exchange and Inorganic Adsorption,” in *Water Encyclopedia*, J. H. Lehr and J. Keeley, Eds. Hoboken, NJ, USA: John Wiley & Sons, Inc., 2005.
- [242] F. C. Richard and A. C. M. Bourg, “Aqueous geochemistry of chromium: A review,” *Water Res.*, vol. 25, no. 7, pp. 807–816, Jul. 1991, doi: 10.1016/0043-1354(91)90160-R.
- [243] S. Boursiquot, M. Mullet, and J.-J. Ehrhardt, “XPS study of the reaction of chromium (VI) with mackinawite (FeS),” *Surf. Interface Anal.*, vol. 34, no. 1, pp. 293–297, Sep. 2002, doi: 10.1002/sia.1303.
- [244] X. Li, P. G. Green, C. Seidel, C. Gorman, and J. L. Darby, “Meeting California’s hexavalent chromium MCL using strong base anion exchange resin,” *J. - Am. Water Works Assoc.*, vol. 108, pp. E474–E481, Sep. 2016, doi: 10.5942/jawwa.2016.108.0112.
- [245] I. J. Buerge and S. J. Hug, “Influence of mineral surfaces on chromium(VI) Reduction by Iron(II),” *Environ. Sci. Technol.*, vol. 33, no. 23, pp. 4285–4291, Dec. 1999, doi: 10.1021/es981297s.

- [246] I. J. Buerge and S. J. Hug, “Kinetics and pH dependence of chromium(VI) reduction by Iron(II),” *Environ. Sci. Technol.*, vol. 31, no. 5, pp. 1426–1432, May 1997, doi: 10.1021/es960672i.
- [247] R. R. Patterson, S. Fendorf, and M. Fendorf, “Reduction of hexavalent chromium by amorphous iron sulfide,” *Environ. Sci. Technol.*, vol. 31, no. 7, pp. 2039–2044, Jul. 1997, doi: 10.1021/es960836v.
- [248] L. Di Palma, M. T. Gueye, and E. Petrucci, “Hexavalent chromium reduction in contaminated soil: A comparison between ferrous sulphate and nanoscale zero-valent iron,” *J. Hazard. Mater.*, vol. 281, pp. 70–76, Jan. 2015, doi: 10.1016/j.jhazmat.2014.07.058.
- [249] G. Qin, M. J. McGuire, N. K. Blute, C. Seidel, and L. Fong, “Hexavalent chromium removal by reduction with ferrous sulfate, coagulation, and filtration: A pilot-scale study,” *Environ. Sci. Technol.*, vol. 39, no. 16, pp. 6321–6327, Aug. 2005, doi: 10.1021/es050486p.
- [250] J. C. Bare, “Traci.: The Tool for the reduction and assessment of chemical and other environmental impacts,” *J. Ind. Ecol.*, vol. 6, no. 3–4, pp. 49–78, Jun. 2002, doi: 10.1162/108819802766269539.
- [251] “Impact of Water Quality on Hexavalent Chromium Removal Efficiency and Cost,” *The Water Research Foundation*.
- [252] J. Zhang *et al.*, “Life cycle assessment of a microbial desalination cell for sustainable wastewater treatment and saline water desalination,” *J. Clean. Prod.*, vol. 200, pp. 900–910, Nov. 2018, doi: 10.1016/j.jclepro.2018.07.197.
- [253] H. E. Muga and J. R. Mihelcic, “Sustainability of wastewater treatment technologies,” *J. Environ. Manage.*, vol. 88, no. 3, pp. 437–447, Aug. 2008, doi: 10.1016/j.jenvman.2007.03.008.
- [254] S. Foteinis, A. G. L. Borthwick, Z. Frontistis, D. Mantzavinos, and E. Chatzisyneon, “Environmental sustainability of light-driven processes for wastewater treatment applications,” *J. Clean. Prod.*, vol. 182, pp. 8–15, May 2018, doi: 10.1016/j.jclepro.2018.02.038.

- [255] M. Schulz, M. D. Short, and G. M. Peters, “A streamlined sustainability assessment tool for improved decision making in the urban water industry,” *Integr. Environ. Assess. Manag.*, vol. 8, no. 1, pp. 183–193, Jan. 2012, doi: 10.1002/ieam.247.
- [256] A. J. Balkema, H. A. Preisig, R. Otterpohl, and F. J. D. Lambert, “Indicators for the sustainability assessment of wastewater treatment systems,” *Urban Water*, vol. 4, no. 2, pp. 153–161, Jun. 2002, doi: 10.1016/S1462-0758(02)00014-6.
- [257] Ll. Corominas *et al.*, “Life cycle assessment applied to wastewater treatment: State of the art,” *Water Res.*, vol. 47, no. 15, pp. 5480–5492, Oct. 2013, doi: 10.1016/j.watres.2013.06.049.

## APPENDIX

We design for a small water treatment plant that serves about 2500 people (150 gallons per capita per day), so we can calculate the annual flowrate

$$Q = 2500 \text{ people} * 150 \text{ gallons/capita/day} * 365 \text{ days/yr} = 136,875,000 \text{ gallons/yr}$$

The total volume of water needed to be treated annually

$$= 136,875,000 \text{ gallons/yr} * 3.785 \text{ L/gallon} = 5.2 \times 10^8 \text{ L}$$

$$\text{The amount of Cr(VI) needed to be removed} = \Delta C * V = \frac{25 \mu\text{g}}{\text{L}} * 5.2 \times 10^8 \text{ L} * 20 \text{ years} = 260 \text{ kg}$$

### 1. Adsorbent/Resin Mass Determination

Table S1. Design parameters for adsorber and ion-exchange units

Design Parameters	Adsorber	Ion-exchange
Number of units with maximum packing volume of 80 ft <sup>3</sup>	3 units, 1 unit standby	2 units, 1 unit standby
Hydraulic loading rate (ft/min)	0.26	0.5
Actual EBCT (min)	10	5
Media height (ft)	6	6

Table S2. Design parameters for reduction-coagulation-filtration unit

Design parameters	RCF unit
Reduction contact time(min)	15
Filter units	2 units, 1 unit standby for backwash period
Silica sand depth (m)	0.3
Anthracite depth (m)	0.6
Filter loading rate (gpm/ft <sup>2</sup> )	4.1

The mass and volume ratio for adsorber unit is fixed at 20g adsorbent/L water. This ratio is determined for MCS using information given in batch study. *The amount of MCS packed in adsorber units =*

$$80 \text{ ft}^3 * 2 * \frac{1538 \text{ kg}}{\text{m}^3} = 8162.2 \text{ kg}$$

$$\text{MCS will exhausted at} = \frac{8162.2\text{kg}}{\frac{20\text{g}}{\text{L}} * 5.2 \times 10^8\text{L}} * 365\text{days} = 286\text{days}$$

$$\text{The amount of MCS needed for 20 years} = 8162.2\text{kg} * 9.5 = 77540.9\text{kg} = 77.54\text{ton}$$

MCS will be used until full exhaustion in each cycle and can be regenerated for three times with 0.01N NaOH before disposed as spent adsorbent. Adsorption capacity of MCS will decrease 10% after each regeneration cycle.

Adsorption capacity of resin is given by manufacturer literature. The resin can be regenerated for five times with 1.7N NaCl before its disposal. For each cycle of regeneration, a decrease in the exchange capacity of the resin is 5%.

$$\text{The amount of resin packed in adsorber units} = 80\text{ft}^3 * \frac{750\text{kg}}{\text{m}^3} = 1699\text{kg}$$

$$\text{Resin will exhausted at} = \frac{\frac{4.02\text{g}}{\text{L}} * 2265.35\text{L}}{13\text{kg}} * 365\text{days} = 254\text{days}$$

$$\text{The amount of resin needed for 20 years} = 1699 * 10.1 = 17159.9\text{kg} = 17.16\text{ton}$$

For reduction-coagulation-filtration unit, Cr(VI) is first reduced into Cr(III) by ferrous sulfate (FeSO<sub>4</sub>), then Cr(III) and Fe(III) are subsequently precipitated by adding coagulants upstream before flowing through filtration unit. The mass ratio of Fe(II): Cr(VI) is derived from a pilot study of the RCF system as 45:1.

$$\begin{aligned} \text{The amount of ferrous sulfate needed for Cr(VI) reduction for 20 years} &= 260\text{kg} * 45 \\ &= 11700\text{kg} = 11.7\text{ton} \end{aligned}$$

$$\text{The amount of coagulant needed for 20 years} = \frac{3\text{mg}}{\text{L}} * 5.2 \times 10^8\text{L} * 20 = 31200\text{kg} = 31.2\text{ton}$$

The amount of filter media needed *for 20 years, assuming that 10% media loss per year:*

$$\begin{aligned} \text{The amount of silica sand needed} &= \left( \frac{1580\text{kg}}{m^3} * 1.98m^3 \right) + 19 * 10\% * \left( \frac{1580\text{kg}}{m^3} * 1.98m^3 \right) \\ &= 9075\text{kg} \end{aligned}$$

$$\begin{aligned} \text{The amount of anthracite needed} &= \left( \frac{850\text{kg}}{m^3} * 3.96m^3 \right) + 19 * 10\% * \left( \frac{850\text{kg}}{m^3} * 3.96m^3 \right) \\ &= 9762\text{kg} \end{aligned}$$

For the functional unit selected in this study, we can calculate all the chemical and material demands for the lifetime (20 years) of a small water treatment plant (Table S2).

Table S2. Total materials demand for the running length of 20 years

Adsorber unit	Materials	units		Total demand(kg)
Adsorbent	silica sand	kg silica sand·kg <sup>-1</sup> adsorbent	1	77540.9
	MnSO <sub>4</sub> ·H <sub>2</sub> O	kg MnSO <sub>4</sub> ·H <sub>2</sub> O·kg <sup>-1</sup> adsorbent	0.2113	16384.4
	Na <sub>2</sub> CO <sub>3</sub>	kg Na <sub>2</sub> CO <sub>3</sub> ·kg <sup>-1</sup> adsorbent	0.1325	10274.2
Regeneration	NaOH	kg NaOH·kg <sup>-1</sup> adsorbent	0.02	4652.5

IX unit	Materials	units	Total demand(kg)
Resin	A600E/9149	kg	17159.9
Regeneration	NaCl	kg NaCl·kg <sup>-1</sup> resin	16473.5

RCF unit	Materials	units	Total demand(kg)
Reduction	FeSO <sub>4</sub>	kg	11200
Coagulant	Al <sub>2</sub> (SO <sub>4</sub> ) <sub>3</sub>	kg	31200
Filter media	silica sand	kg	9075
	anthracite	kg	9762

## 2. Energy Requirements

$$\text{Power} = (K * Q * THD * \rho) / E$$

Where K is 1/550, Q is the volumetric flow rate of water (ft<sup>3</sup>/s), TDH is total dynamic head for pumping (ft),  $\rho$  is water density (lb/ft<sup>3</sup>), and E is efficiency.

Head loss are inversely proportional to particle sizes, therefore TDH for adsorber and ion-exchange unit are different despite of same media depth.

For annual operation of pumping of adsorber unit,

$$Power = \frac{\left(\frac{1}{550} * 0.6 * 12 * 62.4\right)}{0.8} = 1.02hp = \frac{0.76kJ}{s}$$

$$Energy\ requirement = \frac{0.76kJ}{s} * (24 * 3600 * 365s) = 23967360kJ = 6657.6kW \cdot h$$

For annual operation of pumping of ion-exchange unit

$$Power\ for\ pumping = \frac{\left(\frac{1}{550} * 0.6 * 9 * 62.4\right)}{0.8} = 1.02hp = \frac{0.57kJ}{s}$$

$$Energy\ requirement\ for\ pumping = \frac{0.57kJ}{s} * (24 * 3600 * 365s) = 17975520kJ \\ = 4993.2kW \cdot h$$

For annual operation of pumping of RCF filter unit,

$$Power\ for\ pumping = \frac{\left(\frac{1}{550} * 0.6 * 6 * 62.4\right)}{0.8} = 0.51hp = \frac{0.38kJ}{s}$$

$$Energy\ requirement\ for\ pumping = \frac{0.38kJ}{s} * (24 * 3600 * 365s) = 11983680kJ \\ = 3328.8kW \cdot h$$

The backwash volume is nearly 4% of total treated water,

$$\text{Power for backwash} = \frac{\left(\frac{1}{550} * 0.024 * 6 * 62.4\right)}{0.8} = 0.0408hp = \frac{0.0304kJ}{s}$$

$$\text{Energy requirement for backwash} = \frac{0.0304kJ}{s} * (24 * 3600 * 365s) = 958695kJ = 266.3kW \cdot h$$

### 3. Transportation

Table S3. Transportation calculation of chemicals and materials and their selected manufacturer

Materials	Manufacturer	Distance (miles)	Transport(tkm)
Silica sand	J R Simplot Co, 3630 Gateway Dr, Grand Forks, ND 58203	721	89973.8
MnSO <sub>4</sub> · H <sub>2</sub> O	Jost Chemical Co. 8150 Lackland St. Louis, MO 63114	319	8411.5
Na <sub>2</sub> CO <sub>3</sub>	GFS Chemicals Inc 851 McKinley Ave, Columbus, OH 43222	352	5820.2
NaOH	GFS Chemicals Inc 851 McKinley Ave, Columbus, OH 43222	352	2635.6

Materials	Manufacturer	Distance (miles)	Transport(tkm)
NaCl	GFS Chemicals Inc 851 McKinley Ave, Columbus, OH 43222	352	9332.1
Purolite A600E/9149	Purolite Corporation 3620 G Street Philadelphia, PA, USA 19134	770	21264.4

Materials	Manufacturer	Distance (miles)	Transport(tkm)
FeSO <sub>4</sub>	GAC Chemical Corporation, 34 Kidder Point Rd, Searsport, ME 04974	1190	21448
Al <sub>2</sub> (SO <sub>4</sub> ) <sub>3</sub>	GAC Chemical Corporation, 34 Kidder Point Rd, Searsport, ME 04974	1190	59748
Silica sand	J R Simplot Co, 3630 Gateway Dr, Grand Forks, ND 58203	721	10530.1
Anthracite	Lehigh Anthracite, 1233 E. Broad Street Tamaqua, PA 18252	684	10745.9

#### 4. Economic Calculations

##### 1. Capital Investment

Estimated equipment costs:

Vessel cost

For ion-exchange,

Two fix-bed columns, the estimated cost is  $(\$20,000*2) = \$40,000$

Labor and travel cost = \$17,500

For adsorber,

Three fix-bed columns, the estimated cost is  $(\$20,000*3) = \$60,000$

Labor and travel cost = \$10,000

For RCF,

One reduction tank, one coagulation tank, and one dual-media filter unit cost is

$=\$20,000+\$30,000+\$50,000= \$100,000$

Labor and travel cost = \$30,000

Detailed chemical costs for each system is tabulated in Table. S4 based on quotes from vendors.

Table.S4 Total costs of chemicals for SBA, adsorber, and RCF systems

Materials	Total demand (kg)	Unit price (\$/kg)	Total cost (\$)
Silica sand	77540.9	0.075	5,816
MnSO <sub>4</sub> ·H <sub>2</sub> O	16384.4	2	32,769
NaOH	4652.5	0.1	466
Na <sub>2</sub> CO <sub>3</sub>	10274.2	0.3	3083
A600E/9149	17159.9	50	857,995
NaCl	16473.5	0.4	6590
FeSO <sub>4</sub>	11200	1.5	16,800
Al <sub>2</sub> (SO <sub>4</sub> ) <sub>3</sub>	31200	2	62,400
Silica sand	9075	0.075	681
Anthracite	9762	0.2	1952

## 2. Estimated Engineering Costs

For ion-exchange, engineering cost = \$30,000

For adsorber, engineering cost = \$16,000

For RCF, engineering cost = \$50,000

## 3. Estimated Installation Costs

For ion-exchange, total costs (including materials, labor, and subcontractor) = \$50,000

For adsorber, total costs (including materials, labor, and subcontractor) = \$38,000

For adsorber, total costs (including materials, labor, and subcontractor) = \$60,000

The unit capital investment for adsorber = \$8,308/year, ion exchange = \$50,105/year, and RCF = \$16,092/year

#### 4. Estimated Operation and Maintenance Costs

O&M costs include media replacement and disposal, electricity consumption, and labor

Labor cost = \$6,000/year for both systems

The media replacement cost, which includes material, freight, labor, travel expense, and media profiling and disposal fees

##### 1. The waste brine is discharged to the sewer without treatment

For ion exchange, the media replacement cost = \$28,000/year

For adsorber, the media replacement cost = \$30,000/year

For RCF, the media replacement cost = \$32,000/year

The unit O&M cost for adsorber = \$36,000/year, for ion-exchange = \$34,000/year, and for RCF = \$38,000/year

##### 2. The waste brine is treated and then returned to the head of the plant or hauled off-site for disposal

For ion exchange, the media replacement cost = \$42,000/year

For adsorber, the media replacement cost = \$30,000/year

For RCF, the media replacement cost = \$50,000/year

The unit O&M cost for adsorber = \$36,000/year, for ion-exchange = \$48,000/year and for RCF = \$56,000/year

## 5. LCA Results

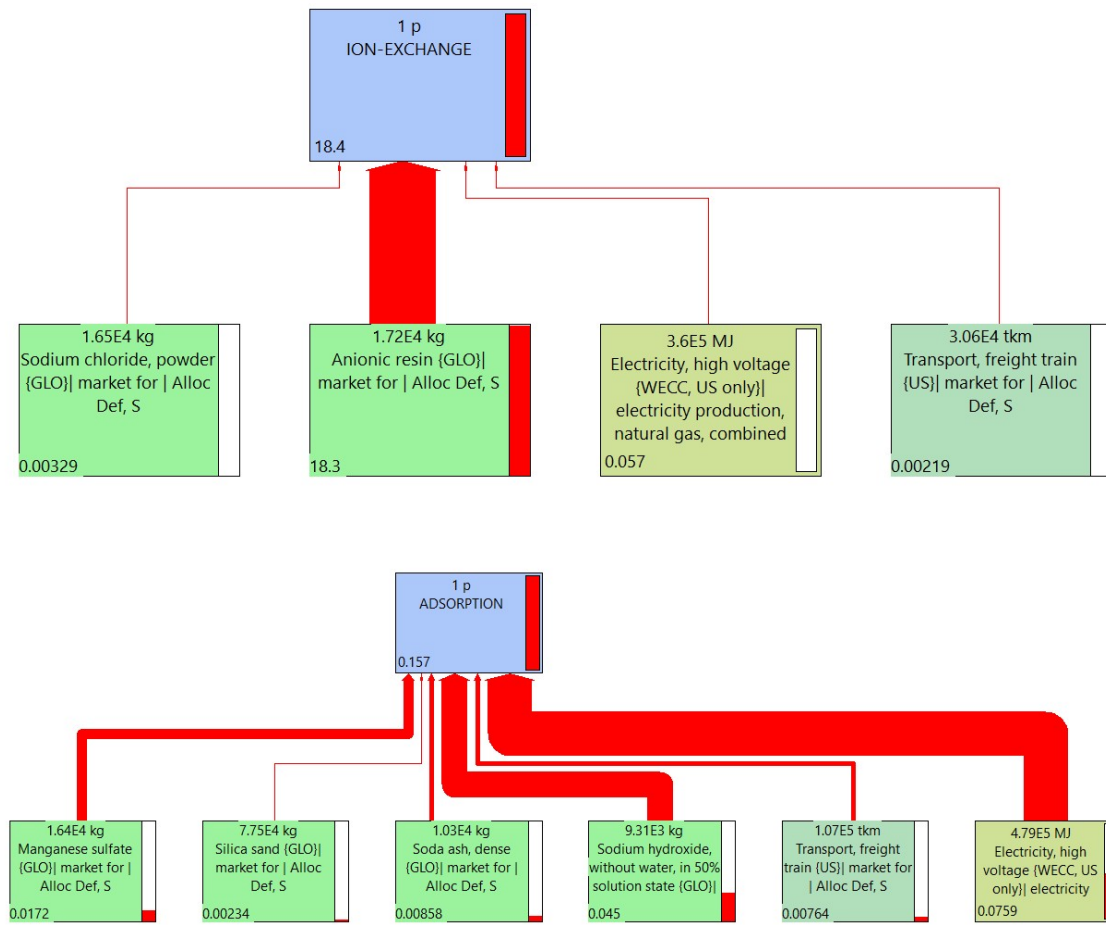


Figure S1. Tree diagram of adsorption and ion-exchange treatment system

Table S5. Characterization and normalization of impact assessment using TRACI 2.1

Impact category	Unit	Adsorption	Ion-exchange	RCF
Ozone depletion	kg CFC-11 eq	0.025265962	2.961049865	0.01147023
Global warming	kg CO <sub>2</sub> eq	97993.37537	101929.9535	64855.7475
Smog	kg O <sub>3</sub> eq	5469.90592	3800.538704	4485.127797
Acidification	kg SO <sub>2</sub> eq	851.9117378	456.0236921	535.2759371
Eutrophication	kg N eq	207.9062429	170.1984915	139.31258
Carcinogenics	CTUh	0.003381289	0.003250313	0.010534177
Non carcinogenics	CTUh	0.019003722	0.017629114	0.019596296
Respiratory effects	kg PM <sub>2.5</sub> eq	100.5048538	61.65666383	62.81392581
Ecotoxicity	CTU <sub>e</sub>	445221.2222	421598.9928	596128.1459
Fossil fuel depletion	MJ surplus	201799.1254	235344.3488	119788.4165

Impact category	Adsorption	Ion-exchange	RCF
Ozone depletion	0.156671534	18.36115394	0.071125672
Global warming	4.045352723	4.207862146	2.677368483
Smog	3.92977733	2.730443824	3.222277274
Acidification	9.379195542	5.020632057	5.893166464
Eutrophication	9.618264225	7.873809074	6.444949347
Carcinogenics	64.13794214	61.65352823	199.8174338
Non carcinogenics	18.09350437	16.78473566	18.65769588
Respiratory effects	4.144875651	2.542754851	2.590480974
Ecotoxicity	40.21888102	38.08497638	53.85099761
Fossil fuel depletion	10.72237455	12.5047631	6.364825742

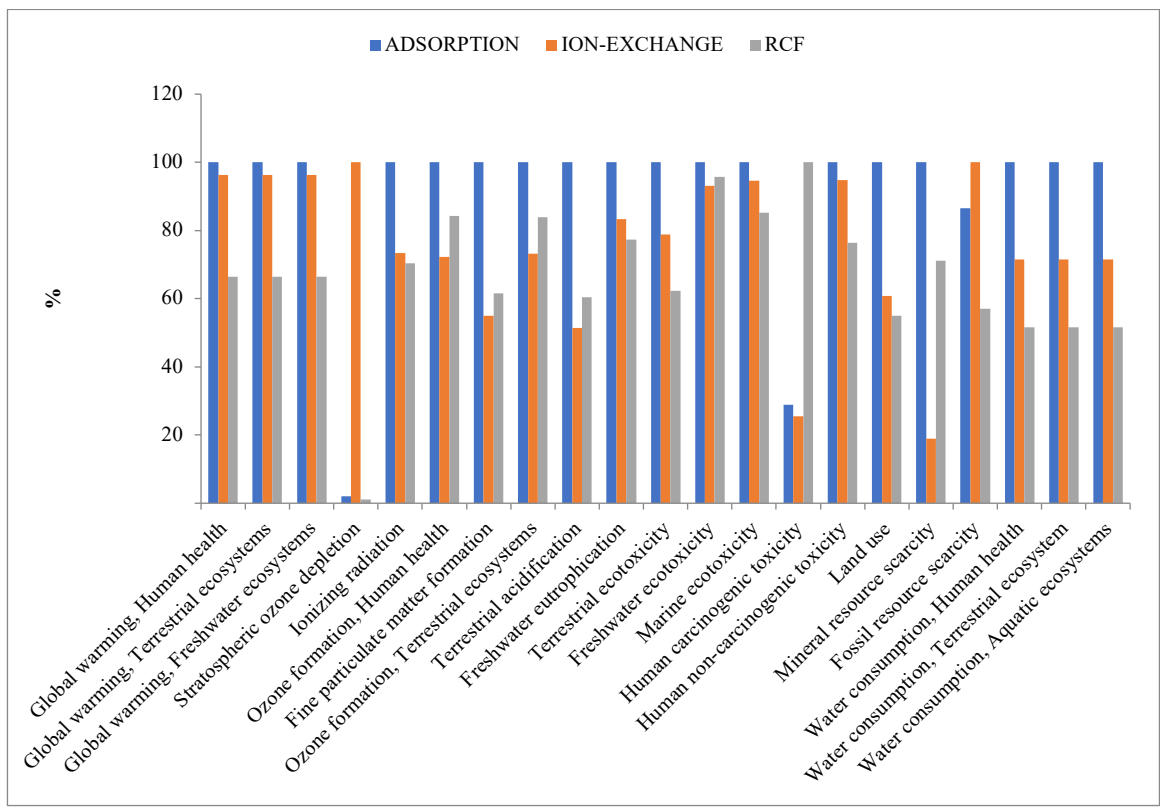


Figure S2. Characterization of impact assessment using ReCiPe Endpoint E method

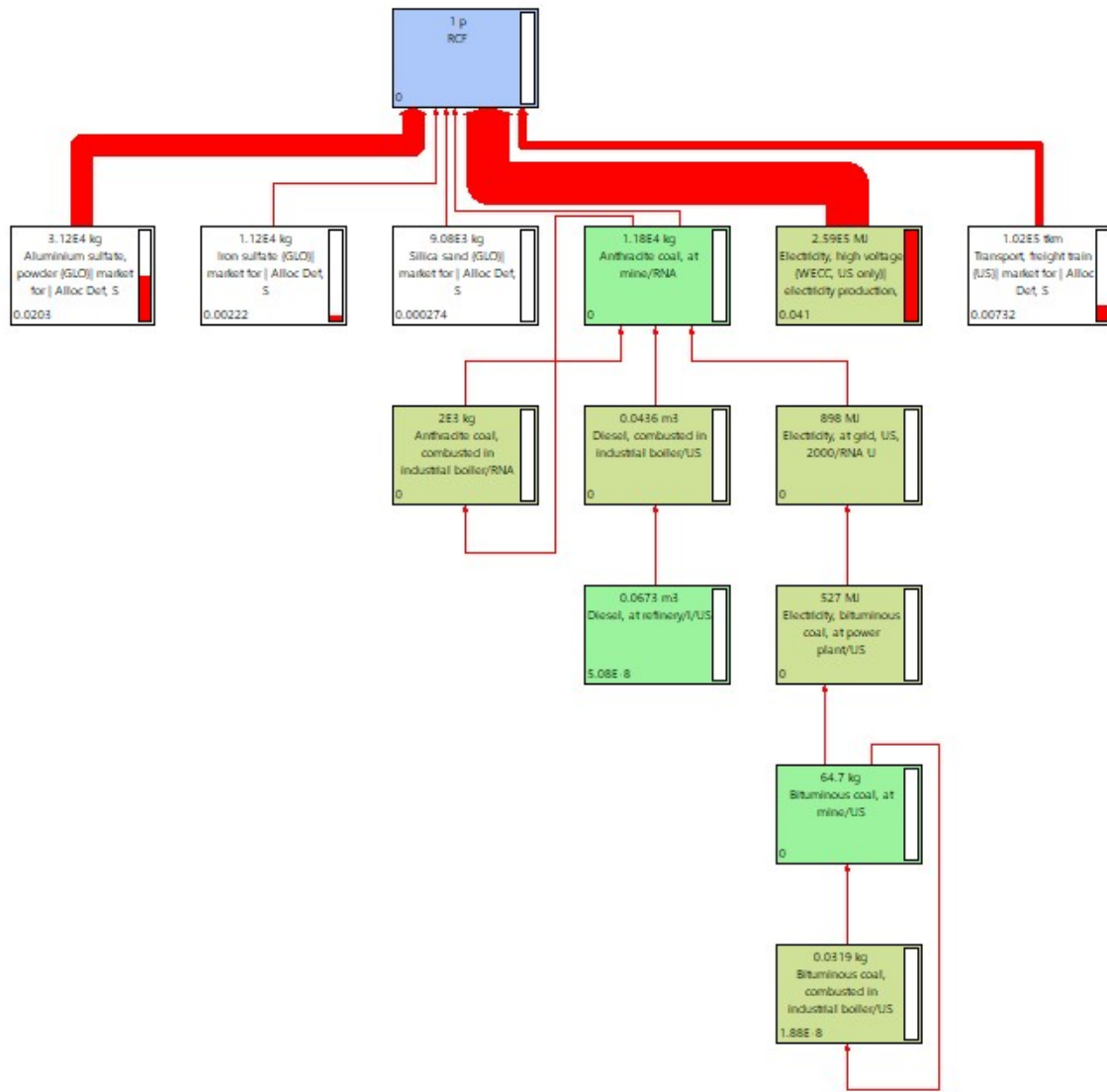


Figure S4. Network scheme of RCF treatment system

## VITA

**NAME:**

Lisha Wu

**EDUCATION:**

Ph.D., Civil and Material Engineering, University of Illinois at Chicago, Chicago, Illinois, 2020

M.S., Environmental Science and Engineering, Beijing University of Chemical Engineering, Beijing, China, 2014

B.S., Chemical Engineering, Wuhan Institute of Technology, Wuhan, Hubei, 2011

**PROFESSIONAL MEMBERSHIP:**

American Society of Civil Engineering

Society of Women Engineers

**AWARDS:**

ASCE IL section The Environmental and Water Resources Institute Scholarship

Christopher B. Burke and Susan S. Burke Graduate Student Award

Chancellor's Graduate Research Award

**PUBLICATIONS:**

U.S. Environmental Protection Agency First Place in Master Plan Campus Rain Works Challenge Punia, Snover, Kamel Babaeiveli, Lisha Wu, and Amid P. Khodadoust. "Removal of Arsenic from Coal Fly Ash Leachate Using Manganese Coated Sand." [Geotechnical Special Publication](#), Vol. 2016-January, Issue 273 GSP, 62-69.

Wu, Lisha, Snover Punia, and Amid P. Khodadoust. "Removal of Chromium, Copper, and Arsenic from Contaminated Water Using Manganese Oxide Based Adsorbents." [Geotechnical Special Publication](#), Vol. 2016-January, Issue 273 GSP, 2016, 53-61.

Wu, Lisha and Amid P. Khodadoust. " Adsorption of Cr(III) and Cr(VI) from Water Using Crystalline Manganese (II, III) Oxides." Submitted to [Journal of Colloid and Interface Science](#).

